Design of freeze-dried formulations for the enhancement of drug release

Alqurshi, Abdulmalik Abdulrahman M

Awarding institution:
King's College London

Design of freeze-dried formulations for the enhancement of drug release

Abdulmalik Alqurshi B.Sc. (Hons) M.Sc.

A thesis submitted for the degree of Doctor of Philosophy of King's College London

Faculty of Life Sciences & Medicine, Institute of Pharmaceutical Science, King's College London, Franklin-Wilkins Building, 150 Stamford Street, London, SE1 9NH

Certificate

This is to certify that research work embodied in this thesis entitled “Design of freeze-dried formulations for the enhancement of drug release” has been carried out by myself under the supervision and guidance of Dr Paul G Royall.

Abdulmalik Alqurshi

Abstract

A commonly used approach for the improvement of dissolution and disintegration is to render a poorly soluble drug into its amorphous or disordered form. However, such amorphous materials are physically unstable and are difficult to formulate into oral dosage forms due to their sensitivity to the physical and thermal processes that are involved in production. The first aim of work presented here was to produce the amorphous form of a drug *in-situ* within a capsule. The second aim was to develop a predominantly amorphous freeze-dried buccal tablet for the rapid delivery of emergency medicine. Nifedipine and naloxone were used as the test compounds to achieve aims 1 and 2 respectively.

Nifedipine and polyvinylpyrrolidone K10 (PVP) were dissolved in tert-butanol at 37 ^{o}C to provide a range of drug to polymer ratios. These solutions were dispensed into gelatin capsules, freeze-dried, sealed and packaged in amber vials under nitrogen. The nifedipine content was maintained at 10 mg per capsule, but the PVP concentration was increased from 0 to 90% w/w. Differential scanning calorimetry, infra-red spectroscopy, polarization light microscopy and USP *in vitro* dissolution were used to optimise and characterise drug-polymer interactions in the freeze-dried formulations. The optimised *in-situ* freeze-dried capsule formulation (10% w/w nifedipine in PVP) formed a predominantly amorphous and porous formulation, with 3 months shelf life at 40 ^{o}C, stabilised by drug-polymer hydrogen bond intermolecular interactions. Drug released *in vitro* dissolution by optimized formulation reached 80% in < 6 min, approximately half the time required by the marketed nifedipine formulation.

Excipients and naloxone HCl were dissolved in aqueous solution and dispensed into aluminium blisters to be freeze-dried. The optimised tablet composition (mannitol 24% w/v, gelatin 65% w/v, sodium bicarbonate 11% w/v and naloxone 800 µg) formed stable predominantly amorphous tablets. Sodium bicarbonate was found to be essential in preventing mannitol from recrystallizing in freeze concentrates, while high gelatin to mannitol ratio ensured the stability of amorphous mannitol during and after freeze-drying. A novel disintegration assay was developed to represent conditions in the buccal cavity: i.e. temperature 33-37 ^{o}C, dissolution volumes (0.1-0.7mL), mucin containing disintegration medium. The amorphous tablet has shown to disintegrate in less than 10 s. The disintegration assay was discriminatory for quality control purposes and has potential for future development as an assay to predict *in vivo* performance. In conclusion, rapidly dissolving tablets have been developed which are suitable for proof-of-concept clinical trial in humans to determine the pharmacokinetics of naloxone delivered via the buccal route.

Table of Contents

List of Figures

List of Tables

List of Abbreviations

Ave	Average
BCS	Biopharmaceutical Classification System
BN	Batch Number
BP	British Pharmacopeia

CAS	Chemical Abstracts Service
CC	Catalogue Code
DIDA	Digital Image Disintegration Assay
DSC	Differential Scanning Calorimetry
EP	European Pharmacopeia
FD	Freeze-dried
FD-10%	FD 10% w/w nifedipine in PVP, similarly **FD-30%, FD-50%, FD-70%** and **FD-100%** may be used for FD 30, 50, 70 and 100% w/w nifedipine in PVP respectively.
FDA	Food and Drug Agency
FDT	Fast Disintegrating Tablet
FT-IR	Fourier Transform Infrared
IN	Instrument Number
MHRA	Medicines & Healthcare Products Regulatory Agency
MN	Manufacture Number
NCE	New Chemical Entities
NIF	Nifedipine
NIF-AR	Nifedipine As Received
NLX	Naloxone
PA	Peak Area
PC	Product Code
PEG	Polyethylene glycol
PM	Physical-Mix
PM-10%	Physical-mix 10% w/w nifedipine in PVP, similarly FD-30%, FD-50%, FD-70% and FD-100% may be used for physical-mix 30, 50, 70 and 100% w/w nifedipine in PVP respectively.
PN	Product Number
PT	Product Type
PVP	Polyvinylpyrrolidone
PWSD	Poorly Water-Soluble drug
Rs	Resolution
RT	Retention Time
SD	Solid Dispersion
SE	Standard Error
SN	Serial Number
Std	Standard Deviation
T'_g	Primary Glass Transition Temperature
TBA	Tert-butanol
T_c	Collapse Temperature
T_g	Glass transition Temperature
TGA	Thermogravimetric Analyser
T_p	Target Product Temperature
USP	United States Pharmacopeia

List of publications

Abstracts

Alqurshi, A., Royall, P. G. & Forbes, B. Digital Image Disintegration Assay (DIDA) for the Quality Control (QC) of fast disintegrating tablets. Maximising productivity in pharmaceutical QC and stability testing, 10-12-2015 2015 The Royal Society of Chemistry Burlington House. Joint Pharmaceutical Analysis Group, 10. (see appendix 5)

Alqurshi, A., Riggs, P. & Royall, P. G. Design of a novel *in-situ* freeze-dried capsule for dissolution rate enhancement. AMORPH 2014 THE FELIX FRANKS SYMPOSIUM, 14-16th July 2014 Girton College, Cambridge. The BioUpdate foundation. (see appendix 6)

Mcdonald, R., Alqurshi, A., Forbes, B., Royall, P. G., Taylor, D. & Strang, J. Buccal naloxone for opioid overdose reversal: rationale for and development of a novel instant-dissolving tablet. Neuroimaging and Experimental Medicine Advances, 30th Nov 2015 Denmark Hill, ORTUS learning and events centre. Biomedical Research Centre and Dementia Biomedical Research Unit. (see appendix 7)

Papers

Alqurshi, A., Kumar, Z., Mcdonald, R., Strang, J., Buanz, A., Ahmed, S., Allen, E., Cameron, P., Rickard, J., Sandhu, V., C., H., Stansfield, R., Taylor, D., Forbes, B. & Royall, P. G. submitted. Instant disintegrating buccal tablets for the emergency delivery of naloxone. *Molecular pharmaceutics*. (see appendix 8)

Strang, J., Mcdonald, R., Alqurshi, A., Royall, P. G., Taylor, D. & Forbes, B. submitted. Naloxone without the needle – structured review of potential non-injectable routes, the consequent rationale for, and next steps in development of new nasal and buccal naloxone formulations. *Drug and alcohol dependence*. (see appendix 9)

Patent

Novel formulation: buccal naloxone fast disintegrating tablet, King's College London has registered intellectual property under patent number **GB 1504482.9**. The following authors are involved: Alqurashi, A., Royall, P.G., Forbes, B., Strange, J., McDonald, R.

Acknowledgment

I thank God (ALLAH) the most merciful and the most gracious for giving me the strength, knowledge and patience to be able to complete this study.

My deepest gratitude goes to my supervisor Dr. Paul Royall, who has been a true source of inspiration and motivation. Not only was Dr. Royall's guidance key to the success of this project, but he was also a very patient and supportive role model. His words and advice have guided me through this research, and will form the bases of my future work. I would like to thank my parents, Abdulrahman and Fatma, my brothers, sisters, my beloved in-laws and my dear friend Khalil for their continuous support, guidance and encouragement. I would also like to thank my loving wife Somaiah, who has been a truly caring friend, a source of joy and happiness, and who, most importantly, fed me well through my writing phase.

My sincere gratitude goes to Prof. Ben Forbes, for his direct & most valuable advice, and for relentlessly motivating me to publish. Prof. Forbes has informally co-supervised me through a great research opportunity; working with him has allowed me to build a range of important skills, which I am quite thankful for. I am also very grateful to the Pharmacy manufacturing unit team at Guy's hospital, especially Rebecca Stansfield, Verity Sandhu, James A. Rickard, Peter Cameron, and Chris Holt for taking the time to advice, support and train me to implement good manufacturing practice in all aspects of pharmaceutical production.

A special thanks goes to David McCarthy and the extremely helpful team of technicians at Franklin-Wilkins building, especially Steve Ingham, Dan Asker, Richard Harper, Calum King, Tom Littlewood and David Stanton for their priceless practical help. I would also like to thank my wonderful friends and previous master student namely Zahrae Kumar, Mireille Hassoun, Samana Abidi and Qudsia Afzal for their great friendship and hard work.

Last but not least, I would like to thank the Saudi ministry of education and the Saudi Arabian Embassy for funding this study, and for giving me this great opportunity.

Chapter 1. General introduction

The oral route, from the patient's perspective, is the most familiar and convenient form of consuming medication, the assistance of trained medical staff in the administration process is not usually needed, and therefore a greater patient compliance is seen when administering oral formulations (Sugawara *et al.*, 2005, Youn *et al.*, 2006). Medications delivered through the oral route are most commonly presented as a solid dosage form, such as capsules and tablets, or as liquid dosage forms such as solutions and suspensions (Strickley *et al.*, 2008). While liquid oral formulations are easier to swallow, the bitter taste of some active pharmaceutical ingredients (API) can sometimes be challenging to overcome with taste masking excipients, and may therefore reduce the compliance of patients (Jin *et al.*, 2008, Venables *et al.*, 2015). Solid dosage forms on the other hand overcomes the taste barrier by encapsulating the active pharmaceutical ingredient (API) or by coating it, thus preventing its direct contact with taste buds on the tongue (Jin *et al.*, 2008). Moreover, solid dosage forms eliminate the patient's responsibility to measure the appropriate volume of medication as generally observed with liquid oral formulations (Marwaha *et al.*, 2010). Economically, the pharmaceutical industry is more attracted to formulating a drug into a solid dosage form due to its low cost in production and transportation (Marwaha *et al.*, 2010). Solid dosage forms are also a safer investment for community pharmacies, as they tend to have a long shelf-life, 4 - 5 years (FDA, 2008) in comparison to 1 - 2 years for liquid dosage forms. Moreover, solid dosage forms may be stored at 40 ^{o}C or below, which in some climates falls under room temperature (WHO, 2009, ICH, 2006).

Solid oral formulations have a long history of development, and therefore a wide range of materials have been explored for their role as excipients, providing the formulator with a large library of generally regarded as safe (GRAS) excipients (Marwaha *et al.*, 2010). A good understanding of the underpinning science behind the design, manufacture and packaging of solid oral dosage forms has developed over time (Zhang *et al.*, 2004), this has led to the development of accurate methods for measuring

quality in performance of solid oral dosage forms, e.g. British Pharmacopeia (MHRA, 2014b). Organizations such as the medicine and health care regulatory agency (MHRA) have in place thorough guidelines and regulations to help develop new and safe solid oral dosage formulations (MHRA, 2014a).

Due to these advantages, pharmaceutical companies strive to formulate new chemical entities (NCE) into solid dosage forms that provide desirable and reproducible drug plasma concentration (Ikegami *et al.*, 2006). A problem that is frequently encountered, is that most NCEs have low water solubility, and despite the high permeability of some of them, their absorbance into the circulatory system and hence their bioavailability is dependent on their dissolution into the aqueous gastrointestinal fluid (Kaur *et al.*, 2012, Vasconcelos *et al.*, 2007, Streubel *et al.*, 2006, Gardner *et al.*, 1997). Drug research teams were reported, by Thomas *et al.* (2006), to rottenly target a solubility of > 60 µg/mL for new developable drugs, as this solubility is believed to usually lead to a satisfactory absorption provided the drug has average permeability (Figure 1.1) However, it can be misleading to assume a single solubility limit for all drugs as potency and metabolism can vary considerably from one drug to another, and thus the amount of drug, or dose, that must dissolve to achieve a satisfactory effect is the dominant factor in evaluating drug solubility.

Fick's first law illustrates that drug absorption is a product of drug solubility and permeability (Flynn *et al.*, 1974):

$$J_{wall} = C_{int} \cdot P_{wall} \qquad \text{Equation 1.1}$$

Where J_{wall} is the drug flux across a homogeneous intestinal membrane measured in mass unit often µg, for a specific cross sectional area and a period of time, such as µgcm^{-2}h^{-1} (Brodin *et al.*, 2010). C_{int} is the drug concentration in the luminal fluid, often measured in µg/mL, and P_{wall} is the effective permeability measured in Darcy units (D), named after Henry Darcy (Simmons, 2008). The most promising NCEs are generally limited to absorption in the upper small intestine, which therefore narrows the window of absorption (Gardner *et al.*, 1997, Streubel *et al.*, 2006). This dilemma presents the pharmaceutical industry with one of its most challenging objectives; to

design formulations that would enable poorly water-soluble drugs (PWSD) to dissolve rapidly into the aqueous gastrointestinal fluid (Vippagunta *et al.*, 2007, Tanaka *et al.*, 2006, Ohara *et al.*, 2005). If this objective was successfully fulfilled, such formulation design would be expected to have improved dissolution rate for the PWSD, and thus enhanced bioavailability and minimised gastrointestinal side effects for the active pharmaceutical ingredient (API) (Streubel *et al.*, 2006, Tanaka *et al.*, 2006, Leuner and Dressman, 2000, Majerik *et al.*, 2007, Prabhu *et al.*, 2005).

The biopharmaceutical classification system (BCS) helps classify drugs in accordance to their solubility and permeability (Leucuta, 2014), which are the dominating factors in influencing oral bioavailability of drugs (Flynn *et al.*, 1974, Pouton, 2006).

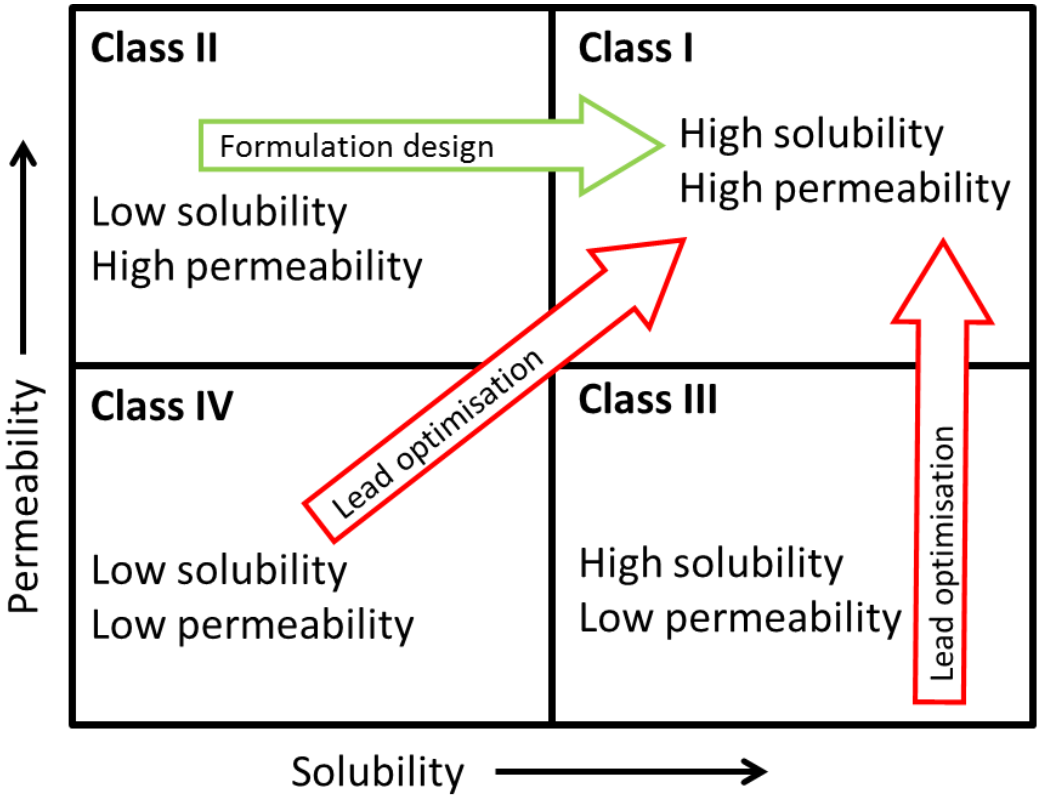

Figure 1.1 The biopharmaceutical classification system (Pouton, 2006), with indications of how the solubility and permeability of drugs in Class II-IV may be enhanced to match drugs in class I.

Class I of the BCS classification system includes drug molecules with high solubility (Thomas *et al.*, 2006) and permeability. Class II, most common in currently used active pharmaceutical ingredients (Patil *et al.*, 2015), include drugs with high permeability but low solubility, caused by a large molecular weight or the presence of hydrophobic groups, such as benzene rings, or in some cases due to a planer molecular geometry

that encourages strong π-π intermolecular bonding (Chowdary and Pavan Kumar, 2013, Leucuta, 2014). Due to solubility limitations, absorption of a class II drug is hindered, this however may be markedly improved if the drug is maintained in a solubilized state while in the lumen of the gut, this may be achieved through formulation strategies (Pouton, 2006, Chowdary and Pavan Kumar, 2013). The absorption of class III and class IV drugs on the other hand are very difficult to improve, as both suffer from low permeability, which requires structural optimisation to bypass (Leucuta, 2014).

1.1. Solid dosage forms and the solid state

In order to understand the behaviour of solid dosage forms and thus allow for the enhancement of favoured properties, it is important to understand the properties of the solid-state. Unlike gases or liquids, solids retain their shapes unless a compressive force is applied (Milanovic *et al.*, 1998). This indicates that the molecules of a solid state material are held up in close proximity to one another through strong non-covalent intermolecular forces such as hydrogen bond or van der Waals forces (George Burton, 2000). The type, strength and frequency of intermolecular forces in addition to the presence of an order in which they occur are all of a great impact on the physicochemical properties of the resulting solid (Florence and Attwood, 1988). These factors in return are influenced by the content and structure of the individual molecules, hydrogen bonding for example occurs between a hydrogen atom from one molecule and an electronegative atom from another, or from the same macromolecule, given that the two atoms are within close proximity (Stone and Editor, 1996).

1.1.1. Crystalline state

Molecules in a crystalline material are packed in a defined and repeated order, held in place by intermolecular forces such as van der Waals forces to form a crystal lattice. The strength of these intermolecular forces determines the energy of the lattice and vice versa. (Vippagunta *et al.*, 2001, Mullin, 2001). A melting point is a characteristic

property of crystalline material, it indicates the temperature at which the individual molecules of a lattice have gained sufficient energy to overcome the intermolecular forces holding the lattice together, and therefore the temperature at which the crystal lattice converts to liquid (Vippagunta *et al.*, 2001). A high melting temperature is indicative of a high energy crystal lattice which as a result indicates that strong intermolecular forces such as hydrogen bonding are holding the molecules together. Low melting temperatures on the other hand indicate the presence of only weak intermolecular forces in the lattice, such as van der Waals (George Burton, 2000). The shape of the molecule has a great effect on the energy of the lattice, as molecules with planer geometry such as nifedipine are easily packed very closely, allowing stronger π-π intermolecular bonding, therefore resulting in higher lattice energy and thus a higher melting temperature. (Ahmed *et al.*, 1996, Allen *et al.*, 1978, Aulton, 2007, Briggner *et al.*, 1994, Royall *et al.*, 2001).

1.1.2. Amorphous state

A solid material is said to be in an amorphous state when it lacks the long-range order characteristic of a crystal (Kaushal *et al.*, 2004, Santivarangkna *et al.*, 2011, Craig *et al.*, 1999). In other words, the arrangement of its molecules, and the interactions between them, resemble that of a liquid form while maintaining a solid like viscosity (Raudonus *et al.*, 2000, Paterson *et al.*, 2015). When heating an amorphous material a noticeable change in viscosity and molecular mobility takes place at a temperature specific to the material, this transition is known as the glass transition (Paterson *et al.*, 2015), and the temperature at which it takes place is referred to as the glass transition temperature (T_g) (Paterson *et al.*, 2015). Despite the change in viscosity, intermolecular interactions before and after the glass transitions remain approximately the same, as a result no endothermic melting peak appears in thermal analysis of such materials (Craig *et al.*, 1999).

1.1.3. Physical stability of amorphous material

When storing an amorphous material below its glass transition it appears brittle, sometimes described as being in the glassy state (Santivarangkna *et al.*, 2011), and

very viscous, approximately ≥ 1.1 x 10^{14}Pa (Craig *et al.*, 1999), and therefore its molecules lack mobility (Paterson *et al.*, 2015). Molecular mobility is represented by the average relaxation time (τ), which may be described as the average time taken for a molecular motion to occur (Hancock *et al.*, 1995). The specific type of motion really depends on the analytical method employed for their characterisation (Roudaut *et al.*, 2004). For example, if viscosity is used to measure relaxation behaviour, this is relative to intermolecular translational diffusion (Roudaut *et al.*, 2004), whereas if IR or NMR are used to determine relaxation times, these will relate to motion within specific parts of the molecules and theirs environment (Roudaut *et al.*, 2004). Therefore, its overall magnitudes behind different relaxation times within glass will be similar, but the specific values may change depending on the analytical technique used.

Molecular mobility, and relaxation time, is directly influenced by storage temperature; at high temperatures the mean relaxation times, of amorphous materials, is very rapid (≤ 10 h) compared to the speed of transition molecular motion at temperatures below the glass transition (> 1000 h for PVP and > 1x10^5 h for indomethacin at approximately 50 ^{o}C below T_g) as measured by Hancock *et al.* (1995). Short relaxation times (< 1h) for amorphous products, above their $T_{g,}$ may be determined via conventional solid state nuclear magnetic resonance and thermal techniques (Hancock *et al.*, 1995), while determining long relaxation times requires aging experiments as described by Struik (1977) and applied by Guo (1994) and (Hancock *et al.*, 1995). Glassy material experiences gradual losses in enthalpy (ΔH) and volume (ΔV) when stored, under T_g (Hancock *et al.*, 1995), due to molecular motion towards the more thermodynamically stable crystalline structure (Hancock *et al.*, 1995). Measuring endothermic relaxation using differential scanning calorimetry (Hancock *et al.*, 1995), before and after various lengths of controlled aging at specific temperatures permits the determination of molecular mobility in the non-equilibrium amorphous sample (Hancock *et al.*, 1995). However the impact of extended periods of relatively high temperature aging on the chemical stability of the amorphous material understudy is rarely reported, and this casts a general concern over such approaches.

If amorphous materials are stored above their glass transition, they appear, less viscous and thus molecules are more mobile and are able to diffuse (White and Cakebread, 1966). This quickly leads to crystal nucleation and therefore crystallization, a process where the amorphous matter reverts back to the more stable ordered crystal structure. Crystallization is difficult to avoid but maybe slowed down by limiting molecular mobility, which is the dominating factor in the kinetics of recrystallization. As temperature directly influences molecular mobility, the T_g is commonly used as a marker for the process of recrystallization. (Kaushal *et al.*, 2004, Royall *et al.*, 1998, Hancock and Zografi, 1997, Yoshihashi *et al.*, 2006, Aso *et al.*, 2004). Despite the reduction in molecular mobility below T_g, this is found to have a profound influence over the life-time of an amorphous pharmaceutical product, which is usually in the order of a few years (Hancock *et al.*, 1995). Zografi's rule states that recrystallization of an amorphous material may be slowed down by storing the product 50 ^{o}C below its T_g (Hancock and Zografi, 1997).

The glass transition temperature of an amorphous solid material is mainly influenced by the physiochemical properties of the material, such as intrinsic properties that directly influence molecular mobility and macroscopic fluidity (Craig *et al.*, 1999). These include molecular structure, weight, size and shape. For example polymers with high molecular weight and long chains are less mobile than small organic molecules which form a large proportion of drugs. As a result polymers tend to show a higher T_g than amorphous small organic molecules (Meng *et al.*, 2015). Polymers with stiff backbones tend to have higher T_g values than those with a more flexible, and therefore mobile, backbone; mobile backbones are composed of bond sequences that can easily rotate (e.g. $–CH_2CH_2–$ or $–CH_2OCH_2–$). The mobile flexibility of a polymer may be hindered by bulky side groups. In addition, the purity of an amorphous material can also influence the T_g, for example the T_g of a pure organic material may be increased by the addition of high T_g long chain polymer (Raudonus *et al.*, 2000), or decreased by the addition of smaller molecules with lower T_g, a process known as plasticisation (Craig *et al.*, 1999). One of the most commonly dealt with plasticizers is water (with a T_g at 135K), and as water is present in ambient air (Craig *et al.*, 1999) it is therefore important to keep amorphous material sealed and protected to avoid adsorption of

water molecules; a process that can eventually lead to accelerating recrystallization and therefore shortening the life-time of amorphous pharmaceutical products (Royall *et al.*, 1999). It may therefore be concluded that the rate of crystallisation of amorphous drugs will vary depending on two major factors, the environmental storage conditions and the physicochemical properties of drug.

In the field of investigating the stability of amorphous products, it is useful to look at the kinetics of crystallization, as it would allow better estimation and understanding of the shelf-life of amorphous pharmaceutical products. Crystallization kinetic data, expressed as an extent of conversion or relative crystallinity (θ_t) as a function of time (Kaushal *et al.*, 2004, Gaisford *et al.*, 2009), maybe fitted to different models at each temperature. The model that best fits the data is then selected and assumed to represent the mechanism at hand. One of the commonly used models is the Avrami model:

$$\theta_t = 1 - \exp[-(k_a t)^{na}] \qquad \text{Equation 1.2}$$

Where k_a is the Avrami rate constant, which gives a quantitative parameter for the stability of the system, and n_a is the Avrami exponent, which provides information of the mechanism of nucleation and crystal growth (Gaisford *et al.*, 2009).

1.2. Solubility

The thermodynamic solubility of a solid drug in an aqueous phase is defined as the concentration of the drug in a solution when in equilibrium with its pure solid form at a constant temperature and pressure, following scheme given below equation 1.4 where $[Drug]_s$ is the concentration of drug in solid state and $[Drug]_{aq}$ is the concentration of drug in the saturated aqueous solution (Johnson and Zheng, 2006).

$$[Drug]_s \rightleftharpoons [Drug]_{aq} \qquad \text{Equation 1.3}$$

Thermodynamic solubility for a drug at a specific temperature and pressure is typically measured by adding an excess amount of solute to a vessel containing the solvent, which is then sealed and kept at constant conditions (a temperature and pressure of

interests). Enough time is then given to allow equilibrium to be reached between drug in the solid state and drug dissolved within an aqueous solution (typically 5 days). Once the duration is completed, the concentration of drug in solution is noted to be the aqueous solubility of the drug under the specified temperature and pressure (Soltanpour *et al.*, 2014).

Typically the driving force for the formation of a solution from the starting point of a pure solute and solvent is the increase in disorder, which may be expressed as the change in entropy (ΔS), which is a result of the increase in the random arrangements of the solute molecules in the solvent upon formation of a saturated solution (Liu, 2008). The change in enthalpy (ΔH) is also an important factor that determines the likelihood for the formation of a solution. There are several steps which contribute to this enthalpy change: Firstly the change in enthalpy associated with the endothermic process of breaking non-covalent intermolecular forces which are present between solute molecules as well as the solvent molecules. Secondly the exothermic process of non-covalent bond formation between solute and solvent molecules. Thus heat flow is typically observed when a solution, or saturated solution, is formed. Such heat flow usually indicates an overall endothermic process for the dissolution of crystalline materials. *Gibbs free energy* (G) is a function that is derived from the entropy and enthalpy of a closed system under constant temperature and pressure. For a process to favour the product, the change in free energy or ΔG must be negative (Florence and Attwood, 1988).

$$\Delta G = \Delta H - T\Delta S \qquad \text{Equation 1.4}$$

From equation 1.5 it can be seen that the main limitation of achieving a large negative change in ΔG is the presence of a large positive ΔH value. Therefore, solutes with strong intermolecular forces are less likely to be soluble, with the exception of solutes that have a high tendency to interact with the solvent molecules to form strong solute-solvent interactions, such as ionic materials, electrolytes and salts, for example NaCl. In such cases the exothermic reaction of bond formation between solute and solvent molecules outweighs the endothermic breakage of solute-solute interactions as well as solvent-solvent interactions.

Applying a thermodynamic approach to the formation of a saturated solution, to determine the solubility in thermodynamic terms, the following equation has been derived and reported by many authors for example (Liu, 2008, Smith, 1982):

$$\ln X_2 = -\frac{\Delta H_f}{RT_m}\left(\frac{T_m - T}{T}\right) - \ln \gamma_2 \qquad \text{Equation 1.5}$$

Were X_2 is the solubility concentration expressed as the mole fraction of solute within the solution, calculated by dividing the number of moles of solute by the total number of moles of solute and solvent present in solution. ΔH_f is the change in enthalpy of fusion. R is the gas constant (8.314Jk^{-1}mol^{-1}), T_m is the melting temperature of the solute, T is the temperature of solution in Kelvin, and finally γ_2 is the activity or effective coefficient (Smith, 1982). From the middle term $\left(\frac{T_m - T}{T}\right)$ the melting temperature of the solute can have an inverse effect on the solute's solubility. The later part of the equation ($\ln \gamma_2$) accounts for the activity and interactions of the solute with the solvent in a non-ideal solution. Also an important factor which can influence solubility is the heat of fusion, as an increase in ΔH_f causes a lowering of solubility (Smith, 1982, Liu, 2008). It is difficult to apply the above equation to solid amorphous materials where the molecules are present in a disordered manner as they are far from equilibrium. In these systems the interactions or non-covalent bonding between molecules is reduced relative to the analogous crystalline form. However extrapolating equation 1.5 to highly viscous or slow to reach equilibrium amorphous systems may be useful as it can be seen that due to a lowering of the interactions between the molecules, because of the disordered structure, a higher *apparent* solubility would be observed (Leuner and Dressman, 2000).

An alternative to measuring solubility using thermodynamic methods i.e. measuring the concentration of a saturated solution above the solid once equilibrium is reached, the kinetic solubility has been proposed. This is considered to be the more favourable method at drug discovery stage, as it requires virtually no equilibrium time and relatively low amounts of the sample (Dehring *et al.*, 2004, Thomas *et al.*, 2006). Kinetic solubility is the measurement of the solute solubility where it is pre-dissolved in dimethyl sulfoxide (DMSO), then titrated with an aqueous medium to precipitation

point (Thomas *et al.*, 2006, Dehring *et al.*, 2004). This method is very useful for obtaining an apparent solubility but if the system were allowed to equilibrate over many hours the values for the solubility measured at equilibrium can be expected to differ when compared to the kinetic or apparent solubility. For drugs in the amorphous state, this is more than likely as over time they have a well-reported tendency to crystallise in the presence of solvents especially water (Thomas *et al.*, 2006). Verma and Rudraraju have shown in a recent study, that presenting cilostazol in its amorphous form can enhance its apparent solubility to be > 80.0 µg/mL, while its thermodynamic solubility was reported to equal 2.63 µg/mL. However, the supersaturated solutions of cilostazol lead to the recrystallization and precipitation of drug (Verma and Rudraraju, 2015).

Kinetics is concerned with rates of reactions and in order for a product to form (e.g. solute in the aqueous form) the reactant molecules must interact with one another (Laidler, 1987). Therefore mobility and concentration are two of the factors that govern the rate of reaction (Laidler, 1987, Varma *et al.*, 2004). Furthermore, the reactant molecules must carry enough energy to overcome an energy barrier known as the activation energy (E_a). If the reactant molecules do not hold enough energy, the reaction and therefore the product will not be formed (Figure 1.2). Arrhenius equation below summarises the relation between k, $T$and E_a were (A) is the pre-exponential factor (Laidler, 1987, Varma *et al.*, 2004):

$$k = Ae^{\left(-E_a/RT\right)} \qquad \text{Equation 1.6}$$

Arrhenius equation implies that T has a positive effect on k i.e. the rate of reaction increases with temperature, while E_a, the activation energy, acts as a barrier to the rate of a reaction (Laidler, 1987). As sketched in Figure 1.2, changes in the physical form of a solid material will also alter the activation energy and if solution formation is being considered then the rate of solution will be affected by the solid form of the solute i.e. whether it is presented in either the amorphous or crystalline form (Ozaki *et al.*, 2012).

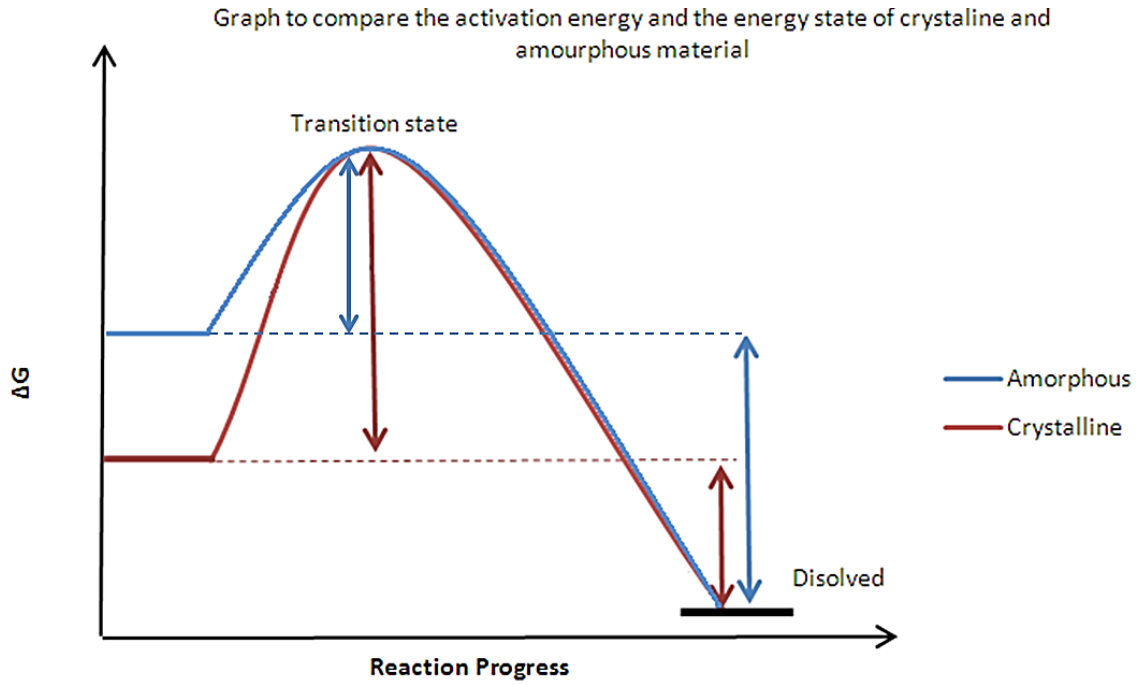

Figure 1.2 Comparing activation energy (E_a) between the amorphous and the crystalline state.

1.3. Dissolution

Dissolution can be defined as the process or rate by which a solid substance or a solute dissolves in a solvent. The rate of such process is measured as the mass of drug that goes into solution per unit time under defined conditions of temperature, pressure, solid/liquid interface and the composition of the solvent (Aulton, 2007). The Noyes-Whitney equation (Noyes and Whitney, 1897) below describes the factors affecting the rate of dissolution:

$$\frac{dW}{dt} = \frac{DA(C_s - C)}{L} \qquad \text{Equation 1.7}$$

Where $\frac{dW}{dt}$ is the rate of dissolution, A is the surface area, C is the concentration of the solid in the bulk dissolution medium, C_s is the solubility of the compound in the dissolution medium, D is the diffusion coefficient and L is the diffusion layer thickness (Leuner and Dressman, 2000). Equation 1.7 implies that the surface area has a direct effect on the rate of dissolution, while L has an inverse effect on the rate of dissolution. Reduction of particle size and optimisation of wetting characteristics of solute surface, thus reducing the value of L, may therefore have a considerable positive effect on the rate of dissolution (Leuner and Dressman, 2000). Equation 1.7

also implies that C_s has a direct effect on the dissolution rate, thus improving the apparent solubility of a solute can enhance dissolution rate and thus in the case of drugs, it may enhance bioavailability (Leuner and Dressman, 2000, Vasconcelos *et al.*, 2007).

It is important to understand that enhancing the dissolution rate would not improve the final solubility of a solute (Florence and Attwood, 1988). Such concentration is achieved when equilibrium is reached between the rate of solute dissolving into solution and solute recrystallizing and precipitating out of solution. It is however possible to produce a supersaturated solution by increasing the apparent or kinetic solubility to be greater than the equilibrium concentration (Aulton, 2007, Brouwers *et al.*, 2009). However as solutes do not precipitate out of solution as amorphous solid but as the crystalline form (Verma and Rudraraju, 2015), it is misleading to believe that the thermodynamic solubility of the amorphous form of a drug can be measured.

$$Drug_{\,(Amorphous\ solid)} \rightarrow Drug_{\,(aq)} \rightleftharpoons Drug_{\,(\mathrm{Crystalline})} \qquad \text{Equation 1.8}$$

Dissolution profile of a drug, and hence the rate of reaching drug solubility, can be greatly influenced by external factors, namely: temperature, volume, pH & composition of dissolution medium and physical agitation of the system such as speed and shape of peddle rotation (Ghayas *et al.*, 2013). The solubility of the test drug can be influenced by the temperature, pH & composition of dissolution medium and thus in return can influence the dissolution rate as described by the Noyes-Whitney equation (Noyes and Whitney, 1897). Wu et al. has shown the speed of peddle rotation to negatively influence the thickness of diffusion layer (*L*) in the dissolution of naproxen tables (Wu *et al.*, 2004). As a result, increasing speed of peddle rotation caused a faster drug release, as predicted by the Noyes-Whitney equation (Noyes and Whitney, 1897). Furthermore, assuming sink conditions are not met, the volume of dissolution can have a great effect on the rate of dissolution. Due to the great effect external parameters have on a dissolution profile, a standard method of monitoring dissolution for conventional oral solid dosage forms has been designed to allow comparison of different formulations (MHRA, 2014b). This method was adjusted to simulate conditions of the gastric luminal fluid and thus to improve correlation

between *in vitro* and *in vivo*. For an oral medicine to be marketed, its dissolution is legally required to be measured using a pharmacopeia method, appropriate to the formulation type (MHRA, 2014b). The conventional oral tablets and capsules are required to be tested using the United States Pharmacopeia (USP) Apparatus 2, also known as paddle apparatus (MHRA, 2014b) in which the formulation is dropped in a dissolution bath of a specific shape containing a large but exact volume of dissolution medium to ensure sink conditions, and at a controlled temperature, to simulate gastric conditions. The solution is continuously stirred by a paddle with a specific shape and size, a controlled speed of rotation and a fixed position to ensure equal diffusion of released drug. Content, and hence rate, of drug released is monitored by measuring the concentration at various time intervals (MHRA, 2014b).

1.4. Dissolution and apparent solubility enhancement techniques

Dissolution rate enhancement techniques have been developed on the basis of the governing factors suggested by the Noyes-Whitney equation (Vasconcelos *et al.*, 2007, Leuner and Dressman, 2000, Kaur *et al.*, 2012). Increasing the surface area by reducing particle size is usually achieved by physical techniques such as spray drying or milling. However such techniques exert physical and thermal stress on drug particles and therefore are unsuitable for thermally sensitive drugs such as nifedipine (Kumar *et al.*, 2011, Chaumeil, 1998, Vogt *et al.*, 2008, Ali, 1989) . Furthermore, it has been argued that the micronized powder, if stored incorrectly, tends to agglomerate, thereby negating the micronization procedure (Leuner and Dressman, 2000). Nano-suspension is another potential candidate for efficient delivery of PWSD, as a sharp increase in the surface area is associated with the reduction in drug particle size from micro to nano (Muller *et al.*, 2000, Patravale *et al.*, 2004). Nevertheless, many fundamental challenges such as the physical stability and shelf life are yet to be overcome (Agarwal and Bajpai, 2013), in addition carrier toxicity presents a limitation to the number of carriers suitable for nanosuspentions.

The dissolution rate of a PWSD may also be enhanced through modification of crystal habit and the use of polymorphs (Horter and Dressman, 1997), this technique is however limited to the ability of the drug to exist in more than one crystal habit (Brittain *et al.*, 2009). A classic example of the effect of using the right polymorph on drug kinetic solubility is that of chloramphenicol palmitate suspensions. It was shown by Aguiar Aguiar *et al.* (1967) that when using the stable α-polymorph of chloramphenicol palmitate in an oral formulation produces low serum levels when compared to the same dose of the unstable β-polymorph . Due to the large differences in the physiochemical properties of the different polymorphic forms of the same drug, it is essential for the manufacturers to ensure that the same appropriate polymorphic form is produced every time (FDA, 2007). Moreover it is also important to ensure the physical stability of the more water soluble polymorphic form, as it may convert to the more stable polymorphic form during the shelf life of the product, resulting in a reduction of the expected bioavailability (Savjani *et al.*, 2012).

Poor aqueous solubility may also be overcome by the use of complexing agents, one of the commonly employed class of complexing agents is the cyclodextrin (CD) family (Loftsson and Brewster, 1996). CD are enzymatically modified starches composed of specific number of glucopyranose units that form a, controlled size, ring shaped molecules with a hydrophilic outer surface and a lipophilic inner cavity (Savjani *et al.*, 2012). PWSD's can fit into the lipophilic cavity to form soluble inclusion complexes (Loftsson and Brewster, 1996, Savjani *et al.*, 2012). The antifungal miconazole is one example of the PWSD's that showed enhanced water solubility, and hence a higher oral bioavailability, in the presence of a seven unit ring cyclodextrin (β-cyclodextrin) (Tenjarla *et al.*, 1998). Despite the solubility advantages of including cyclodextrin in oral formulations, limitations to the amount of cyclodextrin used can arise due to toxicity limits as well as costs and production capacities (Loftsson, 1998).

Although particle size reduction can lead to dissolution rate enhancement, poor solubility of a drug may act as a limit to the amount of drug that dissolves into the dissolution medium, therefore limiting the drug influx and thus the bioavailability of the drug (Noyes and Whitney, 1897, Flynn *et al.*, 1974). The enhancement of drug

solubility is therefore also very important. One of the most common technique of enhancing aqueous solubility of PWSD's is a process known as hydrotrophy (Savjani *et al.*, 2012), where a second solute, referred to as hydrotrope or hydrotropic agent (Savjani *et al.*, 2012), is added to the aqueous dissolution medium, as a result the solubility of the primary solute (i.e. the drug) increases (Savjani *et al.*, 2012). The mechanism behind this process is based on complexation involving weak interactions between the hydrotropic agents such as sodium acetate, sodium benzoate or sodium alginate and the PWSD (Savjani *et al.*, 2012). Advantages of this technique include the absence for the need of chemical modification of the PWSD, the use of organic solvent or the preparation of emulsion systems. This approach is very beneficial for *in vitro* tests of water insoluble drugs; nevertheless, it may be impractical for the delivery of solid oral dosage forms as a large amount of hydrotropic agent maybe needed per dosage unit (Savjani *et al.*, 2012).

A widely known technique that is seen to improve both the dissolution rate and apparent solubility of PWSD's is the use of solid dispersions; where by PWSD's are fully dispersed into a water soluble carrier (Leuner and Dressman, 2000, Kaushal *et al.*, 2004, Vasconcelos *et al.*, 2007), therefore reducing the drug's particle size to the absolute minimum (Bates, 1969). As a result the dissolution rate of the drug is determined by the dissolution rate of the soluble carrier (Goldberg *et al.*, 1966, Leuner and Dressman, 2000). To enhance the dissolution rate even further an amorphous solid dispersion, otherwise known as a solid solution, can be developed, where the drug is dispersed molecularly within the amorphous carrier which acts as a solvent (Leuner and Dressman, 2000, Ozaki *et al.*, 2012, Brouwers *et al.*, 2009, Chiou and Riegelma.S, 1969). This was reported to enhance drug dissolution by 5 to 11 times when compared to micronized drug depending on the drug/polymer ratio (Mayersoh.M and Gibaldi, 1966).

1.5. Solid dispersions

The term solid dispersions (SD) signifies a range of pharmaceutical products containing one or a number of drugs homogeneously dispersed within a matrix of carrier(s),

traditionally prepared by heat melt or solvent evaporation methods. The methods of preparing SD and the effect of each method will be discussed in more detail in later sections of this chapter.

1.5.1. First generation solid dispersions

It was first noted by Sekiguchi and Obi in 1961 that formulations of eutectic mixtures improves the rate of drug release and, consequently, the bioavailability of drugs with poor aqueous solubility (Sekiguchi *et al.*, 1964). Eutectic mixtures consist of a fine dispersion of crystals of two different components, in this case the PWSD's and the carrier, the melting point of the drug and polymer mixture presented as a fine dispersion is lower when compared to pure drug and polymer. Reduction in melting point, as presented by Equation 1.5 in section 1.2, enhances the solubility of the water PWSD, given all other variables in Equation 1.5 are maintained constant.

Urea was one of the first highly water soluble carriers used formulating PWSD's such as sulfathiazole (Sekiguchi and Obi, 1961) and chloramphenicol (Sekiguchi *et al.*, 1964) into SD. The observed increase in rate of drug release and bioavailability were attributed to the decrease in drug particle size and better wettability (Vasconcelos *et al.*, 2007). (Levy, 1963) & (Kanig, 1964) later developed molecularly dispersed solid systems using mannitol as a faster dissolving carrier, which has proved to increase the rate of drug release further. Nevertheless these SD, sometimes referred to as first generation SD (Vasconcelos *et al.*, 2007), have the disadvantage of using crystalline carriers, such as urea (Goldberg *et al.*, 1966, Sekiguchi and Obi, 1961, Sekiguchi *et al.*, 1964) and sugars (Kanig, 1964) rather than amorphous carriers. This allows the formation of crystalline solid dispersions which are thermodynamically stable. Crystalline solid dispersions do not release drugs as fast as amorphous carriers which makes them less attractive as a formulation platform for water PWSD's (Vasconcelos *et al.*, 2007).

1.5.2. Second generation solid dispersions

In the late sixties it was first observed that maintaining the drug in its less thermodynamically stable state, the amorphous form, rather than the crystalline state, a faster drug release was achieved (Simonelli *et al.*, 1969, Vippagunta *et al.*, 2007, Urbanetz, 2006, Chiou and Riegelma.S, 1969). Therefore creating a second generation of SD (Vasconcelos *et al.*, 2007), whereby PWSDs are molecularly dispersed in a solubilizing carrier (Kaushal *et al.*, 2004).

Second generation SD can be further categorised in accordance to the drug-carrier interactions (van Drooge *et al.*, 2006). When the drug is completely miscible and soluble in the carrier, homogeneous molecular interactions between the drug and carrier are frequent, such interactions include hydrogen bonding and van der Waals interactions, which when very high result in a true one phase solution (Leuner and Dressman, 2000) as the affinity of the drug for the carrier outweighs the drug's affinity for itself. The use of a high molecular weight, amorphous stabilizing, polymer such as PVP (Kaushal *et al.*, 2004) to act as a carrier for such systems, creates a one phase molecularly homogenous glassy product where by the PWSD is fully dissolved in the polymer (van Drooge *et al.*, 2006, van den Mooter *et al.*, 2006).

In some cases the solubility of the drug, usually drugs with very high melting points and thus low solubility (Chiou and Riegelman, 1971), in the carrier maybe very limited, resulting in a two phase amorphous solid system otherwise known as a solid suspension (Vasconcelos *et al.*, 2007) where regions of amorphous drug and amorphous carrier are separated by a boundary, such as 50% w/w iopanoic acid in polyvinylpyrrolidone (Chiou and Riegelman, 1971). Although the obtained dispersions are molecularly nonhomogeneous, small drug particles, when dispersed in polymeric carriers, are able to provide an amorphous final product (van Drooge *et al.*, 2006, Goldberg *et al.*, 1966). Finally some systems are a mixture of both solid solutions and solid suspensions, where by the drug is both dissolved and suspended in the carrier. Such heterogeneous systems show mixed characteristics of solid solutions and solid suspensions (van Drooge *et al.*, 2006, Goldberg *et al.*, 1966).

1.5.3. Factors to consider when choosing carriers for a solid solution

For a polymer to be utilised as a carrier and thus to be included in a medicinal product that is a solid solution, it must always be chemically stable, compatible with the drug and generally regarded as safe (GRAS). Furthermore, in order to develop efficient solid solutions, carriers are chosen with relation to the following three factors:

1.5.3.1. Drug-polymer miscibility

For a polymer to act as an efficient carrier, it must firstly be miscible with the drug, this would allow molecular dispersion of the drug with in the polymer and may also encourage drug-polymer interactions. Several mathematical models have been constructed to allow estimation of drug-polymer thermodynamic miscibility and interactions. The Flory-Huggins (FH) interaction theory (Flory, 1942), is one that uses melting point depression to predict the interaction parameter, x, using Equation 1.9 below. It accounts for the entropy and enthalpy of mixing between molecules with a large dissimilarity in molecular weight, such as polymer and drug in the case of solid dispersions.

$$\left(\frac{1}{T_m^{mix}} - \frac{1}{T_m^{pure}}\right) = \frac{-R}{\Delta H_{fus}}\left[\ln \emptyset_{drug}\left(1 - \frac{1}{m}\right)\emptyset_{polymer} + x\emptyset_{polymer}^2\right] \quad \text{Equation 1.9}$$

Where T_m^{pure} and ΔH_{fus} are the pure drug's melting point and enthalpy of fusion respectively; T_m^{mix} is the melting point of the drug when mixed with the polymer; m is the molecular volume ratio of a polymer molecule to a drug molecule; $\emptyset_{polymer}$ and $\emptyset_{drug}$ are the volume fractions of the polymer and drug respectively (Marsac *et al.*, 2009, Marsac *et al.*, 2006).

Another approach of predicting the drug-polymer miscibility is by calculating the Hansen solubility parameter, δ, from their chemical structures. This may be achieved by using the van Krevelen and Hoftyzer method according to equation 1.10 and 1.11 below.

$$\delta^2 = \delta_d^2 + \delta_p^2 + \delta_h^2 \quad \text{Equation 1.10}$$

Where the total solubility parameter (δ^2) is determined from the interactions between the dispersion forces (δ_d^2) and the polar interactions (δ_p^2), and hydrogen bonding (δ_h^2) of the functional group of the parent molecule divided by the molar volume (V). The units of the solubility parameters are $MPa^{1/2}$

$$\delta = \sqrt{\left(\frac{\sum F_{di}}{V}\right)^2 \left(\sqrt{\frac{\sum F_{pi}^2}{V}}\right)^2 + \left(\sqrt{\frac{\sum E_{hi}}{V}}\right)^2} \qquad \text{Equation 1.11}$$

Where (F_{di}), (F_{pi}^2) and (E_{hi}) are the group contribution for different components (dispersion forces, polar interactions and hydrogen bonding respectively) of structural groups that are reported in the literature at 25 ^{o}C. The drug-polymer interaction parameter (x) may then be calculated from the difference in the solubility parameters between the drug and the polymer. This can be estimated as follows:

$$x = \frac{V_0}{RT}(\delta_{drug} - \delta_{polymer})^2 \qquad \text{Equation 1.12}$$

Where (V_0) is the volume of the lattice site, (R) is the gas constant, and (T) is the absolute temperature.

1.5.3.2. Solubilization effect

The choice of carrier also depends on its suitability to act as a solubilizing agent. Although all of the most explored carriers in the past 3 decades (table 1.1) have been frequently reported to have drug solubilizing properties, there is a clear difference in the degree of solubilization between carriers that are high molecular weight polymers and low molecular weight carriers such as sugars. (Kaushal *et al.*, 2004). Polyethylene glycol (PEG) and polyvinyl(pyrrolidone) (PVP) are 2 of the most successful solubilizing polymers (Kaushal *et al.*, 2004) due to their inherent drug solubilization capacity which is built on their ability to interact with drug molecules via electrostatic bonds such as van der Waals and hydrogen bridges forming soluble drug-polymer complexes. However, drug-polymer interactions can vary depending on the chemical structures and the physiochemical properties of the drug and polymer, as well as the method of preparing the solid solution.

Table 1.1 Most successful solubilizing carriers explored in the past three decades in development of SD, PEG: poly(ethylene glycol), PVP: poly(vinyl pyrrolidone), FUR: furosemide, NSAIDs: non-steroidal anti-inflammatory drugs, CEL: celecoxib, PVP/VA: poly(vinyl pyrrolidone/vinyl acetate), HPMC: hydroxyl propyl methylcellulose, PVM/MA: poly(vinyl methyl ether/maleic anhydride) (Kaushal *et al.*, 2004, Papadimitriou *et al.*, 2012).

Solubilizing carrier	Drug
PEG	Griseofulvin, phenytoin, prednisolone, nortriptyline HCl, piroxicam, oxazepam, fenofi brate, ketoprofen, glyburide, nifedipine, carbamazepine, ibuprofen, zolpidem.
PVP	Griseofulvin, sulfathiazole, hydrochlorothiazide, carbamazepine, FUR, NSAIDs, mefenamic acid, azapropazone, glafenin, flotafenin, oxodipine, etoposide, benidipine HCl, atenolol, piroxicam, clofazimine, lonidamine, CEL.
PVP/VA	Carbamazepine, atenolol
HPMC	Benidipine, nilvadipine, albendazole
PVM/MA	Griseofulvin, clofazimine
Crospovidone	FUR
Croscarmellose Na	Itraconazole
Sorbitol	Prednisolone
Mannitol	Triamterene
Lactose	Nitrazepam
Urea	Ofloxacin
Chitosan	Nifedipine
Gelita Collagel*	Oxazepam
Egg albumin	Mefenamic acid

*Gelita Collagel is an enzymatically synthesised collagen hydrolysate (Jachowicz and Nürnberg, 1997).

1.5.3.3. Stabilization

Choice of carrier can also, greatly influence the shelf-life of a solid solution product by acting as a stabilizer (Khougaz and Clas, 2000, Kaushal *et al.*, 2004). Using long chain, and high T_g, polymers such as PVP as carriers, can increase the T_g value of an amorphous drug to be substantially higher (by ≥ 50 ^{o}C) than storage temperature (25 ^{o}C) (Kaushal *et al.*, 2004, Ikegami *et al.*, 2006, Khougaz and Clas, 2000, Raudonus *et al.*, 2000, Shamblin *et al.*, 1996, Zeng *et al.*, 2001). This in return gives more confidence in the physical stability of the product when stored at room temperature (Hancock and Zografi, 1997). In addition to increasing T_g values, PVP, unlike PEG, has repeatedly shown the ability to further stabilize amorphous drug by limiting their molecular mobility (Kaushal *et al.*, 2004, Yoshioka *et al.*, 1995, Matsumoto and Zografi, 1999a, Crowley and Zografi, 2003, Shamblin *et al.*, 1996, Shamblin and Zografi, 1999, Zeng *et*

al., 2001, Miyazaki *et al.*, 2004, Broman *et al.*, 2001, Khougaz and Clas, 2000, Karavas *et al.*, 2006b, Yuan *et al.*, 2014, Hosono *et al.*, 1980, Aso and Yoshioka, 2006, Matsumoto and Zografi, 1999b). This is done by forming strong and very specific drug-polymer interactions, such as hydrogen bonding and dipole induced dipole forces (Table 1.2) (Hosono *et al.*, 1980). As a result mobility of molecularly dispersed molecules is decreased and thus recrystallization is discouraged (Miyazaki *et al.*, 2004, Kaushal *et al.*, 2004, Broman *et al.*, 2001, Khougaz and Clas, 2000, Hosono *et al.*, 1980). A number of studies have even shown that the addition of a low content of PVP can substantially reduce the molecular mobility of nifedipine (Aso *et al.*, 2004), phenobarbital (Aso *et al.*, 2004), acetaminophen (Miyazaki *et al.*, 2004) and Indomethacin (Matsumoto and Zografi, 1999b) thus inhibiting recrystallization. This makes PVP a very desirable carrier as stabilizing the drug in its amorphous form has substantial effects on apparent solubility and the rate of dissolution (Kaushal *et al.*, 2004). Table 1.2 lists a number of published specific drug-carrier interactions for stabilization of amorphous drugs observed between PVP and a number of drugs.

Furthermore, one of the important factors to consider when choosing a polymer to use as a carrier is the molecular weight (Zeng *et al.*, 2001). An increase in molecular weight usually causes an increase in T_g of the polymer and therefore making it a more appropriate polymer to use for stabilizing drug in the amorphous form (Zeng *et al.*, 2001). On the other hand it is also important to note that the molecular weight is directly related to the intrinsic viscosity (Kaushal *et al.*, 2004), which has a great influence on the rate of drug release. A very high molecular weight polymer can introduce a high viscosity diffusion boundary layer around the solid dispersion particles containing the drug, and thus the release of drug would be diffusion controlled. A correlation was found between a reduction in the aqueous solubility of PVP and the increase in chain length. Therefore when choosing the molecular weight of PVP to use in the development of a solid solution, it is important to balance the need for stabilization and solubilization. PVP MW 10,000 for example, has shown to have a high aqueous solubility and dissolution rate as well as high stabilizing properties (Kaushal *et al.*, 2004).

Table 1.2 Drug-polymer interactions between PVP and a range of drugs. It is well known that PVP can reduce the crystallization process of many drugs (Aso and Yoshioka, 2006).

Drug	Chemical interaction	Remark
Ajmaline-PVP k15	-OH----O=C-	A dipole-induced dipole of a drug-polymer complex was formed, which enhanced the solubility of ajmaline (Hosono *et al.*, 1980).
Nabilone-PVP	OH----O=C-	Hydrogen bonding forming between nabilone and the chains of PVP stabilized the amorphous form of nabilone for 2 years (at 25 ^{o}C) (Thakkar *et al.*, 1977).
Indomethacin-PVP (K12, 17, 30, 90)	OH----O=C-	Hydrogen bonding forming between amorphous indomethacin and polymer chains, inhibited drug recrystallization at 30 ^{o}C for 20 weeks, using 5% w/w PVP only (Matsumoto and Zografi, 1999b).
MK-0591 (An investigational drug)-PVP K30	-COO^{-} Na^{+} -O=C=$^{+}$N-	Ion-dipole interaction resulted in higher *Tg* values than those predicted by Gordon-Taylor equation (Khougaz and Clas, 2000).
Probucol-PVP K30	OH----O=C-	Hydrogen bond complex formed between probucol and polymer, resulting in stabilization of the amorphous drug (Broman *et al.*, 2001).
Nifedipine-PVP k40	-NH----O=C	Hydrogen bonding between nifedipine and PVP helped in stabilizing the amorphous form of nifedipine (Aso and Yoshioka, 2006).
Acetaminophen-PVPK40	OH----O=C	Hydrogen bonding between drug and PVP prevented molecular mobility and hence limited crystallization (Miyazaki *et al.*, 2004).

1.5.4. Barriers to using solid solutions as pharmaceutical products

Despite the extensive research performed on solid solutions over the past decades and despite their much needed ability in enhancing the oral bioavailability of PWSDs, they are not broadly used in commercial products. Table 1.4 below includes some of the amorphous or partially amorphous products that have made it to the market. The lack of their usage as pharmaceutical products can be related to the following challenges:

1.5.4.1. Low physical stability

Physical stability referred to here, is the stability of the physical state at which the organic drug is intended to be dispensed in, for the life time of the product which is typically in the range of 2-3 years (Trasi *et al.*, 2014). Solid solutions are designed to

provide the drug in its amorphous state; therefore their physical stability is defined by the absence of the crystalline state of the drug (Craig *et al.*, 1999). Nevertheless, amorphous organic drugs are thermodynamically metastable, when compared to the crystal state (Craig *et al.*, 1999), and can revert back to the crystalline form when maintained in a temperature range where nucleation is thermodynamically and kinetically favourable (Trasi *et al.*, 2014, Baird *et al.*, 2010). This poses a problem, as the physicochemical properties of the crystalline form of a drug may be very different from the amorphous form (Baird *et al.*, 2010). Undergoing crystallization may therefore take away the enhancement of intrinsic solubility and dissolution rate seen with the amorphous state. As a result the medicinal product may no longer meet the required specifications of drug delivery. As described in earlier sections (1.1.3), crystallisation is greatly influenced by environmental conditions, such as temperature and humidity. This makes manufacturing, processing, packaging and storage to be steps with high risk of drug crystallisation, as it would be difficult to control and implement anti-crystallization environmental conditions, especially with large scale production (Kaushal *et al.*, 2004, Craig *et al.*, 1999, Vasconcelos *et al.*, 2007). In addition unit operations in manufacturing, such as size reduction, drying, dry and wet granulation and compression may induce mechanical, thermal or solvent related stress that may also lead to increasing the rate of crystallisation (Kaushal *et al.*, 2004). The high sensitivity of amorphous formulations to environmental conditions, the risk of high rate recrystallisation taking place and the effect it has on the shelf-life of amorphous pharmaceutical products makes them less attractive to pharmaceutical companies (Kaushal *et al.*, 2004).

The sensitivity of amorphous formulations to crystallisation does not stop at the manufacturing and storage stages, but also extends to the administration of the medicine, such as the duration of exposing the medicine to the ambient air once outside its packaging. For example, it is a common practice in many countries for pharmacies to repackage solid dosage form medicines, such as tablets and capsules, from their original blisters, and into an easily accessible compliance packages for geriatric patients (Gerber *et al.*, 2008, Gilmartin *et al.*, 2013, Tan and Kwan, 2014). Such packages do not provide environmentally controlled conditions, and therefore

increasing the risk of recrystallizing the drug. Physical stability is also at risk after ingesting the amorphous drug, as it was observed with many amorphous organic drugs, when solid solutions disperse in an aqueous solution, such as the luminal content, drug recrystallisation and precipitation may occur, therefore reducing the expected oral bioavailability of drug in the amorphous state. The physical stability of amorphous drugs is therefore undoubtedly the greatest barrier to using solid solutions as platforms for PWSD as marketable pharmaceutical products.

1.5.4.2. Chemical stability

The rate of chemical degradation of drugs is reported to be higher in the amorphous state than when in the crystalline state (Yu, 2001, Bhugra and Pikal, 2008). This has been attributed to the increase in surface area and the enhanced level of molecular mobility, which reduces the activation energy for solid-state chemical reactions. Furthermore the higher hygroscopicity of amorphous material in comparison to the crystalline form enhances the rate of degradation by mediating the drug and indirectly by increasing molecular mobility through the plasticising effects. The chemical stability of the amorphous form of quinapril HCL was determined to be lower than the crystalline form, in addition, it was found to correlate with increased molecular mobility at high temperatures (Kaushal *et al.*, 2004).

In addition, the chemical instability of amorphous drugs can further lead to undesirable drug-excipient interactions promoting instability. Although drug-polymer interactions are generally described as a favoured interaction, however in certain cases may come as a disadvantage, as strong binding and interaction between a PWSD and a polymer can retard the dissolution rate of the polymer through polymer swelling (Kaushal *et al.*, 2004). Studies with PVP, PEG, Renex^{TM} and β-cyclodextrin showed a decrease in the dissolution rate of the polymer due to strong drug-polymer interactions (Singh *et al.*, 1966, Gibaldi and Weintrau.H, 1968).

1.5.4.3. Lack of characterization tools

Although amorphous systems are not new to the pharmaceutical field, there is a lack of analytical tools that allow the quantification of amorphous content rather than crystalline content (Kaushal *et al.*, 2004, Shah *et al.*, 2006). The current analytical tools

that are typically used are designed to measure the amount of amorphous material in an otherwise crystalline sample, rather than the amount of crystalline in an otherwise amorphous material (Kaushal *et al.*, 2004, Shah *et al.*, 2006). This as a result can introduce a difficulty when undertaking quality control procedures on amorphous pharmaceutical products. Furthermore, the T_g value, which is one of the key characteristics of amorphous materials (Shah *et al.*, 2006), may differ depending on the analytical method used and the parameters implemented within the method (Tropin *et al.*, 2011). For example determining the T_g value using a diffraction scanning calorimetry can vary depending on the rate of heating and cooling (Tropin *et al.*, 2011, Kerc and Srcic, 1995).

1.5.5. Evaluation of solid solutions using model drugs

Novel solid solutions are evaluated for efficiency of physical stability and the enhancement of intrinsic solubility and dissolution rate, of water insoluble drugs, as part of research and development. To allow accurate evaluation, suitable model drugs must be used. Table 1.2 shows a wide range of model drugs that have been used to evaluate and determine the mechanism behind novel solid solutions. A suitable model drug must have a low water solubility (< 60 µg/mL), but preferably has an acceptable permeability (BCS class II), in which case an enhancement in solubility and dissolution rate would improve the drug's bioavailability. As 50% of currently used API's are categorised as class II of the BCS (Patil *et al.*, 2015), it is ideal for the model drug to be of this popular group.

In addition to water insolubility, there are a number of other physicochemical and chemical properties that, if present in the model drug, can allow a better evaluation of the solid solution. These include low physical and chemical stability, which will allow the stabilization by the solid solution platform to be more apparent. Similarly the drug should have low wettability, which as a result would also make the enhancement in dissolution rate more apparent. Using a model drug with a published UV and chromatographic analysis can also help in adapting analytical methods for the novel solid solution. Furthermore a model drug should be relatively cheap and easily

accessible for academic research, and has approved marketed formulation to allow novel formulations to be compared with the conventional marketed formulations.

1.6. Manufacturing solid solutions

Traditionally solid solutions were prepared using hot-melt extrusion (HME) processing, a technology that was first utilised in the plastic, rubber and food industry, but was quickly found to have great potential in the pharmaceutical industry in early 1970s (Patil *et al.*, 2015). In the pharmaceutical industry HME was applied as a continued process of a mechanical pressure on mixtures of polymeric materials and API's with a rotating screw. The temperature of the mixtures is raised above the T_g and/or melting temperatures of its components. In some systems, the mixtures are also passed through a high-pressure homogenizer, to achieve molecular dispersion of API in polymer (Patil *et al.*, 2015). The final products are solid solutions with uniform density and shape (Patil *et al.*, 2015), which may then be milled to reduce the overall particle size (Leuner and Dressman, 2000). HME, once established, was found to be less time consuming and more efficient than conventional pharmaceutical manufacturing processes, and thus was used as an alternative platform technology for manufacturing pharmaceutical dosage forms, such as tablets and capsules (Patil *et al.*, 2015). However, HME process was found to be limited to thermostable compounds with acceptable chemical and physical stability to the high temperatures, and in some cases high pressures, experienced during HME processes (Patil *et al.*, 2015).

As the HME process is limited to thermally stable drugs, a solvent evaporation method was adapted (Tachibana and Nakamura, 1965), where the polymer and the drug were dissolved in a common volatile solvent such as chloroform (Vasconcelos *et al.*, 2007, Hasegawa *et al.*, 2005, Lloyd *et al.*, 1999); The solvent was then removed by an evaporation process usually including vacuum drying (Karavas *et al.*, 2006a, Yoshihashi *et al.*, 2006, Wang *et al.*, 2005), moderate heating via the use of hot plate (Desai *et al.*, 2006), slow evaporation at low temperatures (Lloyd *et al.*, 1999, Yoshihashi *et al.*, 2006), using a rotator evaporator, a stream of nitrogen, spray-drying, freeze-drying and the use of supercritical fluids (Vasconcelos *et al.*, 2007).

1.6.1. Freeze-drying

Freeze-drying, also known as lyophilisation, has been widely used as a process to transform pharmaceutical injectable formulations into stable solid systems with long-term, unrefrigerated-storage stability (Craig *et al.*, 1999). The process has found considerable applications in the formulation of biological pharmaceutical products, as the stability of freeze-dried solid formulations is usually higher than the equivalent aqueous solution based formulation (McPhillips *et al.*, 1999, Tang and Pikal, 2004). In addition freeze-dried formulations have the advantage of ease of handling when it comes to shipping and storage (Pikal, 1993, Pikal, 1994). Nevertheless freeze-drying can be a costly process, and may require periods of many days to complete if the cycle is not optimised (Tsinontides *et al.*, 2004, Tang and Pikal, 2004). Furthermore, freeze-drying has been of high interest in the development of rapidly dissolving oral solid-dispersion formulations as it can results in amorphous solids which can enhance the intrinsic solubility and dissolution rate of water insoluble drugs (van Drooge *et al.*, 2006, McPhillips *et al.*, 1999, Vasconcelos *et al.*, 2007, Corveleyn and Remon, 1997). These factors therefore make freeze-drying an ideal method to manufacture stable solid solutions.

1.6.1.1. Stages of freeze-drying

Freeze-drying consists of 3 stages: Firstly the freezing stage where by the majority of water present in the formulation crystallises at temperatures below 0 ^{o}C typically in the range of -20 ^{o}C to -50 ^{o}C (Tang and Pikal, 2004). This then is followed by a primary drying stage where the ice present is removed by sublimation, this is performed under vacuum pressure which can vary from 0.06 mbar-0.26 mbar (Pikal *et al.*, 1984), and at a temperature range, known as the temperature safety margin, 2-5 ^{o}C below the macroscopic collapse temperature (T_c) of the formulation (Tang and Pikal, 2004). T_c is the temperature above which the freeze-dried product loses macroscopic structure and therefore collapses during freeze-drying. T_c is estimated to be 2 ^{o}C higher than the primary glass transition temperature (T'_g) of the freeze concentrated amorphous matrix (Mackenzie, 1966). Finally the secondary drying stage, whereby water is desorbed from the sample, it is usually performed at elevated temperature and low

pressure (Tang and Pikal, 2004). There are many excellent papers covering the freeze-drying of pharmaceuticals (Pikal, 1993, Pikal, 1994, Pikal *et al.*, 1984, Pikal and Shah, 1990, Pikal and Shah, 1997, Tang and Pikal, 2004, Tsinontides *et al.*, 2004). A review of these papers informed the development of the freeze-drying cycles reported later in the thesis. This stage by stage review is given below:

1.6.1.1.1 Freezing

Freezing is an efficient desiccation step where by most of the water, ≥ 99% v/v, is separated from the solutes, which in this case are drug and excipients, and leaving behind a very concentrated solutions termed "freeze concentrate" (Tang and Pikal, 2004). The typical average water content of freeze concentrate is ≤ 20% w/w (Tang and Pikal, 2004), which is equivalent to ≤ 1% v/v of the total water that was present in the feed solution. Freeze concentration of the remaining solution is a crucial factor to consider when dealing with biological formulations, as this often induces destabilizing stresses such as pH shifts and aggregations. Therefore, the optimal choice of buffer and or surfactants is essential (Tang and Pikal, 2004). The temperature at which the system undergoes a primary glass transition (T'_g) is essential to note, as the product must be kept below this temperature for the whole duration of the primary drying stage. Furthermore the rate of cooling is also an important factor to control, as slow cooling rate (typically > 0.5 ^{o}C/min) can result in the growth of large ice crystals, while this would increase the rate of sublimation in the primary drying stage, it has the potential to increase destabilizing stress, as it prolongs the freezing time, where solutes exists in freeze concentrate (Heller *et al.*, 1999b, Heller *et al.*, 1999a, Tang and Pikal, 2004). Furthermore, this can lead to phase separation and thus crystallisation of amorphous solute, therefore in particular cases defeats the purpose of using freeze-drying to produce an amorphous material (Izutsu *et al.*, 1997, Tang and Pikal, 2004). Rapid cooling using a pre-cooled shelf of -80 ^{o}C or cooling with liquid nitrogen results in small ice crystals, it requires longer periods to sublime and is uneconomical (Jiang and Nail, 1998). A moderate cooling rate of 1 ^{o}C/min has been reported to be a good compromise (Tang and Pikal, 2004). It was reported that once the sample has reached the required temperature, it must be kept for a sufficient length of time (typically 1h

per 1cm depth fill) to allow for all the solution to transform into solid (Tang and Pikal, 2004).

1.6.1.1.2 Primary drying

Primary drying requires the longest period out of all three stages and so it is the most important parameter to optimise. The rate of mass removal is increased by altering the chamber pressure (P_c) which impacts both the temperature and mass transfer (Tang and Pikal, 2004) as presented in equation 1.13 below:

$$\frac{dm}{dt} = \frac{(P_{ice} - P_c)}{R_p + R_s} \qquad \text{Equation 1.13}$$

Where $\frac{dm}{dt}$ is the rate of sublimation (g/h per vial if applicable), P_{ice} is the equilibrium vapour pressure of ice at the sublimation interface temperature (measured in units of Torr), R_p and R_s are the dry layer and the stopper resistance, respectively, to the ice vapour transporting from the sublimation interface (Torr· h/g) (Pikal *et al.*, 1983, Tang and Pikal, 2004). Choosing the right P_c is critical as it impacts on the products temperature $(\mathrm{T_p})$, thus a compromise between high sublimation rate and homogenous heat transfer, to provide sublimation with the required energy is needed. Equation 1.14 below may be used to choose the optimal chamber pressure (Tang and Pikal, 2004, Pikal *et al.*, 1984).

$$P_c = 0.29 \cdot 10^{(0.019 \cdot \mathrm{T_p})} \qquad \text{Equation 1.14}$$

Where P_c is in Torr and T_p in °C Furthermore, rate of sublimation can be related to heat transfer (dQ/dt) using Equation 1.15, where ΔH_s is the heat of ice sublimation (cal/g).

$$\Delta H_s \cdot \frac{dm}{dt} = \frac{dQ}{dt} \qquad \text{Equation 1.15}$$

Tang and Pikal (2004) reported Equation 1.15 as a tool to estimate the duration of the primary drying stage (Tang and Pikal, 2004). In addition to the theoretical approach, the endpoint of primary drying is typically indicated by the absence of water vapour in the freeze-drying chamber in addition to $\mathrm{T_p}$ reaching the shelf temperature (Pikal *et al.*, 1984, Tang and Pikal, 2004).

1.6.1.1.3 Secondary drying

Removing residual water from an amorphous product (typically 5-20% w/w depending on the formulation (Tang and Pikal, 2004)) by desorption requires elevation in temperature. It is crucial to do so at a slow rate (typically 0.1 or 0.15 ^{o}C/min), as a fast temperature ramp might cause the collapse of the amorphous product. It is vital to stay below the gradually rising T_g value of the product, but also to maintain a steady ramp to reach a relatively high temperature (typically 40 ^{o}C) and to maintain at such a temperature for a period of 3-6h (Tang and Pikal, 2004). Higher temperatures induce faster rate of water desorption. Therefore, gradually raising the temperature, while avoiding the product's temperature rising above its T_g, can reduce the duration of the secondary drying stage and improve its efficiency (Pikal *et al.*, 1990). Secondary drying is usually stopped when the water content is ≤ 1% w/w. This ensures optimal freeze-dried cake stability (Tang and Pikal, 2004).

1.6.1.2. Challenges and limitations of using freeze-drying to produce solid solutions to enhance dissolution

1.6.1.2.1 Stability of feed solutions

One of the main challenges with utilizing freeze-drying as a method of manufacturing stable amorphous drugs is to overcome the destabilizing stress induced by the creation of freeze concentrate at the freezing stage (Tang and Pikal, 2004, Heller *et al.*, 1999b, Costantino and Pikal, 2004). These include sharp increase of solute concentration which enhances solute-solute interactions leading to aggregation and precipitation; sharp change in pH of solution due to crystallization of buffer, a very large increase in ionic strength and, in the case of biopharmaceuticals, denaturation of proteins (Tang and Pikal, 2004, Costantino and Pikal, 2004). Freeze related stress can be overcome by incorporating specific stabilizing excipients known as cryoprotectants. Examples of cryoprotectants include sucrose, trehalose, sorbitol, mannitol and PEG (Costantino and Pikal, 2004). Many hypothesis were developed to describe the mechanism by which cryoprotectants function, the mechanism that seems most applicable to all known cryoprotectants is the preferential exclusion mechanism (Arakawa *et al.*, 2001). This describes the co-solute cryoprotectants to create a thermodynamically unfavourable

situation, which as a consequence prevents the denaturation of proteins (Arakawa *et al.*, 2001).

Additionally, physical and chemical degradation may also occur during the drying stages (Bhugra and Pikal, 2008), such degradation can lead to sample collapse and hence the crystallization of amorphous drug. Several excipients, known as lyoprotectants, may be incorporated into the formulation to enhance the physical and chemical stability of the drug at the drying stages of the process; via the formation of stabilising hydrogen bonds (Arakawa *et al.*, 2001). These Lyoprotectants include small carbohydrate molecules such as sucrose (Roy and Gupta, 2004).

1.6.1.2.2 Low aqueous solubility

An obvious obstacle to freeze-drying organic drugs with low aqueous solubility is the need to work with large volumes of feed solutions and therefore large amounts of ice to sublime. This will not only be expensive and time consuming but also impractical. Many have therefore, resulted to freeze-drying using organic solvents either alone or as a co-solvent (Teagarden and Baker, 2002a, Wittaya-Areekul *et al.*, 2002, Oesterle *et al.*, 1998, Ni *et al.*, 2001, Teagarden and Baker, 2004). Solvents used in the freeze-drying process must have a number of critical physical and chemical properties, including a freezing point between 30 to -10 ^{o}C and relatively high vapour pressure at low temperatures (typically higher than vacuum pressures 0.06 mbar - 0.26 mbar (Pikal *et al.*, 1984)). One of the most popular organic solvents used in this capacity is *tert*-butanol (Ni *et al.*, 2001, Vessot and Andrieu, 2012). CAVERJECT® is one of the marketed pharmaceutical products which utilized *tert*-butanol in freeze-drying (Teagarden and Baker, 2002a).

1.6.1.2.3 Low density

Finally producing a hard solid oral dosage form via freeze-drying may be a challenge especially when the solid solution consists of low density organic polymer (Leuner and Dressman, 2000). Making a tablet out of such material may not be practical. In addition the process of tableting can exert thermal and physical stress that may induce crystallisation. As a solution and to keep the freeze-dried porous structure intact, one may result to freeze-drying a formulation while inside a degradable vessel that can be

orally administered and can withstand the temperatures of freeze-drying. A standard gelatin capsule may be fit for such a role.

1.7. Rapid buccal delivery

Another approach to improving the oral bioavailability of water insoluble drugs is through the use of rapid buccal delivery systems (Kassem *et al.*, 2014, Badgujar and Mundada, 2011, Lam *et al.*, 2014). This is mainly because the buccal route bypasses the first pass metabolism and drug degradation or metabolism in the gastrointestinal system (Lam *et al.*, 2014). Furthermore, the high blood flow and relatively high permeability of the oral mucosa allows a quick onset of action to be achieved (Lam *et al.*, 2014). This makes the buccal route ideal for when a rapid clinical effect is required (Lam *et al.*, 2014).

Traditional oral solid dosage forms such as capsules and tablets share a common disadvantage of difficulty in swallowing which is thought to affect patients in all age groups. A study by (Sastry *et al.*, 2000) has shown that dysphagia, or difficulty in swallowing is a problem encountered by approximately 35% of the general population as well as 30-40% of elderly institutionalized patients, and 18-22% of all persons in long-term care facilities (Fu *et al.*, 2004). It has been repeatedly published that paediatric and geriatric patients alongside bedridden or developmentally disabled patients; patients with persistent nausea and patients with limited fluid intake, due to their condition, as well as travelling patients with limited access to water are all in need of a new dosage form that can readily disintegrate or melt once placed inside a patient's mouth (Dobetti, 2001, Seager, 1998). This in return will eliminate the faced difficulties with swallowing a solid dosage form as a whole and thus enhance patient compliance.

1.7.1. Orally fast disintegrating tablets

In the past two decades a great deal of attention has been drawn to a new form of solid dosage form commonly known as fast disintegrating tablets, which has the ability to quickly dissolve, disintegrate or melt inside a patient's mouth without the need of

water intake (Fu *et al.*, 2004). Such tablets are also known as fast dispersing, rapid dissolve, rapid melt, quick disintegrating and/or instant melt tablets (IMTs), in relation to the properties of the tablet and thus the time it requires to fully disperse or disintegrate (Fu *et al.*, 2004). The European pharmacopeia has adopted the term orodispersible tablet for all tablets that disintegrate or disperse inside the mouth with in a period equal to or less than 3 min or alternatively, disintegrate within 3 min under the USP disintegration test. Nevertheless a good FDT should disintegrate within one minute of administration to enable rapid drug absorption (Fu *et al.*, 2004), an additional advantage of FDTs is the possibility of a pre-gastric drug absorption and thus avoiding the first-pass metabolism which in return can induce a rapid drug therapy intervention and enhance the drug's bioavailability (Fu *et al.*, 2004). Furthermore FDTs must also share all of the advantages of using the conventional oral solid dosage form, such as accurate dosing, easy manufacturing, ease in handling and transport in addition to easy handling by patients (Dobetti, 2001, Habib *et al.*, 2000, Seager, 1998, Fu *et al.*, 2004).

Unlike the conventional tablets, FDTs are required to disintegrate and sometimes dissolve in a very short period of time and in the presence of a limited amount of water despite the large difference in performance. Listed below, are each of the factors that contribute to the overall performance of the FDTs (Fu *et al.*, 2005).

1.7.2. Disintegration and dissolution.

As the disintegration fluid is provided by the patient's saliva, FDTs are presented with a challenge of disintegrating in a very limited volume of solvent. On average the minimum salivary volume, being the residual volume in the mouth after swallowing, is 0.8 mL. While the maximum salivary volume (Vmax), being the volume in the mouth just before swallowing, is 1.1 mL (DiSabato-Mordarski and Kleinberg, 1996). Furthermore, when aiming to deliver an emergency drug via the buccal absorption, FDTs must have rapid dissolution as a vital property. The key properties for FDTs are therefore fast absorption of water and rapid dissolution, such process is usually expected to take place in less than one minute.

1.7.3. Physical properties of FDTs

To ensure fast disintegration and dissolution, FDTs should maintain a very porous structure. Methods and parameters of manufacturing have great influence over pore diameter, freeze-dried ODT formulations for example, produce tablets with more porous structures than any other of the methods used in manufacturing FDTS, such as compressions. However the pH of the feed solution used in freeze-drying, has a further effect on the pore diameter. A study by (Jones *et al.*, 2011) has shown that adjusting the pH of the feed solutions to approximately 8, may be done by incorporating sodium bicarbonate in the formulation, can improve the average pore diameter from 90 µm to 140 µm, while the wall thickness was seen to reduce from 40 µm to 20 µm, therefore making the structure of the tablet more porous. Nevertheless porosity could have a negative effect on the mechanical strength of tablets, otherwise known as tablet's hardness (Shang *et al.*, 2013), which also is greatly influenced by the method and parameters of manufacturing (Shang *et al.*, 2013). For industrial convenience, tablets should have hardness strength of 5 to 8 Kg/cm^3 to survive packaging processes, the pressure of being pushed through the foil of the conventional blister packages and the physical handling of the tablet by patients. One way of overcoming the friability of porous tablets is to design a special packaging.

1.7.4. Stability

FDTs usually consist of highly water soluble excipients to enhance its ability to absorb water and thus disintegrate and dissolve faster, this in return makes FDTs very sensitive to moisture and thus can shorten their shelf life considerably (Malik *et al.*, 2012b). A typical shelf life of solid dosage form is 2 to 5 years (FDA, 2004). To ensure an acceptable shelf life, FDTs should be packaged by hermetically sealing under inert gas in protective blisters, impervious to air or any other gas under normal handling and shipment, following the World Health Organization (WHO) and International conference of harmonization (ICH) guidelines for packaging pharmaceutical products (WHO, 2002, ICH, 2009).

1.7.5. Drug taste and properties.

One of the critical factors to patients' acceptance and thus compliance is taste (Badgujar and Mundada, 2011). As FDTs are to be disintegrated and/or dissolved inside the patient's mouth, it is important to ensure that while dealing with a bitter tasting drug, an ideal taste-masking technology is implemented (Badgujar and Mundada, 2011). Nevertheless, it is also critical to ensure that the physiochemical properties of the drug and that of taste-masking compounds are compatible with the tablet's properties (Badgujar and Mundada, 2011). This includes drug's solubility, crystal morphology, particle size, hygroscopicity, compressibility and bulk density, as each may have an impact on the tablets final characteristics (Fu *et al.*, 2004).

1.7.6. Formulation process for manufacturing FDTs

There are several different commercial technologies for manufacturing FDT. Table 1.4 below presents an example of some of the commercial products that use FDT manufacturing technologies. Although they all, to some extent, meet the special requirements of the FDTs, none provide all desired components of an optimum FDT, specially the requirement of hardness and porosity. The current technologies have been reviewed in the following literature (Dobetti, 2001, Fu *et al.*, 2004, Habib *et al.*, 2000, Sastry *et al.*, 2000). Although the FDT manufacturing technologies differ from one another, they can be grouped under the general producing methods table 1.3; (Fu *et al.*, 2004). The most dominant ones are: freeze-drying, molding and compressions. While freeze-drying produces porous tablets with instant disintegration (2-10sec) and enhanced dissolution (Fu *et al.*, 2004), they lack mechanical strength and are very sensitive to humidity and hence require special packaging to ensure physical stability. Moreover, freeze-drying is a more expensive manufacturing method, making it less profitable for the pharmaceutical industry (Fu *et al.*, 2004). Compression on the other hand is an ideal choice for the pharmaceutical industry, as it simply utilises standard tabletting equipment and materials. However the standard compression procedures used in tabletting are not designed to FDT specifications, as a result, FDTs produced by compression take much longer to disintegrate. This may not be a great problem in general, but may act as a barrier when it comes to the delivery of emergency medicine.

Several strategies have been implemented in the standard tabletting method in order to produce higher porosity while maintain the tablets strength. One of the strategies included several granulation methods that are thought to be more suitable for making FDT. These include wet granulation, dry granulation, spray drying and flash heating methods. Another was looking at varying the compressing pressure and applying after treatments (Fu *et al.*, 2004).

Table 1.3 Summary of technologies used to manufacture FDTs (Fu *et al.*, 2004).

Method	Technology	Company
Freeze-drying process	Zydis®	Cardinal Health
	Quicksolv	Janssen Pharmaceutica
	Lyoc	Pharmalyoc
	NanoCrystal	Elan
Tableting process	FlashDose	Biovail (Fuisz)
	OraSolv /DuraSolv	Cima Labs
	WOWTAB	Yamanouchi
	Fast Melt	Elan Corp.
	Flashtab	Ethypharm
	AdvaTab /Ziplets	Eurand
	OraQuick	KV Pharmaceutical
	Pharmburst	SPI Pharma
	Frosta	Akina

Table 1.4 Examples of Marketted predominantly amorphous FDTs with details on drug solubility, BCS class and the technology used to manufacure the FDT (Fu *et al.*, 2004).

Brand name	Application	Drug	Solubility of drug in water (µg/mL)	Temp at which solubility was determined (^{o}C)*	BCS class	Company	FTD Technology	Ref
Claritn® RediTabs®	Antihistamine	Loratadine	3.31	25	II	Schering Corporation	Zydis®	(Popović *et al.*, 2009)
Tempra Quicklets Tempra Firs Tabs	Analgesic	Paracetamol	12.65 x 10^{3}	20	III	Bristol-Myers Squibb	OraSolv®	(Chahiyan *et al.*, 2014, Nainar *et al.*, 2012)
Excedrin® QuickTabs	Pain reliever	Acetaminophen also known as Paracetamol	12.65 x 10^{3}	20	III	Bristol-Myers Squibb	Quicksolv®	(Nainar *et al.*, 2012, Chahiyan *et al.*, 2014)
Nurofen® Flashtab®	NSAID	Ibuprofen	21.0	25	II	Boots Healthcare	Flashtab®	(Yalkowsky and Dannenfelser, 1992)
Hyoscyamine Sulfate ODT	Anti-ulcer	Hyoscyamine Sulfate	3.56	20 in pH 9.5	II	ETHEX Corporation	OraQuick	(Maynard, 1997)
Cibalginadue FAST	NSAID	Ibuprofen	21.0	25	II	Novartis Consumer Health	Ziplets™	(Yalkowsky and Dannenfelser, 1992)

* In water if not specified.

1.8. Research aim and objectives:

The aim of the research reported here was to develop two novel freeze-dried formulation platforms. The aim of the first formulation platform was to enhance the release of PWSD's, and the aim of the second was to enhance the rapid disintegration of the formulation matrix, to release soluble drugs in biorelevant conditions to the buccal cavity. The purpose of investigating these two platform designs was to gain better insights into the underpinning science and applications of freeze-dried formulations destined for the oral & buccal delivery routes.

1.8.1. Research Objectives

1) To develop a simple freeze-dried formulation of a poorly water-soluble model drug by exploring the relationship between the concentration of the ingredients and the quality of the freeze-dried material.

2) To transfer this design from ampoules into capsules.

3) To test the physical & chemical stability of these formulations.

4) To investigate the dissolution rates and compare to the marketed formulation.

5) To develop a fast disintegrating tablet that contains a model drug used as an emergency medicine.

6) To develop a simple buccal dissolution model to test the new design.

7) To manufacture the novel FDT under GMP and prepare this for a clinical trial.

Chapter 2. Production and characterization of freeze-dried nifedipine solid solutions

The following chapter reports the investigation of the freeze-drying method used for the production of solid solutions, containing the class II BCS drug nifedipine dispersed in a solubilizing and stabilizing polymer PVP. The effects of varying the w/w % of drug in polymer on the physical characteristics of the freeze-dried materials are also described in detail.

2.1. Introduction

Patients are more accepting of medications delivered by the oral rout, thus making this delivery route more favourable for patients with regards to compliance(Andrews, 2007, Marwaha *et al.*, 2010, Jin *et al.*, 2008). Moreover, pharmaceutical companies are interested in oral solid dosage forms, as they are more economically effective (Rasenack and Muller, 2002). Nevertheless for a drug to be absorbed into the circulatory system, it must first be in solution. Drugs with high permeability but low water solubility and dissolution rate, i.e. class II BCS drugs, have a limited oral bioavailability (Leucuta, 2014).

Several techniques have been developed over the years to overcome the challenge of formulating PWSD's into solid dosage forms (Pouton, 2006). One of the most effective techniques in enhancing the intrinsic solubility and dissolution rate is to molecularly disperse the drug in a solubilizing carrier, either by a heat melt or a solvent evaporation technique, and therefore rendering the drug into its amorphous form (Kaushal *et al.*, 2004). However, despite the amorphous form's high efficiency in enhancing solubility and dissolution rate, it is not widely used in the pharmaceutical industry (Kaushal *et al.*, 2004, Van den Mooter, 2012). This is due to the lack of a robust, manufacture convenient, method of rendering PWSD's into amorphous materials, without the exposure to devitrification inducing conditions, such as excess heat or humidity (Kaushal *et al.*, 2004).

2.1.1. Freeze-drying

One of the methods that have attracted the interest of many researchers, in the field of solid dispersions, is freeze-drying (Vessot and Andrieu, 2012). Which unlike other methods of producing solid dispersions, it does not expose samples to high temperatures and therefore lowers the possibility of inducing thermal based chemical degradation and in some instances crystallization (Craig *et al.*, 1999, Bhugra and Pikal, 2008). Freeze-drying is widely recognized by the pharmaceutical industry as an important preservation technique that can enhance the shelf life of pharmaceutical products (Craig *et al.*, 1999, McPhillips *et al.*, 1999, Tang and Pikal, 2004). Modern freeze-drying was developed in the second world war as a solution of overcoming the instability of serum, which was spoiling upon transport from the United States to Europe due to lack of refrigeration during transport (Meryman, 1976). The process of freeze-drying allowed serum to be rendered chemically stable and viable, without having to be refrigerated. More importantly, freeze-dried serum was very easy and fast to hydrate, which makes freeze-drying an effective technique to use in developing solid oral dosage forms intended for rapid hydration and therefore dissolution.

2.1.1.1. Tert-butanol

The conventional solvent used in freeze-drying feed solutions is water, this puts freeze-drying at a great disadvantage when dealing with PWSDs. Depending on the solubility of the drug, large amounts of ice may need to be sublimed for very little mass of drug in the final product, which is not cost effective and hence unattractive to the pharmaceutical industry. Recent research has shown that organic solvents may also be used in combination with, or in place of water (Srinarong *et al.*, 2010). One of the most successful organic solvents that have been used in freeze-drying is tert-butanol (TBA). The reason behind its success is the favourable physicochemical properties of TBA. TBA has a convenient freezing point of 24 ^{o}C (Teagarden and Baker, 2002b), this is beneficial for freeze-drying as maintaining TBA based feed solutions under freezing point is possible using the standard freeze dryers used for water based feed solutions. Additionally high freezing points can help with reducing the chance of sample collapse (Vessot and Andrieu, 2012). Furthermore, TBA has a high vapour pressure of 35.72 mbar at 20 ^{o}C (Teagarden and Baker, 2002b). High vapour pressure leads to faster

sublimation (Vessot and Andrieu, 2012), this makes TBA a highly appropriate solvent to use in the process of freeze-drying. Not only is TBA a good solvent for water insoluble drugs, but it is also freely miscible in water. This is an important advantage as it allows water to be used as a co-solvent with TBA, to allow the mixing of TBA insoluble carriers with a water insoluble drug. Nevertheless commonly used water soluble carriers, such as PVP, are found to be freely soluble in TBA (Vessot and Andrieu, 2012).

A major disadvantage to using TBA is its toxicity (McGregor, 2010). TBA is absorbed rapidly upon inhalation or oral ingestion and is then distributed to all tissues around the body. The elimination of TBA from blood is a slow process with half-life being dependent on the dose. Metabolism of TBA in the body is mostly by oxidation through 2-methyl-1,2-propanediol to 2-hydroxyisobutyrate, which are the main metabolites found in urine (NSF-Toxicology-Services., 2003). Conjugation can take place, which leads to the presence of acetone in urine at high doses. Although a single dose of TBA has a low systemic-toxicity, it is however an irritant to skin and eyes. Large oral doses cause ataxia while repeated small exposures may induce dependence. The maximum accepted oral reference dose published by the NSF international is 1.0 mg/kg-day (NSF-Toxicology-Services., 2003). Studies on rats show the target organs for TBA's toxicity are the kidney and urinary bladder (NSF-Toxicology-Services., 2003).

Using TBA as a solvent in the production of a solid oral dosage form may therefore introduce a health risk. However, considering that the industrial standard of residual solvent after freeze-drying is ≤ 1.0 %, the expected content of TBA to reach a patient is much lower than the maximum accepted oral reference dose published by the NSF international. Additionally, several authors found TBA or TBA/water freeze-dried systems to be useful in preparing clinically acceptable medicinal products on a large scale (Li and Deng, 2004, Cui *et al.*, 2006).

2.1.1.2. Freeze dryers

Freeze dryers are instruments that subject feed solutions to controlled conditions of temperature and pressure, in order to optimise the rate of sublimation. While maintaining the same principles, freeze driers have greatly developed over the past few years, making the process of freeze-drying more practical and cost effective for

large scale manufacture (Tsinontides *et al.*, 2004). Many university laboratories however use bench top freeze dryers for development purposes. A bench top freeze dryer, such as Lyotrap from LTE scientific, provides the bench top conditions of freeze-drying which are low temperature (-50 to -40 ^{o}C) and pressure (≥0.1 mbar). Such bench top or laboratory freeze dryers are commonly used for developing new formulations (Crum *et al.*, 2013, de Waard *et al.*, 2008). Such freeze-drying cycles may then be transferred into large scale production freeze dryers (Kuu *et al.*, 2005).

The structure of a typical bench top freeze dryer (figure 2.1), for example the Lyotrap, consists of a condensing chamber (figure 2.1 a) which is a cylindrically shaped metal chamber (18.0 cm in diameter and 35 cm in length) located to the bottom of the freeze-drying shelf (FDS) (figure 2.1 c), on which samples are placed to be freeze-dried. The walls of the condensing chamber may be set to -55 ^{o}C using an inbuilt cooling unit. The condensing chamber is designed to act as a trap for all solidified solvent that sublimes from the samples while freeze-drying.

The freeze-drying shelf (FDS) (figure 2.1 c) is cooled by conduction as it is in contact with the walls of the condensing chamber. Figure 2.1 illustrates how the FDS (diameter of 17.7 cm, thickness of 6 mm) stands on three metal rods (40 cm in height), which extend to the bottom of the condensing chamber. The position of the FDS is adjustable with regards to height, this gives some manipulation over the initial shelf temperature prior to pulling a vacuum. For example, if the samples are required to be introduced to FDS of a lower temperature, i.e. closer to the condensing chamber's temperature, the FDS is simply lowered down to be closer to the condensing chamber.

The chamber located directly above the condensing chamber (figure 2.1 b) is the drying chamber at which samples are freeze-dried. This chamber consists of a see-through pressure resistant acrylic cylinder (26.6 cm in diameter and 30.5 cm in length) that is situated directly on top of the condensing chamber. The drying chamber is partially separated from the condensing chamber by the FDS, which contains sufficient number of holes (0.5 cm in diameter) to allow free movement of sublimed solvents from the drying chamber to the condensing chamber. Sublimation of solidified solvent

in samples is enhanced by creating a high vacuum in both chambers, this is achieved by connecting the condenser chamber to a vacuum pump (Fig 2.1 f-h).

Simply by assembling the different parts of the set-up illustrated in figure 2.1, both the drying and condensing chambers become sealed, preventing external air from entering the chambers. However, the draining valve (figure 2.1 i), which is connected directly to the condensing chamber, may allow air flow into the freeze-drying chambers if opened. To allow the build-up of vacuum inside the freeze-drying chambers, the draining valve must be sealed and the vacuum pump must be turned on. This set-up (figure 2.1) is designed to reduce the temperature of the condensing chamber to a minimum of -55 ± 5 ^{o}C (measured via a built in digital thermometer). In addition the vacuum pump used with the setup in figure 2.1 is designed to reduce the pressure inside both the drying chamber to a minimum of 0.03 mbar (± 0.002 mbar) (measured via a built in digital pressure meter). However, the achievement of such conditions may be subject to the size of sample batch as well as the physicochemical properties of the solvent to be removed such as vapour pressure and melting temperature.

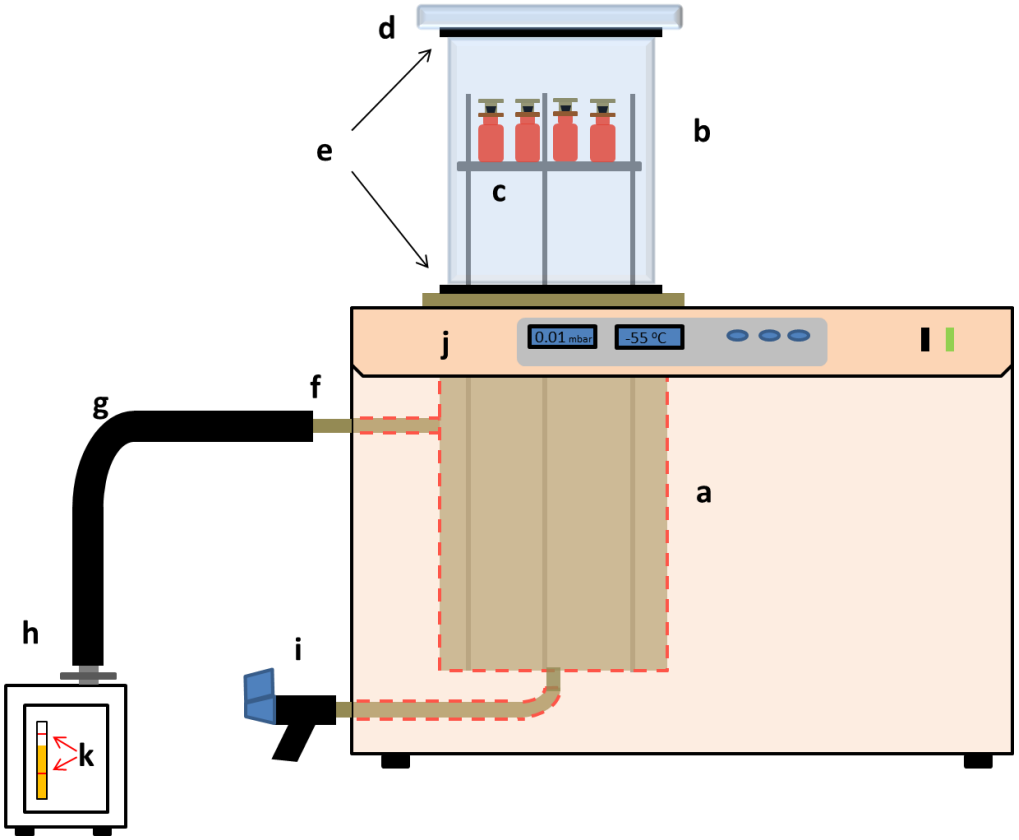

Figure 2.1 Structural diagram of the Lyotrap freeze dryer. The structure of the lyotrap is based on LTE Lyotrap operating instructions (Ltd, 2014). This diagram was created using Microsoft PowerPoint.

2.1.1.3. Freeze-drying accessories

Commonly freeze-drying feed solutions are held in freeze-drying vials (figure 2.2). Such vials can be designed to allow practical packaging of freeze-dried formulations while maintaining an efficient freeze-drying process by ensuring a sufficient surface area, allowing sublimation to undergo at a cost effective rate (Hibler *et al.*, 2012). The design and thickness of vial walls ensures good conductivity, allowing sufficient heat flux, which is vital for the process of sublimation (Hibler *et al.*, 2012). Freeze-drying vials come with useful accessories such as rubber stoppers that prevent the escape of large particles during freeze-drying whilst allowing sublimed solvent to be freely removed (figure 2.2 a). The same rubber stopper may be used to temporary seal the vial, at the end of a freeze-drying cycle, to prevent water vapour in ambient atmosphere from entering the vial (figure 2.2 b) (Barbaree *et al.*, 1985). This is very important as water vapour can greatly influence the physical and chemical stability of freeze-dried products (Craig *et al.*, 1999). Finally for long term storage, a metal cap may be crimped or screwed on top of the stopper rubber to ensure the vial is absolutely sealed (Barbaree *et al.*, 1985).

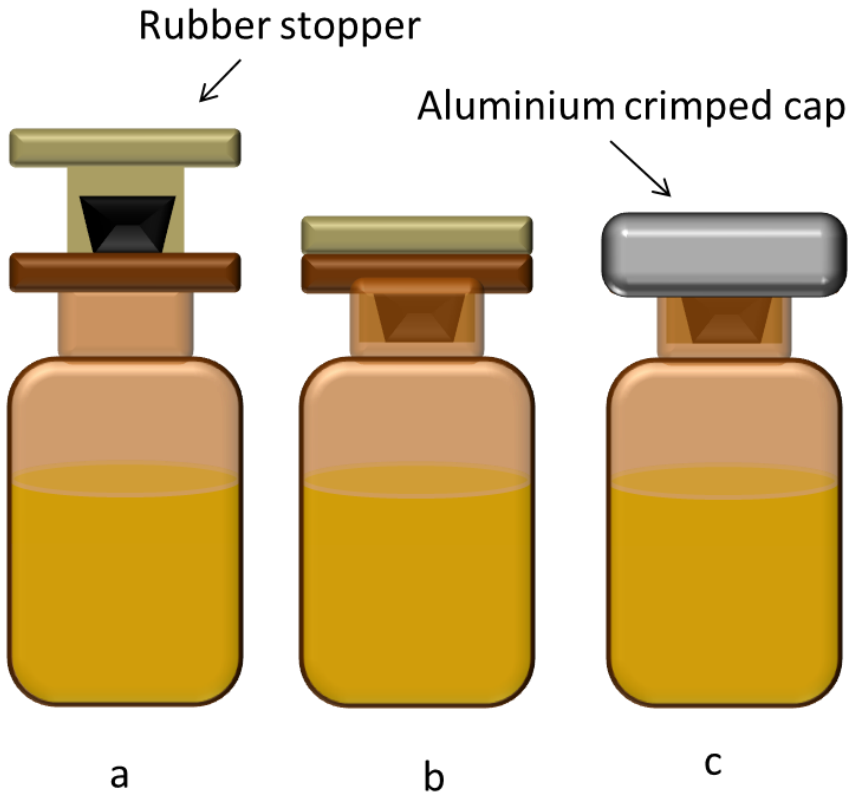

Figure 2.2 Freeze-drying vial in different closure positions. A typical volume of feed solution per vial is 2 mL. This diagram was created using Microsoft PowerPoint.

2.1.1.4. Nifedipine

To investigate the enhancement in drug solubility, dissolution rate, physical and chemical stability by a freeze-dried solid solution platform, a representative model for water insoluble drugs, nifedipine, was chosen to be incorporated into the formulation platform.

Nifedipine (4-(2-nitrophyenyl)-2,6-dimethyl-3,5-dicarbomethoxy-1,4-dihydropyridine) Figure 2.3 (Ali, 1989), which was used as a model for water insoluble drugs in this research, is a class II BCS drug that is widely used in the treatment of cardiovascular disorders. It was first synthesised in 1966 by F. Bosset in search for orally active drugs for the treatment of coronary insufficiency, following its introduction as nifedipine (Adalat) in 1975, it since became one of the major cardiovascular drugs (Ali, 1989). The synthesis of nifedipine is based on the classical Hantzsch 1,4-dihydropyridine synthesis, i.e. the reaction of 1 mole 2-nitro-benaldehyde with 2 moles methyl acetoacetate and 1 mole concentrated aqueous ammonia in refluxing methanol which leads to the formation of nifedipine (Ali, 1989). Although nifedipine has a high permeability, it is known to often show low bioavailability after oral administration, due to being practically insoluble in water (0.0058 g/L at pH:4, 0.0056 g/L at pH:7,0.0078 g/L at pH:9 and 0.006 g/L at pH:13)(Ali, 1989), therefore making nifedipine a good model for hydrophobic drugs. The reason nifedipine is practically insoluble in water, is because of its flat molecular shape which allows close and organised stacking of molecules into high energy lattice crystals. The presence of delocalised benzene rings introduces pi to pi stacking which holds the crystal lattice together and leads to a high melting point, for nifedipine (172-174 ^{o}C), in comparison to a hydrocarbon molecule of a similar molecular weight. Furthermore nifedipine molecules consist of hydrophobic functional groups as presented in figure 2.1. Nifedipine has a T_g value of 46.2 ± 0.2 ^{o}C (Miyazaki *et al.*, 2007), which makes it a good model drug to illustrate the challenges of physical instability observed when dealing with small organic amorphous molecules with low T_g values.

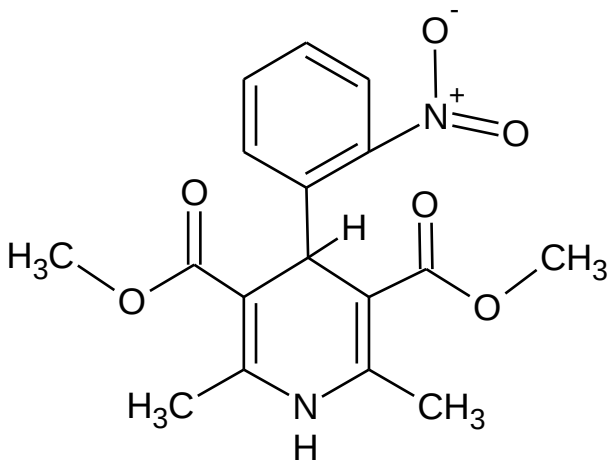

Figure 2.3 Structure of nifedipine. Molecular mass: 346.3g, melting point: 172-174°C, crystalline form, very insoluble in water. Log P = 2, pKa = 2.6 (Shalaeva *et al.*, 2008). Nifedipine exists as a yellow crystal with a melting point between 172-174 ^{o}C (Ali, 1989, Vippagunta *et al.*, 2002, Mehta *et al.*, 2002, Cilurzo *et al.*, 2002). This figure was constructed using ACD/ChemSketch.

Nifedipine is also a good model drug to illustrate the problems encountered with chemical instability of amorphous material, as nifedipine is a relatively sensitive compound. Exposure to light, high temperature and presence of oxidizing agents can cause nifedipine to degrade to predominantly two degradation products as illustrated in figure 2.2 (Ali, 1989). It was found that nifedipine partially decomposed within five minutes when exposed to day light and up to thirty minutes when exposed to bulb light (Ali, 1989). Nifedipine in solution is extremely sensitive to visible and ultra-violet light. On exposure to day light its UV-Vis spectrum changes very quickly (Ali, 1989). Under constant conditions the degradation of nifedipine is found to follow a first order kinetics, table 2.1. Working with nifedipine solutions in day light is challenging (Ali, 1989) due to the effect of day light on its decomposition rate. Therefore it has been recommended to perform all experimental work with nifedipine solutions under red or yellow light. Nifedipine is only affected by light with wavelengths of < 450 nm. When placing nifedipine solutions in amber vials it was found to degrade by 10 % of its original value within the first 20min, where as in clear vials, nifedipine is found to degrade by 50 % for the same period of time (Ali, 1989). The photolytic decomposition of solid crystalline nifedipine is not substantial, this is thought to be due to the inability of light rays to deeply penetrate the crystalline surface (Ali, 1989).

Table 2.1 Light degradation of dissolved nifedipine in alcoholic solutions, where irradiated by a different light sources (Ali, 1989). t_{10} and t_{50} time needed for 10% and 50% degradation respectively.

Light source	**k min^{-1}**	**t_{10} /min**	**t_{50} /min**
Day light	0.015	7	45
Light bulb	0.005	20	135
Spectro-test (xenon lamp) 700-372 nm	0.798	0.5	3.5
Spectrotest (xenon lamp) 700-471 nm	0.04	2.5	17

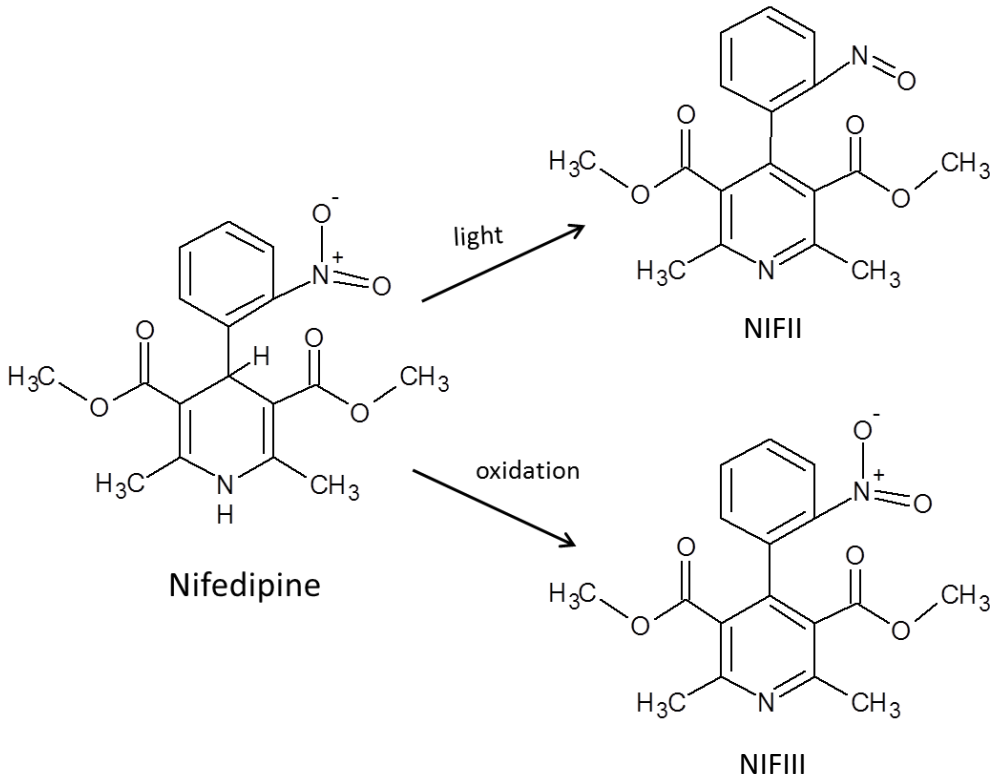

Figure 2.4 In vitro degradation of nifedipine to nitrophenylpyridine (NIF II) and nitrosophenylpyridine (Ali, 1989). This figure was constructed using ACD/ChemSketch.

An additional advantage of using nifedipine as a model drug in this research, is that it has been extensively investigated in the literature, and thus a verity of analytical methods have been established and published, of these references (Potter and Hulm, 1988, Chan *et al.*, 2004, Iqbal and Chan, 2015, Ali, 1989). Nifedipine does not require a controlled drug licence and is relatively cheap to buy, which makes it easy to obtain by university laboratories around the world. Another advantage to choosing nifedipine as a model drug for this research is that marketed forms are available for comparison.

From the clinical point of view, nifedipine works by slowing the influx of calcium ions into vascular smooth muscles, muscle cells that are found in the walls of blood vessels, it does so by acting as a highly specific antagonist to the voltage-dependent Ca^{2+} channels present on the cell membrane of such muscles (Opie, 1987). Calcium ions are essential for the contraction of muscle cells and thus deprivation of calcium ions inhibits the ability to contract, therefore inducing vascular smooth muscles to relax (Opie, 1987). This results in vasodilation of blood vessels, specifically arteries as they are more targeted by nifedipine. The induced effect of nifedipine has two main uses; the relaxing and widening of arteries in the body, thus minimising resistance to pump blood around the body, lowering the work load on the heart to circulate blood. This reduces pressure within blood vessels, therefore making nifedipine a good drug to treat high blood pressure. Vasodilation of small arteries in the heart improves oxygen supply to cardiac muscles, these properties show that nifedipine may also be used to treat, manage and prevent angina, chest pain caused by insufficient oxygen supply to the heart (Opie, 1987, Crum *et al.*, 2013, Garbacz *et al.*, 2009, Snider *et al.*, 2008, Huang *et al.*, 2006, Vippagunta *et al.*, 2002, Mehta *et al.*, 2002, Cilurzo *et al.*, 2002, Mehta *et al.*, 1995, Fujii *et al.,* Ali, 1989). A fast release nifedipine dosage form is advantageous as an emergency medicine to treat life threatening heart conditions.

Nifedipine is also used to treat the symptoms of a circulatory disorder called Raynaud's phenomenon. In this condition the blood vessels in the hands go into spasm and contract excessively when the hands are cold (Opie, 1987, Snider *et al.*, 2008). This causes the hands to go white, numb and painful. Nifedipine relaxes the peripheral arteries in the hands, causing them to widen and the blood circulation to the fingers to improve (Opie, 1987, Snider *et al.*, 2008).

The pharmacokinetic studies of nifedipine show that, independent of the method of administration, 70 to 80 % of the absorbed nifedipine is eliminated via urine. Majority of which, approximately 90%, was eliminated with in the first day of administration, giving nifedipine a half-life of 4 to 5 hours. Figure 2.5 below presents the metabolites of nifedipine (Ali, 1989).

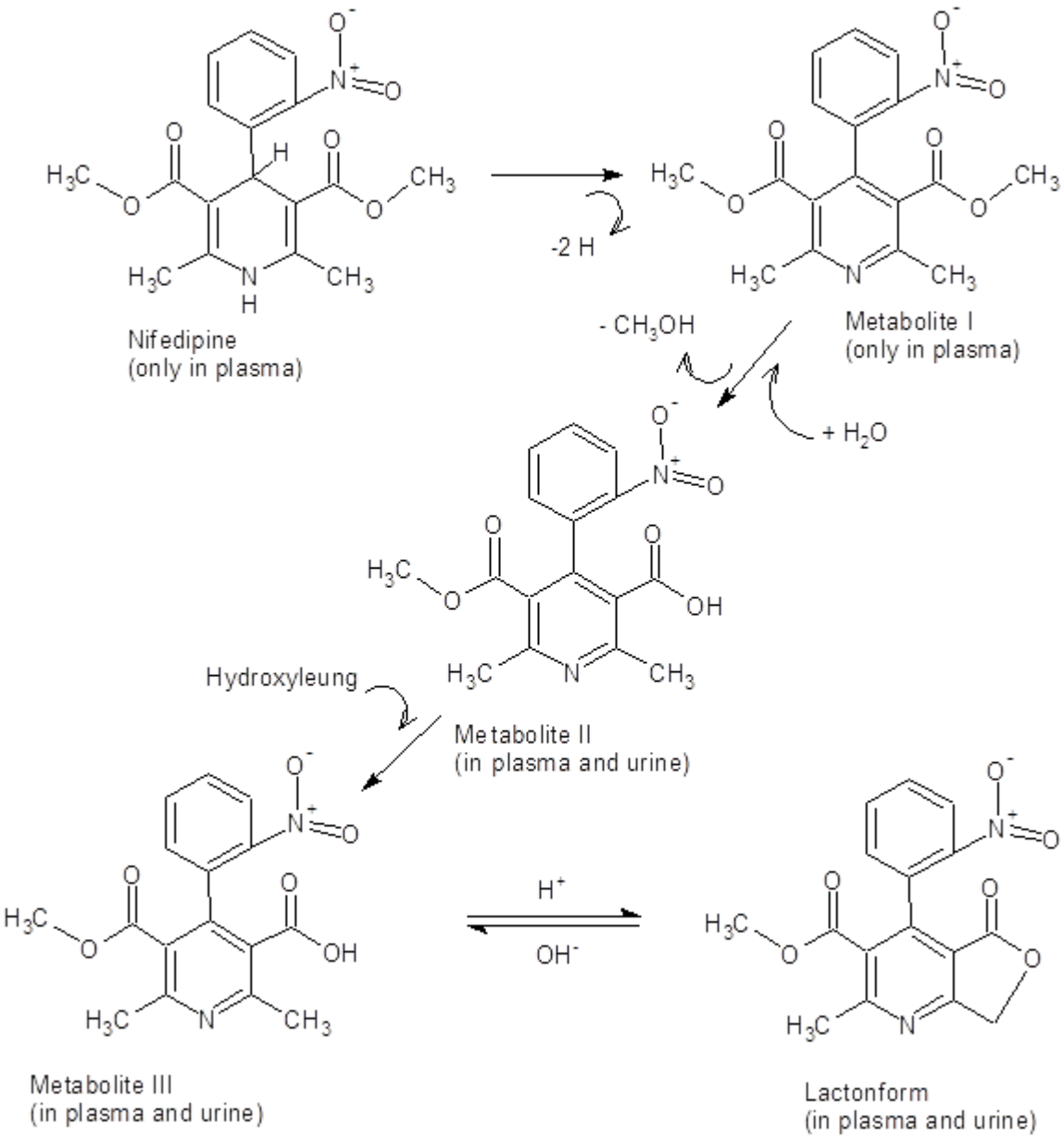

Figure 2.5 Metabolism of nifedipine (Ali, 1989). This figure was constructed using ACD/ChemSketch.

As discussed in chapter 1, there are great stability benefits to using a large molecular weight carrier compared to a small carrier, due to the substantial increase it provides in glass transition as it can increase the physical stability of amorphous drug (Kaushal *et al.*, 2004). Polyvinylpyrrolidone (PVP) is one of the most successful carriers due to its efficient and stabilising properties (Kaushal *et al.*, 2004). Not only does PVP increase the glass transition of the amorphous drug when incorporated into the solid dispersion, PVP has been found to enhance the physical stability of amorphous drugs even further by forming hydrogen bond complexes that inhibit molecular mobility and therefore considerably reduce the rate of crystallization. The addition of 10% w/w of

PVP K40 to amorphous nifedipine can reduce the rate of drug crystallization by 2 to 3 orders of magnitude, which has been attributed to hydrogen bond interactions between the carbonyl group of PVP and nifedipine (Aso and Yoshioka, 2006). Although many studies have concluded that PVP inhibits the recrystallisation rate of nifedipine through hydrogen bond interactions, rather than just by increasing the T_g value of the solid dispersion, very few of the related studies attempted using a PVP from the far lower end of the molecular weight range such as PVP K10 (K = 1000).

PVP has shown to increase the solubility of nifedipine as well as many other water insoluble drugs. This is by firstly increasing the life of amorphous nifedipine and therefore, maintaining the enhanced intrinsic solubility. Secondly, as mentioned above, PVP was found to interact through hydrogen bonding with nifedipine, as well as other water insoluble drugs, this as a result prevents nifedipine molecules from recrystallizing and precipitating out of solution, instead the drug is maintained in solution as a soluble drug-polymer complex. PVP is therefore an ideal carrier to use in the formation of a nifedipine solid dispersion. Another advantage to using PVP is that it is freely soluble in TBA, which therefore means that no co-solvents are needed to mix PVP and nifedipine when forming feed solutions.

PVP comes in a range of molecular weights, the most commonly used PVP molecular weights are K30 and K40. Despite the stability enhanced benefits of using the larger molecular weights of PVP, the dissolutions of lower molecular weights of PVP are much higher (Kaushal *et al.*, 2004), therefore low molecular weight PVP are more fit for purpose when it comes to developing fast releases formulations.

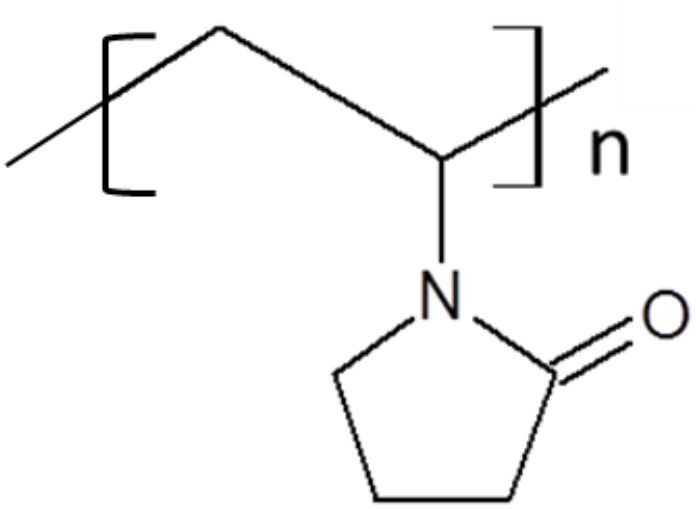

Figure 2.6 Structure of a PVP monomer. The molecular weight of 1 monomer = 111.14 with one hydrogen bond acceptor per monomer. T_g = 65 to 123 ^{o}C (Buera *et al.*, 1992). This figure was constructed using ACD/ChemSketch.

Therefore aims of the study reported in this chapter were to establish a robust freeze-drying method of producing a solid solution of nifedipine in PVP, to determine the effect of changing the w/w % of PVP on the physical state of nifedipine and to investigate any possible interaction.

To fulfil the aims, the following objectives were set:

1. Developing a robust and easily transferable method for producing un-collapsed freeze-dried cakes of amorphous nifedipine in PVP.
2. Production of freeze-dried 0-100 w/w % range of nifedipine in PVP using the developed method.
3. To characterise the physical properties of freeze-dried and physical mixtures of nifedipine and PVP by:
    a. Differential scanning calorimetry (DSC)
    b. Optical microscopy
    c. FT-Infra red spectroscopy
4. To use DSC, optical microscopy and FT-IR data to evaluate phase behaviour in the different nifedipine – PVP systems.
5. Investigating the presence of chemical interactions such as hydrogen bonding between nifedipine and PVP using FT-IR

2.2. Equipment & Materials

2.2.1. Equipment

Alcohol thermometer: G H ZEAL Ltd London UK, product number (PN): L3000, specification: +10 ^{o}C to -40 ^{o}C; **Aluminium foil**: Fisher scientific Ltd Leicestershire UK, Catalogue code (CC): 12369548, specification: 12 µm thickness 450 mm width x 75 m length; **Analytical balance**: Sartorius Ltd Surrey UK, Manufacture number (MN): ME215S Genius Series, Serial number (SN): 13507552, specification: 0.01 mg readability 60/210 g capacity; **AtmosBag^{TM}**: Sigma-Aldrich Gillingham UK, product type (PT): Two hand non-sterile closure type made from polyethylene, SN: Z112828-1EA, Batch number (BN): 3110, specification: medium size; **Capillary piston tips**: Gilson Inc Bedfordshire UK, PT: sterilized, PN: CP1000ST, BN: B00696113S; **Complete tear off aluminium vial seal**: Adelphi health care packing West Sussex UK, PN: COTW20, BN: 20110778; **Crimper for solid aluminium seals**: OPS Diagnostics LLC NJ USA, PT: 20 mm crimper, PN: SKU:KIHC20-18; **Diamond tips**: Gilson Inc Bedfordshire UK, PN: D1000, specification: 100-1000 µL; **Diamond tips**: Gilson Inc Bedfordshire UK, PN: D5000, specification: 1-5 mL; **Differential scanning calorimetry**: TA Instruments - A Division of Waters Ltd Herts UK, model: Q20, Instrument number (IN): 07051.902, SN: 0020-5023; **Digital microscope camera**: QImaging Surrey BC Canada, PT: QICAM Fast 1394-12 bit, MN: 01-QIC-F-CLR-12, SN: Q23526; **Drying Oven**: Weiss Technik Loughborough UK (formed from two separate companies Weiss Gallenkamp and Design Environmental), CC: OVE.100.1106, SN: 89/07/212; **Freeze-drying Fiolax® amber 6.0 mL vials**: SCHOTT Müllheim Germany; PN: 20110876, BN: 6102393931; **FT-Infra red spectroscopy**: PerkinElmer Inc Seer Green UK, model: Spectrum UATR Two, SN: 92100; **Immersion thermometer (76 mm)**: Medalcard scientific Ltd Christchurch UK, specification: +10 ^{o}C to +50 ^{o}C; **Laboratory Freezer**: Prior laboratory supplies Ltd Leicestershire UK, model: -85 ^{o}C ultra-low freezer; **Laboratory fridge/freezer**: Liebherr UK Ltd Bedford, PT: Premium no frost; **Laboratory microscopeLeitzDialux 22EB**: Leica Microsystems UK Ltd Milton Keynes (predecessor previously known as Ernst Leitz GmbH), PT: 020-452.023 equipped with polarizing filters, SN: 541006; **Lambda plate in holder**: Leica microsystems UK Ltd, Milton Keynes, PN: 11513908; **Lyotrap freeze dryer**: LTE

Scientific Ltd Greenfield UK, model: Lyotrap -55 ^{o}C condenser temperature, SN: J5467/5; **Micro balance**: Sartorius UK Ltd Surrey, MN: MC5, SN: 90802138, specification: 5.1 g capacity and 1 µg readability: 1; **Microscope objective 10/0.25**: Leica microsystems UK Ltd Milton Keynes, SN: 519864; **Microscope objective 25/0.60**: Leica microsystems UK Ltd Milton Keynes, SN: 519864; **Microscope objective 40/0.7:** Leica microsystems UK Ltd Milton Keynes, SN: 519747; **Microscope objective 5/0.12**: PZO, SN: 35516; **Nickel:** TA Instruments - A Division of Waters Ltd Herts UK, PN: T120323; **Oil-Lubricated Rotary Vane Vacuum Pumps**: BUSCH (UK) Ltd Telford, Type: R 5 RA 0160 - 0302 D, SN: C0926000007; **Platinum sample pans**: TA Instruments - A Division of Waters Ltd Herts UK, PN: 952018.908, specification: 50 µL size; **Polystyrene film**: PerkinElmer Inc Seer Green UK, PN: L160-0239; **Rubber vial stopper**: Adelphi health care packing Sussex UK, PN: FDW20RT, BN: 20120010, specification: 20 mm diameter; **Sonorex Ultrasonic bath**: Bandelin electronic Berlin Germany, PT: RK510, PN: GB327.00034435.001, SN: D-12207; **Stage micrometre**: Leitz Wetzlar Deutschland Germany, specification: size of 2 mm and an interval of 0.01 mm; **Stage micrometre**: Graticules Ltd Kent UK, specification: size of 1 mm and an interval of 0.01 mm; **Standard Aluminium Hermetic Lids**: TA Instruments - A Division of Waters Ltd Herts UK, PN: 900793.901, BN: A3881401**; Standard Aluminium Hermetic Pans**: TA Instruments - A Division of Waters Ltd Herts UK, PN: 900794.901, BN: A3925701; **Standard sample presser**: TA Instruments - A Division of Waters Ltd Herts UK, PN: 900680.902, SN: 6173; **Thermogravimetric analyser**: TA Instruments - A Division of Waters Ltd Herts UK, model: Q500, IN: 95300.901, SN: 0500-1858; **Ultraviolet/Visible spectroscopy cells**: PerkinElmer Inc Seer Green UK, Part No: B0631009; **Ultraviolet/Visible spectroscopy**: PerkinElmer Inc Seer Green UK, model: Lambda2S, Identification number (ID): 166351, SN: 6847; **Vacuum desiccator**: Smiths scientific Kent UK, PT: Vacuum with stopcock And perforated ceramic disc, CC: 262D/k/200; **Vacuum pump**: Edwards Ltd West Sussex UK, model: RV3, SN: 129449289; **Variable volume M1000 pipette**: Gilson Inc Bedfordshire UK, model: MICROMAN® 100 µL - 1000 µL SN: GK05911; **Variable volume P1000 pipette**: Gilson Inc Bedfordshire UK, model: PIPETMAN classic™ 100 µL - 1000 µL, SN: K25103M; **Variable volume P5000 pipette**: Gilson Inc Bedfordshire UK, model: PIPETMAN classic™ 100 µL - 5000 µL, SN: CJ58322; **Vortex-Genie 2**: Scientific Industries New York USA, MN: G560E, SN: 2-

153495; **Water bath-controlled temperature**: Grant instruments Ltd Cambridge UK, PT: SS40-D2, SN: 899209003.

All instruments including balances used in this project were validated on an interval of 6 months or less as part of the college instrumental routinely checks.

2.2.2. Materials

Ethanol absolute: VWR International Ltd Leicestershire UK, CAS: 64-17-5, CC: 20821.321, BN: 1213150524; **Hydrochloric acid**: Fisher scientific Ltd Leicestershire UK, CAS: 7647-01-0, PN: J/4320/24, CC: 10284480, BN: 1214805, specification: 1.0M meets analytical specification for BP, EP and USP; **Indium**: Alfa Aesar Heysham UK, CAS: 7440-74-6, BN: 0160615, specification: purity ≥ 99.9999%; **Methanol**: Fisher scientific Ltd Leicestershire UK, CAS: 67-56-1, PN: M/4056/17, CC: 10675112, BN's: 1289045, 1402809, 1498902, 1414862; **Nifedipine**: Sigma-Aldrich Gillingham UK, CAS: 21829-25-4, PN: N7634-5G, BN's: 041M0056V, SLBD7789V, specification: ≥98% pure (HPLC); **Oxygen-free Nitrogen compressed gas**: British oxygen company Windlesham UK, SN: Kings/BHS/NS37/N2-4B; **Polyvinylpyrrolidone**: Sigma-Aldrich Gillingham UK, CAS: 9003-39-8, PN: PVP10-100G, BN: BCBG5331V, specification: Average molecular weight of 10,000 g per mole, water content by Karl Fischer ≤ 5.0 %; ***Tert*-butanol**: Sigma-Aldrich Gillingham UK, CAS: 75-65-0, PN: 360538-1L, BN's: BCBG196IV, BCBH4856V, specification: ACS reagent ≥99.0%, water content by Karl Fischer ≤0.1%; ***Tert*-butanol**: Alfa Aesar Ward hill US, PN: 33278, BN: C25Z023, specification: ACS reagent ≥99.0%, water content by Karl Fischer ≤0.1%.

2.2.3. Software

QCapture Pro6.0: QImaging Surrey BC Canada; **TA explorer:** TA Instruments - A Division of Waters Ltd Herts UK; **Universal Analysis 2000:** TA Instruments - A Division of Waters Ltd Herts UK; **PerkinElmer spectrum:** PerkinElmer Inc Seer Green UK; **OriginPro**: OriginLab Silverdale Scientific Ltd Buckinghamshire UK.

2.3. Method

2.3.1. Production of freeze-dried cakes containing nifedipine and PVP

A w/w % range of freeze-dried cakes of nifedipine in PVP k10 were produced using tert-butanol (TBA) as a solvent. All production steps were performed in a dark room or in isolation from ambient light, using aluminium foil and amber glassware to protect nifedipine from photo degradation.

2.3.1.1. Preparation of feed solutions for freeze-drying nifedipine and PVP

A 100 ± 0.08 mL of 1% w/v stock solution of nifedipine in TBA was prepared by adding a pre weighed 1.0 g ± 1.0% of nifedipine, in a plastic weighing boat, into a clean and dry 100 mL amber glass volumetric flask. The weighing boat was rinsed with liquid TBA (40 ± 0.5 ^{o}C), and the rinsing was poured into the volumetric flask containing the nifedipine. The developing solution was diluted to volume (100 ± 0.08 mL) with liquid TBA (40 ± 0.5 ^{o}C). The volumetric flask was then caped and sealed. The volumetric flask was then placed in a (40 ± 0.5 ^{o}C) water bath for 60 to 80 min, with a 20 to 25 min interval of 60 to 90 sec of vortex shaking (set to maximum shaking speed of 10 units), to ensure full dissolution of drug. A 100 ± 0.08 mL of 1% w/v stock solution of PVP K10 in liquid TBA (40 ± 0.5 ^{o}C) was prepared using the same method. Both stock solutions were checked visually for any precipitation or un-dissolved matter, and were kept in the (40 ± 0.5 ^{o}C) water bath until no particles are visible. Both stock solutions were then transferred into individual, labelled 100 mL sample jars and maintained in a (40 ± 0.5 ^{o}C) water bath to prevent TBA from solidifying, however the sample jars were kept closed at all times unless they were sampled from. As TBA is a very volatile liquid when at 40 ± 0.5 ^{o}C, the M1000 pipette was used to transfer the appropriate volumes of each stock solution (Table 2.2) into labelled, clean and dry, amber freeze-drying vials (figure 2.2) to make up the range of solutions. The amber vials were stoppered with rubber stoppers immediately after filling (figure 2.2 b) and were maintained at room temperature (18-25 ^{o}C). This process was repeated 3 times, in order to make 3 batches of the whole range, each starting with different stock solutions of nifedipine and PVP k10, therefore yielding a total of 30 vials.

An additional 20 vials, of 2 mL ± 1.60 µL pure TBA, were prepared using the same method.

Table 2.2 Composition of feed solutions for the production of freeze-dried nifedipine in PVP solid dispersions (n=3). Volumes were pipetted using the M1000 MICROMAN® pipette, with the following systematic errors calculated by the manufacturer (100 ± 3.00 µL, 500 ± 5.00 µL & 1000 ± 8.00 µL) (Gilson.S.A.S, 2006).

Target percentage of nifedipine in PVP after freeze-drying w/w %	Target volume of nifedipine stock solution /mL	Target volume of PVP k10 stock solution /mL	Total target volume of solution in each FD vials /mL
0	0.00	2.00	2.00
10	0.20	1.80	2.00
20	0.40	1.60	2.00
30	0.60	1.40	2.00
40	0.80	1.20	2.00
50	1.00	1.00	2.00
60	1.20	0.80	2.00
70	1.40	0.60	2.00
80	1.60	0.40	2.00
90	1.80	0.20	2.00
100	2.00	0.00	2.00

2.3.1.2. Freezing solution

Once the feed solutions for freeze-drying were prepared in a total of 50 vials (20 containing pure TBA), the process of freeze-drying was started by holding the feed solutions at room temperature (18-25 ^{o}C) for 20 to 30 min, allowing the TBA based solutions to freeze . Following so the stoppers of all vials were readjusted to the upper position (Figure 2.1 a) thus allowing an escape route for the subliming TBA. The samples were then stored in an external -70 to -80 ^{o}C freezer and held at such temperature for 10 to 14 hours.

2.3.1.3. Preparing the Lyotrap freeze dryer

Prior to the start of all freeze-drying cycles performed in this chapter, the following steps were taken to ensure an efficient, clean and safe freeze-drying was performed. The first step was to clean the condensing chamber from any ice build-up. This was achieved using the defrosting option on the control panel, after switching on the main power supply for the Lyotrap freeze dryer (figure 2.1 j). The drain valve (figure 2.1 i) was also opened to allow the escape of any water that resulted from melting the ice build-up in the condenser chamber. Once all the ice was melted and the water

removed, the walls of both chambers as well as the FDS were cleaned using a lint free cloth and 70% v/v ethanol in distilled water. The cleaning process, involved the removal of any residue or particulate matter from inside the two chambers. Cleaning the drying chamber involved separating the parts of the drying chamber and cleaning them individually, this included the drying chamber's lid and rubber seals (diagram 2.1 d &e). Once both chambers were cleaned, they were assembled to match the set-up in figure 2.1, while the FDS was positioned at 0 to 5 cm above the condensing chamber opening. Following so, it was checked that the oil level inside the vacuum pump is between the upper and lower limits (figure 2.1 k). The condition of the oil was also assessed based on its clarity; cloudy oil indicates the presence of impurities such as water or other residual solvents. This can reduce the pump's efficiency, and therefore cloudy oil was changed with fresh oil by following the instructions described in the RV3 vacuum pump manual (Edwards, 2010). Once cleaned, set up and checked for pump oil, the Lyotrap cooling unit was switched on allowing the condensing chamber to reach ≤ -30 ^{o}C, measured by the inbuilt thermometer. The FDS's temperature on the other hand was measured using an alcohol laboratory thermometer. Once the FDS's temperature reached ≤ -15 ^{o}C, the Lyotrap preparation stage was completed.

2.3.1.4. Primary drying

The 50 vials containing the frozen feed solutions, for freeze-drying, were transferred from the freezer and placed onto the ≤ -15 ^{o}C FDS. Vials containing nifedipine and/or PVP were situated in the centre of the shelf, away from the edges, and the vials containing pure TBA were situated closer to the FDS edges. The drying chamber was fixed in place immediately and the draining valve was ensured to be closed. The RV3 vacuum pump was switched on, and was set to high throughput mode, this sets the vacuum pump to constantly reduce the unified internal pressure of the drying chamber to eventually reaching the minimum possible pressure (which in the absence of any samples is 0.03 mbar (Edwards, 2010)). The vacuum pump and the cooling unit were left on for the entire duration of the primary drying stage: 144 ± 1h. The displayed temperature and pressure of the condensing chambers where monitored and recorded throughout the primary drying stage.

Once the primary drying stage was completed, the pump was switched off, and the vacuum was released using the drain valve which was connected to a nitrogen gas (oxygen free) cylinder, thus allowing the freeze-drying chambers and the vials to be refilled with nitrogen gas. Once the vacuum inside the drying chamber was released, the drying chamber was opened and the stopper, for each of the 30 sample containing vials, was pushed in immediately as shown in fig 2.2b. Once all vials were partially sealed with stoppers, they were transferred out of the freeze drier and into a plastic container at room temperature (18-25 ^{o}C). The remaining 20 empty vials were recycled by rinsing them with 70 % v/v ethanol in distilled water and drying them in a 40 ^{o}C drying oven.

2.3.1.5. Secondary drying

Samples were transferred into a vacuum desiccator containing P_2O_5 at ambient temperature (18-25 ^{o}C) and a reduced pressure of 0.69 to 0.86 bar, applied by an inbuilt facility vacuum system of BUSCH vacuum pumps. The vials were reopened and the stoppers where left in the upper position as shown in figure 2.2 a. The vials were maintained in the reduced vacuum desiccator for the entire duration of the secondary drying stage 24 ± 1h (Srinarong *et al.*, 2010).

2.3.1.6. End of cycle packaging

The 30 vials containing the freeze-dried samples were removed from inside the desiccator and placed inside a two-hand polyethylene AtmosBag^{TM} which was flushed with nitrogen gas for 1 to 2min, and then filled with nitrogen gas by sealing all gas outlets within the bag. Using the inbuilt hand gloves within the nitrogen bag, the rubber stopper for each vial was pushed in to partially seal the vials (figure 2.1 b). Following so all samples were crimped with aluminium caps to fully seal the vials, using a 20 mm crimper, whilst inside the nitrogen bag (figure 2.1 c). All samples were stored away from light, in a vacuum desiccator containing P_2O_5 at ambient temperature (18-25 ^{o}C) until analysis was performed (Zijlstra *et al.*, 2007).

All freeze-dried samples were analysed via a number of techniques, therefore extracting a sample out of each of the vials for analysis, was performed in a nitrogen

bag, to ensure that the remainder of the vial content was not subject to atmospheric water and thus may be used for other analytical techniques.

2.3.1.7. Lyotrap validation

The Lyotrap system was validated by running a short test run of empty drying and condensing chambers. This was achieved by simply by switching on the cooling unit (fig 2.1 j), sealing the drain valve (fig 2.1 i) and allowing the condenser chamber enough time to fall below -30 ^{o}C, at which point the vacuum pump was switched on. The internal pressure of the drying chamber was allowed to decrease over a period of 30min.

After 30min of switching on the vacuum pump, a check list was filled to ensure all aspects of the freeze-drying system were performing as expected. This included:

1- Displayed temperature reaching ≤-40 ^{o}C with a fluctuation limit of 2 ^{o}C.
2- Displayed pressure reached ≤0.1 mbar with a fluctuation limit of 0.02 mbar

On occasions, where the freeze dryer failed to perform as required, the freeze-drying cycle was ended and both the vacuum pump and the freeze dryer were examined for faults that may be the cause of the failure. A common cause of large pressure fluctuations was the presence of an air leak; such problems were fixed by replacing the appropriate parts and using the following references as the main guide (Edwards, 2010, Ltd, 2014).

2.3.2. Preparation of controlled samples

Physical mixes of nifedipine and PVP with an equivalent w/w % range to the freeze-dried samples were produced. For each w/w %, the required amount of nifedipine and PVP were weighed (table 2.2) and added to a clean and dry ceramic pestle and mortar. The mixture of powder were ground for 2 to 3min and were then transferred to labelled bijou glass vials and stored in a desiccator over P_2O_5. This was repeated 3 times for each w/w %.

Table 2.3 Composition of physical mix controlled samples of NIF in PVP (n=3). The samples were weighed using an MC5 micro balance with a ± 1.0%.

Target nifedipine in PVP w/w % of the final physical mix	Target weight of nifedipine added / mg	Target weight of PVP added / mg	Total target weight of sample / mg
0	0.00	50.00	50.00
10	5.00	45.00	50.00
20	10.00	40.00	50.00
30	15.00	35.00	50.00
40	20.00	30.00	50.00
50	25.00	25.00	50.00
60	30.00	20.00	50.00
70	35.00	15.00	50.00
80	1.60	0.40	2.00
90	1.80	0.20	2.00
100	2.00	0.00	2.00

2.3.3. Thermal analysis

Thermal analysis was used in this research to investigate the physical and thermal characteristics of different w/w percentages of nifedipine in PVP for freeze-dried (produced in section 2.3.1) and physical mixes (produced in section 2.3.2) (van Dooren and Müller, 1984). This included determining the content of crystalline nifedipine, determining the glass transition temperature of amorphous material and the melting temperature of crystalline material. Additionally thermal analysis was used here for determining the content of residual solvent.

Furthermore, as part of developing the freeze-drying method, thermal analysis was used in the process of identifying the temperature at which feed solutions must stay below in order to avoid melting or collapse during freeze-drying, otherwise known as the collapse temperature (T_c). As there were a range of solutions with different nifedipine and PVP concentrations, the T_c value was only determined for the highest and lowest concentrations of nifedipine and PVP (Table 2.1).

2.3.3.1. Differential scanning calorimetry (DSC)

The DSC instrument used in this research was the heat flux differential scanning calorimeter Q20 TA instrument, which consists of a cooling unit, a heating unit and the main DSC chamber(van Dooren and Müller, 1984). The size of the endothermic melt peak was used to calculate the content of crystalline material present in the sample

(Fix and Steffens, 2004). The glass transition temperature (T_g) of samples as well as the primary glass transition temperature (T'_g) of feed solutions were also determined by the literature recognized method (Haines, 2002).

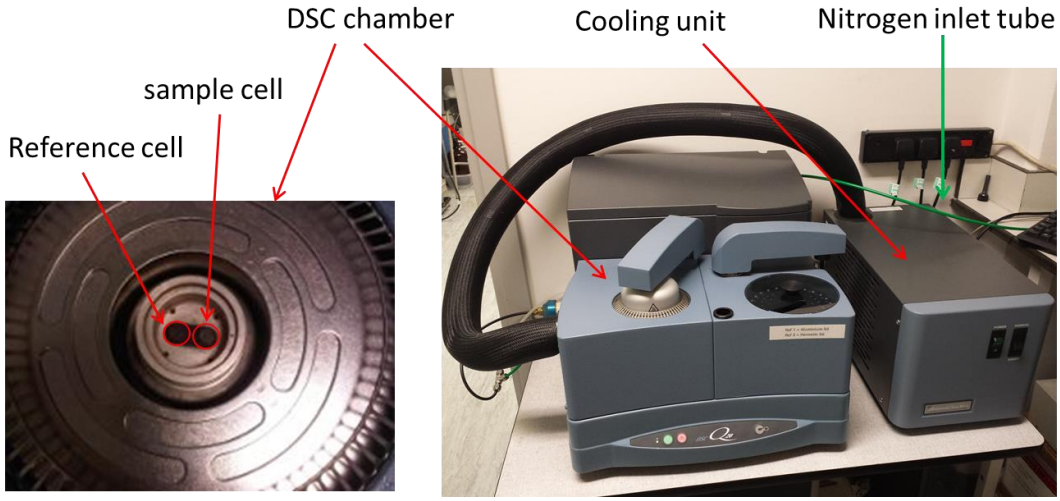

Figure 2.7 Components of the Q20 DSC instrument. Photos on the right contain an overview of the DSC Q20 instrument coupled with a cooling unit. Photo on the left contain an empty DSC chamber illustrating the 2 sensor cells. Photos in this figure were taken on the 20 Sep 2014 in lab number 5.12 Franklin-Wilkins Building, 150 Stamford Street, London SE1 9NH of King's college of London.

2.3.3.1.4 Preparation of the DSC instrument

Before switching on the DSC, a nitrogen gas (oxygen free) cylinder, connected to the DSC instrument, was turned on to a flow rate of 50 ± 5 mL/min. The system was purged with nitrogen gas for 30min prior to the start of any of the experiments, this ensures elimination of all moisture and oxygen from inside the DSC chamber to prevent engross of water by hygroscopic samples as well as oxidation upon heating (Haines, 2002). The nitrogen air flow was maintained at 50 ± 5 mL/min and the DSC instrument was switched on using the main power switch, followed by switching on the cooling unit.

2.3.3.1.5 Preparing DSC pans

The first step that was taken towards preparing DSC pans was to clean them. The presence of any contaminating particles on the inner or outer surface of either parts of the DSC pan (i.e. lid and pan fig 2.6) can act as an impurity and hence may influence the thermal properties of the sample. Therefore, pans with any signs of contamination were washed with 70% v/v ethanol in water and dried by placing inside a 50 to 60 ^{o}C oven for 5 to 10 min, the pans were then left to cool to room temperature (18-25 ^{o}C) for ≥ 10min before usage.

2.3.3.1.6 Creating pin holed DSC pans

To ensure the safety of the DSC instrument, all DSC pans used in a thermal cycle that involved heating samples above 40 ^{o}C were pin holed manually to prevent the build-up of pressure inside the pan when heated. The pin hole was achieved by using a hypodermic needle with a radius of 0.005 mm to puncher a hole in the centre of the lid while reversed and rested on a cushion of clean tissues as illustrated in Figure 2.8. Thus allowing any burs to protrude out words from the pan.

In the addition to serving as a safety precaution, the hole also helps in determining the w/w % of residual solvent present in samples, as the escape of residual solvent would be the dominant contributor to sample weight loss (McPhillips *et al.*, 1999, Haines, 2002, Grodowska and Parczewski, 2010).

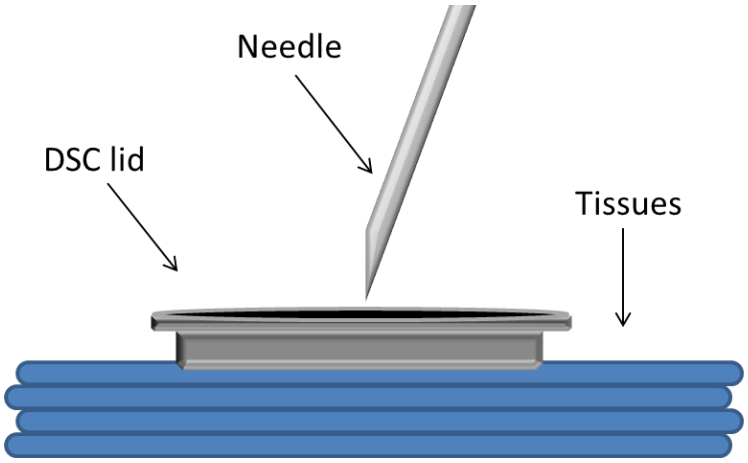

Figure 2.8 Puncturing an outward hole in the lid of a DSC pan to create a pin-holed DSC pan. This diagram was produced using Microsoft PowerPoint.

2.3.3.1.7 Preparing and loading DSC Pans

This method is particularly aimed for the analysis of freeze-dried material and therefore it is designed to prevent sample contact with atmospheric moisture, thus to prevent the ingress of large amounts of water, the DSC pans were typically loaded in a nitrogen atmosphere. This was achieved by firstly cleaning an AtmosBag^{TM} using lint free tissue and 70% v/v ethanol in distilled water, then the required equipment (a pair of tweezers, a small spatula, pre weighed empty DSC pin holed pans, DSC pan crimper, a bijou glass vial and the sample sealed in a freeze-drying vial) were all placed inside the AtmosBag via the sealable mouth. The bag was then connected to nitrogen gas (oxygen free) cylinder, and the bag was flushed with nitrogen gas for 1 to 2 min. The

sealable mouth of the AtmosBag was then sealed and the bag was filled with nitrogen gas. Using the nitrogen bag in-built hands, the freeze-dried sample was opened gently and a 5 to 15 mg sample was extracted from the vial using the available clean spatula. The sample was then loaded into the DSC pan (bottom part) as illustrated in Figure 2.9. Care was taken to avoid contaminating the walls of the DSC pan as this may affect the integrity of the hermetic seal.

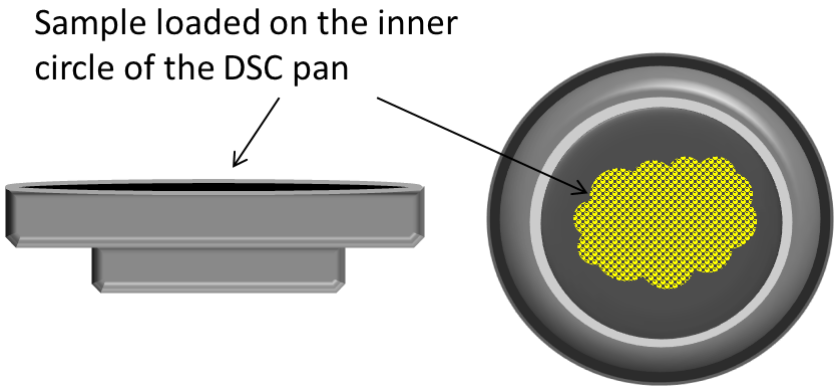

Figure 2.9 Sample loaded inside a DSC pan must be contained within the inner circle of the pan. The lid is not included in this figure. This diagram was created using Microsoft PowerPoint.

After placing the sample into the pan, the hermetic lid and the pan where cold welded (Figure 2.10) and sealed into a labelled sample jar whilst under nitrogen atmosphere. One empty pan was prepared using the same method; this pan was used as a reference pan. Once sample pans are prepared and sealed in nitrogen filled sample jars, they were taken out from the nitrogen bag and stored away from light and at room temperature (18-25 ^{o}C), until analysed, a duration that varied from 0 to 10 days.

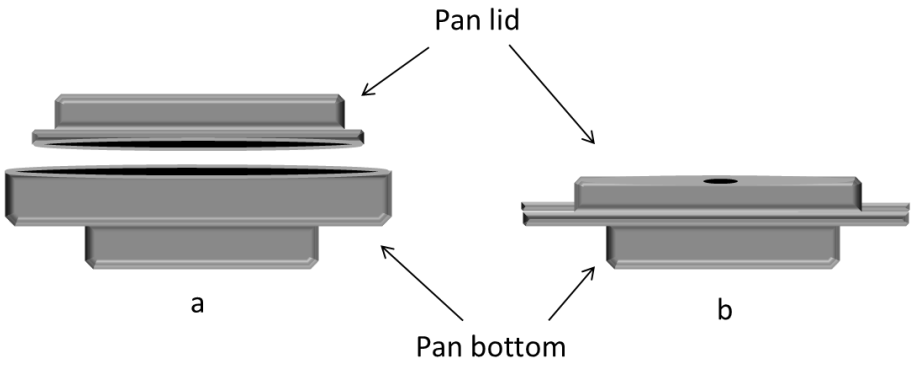

Figure 2.10 Two separate parts of a DSC pan, pan lid and pan bottom, on the left, forming a cold welded DSC pan on the right. This diagram was produced using Microsoft PowerPoint.

2.3.3.1.8 Inserting the DSC pans into the DSC chamber

It is important to note that before it was attempted to load DSC pans to the chamber, the DSC was set to maintain the experimental chamber at 25 ± 1 ^{o}C prior to starting the cycle. This ensures that the sample is not heated or cooled prior to the start of the experiment. To determine the weight of the sample, the full pan was weighed immediately before placing it into the DSC chamber. The sample weight was determined accurately by determining the difference in weight of the pan before and after the addition of sample. The resultant value was put into the details of the thermal cycle (under sample weight in mg) using software TA instrument explorer.

2.3.3.1.9 DSC cycle and data collection

Once the appropriate sample pan and the reference pan were placed on the corresponding sensor cells inside the DSC chamber, a thermal cycle appropriate to the aims of the experiment was programmed through the software TA instrument explorer.

2.3.3.1.10 Thermal cycles to characterise physical state of solid samples of nifedipine in PVP

All DSC cycles performed on solid samples such as the freeze-dried materials and physical mixtures (unless otherwise stated) were started at ambient temperature 25 ^{o}C. The equilibration step allowed the DSC chamber to reach the specified temperature. This was followed by an isothermal step of 5min, which ensured that both the reference pan and the sample pan were at the same temperature, (taking into account the slight difference in weight between the two pans). Following the isothermal step a ramping step was initiated, where the temperature of the DSC chamber was increased to 200 ^{o}C at rate of 10 ^{o}C/min. Followed by a cooling step where the temperature was ramped to 25 ^{o}C at a rate of 10 ^{o}C/min, and lastly a last heating step where the temperature was ramped again to 200 ^{o}C at a rate of 10 ^{o}C/min.

This thermal cycle was applied on the complete w/w % range of freeze-dried and physical mixtures of nifedipine in PVP, in replicates of 3.

2.3.3.1.11 Thermal cycles to determine the primary glass transition of liquid feed solutions

DSC cycles designed for liquid samples such as the TBA based solutions involved temperatures ≤ 40 ^{o}C and therefore the DSC pans used in these cycles were not pin holed. After placing the sample pan and the reference pan in the appropriate places inside the DSC chamber, the chamber was sealed and programmed to undergo the following thermal cycle: An equilibration step at 25 ^{o}C, followed by an isothermal step for 5min, followed by a cooling step where the temperature of the chamber was ramped to -30 ^{o}C at a rate of 10 ^{o}C/min, followed by a heating step where the chamber's temperature was ramped to 40 ^{o}C at a rate of 10 ^{o}C/min.

This thermal cycle was applied on TBA based feed solutions containing 0, 10 and 90 w/w % of nifedipine in PVP, in replicates of 3.

2.3.3.1.12 DSC validation

Prior to using the DSC instrument, the efficiency of the DSC was verified by running two experiments. The first was a test of the heat flow baseline, this was performed by running a cycle of heating and cooling an empty DSC chamber from 25 ^{o}C to 200 ^{o}C and 200 ^{o}C to 25 ^{o}C respectively, at a rate of 10 ^{o}C/min. This allowed the detection of any contaminants or residual precipitation, in the chamber, from previous usage. In the presence of any contamination, the resulting thermo-gram would show fluctuations in the heat flow baseline. In such case the DSC chamber was heated to 300 ^{o}C and cooled down to 25 ^{o}C, both, at a rate of 10 ^{o}C/min. Following so the chamber was cleaned thoroughly using a cotton bud soaked in 50% v/v ethanol in distilled water. Care was taken to avoid scratching the surface of the sensor cells. The chamber was then heated whilst open to ensure all residue solvent from the cleaning process was removed. The heat flow baseline test was then repeated to check that all contaminants were removed.

Once the baseline was proven to be stable, showing no decrease or increase in heat flow, throughout the experimental temperature range (25-200 ^{o}C), the DSC was validated for temperature calibration. This was done by running a sample of Indium using the same method described in section 2.3.3.1.10 to determine the average onset

melting temperature of pure indium, where n=3. This was then compared to the reference melting temperature of indium 156.7 ^{o}C (Kawase *et al.*, 1990). In the event that the determined onset of melting peak for indium deviates from the literature by more than 1.0 ^{o}C, the DSC instrument would have been re-calibrated by a TA engineer.

2.3.3.2. Thermogravimetric analyser (TGA)

The TGA used in this research is the TA instrument TGA Q 500, which may be programmed to heating the sample to a temperature of choice and at a rate of choice, whilst monitoring the weight of the sample(Xiao *et al.*, 2014). TGA is usually used to determine the temperature at which compounds decompose, and the percentage of mass loss at each stage of sample collapse or decomposition. In this chapter the TGA was used to confirm the content of residual solvent in some of the freeze-dried samples(Grodowska and Parczewski, 2010).

2.3.3.2.13 Preparing TGA

The TGA was prepared 30 min prior to the start of experiments by purging the system with nitrogen gas at a flow rate of 10 mL/min. The flow of nitrogen was further adjusted within the instrument and was set to 90 mL/min for the sample chamber and 10 mL/min for the reference chamber as recommended by the TA Q500 manual. Once the purging stage was complete, the weights of empty TGA pans were tarred via the TGA instrument. As the Q500 is equipped with a robotic arm, the pans were simply placed in numbered pan holders (Figure 2.11) and the TGA was programmed to tare the pans with corresponding numbered positions on the pan holder. Nevertheless due to the hygroscopic nature of freeze-dried samples, they were stored in nitrogen filled vials and only placed on the appropriate TGA pans immediately before their individual analysis. This is to avoid samples waiting in ambient atmosphere.

2.3.3.2.14 Programing TGA cycles

Once all pans to be used have been tarred, a TGA cycle was programmed into the software TA instrument explorer. As the instrument used does not come with a cooling unit, the cycle was limited to heating steps only. TGA cycles like DSC cycles are designed depending on the aims of the experiment as well as the thermal properties of the sample. For example determining the content of residual water in freeze-dried

samples required a particular cycle that consists of equilibration at 25 ^{o}C followed by a ramp step to 110 ^{o}C, rate of heating is kept at 10 ^{o}C per min unless other wises stated. It is important to note that when using the Q500, all experiments were force started immediately once the sample has entered the heating chamber, this is because the constant nitrogen air flow that is maintained inside the heating chamber can result in removing adsorbed residual solvent prior to the start of monitoring the weight of the sample.

2.3.3.2.15 TGA calibration and verification

The TGA was calibrated for temperature, by analysing a high purity magnetic standard, Nickel, for its sharp Curie point temperature, 358.28 ^{o}C (Legendre and Sghaier, 2011). This was achieved by firstly selecting the temperature calibration settings through the TA explorer software and erasing the previous temperature calibration values. Following so a thermal cycle was programmed to start with an equilibration step at 250 ^{o}C followed by a ramp step to 450 ^{o}C at a rate of 10 ^{o}C/min. The purging conditions were set to the same conditions as all of the other standard experiments (section 2.3.3.2.1.). The curie material was placed in a clean tared TGA pan, and was inserted into the oven using the auto sampler. The cycle was started, and a magnetic bar was gently placed directly under the furnace. The magnetic bar's position was adjusted in such a manner that a maximum weight gained was detected on the real time display of the sample's weight. The magnetic bar was then fixed in that position, and the instrument was left to complete the experiment. Once the experiment was completed, the resulted thermos gram was analysed for the temperature onset of a sharp drop in sample weight, indicating the observed Curie temperature. The observed Curie temperature and the theoretical Curie temperature (358.28 ^{o}C) were put into the calibration temperature table within the TA explorer software.

The TGA was also verified for weights using TA explorer software inbuilt calibration and verification program, a tared TGA pan and upper and lower range calibration weights supplied by the TGA manufacturer, TA. By following the instructions of the weight calibration program, the observed weights are compared to the theoretical weight of the individual calibration weights. In the case that the TGA fails the

verification test, it is automatically calibrated for on the bases of the TA supplied weights.

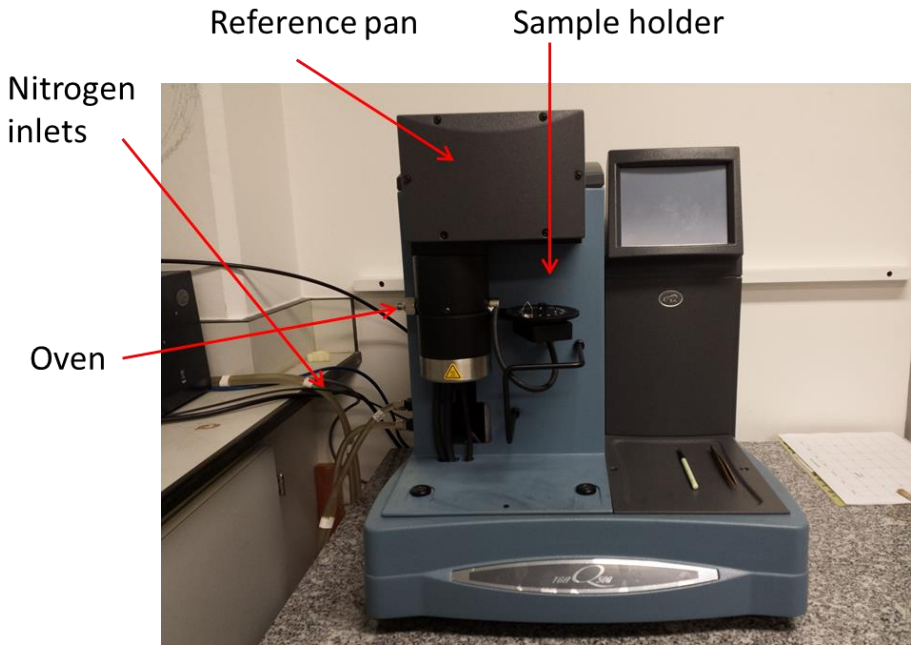

Figure 2.11 Components of the Q500 TGA instrument. The Photo in this figure was taken on the 20 Sep 2014 in lab number 5.12 Franklin-Wilkins Building, 150 Stamford Street, London SE1 9NH of King's college of London.

2.3.4. Fourier Transform infra-red (FT-IR) Analysis

The instrument used to measure IR spectra in this research was a PerkinElmer attenuated total reflectance (ATR) FT-IR spectrometer with a Dura-sampler II-Diamond ATR. One of the main advantages of using this instrument in place of an IR spectrometer is that the FT-IR can easily analyse solid samples without destroying them or mixing them with nujol, which could possibility cause the physical state of the sample to undergo a phase transition. In fact FT-IR may be re-used in other analytical experiments (Iqbal and Chan, 2015) if the samples are not sensitive to the environment in which the experiment was performed in (i.e. sensitivity to ambient light, or atmospheric humidity). The FT-IR analysis performed in this research was particularly aimed at confirming the structural stability of the API as well as excipients after manufacturing and stability studies. Furthermore, comparing FT-IR spectra of freeze-dried formulations to spectra of individual excipients as well as controlled samples (simple physical mixes of drug and carrier) was extremely useful in understanding the drug-carrier interactions, such as the presence of hydrogen

bonding. A recent review on ATR FT-IR can be found elsewhere (Kazarian and Chan, 2013).

2.3.4.1. Experimental settings

All FT-IR spectra were collected at room temperature (18-25 ^{o}C). The resolution was set to 4 cm^{-1} single scan as it is sufficient for determining the present chemical bonds (Zijlstra *et al.*, 2007). Transmittance was recorded over the range 4000– 400 cm^{-1}. The software Spectrum was used to interpret and correct produced spectra. Furthermore, the software was used to convert the transmittance spectra to absorbance spectra.

2.3.4.2. FT-IR validation

The calibration of FT-IR instrument was validated using a polystyrene film supplied by the manufacturer. Were the observed transition peaks in the developed spectrum of the polystyrene film was compared to the theoretical peaks based on the structure of polystyrene and a reference spectrum of polystyrene withdrawn from the literature (Devinder Gupta, 1995).

2.3.5. Cross polarization optical microscopy

An optical microscope slide of each of the samples of interest was produced by carefully placing an amount of 1 to 2 mg of the sample onto the surface of a glass microscope slide which was then covered with a cover-slip. In the interest of spreading the powder into a thin layer, a small amount of pressure and motion was applied to the cover-slip. The slide was then placed under the optical microscope instrument which was fitted with an imaging camera (QiFastCam), a cross polariser and a red 1 (λ) compensator plate to assess birefringence. Magnified pictures, of 5 X, 25 X and 40 X, were generated at ambient temperature and pressure using the QCapture Pro 6.0 software (Carlton, 2011). Representative scale bars were added to all images using previously calibrated in built scale bars.

2.3.5.1. Scale bare calibration

For each microscope objective a scale bar calibration was performed to allow the drawing of scale bars that are representative of the magnification power. The calibration was performed using a 1 mm stage micro-meter (Graticules Ltd, Kent UK)

with an interval of 1.0 µm. The stage micrometre was placed under the microscope and images were taken through different objectives. Using the inbuilt calibration program and the developed images of the stage micro-meter, a scale bar was designed for each objective.

2.4. Results

2.4.1. Method development

The freeze-drying method used in this chapter was monitored and tested to ensure that it does not expose the freeze concentrate solutions to melting or collapse conditions. This was performed by defining the edge parameters of failure, in other words the lowest temperature freeze-drying samples can reach before collapsing in the process, otherwise known as collapse temperature (T_c). Additionally it was important to determine the minimum length of time required for primary drying to produce room temperature (18-25 ^{o}C) stable freeze-dried cake. These conditions were defined specifically for the TBA based feed solutions with the highest and lowest nifedipine concentrations.

2.4.1.1. Collapse temperature

To determine T_c value for the freeze concentrate feed solutions, the primary glass transition must first be determined. DSC thermogram for each of 0%, 10% and 90 % w/w nifedipine in PVP solutions of TBA were produced. Figure 2.12 below presents one of the DSC thermograms developed.

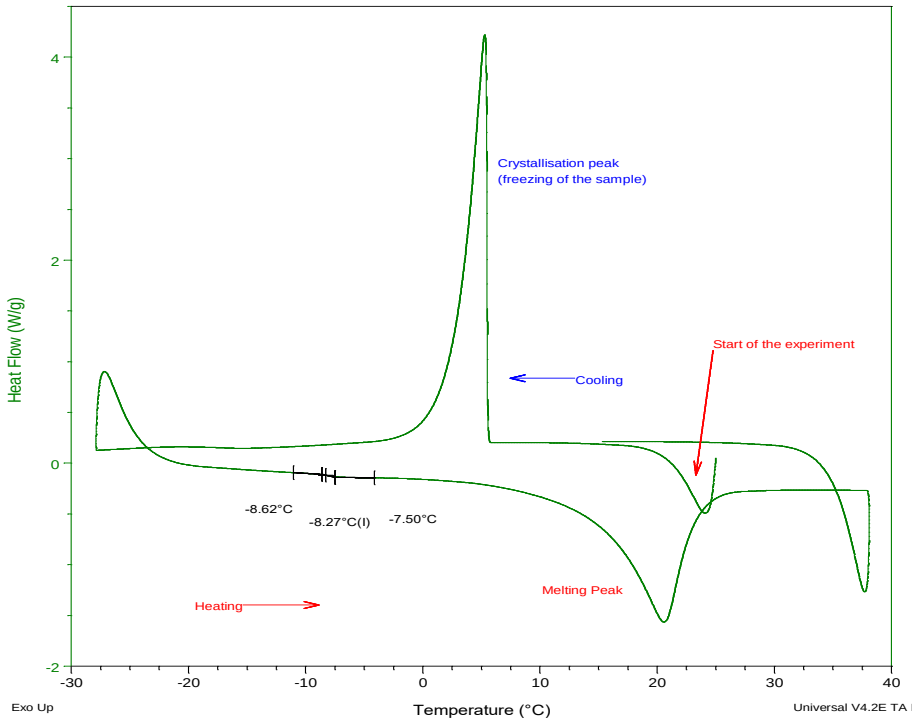

Figure 2.12 Thermogram of a liquid sample of NIF and TBA dissolved in PVP. The sample was cooled to temperatures below -20 °C and heated at a rate of 10 °C/min. T'_g determined to be -8.27 °C. All DSC thermograms in this thesis, unless stated, will have exothermic transitions upwards.

As presented in table 2.4, the lowest T'_g value is - 9.6 ± 0.1 °C (n=3). From the literature, T_c values are estimated to be 2 °C higher than the T'_g (Tang and Pikal, 2004). Therefore the equivalent T_c value is estimated to be -7 °C. As the T_c value is the temperature of failure, a safety temperature margin of 5 °C was implemented between the T_c and the target product temperature (T_p) during the primary drying stage, making the target product temperature to be -12 °C.

To ensure that the products are maintained at the target T_p value, the FDS's temperature was set to be at least 2 °C below the target T_p to account for the temperature difference between the shelf and the product. Shelf temperature was therefore ensured to be ≤ -15.0 °C to avoid sample collapse.

Table 2.4 Average *T'g* determined by DSC of feed solutions containing highest and lowest concentrations of nifedipine in TBA. 0.9% w/v showed the lowest T'_g value. DS of n=3.

Target w/w percentage of nifedipine in PVP dissolved in TBA (1% w/v)	Final target Conc. of nifedipine in feed solution w/v %	Final target Conc. of PVP in feed solution w/v %	Average T'_g °C	Std
0	0	1	-8	0.1
10	0.1	0.9	-8	0.2
90	0.9	0.1	-9.6	0.1

Based on the outcome of this experiment, the FDS's position was lowered, while measuring the temperature of the shelf using an alcohol thermometer, to a point where the shelf's temperature was ≤ - 15.0 ^{o}C. The optimal position of the FDS was determined to be 0 to 5 cm above the condensing chamber. To further ensure the safety of the products while freeze-drying, several temperature measurements of test feed solutions were performed while on the FDS to ensure that the T_p value is ≤ -12 ^{o}C when the displayed temperature of the condensing chamber is -40 ^{o}C or below .

2.4.1.2. Temperature and pressure of freeze-drying chambers

To ensure the temperature of the condensing chamber did not exceed -40 ^{o}C, as this can increase the T_P to be above -12 ^{o}C, the displayed temperature of the condensing chamber was recorded over the primary drying course (figure 2.13). Furthermore, the pressure inside the freeze-drying chambers was also recorded to allow better estimation of the required duration of primary drying. The temperature of the condensing chamber was maintained below -40 ^{o}C at all times (Figure 2.13-A). Pressure, of the drying chamber has shown to reach stability after 4 days of freeze-drying. Thus the primary drying stage of all cycles was given a minimum length of 5 days to avoid any sample collapse up on starting secondary drying. Figure 2.14 shows collapsed samples from a batch that was removed from the freeze dryer after 3 days of primary drying. Figure 2.15 on the other hand presents un-collapsed samples from a successful batch removed from the freeze dryer after 5 days of primary drying. Nevertheless, the efficiency of the 5 days primary drying is dependent on maintaining the sample size at a volume of ≤ 100 mL divided over ≥ 50 vials with a base diameter of ≥ 22 mm, giving the frozen feed solutions a surface area of ≥ 38 cm^2 per vial and a minimal total surface of 19 m^2.

It is also important to note that feed solutions with different nifedipine-PVP compositions may undergo different sublimation rates, therefore including all different compositions in this initial freeze-drying cycle insures that a primary drying stage of 5 days was sufficient for the composition with the slowest sublimation rate.

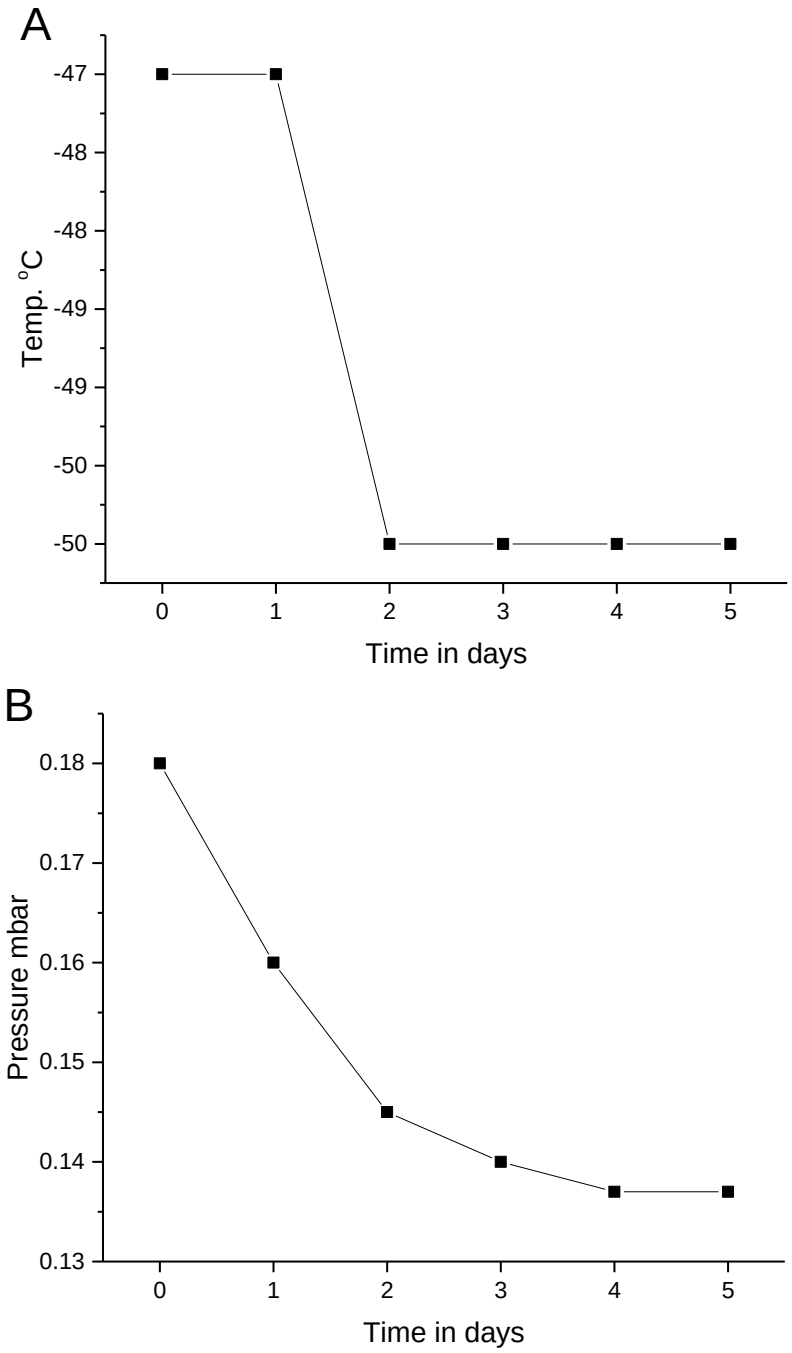

Figure 2.13: **(A)** Temperature & **(B)** pressure of freeze-drying chambers monitored over the course of primary drying NIF in PVP TBA solutions. Batch contained 50 vials.

2.4.1.3. Quality control of freeze-dried cakes

As part of the developed method, a quality control step was implemented where freeze-dried batches were inspected for any sign of FD cake collapse. A successful freeze-dried product is usually expected to appear as a porous consistent cake. Signs of cracks or shrinkage could indicate macroscopic collapse (figure 2.14). As described in earlier sections, this is likely to be caused by insufficient primary drying duration,

which therefor fails to increase the T_c of the product to be above room temperature (18–25 ^{o}C) (Tang and Pikal, 2004). Alternatively, collapse can occur if the T_p was raised above the T'_g during freeze-drying.

Figure 2.14 Collapsed samples from a 3 day only primary drying batch. Collapsed samples show clear shrinkage signs; such as shrinkage away from the walls of the vial and towards the centre of the vial. All vials contain the same formulation 50% w/w nifedipine in PVP.

2.4.1.4. Formulation composition

Varying the ratio of NIF:PVP in freeze-dried formulations had a great impact on the quality of the cake, the w/w % of residual solvent and the w/w % of crystalline NIF present in the formulation. Therefore the impact of each of these variables is described in more detail in the following sections.

2.4.2. Quality of freeze-dried cake

Preliminary results showed that simply freeze-drying TBA solutions of pure nifedipine produced cakes of very poor quality (Figure 2.15). Alternatively freeze-dried cakes composed of 100% w/w PVP showed a high quality porous cake with no sign of shrinkage. Varying the ratio of NIF:PVP has shown to greatly affect the quality of the freeze-dried cake. A minimum of 30% w/w PVP is required to produce a porous freeze-dried cake containing nifedipine (Figure 2.15).

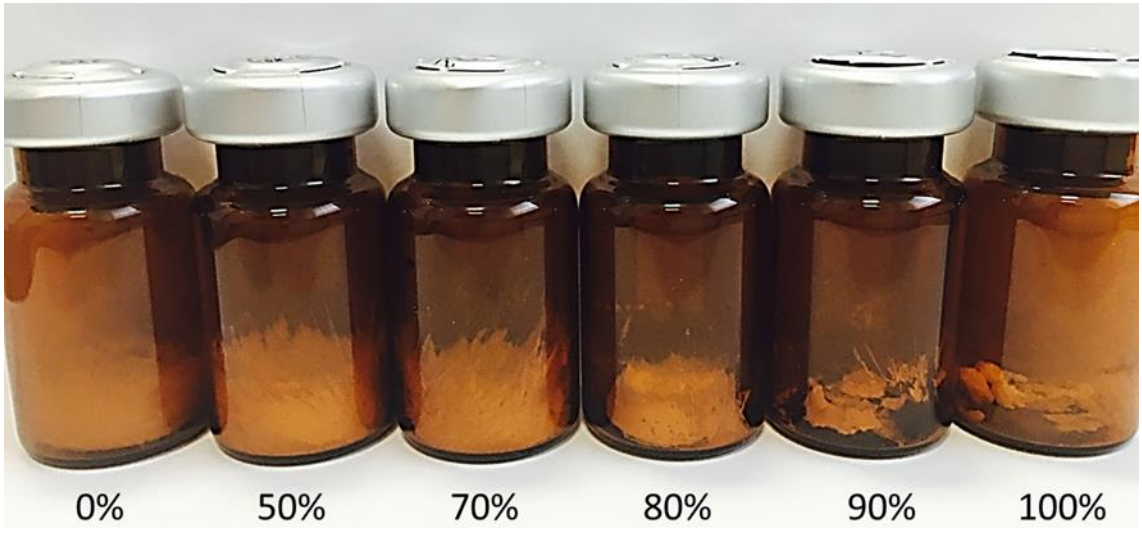

Figure 2.15 Freeze-dried samples from a 5 day primary drying batch. The presented percentage indicates the w/w percentage of nifedipine in the overall weight of vial content. Left to right showing low to high w/w % of NIF in PVP.

2.4.2.1. Residual solvent

Freeze-dried cakes were tested for residual solvent by loss of weight method using differential scanning calorimetry (Grodowska and Parczewski, 2010). Figure 2.16 below presents average (n=3) w/w % residual solvent for each of the freeze-dried compositions, determined as the weight loss upon heating samples between 5 to 8 mg to 200 ^{o}C under nitrogen (Grodowska and Parczewski, 2010). The w/w % of residual solvent was calculated based on the accurately determined weight of the sample before and after heating, measured using a 6 digit figure. The same measurements were performed on physical-mix samples with the same number of replicates. To confirm accuracy of the DSC method, the residual solvent content for FD 50% NIF in PVP was also determined using the TGA. Results generated by the TGA method found to fall within the range of residual solvent content determined by the DSC method (13-14 w/w %).

Results have shown that freeze-dried and non-freeze-dried samples of nifedipine hold similar amounts of residual solvents of just below 2% w/w. Similarly, freeze-dried and non-freeze-dried pure PVP, hold similar amounts of residual solvent: 12.5% and 14.9% w/w respectively (Figure 2.16). The increment in the observed w/w % residual solvent in physical-mix was linear with increasing PVP concentration (w/w % of residual solvent = -0.132 [w/w % of NIF in PVP] + 0.138; R^2 = 0.9, n = 33). This is expected, as for every mole or unit weight of PVP added to the physical-mix, the same amount of water

is added. Freeze-dried formulations on the other hand, showed a jump of approximately 7% in the residual solvent content between pure nifedipine and 90% w/w NIF in PVP, indicating that freeze-dried cakes of NIF-PVP hold more residual solvent. This may be as a result of their open and porous structure.

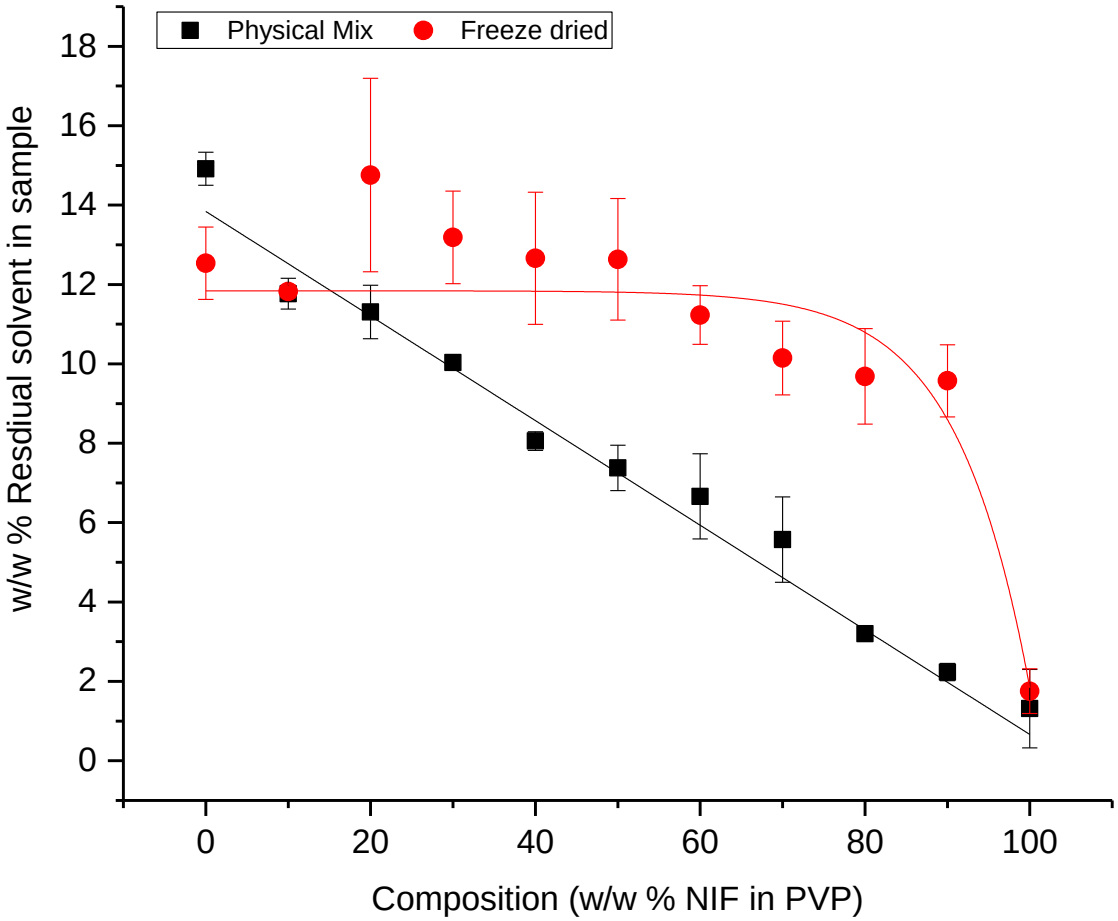

Figure: 2.16 Average w/w % of residue solvent in FD samples and physical mix controls. (Error bars present standard error of n=3).

2.4.3. Crystalline of nifedipine in formulation

The physical state of the freeze-dried material was characterised using thermal, optical microscope and FT-IR techniques. The aim was to determine whether or not nifedipine was molecularly dispersed in PVP, and therefore determining the physical state of nifedipine in different freeze-dried compositions as well as the controlled samples. As a result the effect of w/w % of PVP on the physical state of freeze-dried nifedipine was investigated.

2.4.3.1. Analysis by differential scanning calorimetry

The thermal properties of the individual components were investigated. Figures 2.17 and 2.18 present the thermograms of pure as-received nifedipine and PVP respectively. Using the DSC developed method, it was found that nifedipine as received, when in the crystal form, melts at 172.4 ± 0.1 ^{o}C (Fig 2.17-first heat). Literature value of nifedipine melting onset ranges from 172-174 ^{o}C (Wang *et al.*, 2005). Nifedipine can exist in three mono-tropically related modifications, modification I, otherwise referred to as α-NIF (Gunn *et al.*, 2012), which is thermodynamically stable at room temperature, was reported to melt in the range 169-173 ^{o}C. Modification II or β-NIF, m.p. 161-163 ^{o}C, and modification III or δ-NIF, m.p. 135 ^{o}C, (Gunn *et al.*, 2012) are metastable modifications. DSC thermograms performed in this study have shown that as received nifedipine is present as α-NIF, later confirmed using FT-IR. However, second heat thermograms of as received nifedipine show an additional small peak at 162.9 ± 0.2 ^{o}C (Fig 2.17), this peak is attributed to β-NIF (Wang *et al.*, 2005). The second heat thermogram of NIF, also shows a slight endothermic drop in the bassline at 46.7 ± 0.3 ^{o}C, indicative of the T_g of amorphous nifedipine. Literature T_g of nifedipine equals 46.2 ± 0.2 ^{o}C (Miyazaki *et al.*, 2007). The second heat also shows an exothermic peak at 100.9 ± 0.2 attributed to the recrystallization of amorphous nifedipine.

First and second heat thermograms for the as received PVP (Fig 2.18) appear different. A large broad endothermic peak is observed with an onset of 53.1 ± 8.3 ^{o}C and peak max at 98.03 ± 9.2 ^{o}C on the first heat thermogram. This peak is diminished in the second heat, thus attributed to the evaporation of residual water retained by PVP. Weight loss of sample after first heat (14.9 ± 0.6% w/w) further supports this conclusion. Due to this broad solvent peak, the glass transition of PVP K10 is only apparent in the second heat thermogram 146.06 ± 2.8 ^{o}C. Comparison of the observed T_g for PVP K10, of "zero" moisture content, with data reported by other authors was not possible as the literature values for T_g of dried PVP K10 vary widely from one study to another (65.8-123.8 ^{o}C) (Buera *et al.*, 1992). This could be a result of differences in the method of drying and the rate of heating. The average molecular weight distribution and the cross-linking degree will also influence T_g (Buera *et al.*, 1992).

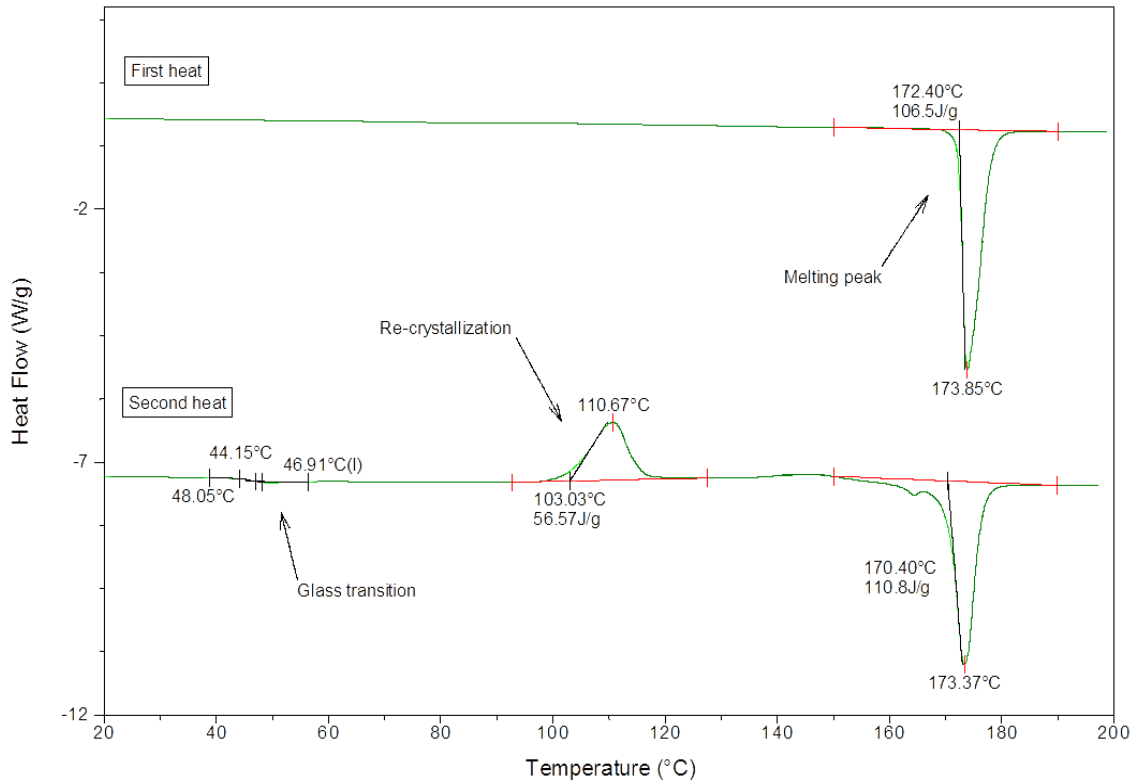

Figure 2.17 First and second heat thermogram of nifedipine as received. Heating and cooling rates were maintained at 10 °C/min.

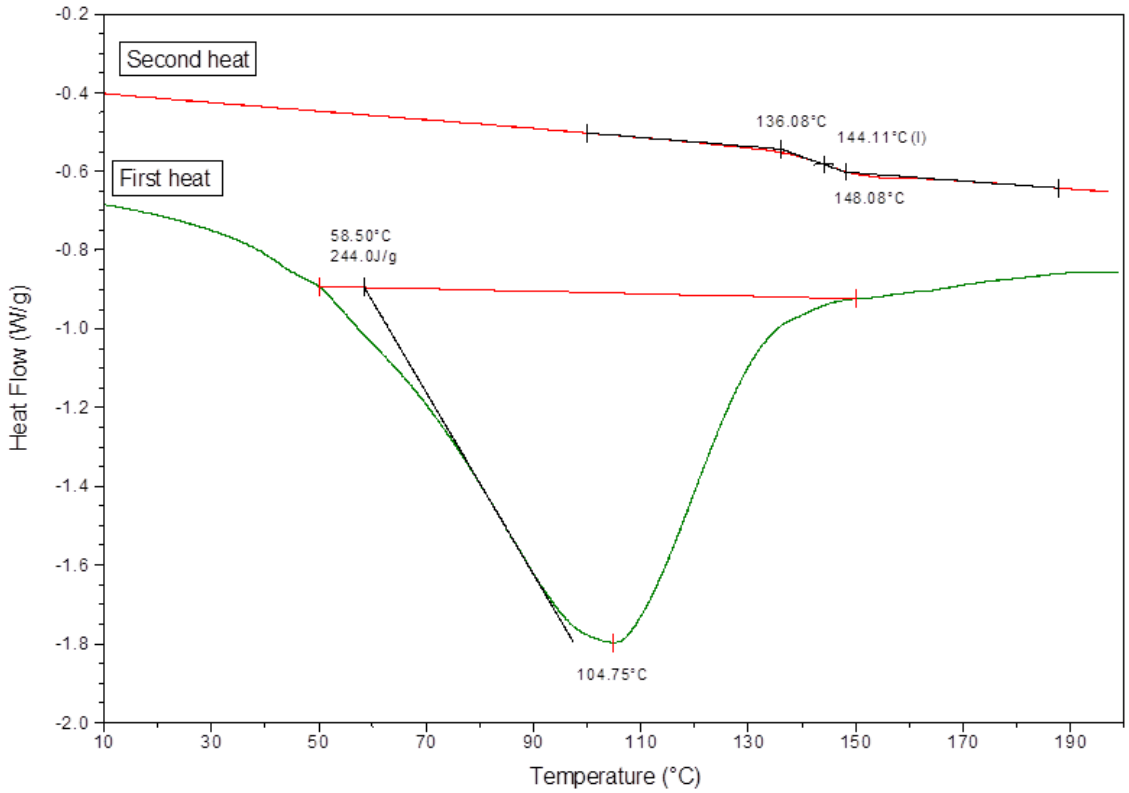

Figure 2.18 First and second heat thermogram of PVP K10 as received. Heating and cooling rates were maintained at 10 °C/min.

Freeze-dried formulations and physical-mix were analysed using the same method as nifedipine and PVP above (Fig 2.19 and 2.20 respectively). First-heat thermograms of freeze-dried formulations in figure 2.19 show the melting peak of nifedipine to broaden and diminish as the w/w % of PVP increases in the formulation, therefore indicating a decrease in the crystallinity of the formulation. The melting peak further disappears completely from thermograms of freeze-dried formulations containing ≤ 50% w/w NIF in PVP, therefore forming predominantly amorphous freeze-dried formulations.

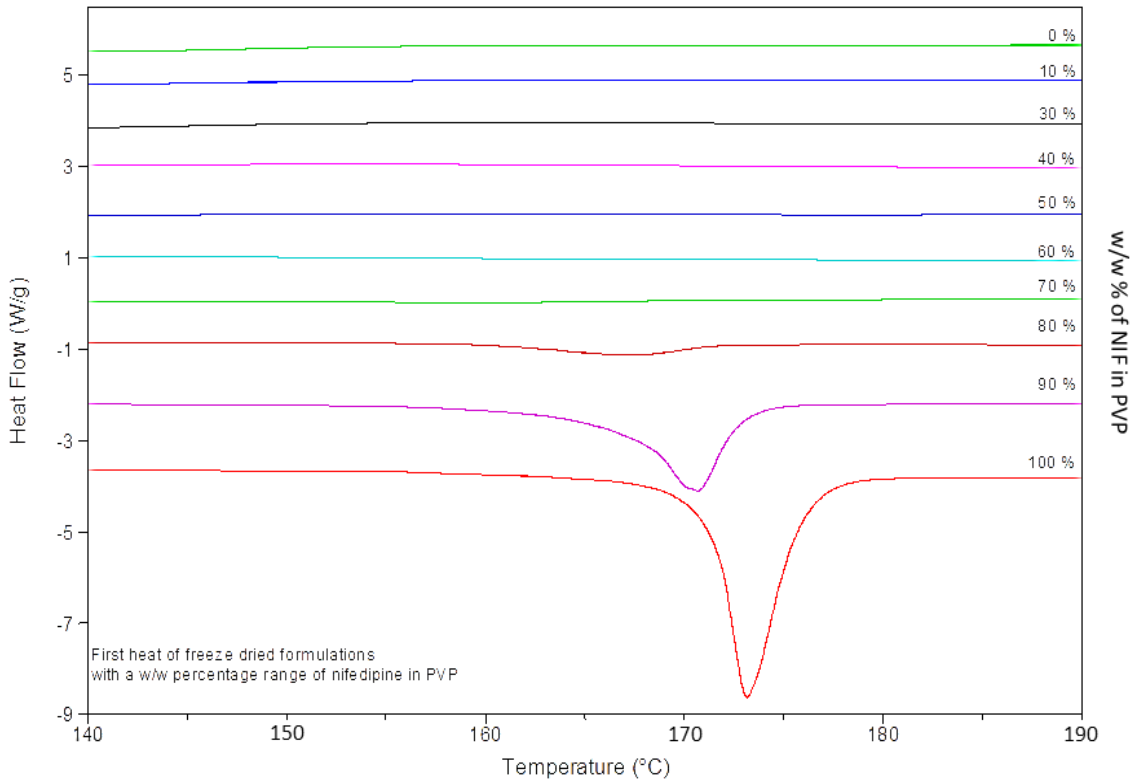

Figure 2.19 First heat of freeze-dried formulations. DSC cycle include a ramp from -10 to 190 °C at a rate of 10 °C/min. Each trace is labelled with the percentage of nifedipine w/w of the formulation it represents.

To accurately determine the content of crystalline nifedipine in formulations, a DSC assay based on enthalpy peak area (PA) was developed (Fig 2.21) for quantifying crystalline NIF in PVP. First-heat thermograms of physical-mix formulations (Fig 2.20) were used as calibration standards where the melting PA of nifedipine in the range 140-180 °C was measured for each of the equivalent nifedipine concentrations (n=3).

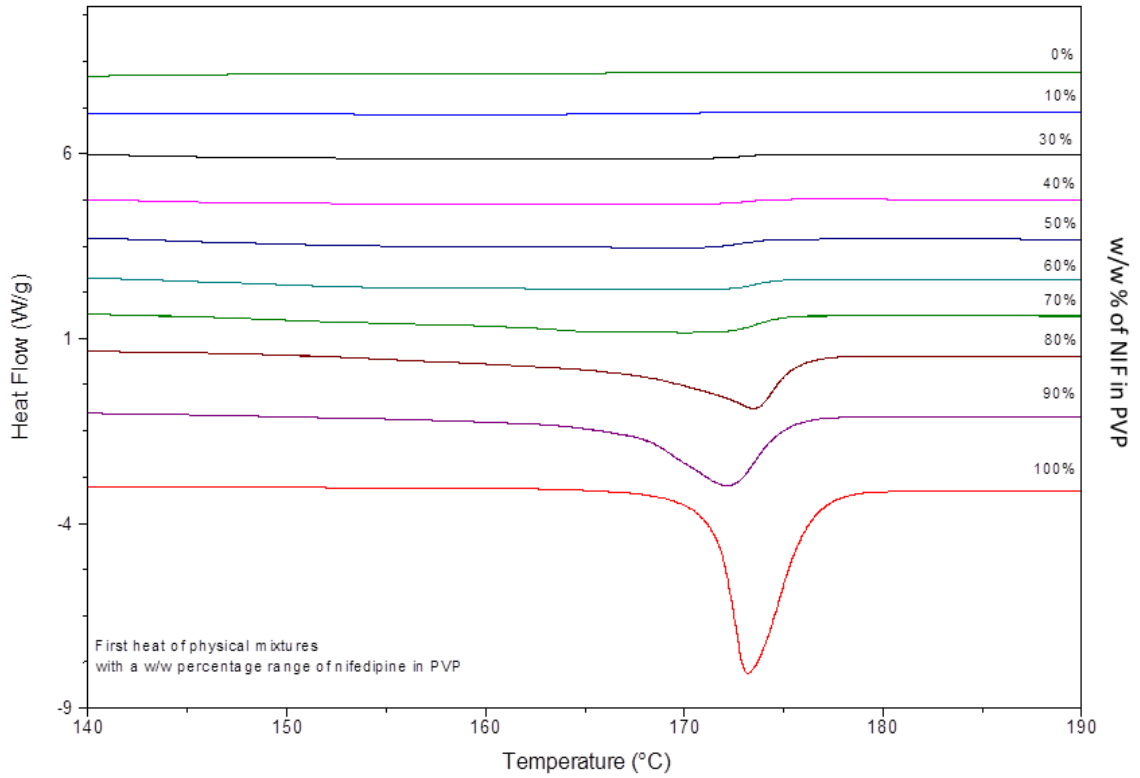

Figure 2.20 First heat of physical-mix formulations. DSC cycle include a ramp from -10 to 190 ^{o}C at a rate of 10 ^{o}C/min. Each trace is labelled with the percentage of nifedipine w/w of the formulation it represents.

PA's were recorded as enthalpy J/g using software TA universal analysis. Once recorded, the PA's were corrected for true sample weights by subtracting weigh of residual solvents. An example is provided below:

Example of PA correction for true sample weight (10% w/w NIF in PVP physical-mix)

Sample weight including residual solvent (RS) = 2.649 mg

Observed PA (for sample weight containing residual solvent) = **5.183 J/g** or 13.730 x10^{-3} J for 2.649 mg of sample

Sample weight after heating (true sample weight) = 2.340 mg

Corrected Enthalpy = 16.995 x10^{-3} J for 3.380 mg of sample or **5.865 J/g**

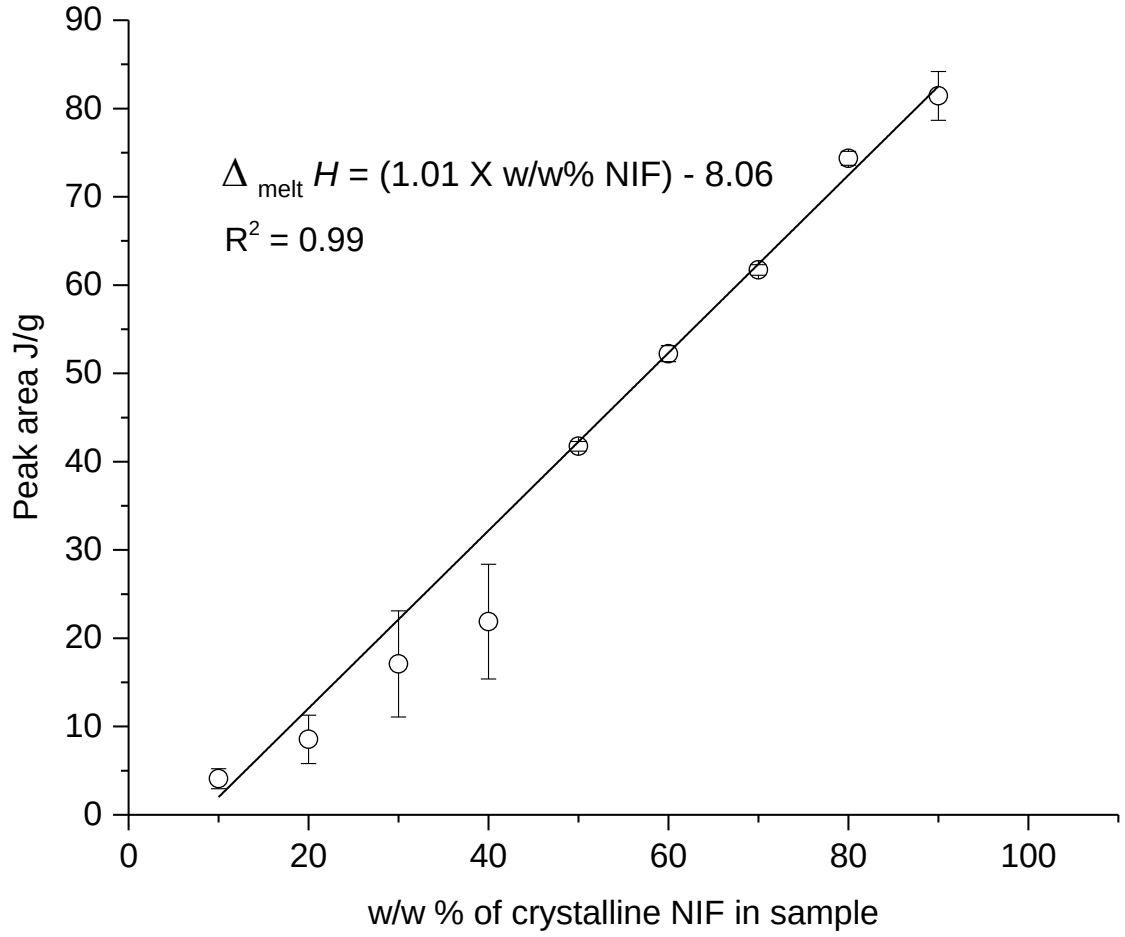

Figure 2.21 DSC assay for crystalline NIF, showing a linear relation between w/w % of crystalline nifedipine in PVP (x-axis) and enthalpy J/g (y-axis) measured in the range 135 – 185 ^{o}C. (Error bars represent the standard error of n=3).

The limit of detecting and quantifying crystalline nifedipine using the melting peak determined via the DSC method was calculated based on the ICH calibration curve method (ICH, 1996). The standard deviation of y-intercept of regression line, otherwise known as standard error of the regression, was calculated by performing regression analysis using Microsoft excel (table 2.5). Limit of detection (LOD) and limit of quantification (LOQ) are in w/w % crystalline nifedipine in PVP as presented in table 2.5 below.

Table 2.5 LOD and LOQ of crystalline nifedipine in PVP (w/w %).

Parameter	Source or equation	Value
Slope (S)	From figure 2.21	1.01
Standard error of intercept (SE)	From figure 2.21	1.57
LOD of crystalline NIF in w/w %	$= 3.3 \times \frac{\sigma}{S}$	5.15%
LOQ of crystalline NIF in enthalpy	$= 10 \times \frac{\sigma}{S}$	15.62%

The developed DSC assay was used to determine the w/w percentage of crystalline nifedipine in freeze-dried formulations and the equivalent melt-cooled formulations formed in DSC second heat. Figure 2.22 below presents a phase diagram of the effect of changing the composition on the crystallinity of the formulation.

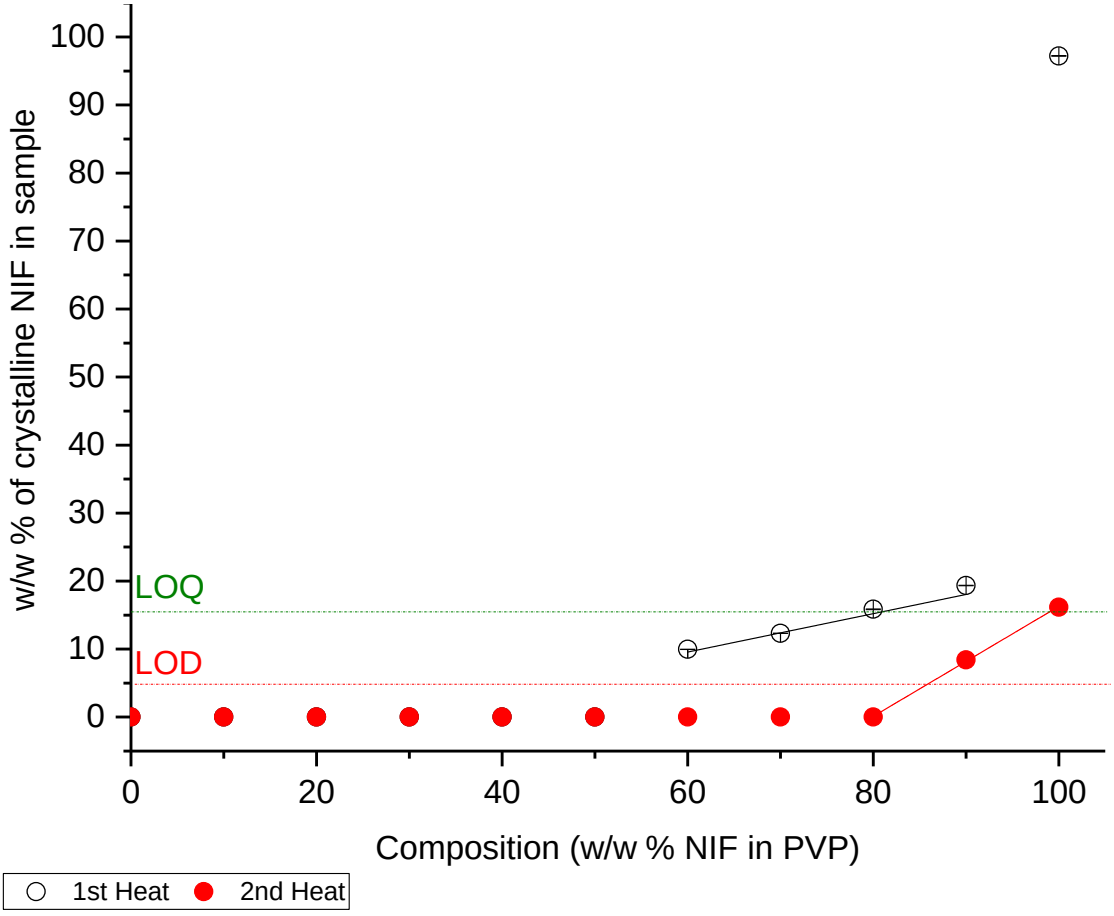

Figure 2.22 Crystallinity phase diagram for freeze-dried samples at first and second heat. Recrystallization peak, if present, was deducted from melting enthalpy to determine original amount of crystalline nifedipine in freeze-dried samples (Error bars represent the standard error of n=3).

2.4.3.2. Cross Polarization microscopy.

Crystals have a specific property of bending polarized light travelling through them, this result in decreasing the speed of light leading to an effect known as birefringence. A full review on this topic can be found in the following reference (Carlton, 2011). This property of crystals allows them to be distinctively visible when observed under cross polarized microscopy. Amorphous material on the other hand, causes light, travelling through them, to scatter. Therefore, in the presence of polarized light, a microscopic image of an amorphous material would show no sign of birefringence. This technique was used in this study to qualitatively analyse freeze-dried formulations. Table 6 below presents the images taken of different freeze-dried compositions using unpolarised and polarized light. A difference was observed between pure amorphous PVP and crystalline nifedipine polarized images. The absence of birefringence indicates the absence of crystalline material. Freeze-dried formulations ≤50% w/w NIF in PVP appeared to be free from crystalline material. Images taken with polarized light for ≥70% w/w NIF in PVP showed a gradual increase of formulation crystallinity as the w/w % of nifedipine increases (replicate images of n=3 show similar results). Nevertheless, quantitatively comparing crystallinity of different formulations was difficult to achieve, as many factors can influence the number of crystals observed, such as mass and thickness of sample.

Table 2.6 Polarized and unpolarised light microscopy images of FD formulations

Images taken with unpolarised light	Images taken with polarized light	Description
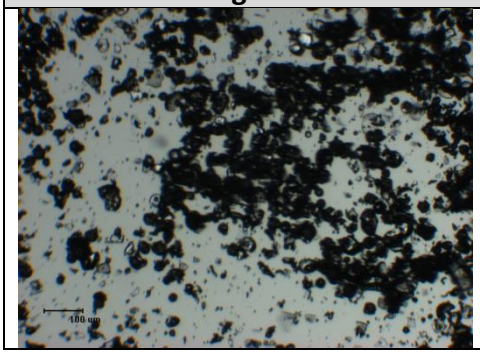	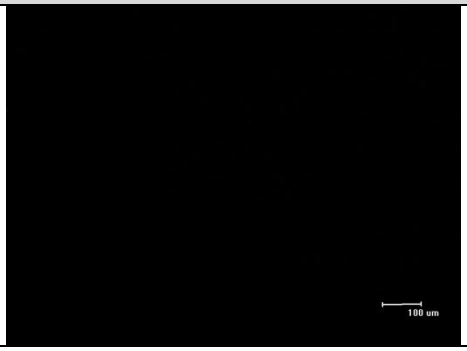	PVP as-received

Images taken with unpolarised light	Images taken with polarized light	Description
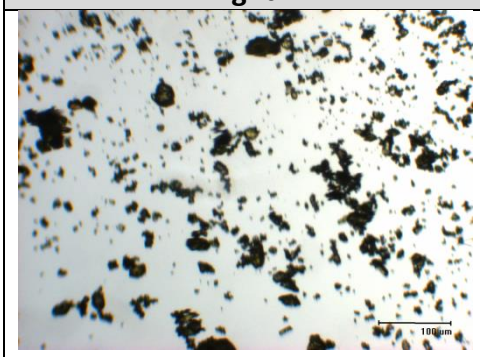	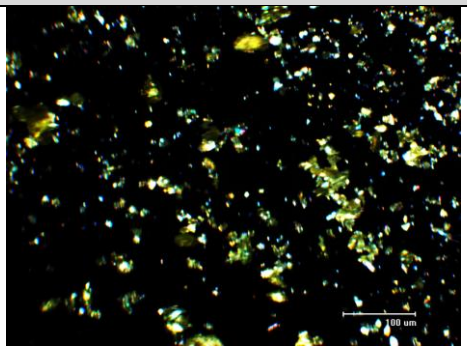	Nifedipine as-received
		0 w/w % freeze-dried nifedipine in PVP. No birefringence is caused by the sample when exposed to polarized light.
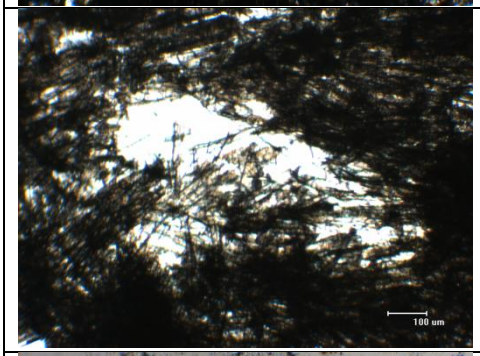		10 w/w % freeze-dried nifedipine in PVP. No birefringence is caused by the sample when exposed to polarized light.
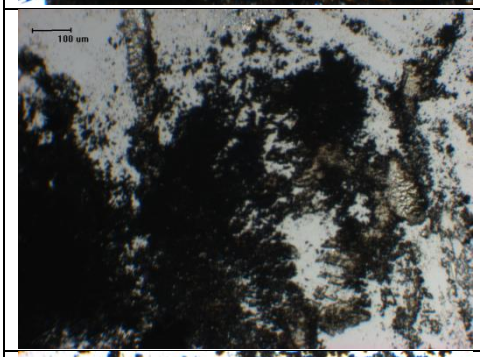	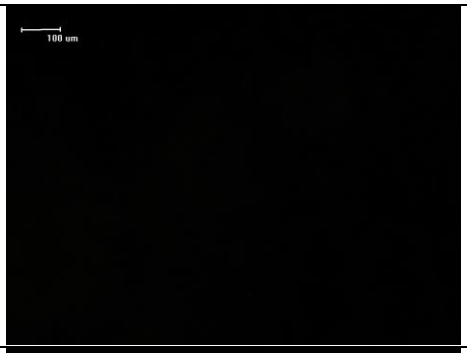	30 w/w % freeze-dried nifedipine in PVP.
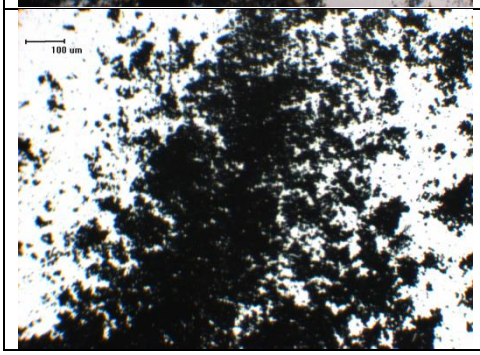		50 w/w % freeze-dried nifedipine in PVP. No birefringence is caused by the sample when exposed to polarized light.

Images taken with unpolarised light	Images taken with polarized light	Description
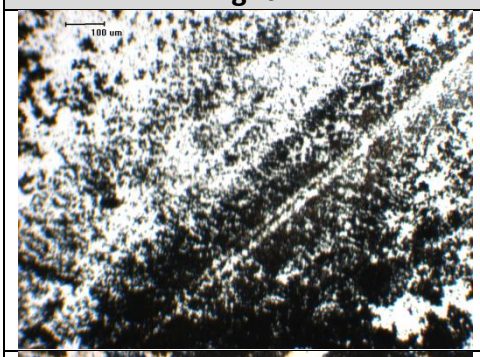		70 w/w % freeze-dried nifedipine in PVP.
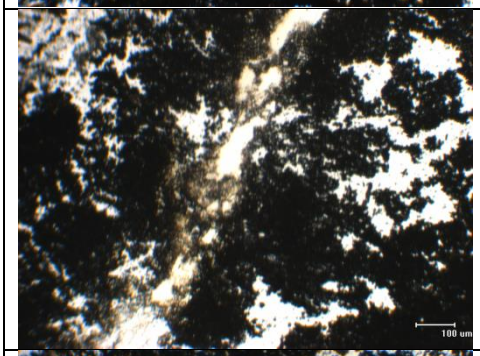	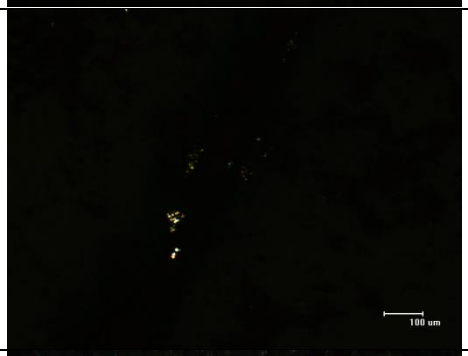	80 w/w % freeze-dried nifedipine in PVP. Birefringence is observed when the sample was exposed to polarized light.
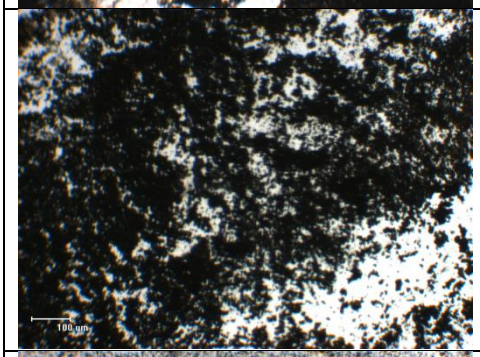	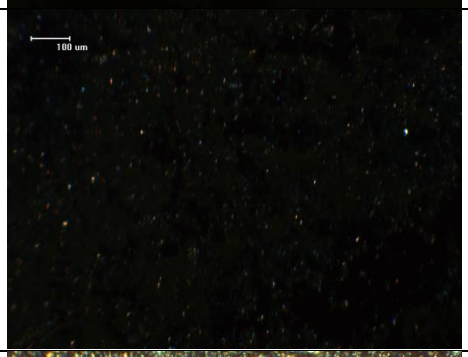	90 w/w % freeze-dried nifedipine in PVP. Birefringence is observed when the sample was exposed to polarized light.
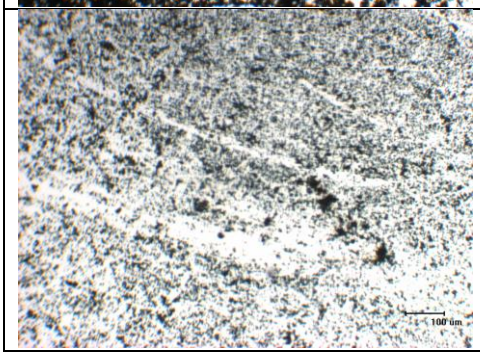	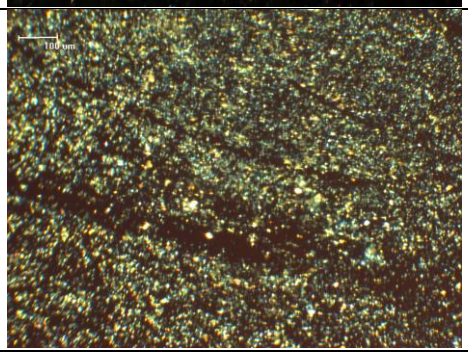	100 w/w % freeze-dried nifedipine in PVP. Birefringence is observed when the sample was exposed to polarized light.

2.4.3.3. FT-IR Amorphous and crystalline content

FT-IR is another analytical tool that was explored in identifying amorphous and crystalline nifedipine (Chan *et al.*, 2004, Hishikawa *et al.*, 1999). Presented below (Figure 2.23) is an FT-IR spectrum of pure nifedipine as received, pure PVP as received, pure amorphous nifedipine (as a result of heat-melt), 50% w/w NIF in PVP freeze-dried formulation (labelled NIF in PVP FD) and 50% w/w NIF in PVP physical-mix (labelled NIF

in PVP PM). FT-IR spectrum of nifedipine as received has shown the main characteristics of the thermally stable α-NIF spectrum reported by (Chan *et al.*, 2004), which exhibits relatively low C=O (doublet centred at 1680 cm^{-1}) and N-H (3328 cm^{-1}) wavenumbers, compared to other nifedipine polymorphs. This is due to strong intermolecular hydrogen bond interactions between the ester carbonyl and the NH group of the adjacent molecule. (Chan *et al.*, 2004) Pure amorphous nifedipine was created by melting nifedipine in a DSC pan and cooled rapidly. The FT-IR spectrum of amorphous nifedipine shows distinct difference to the crystalline nifedipine in the sharpness and definition of peaks, specifically in the 1700 cm^{-1} region, this is characteristic of amorphous material (Grisedale *et al.*). The (N-H) was also shifted to the left indicating less or weaker intermolecular hydrogen bond interactions in amorphous nifedipine.

Freeze-dried nifedipine in PVP (Fig 2.23) also shows clear distinctive IR features from the crystalline physical-mix nifedipine in PVP, with the most pronounced differences also found in the (N-H) and the carbonyl regions. The single peak observed in the (C=O) region in the freeze-dried formulation spectrum is distinctive of molecularly dispersed amorphous nifedipine (Iqbal and Chan, 2015). This distinctive peak is seen to shift to 1678 cm^{-1} in the crystalline physical mix, and therefore may be used as a marker to monitor the crystallization of nifedipine in freeze-dried formulations. However the 1678 cm^{-1} band is thought to be affected by the water band bending mode absorption at ~1640 cm^{-1} (Iqbal and Chan, 2015). Additionally, PVP was shown to absorb in the (N-H) and carbonyl regions (Fig 2.23), which made these regions difficult to use to semi-quantitatively monitor crystalline nifedipine in freeze-dried formulations. Nevertheless, the shape and location of peaks in these regions (N-H and C=O) may be used to qualitatively analyse the physical state of nifedipine in freeze-dried formulations. Figure 2.24 presents the N-H and carbonyl regions of the full range of freeze-dried formulations. A clear change in the shape and location of the C=O peak (1660 – 1680 cm^{-1}) was observed at 70 and 80% w/w NIF in PVP. Due to the presence of strong and broad PVP absorbance in the N-H region, it is very difficult to monitor the change in the N-H peak as the composition of freeze-dried formulations ranges from 10-90 w/w %.

Another region that was observed to be distinctively different between molecularly dispersed amorphous nifedipine in PVP and the crystalline nifedipine in PVP physical-mix is the 800-700 cm^{-1} out of plane δ(C-H) vibration of the ring regions, where PVP has very little absorbance effect (Fig 2.23 and 2.24). Pure crystalline nifedipine shows distinctive peaks at 793, 762 and 744 cm^{-1} which are also shown in crystalline nifedipine in PVP physical-mix (Chan *et al.*, 2004, Iqbal and Chan, 2015). Pure amorphous nifedipine on the other hand, shows distinctive peaks at 784 and 754 cm^{-1} which are also observed in freeze-dried nifedipine in PVP. Peak located at 711 cm^{-1} is a common peak present in all nifedipine containing spectra, independent of the physical state of nifedipine, and may therefore be used as an internal standard for quantitative analysis (Iqbal and Chan, 2015). Iqbal and Chan (2015) was reported to using the ratio of the crystalline indicative 762 cm^{-1} PA against the standard PA at 711 cm^{-1} to semi-quantify crystalline nifedipine in molecularly dispersed nifedipine formulations. The absence of the 762 cm^{-1} peak indicated the absence of crystalline nifedipine on the outer surface of the sample, and thus samples showing PA rations ≤0.05 where considered, by Iqbal and Chan (2015), predominantly amorphous.

Unlike the study performed by Iqbal and Chan (2015), this study has shown all freeze-dried formulations do not show a peak at 762 cm^{-1}. However, a clear change in the 754 cm^{-1} peak shape accompanied with a slight change in peak position was observed (figure 2.25). While amorphous NIF shows a single broad peak at 754 cm^{-1}, crystalline NIF shows two peaks either side this wave number, 744 cm^{-1} and 762 cm^{-1}. The gradual change from amorphous to crystalline NIF, causes the amorphous 754 cm^{-1} peak to gradually change in shape where for example, freeze-dried 90% w/w NIF in PVP shows a clear shoulder towards the 762 cm^{-1} crystalline peak, which maybe early signs of nifedipine crystallization, such as the formation of nifedipine dimers in small clusters.

To semi-quantify the change in peak shape, peak asymmetry was calculated for each formulation (n=3), after adjusting spectra bassline by subtracting pure PVP spectra. The peak asymmetry was calculated using the HPLC frequently used equation (Peak Asymmetry = B/A at 10% peak height) where B and A are the left and right half widths of the peak respectively. Using OriginPro software, peak asymmetry was calculated and plotted for the composition range of the freeze-dried formulations (Figure 2.26).

Freeze-dried 10% w/w NIF in PVP was not included, as peaks in the range 800-700 cm^{-1} were very small and difficult to integrate. Figure 2.26 shows the 754 cm^{-1} peak asymmetry of ≤ 60% freeze-dried NIF in PVP formulations to be in the range 0.9-1.1, which is considered asymmetrically acceptable by HPLC ICH guidelines (Deepti and Pawan, 2013). However, changing the composition of the freeze-dried formulation to contain ≥ 70% NIF in PVP resulted in a sharp increase in the peak asymmetry, indicating a large change in the shape of peak and thus strong early signs of small clusters of crystalline nifedipine.

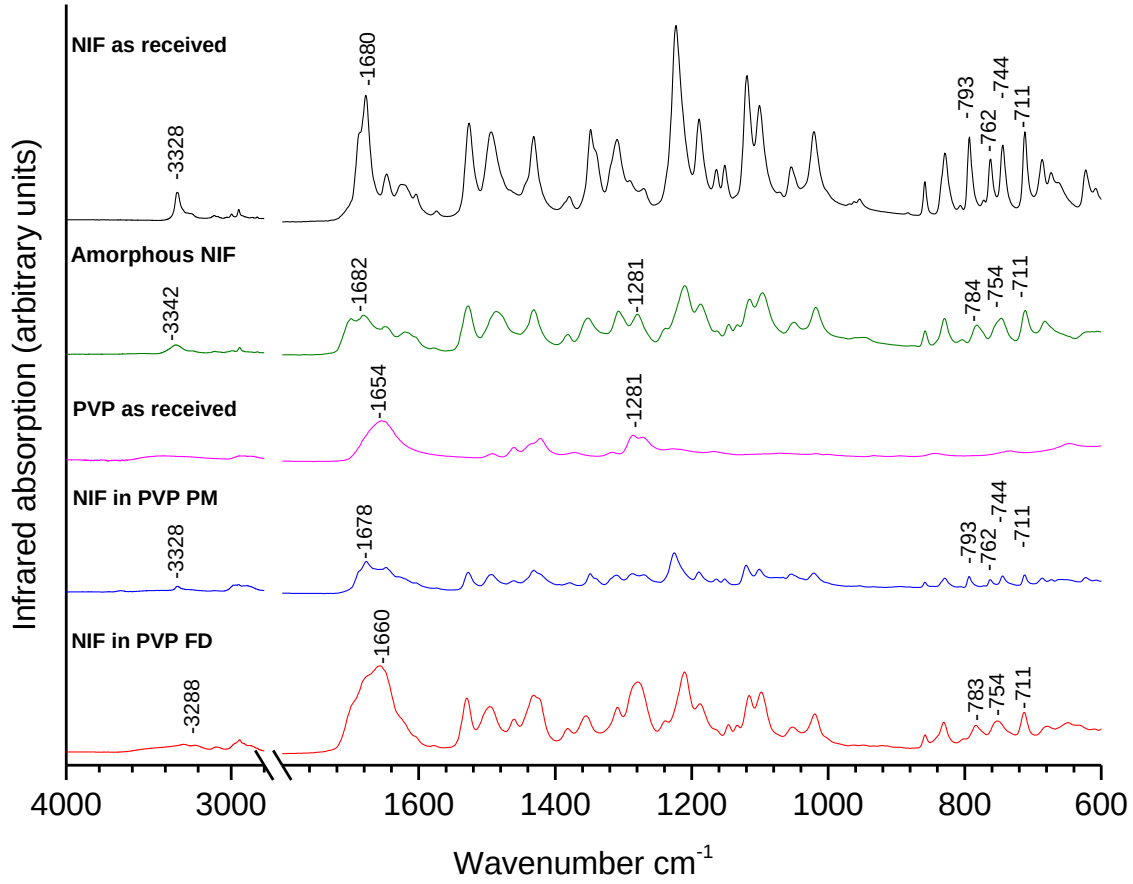

Figure 2.23 FT-IR spectra of crystalline nifedipine as received, amorphous nifedipine (produced by heat melt), PVP as received, 50% w/w crystalline NIF in PVP as physical-mix (NIF in PVP PM) and Freeze-dried 50% w/w NIF in PVP (NIF in PVP FD). FT-IR measurements were repeated to ensure data reproducibility (n=3).

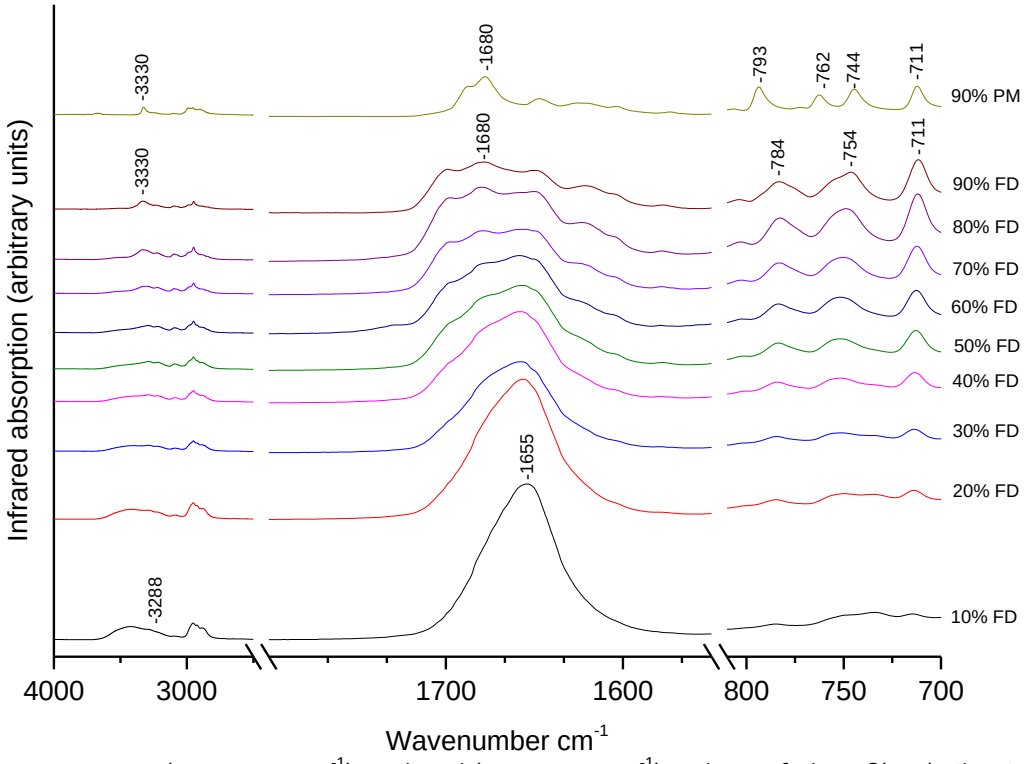

Figure 2.24 N-H (3288-3330 cm^{-1}), Carbonyl (1660-1680 cm^{-1}) and out of plane δ(C-H) vibration of the ring (800-700 cm^{-1}) regions of the FT-IR spectrum for the full range of freeze-dried NIF in PVP formulations compared to the 90% w/w NIF in PVP physical-mix of crystalline NIF in PVP. All percentages listed are of NIF in PVP. FT-IR measurements were repeated to ensure data reproducibility (n=3).

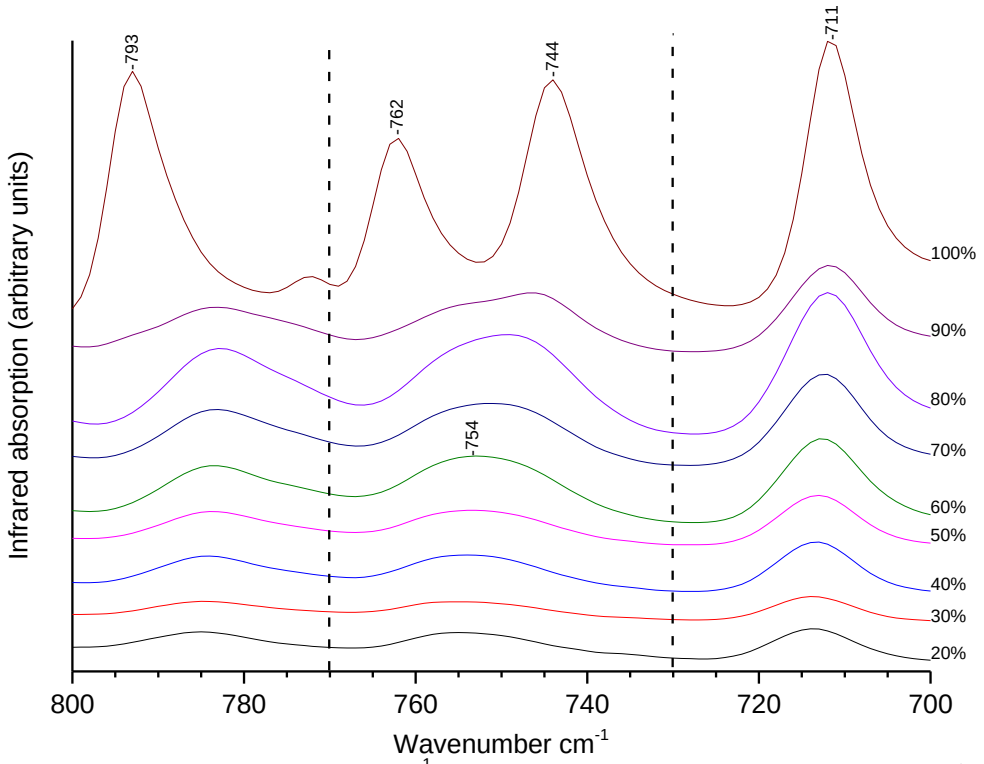

Figure 2.25 FT-IR spectra, (800-700 cm^{-1} only) of freeze-dried formulations 20-100% w/w NIF in PVP. Peak symmetry change at 754 cm^{-1} (peak distinctive of amorphous nifedipine) was examined. 90% w/w NIF shows a clear left shoulder. FT-IR measurements were repeated to ensure data reproducibility (n=3).

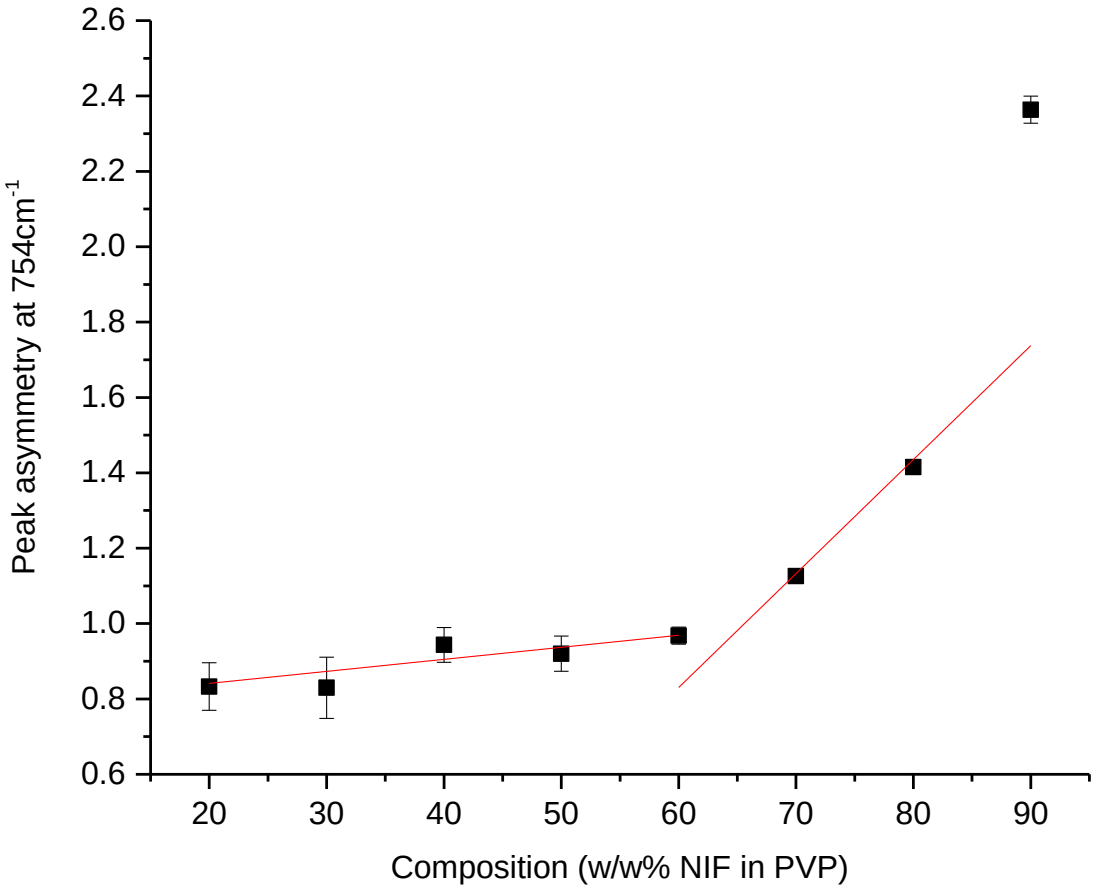

Figure 2.26 Monitoring NIF crystallinity in freeze-dried formulations using FT-IR peak symmetry at 754 cm^{-1}. A change in peak symmetry is indicative of a change in physical state, as amorphous NIF presents a single broad and asymmetric peak at 754 cm^{-1} and crystalline NIF presents 2 separate peaks at 762 cm^{-1} and 744 cm^{-1}, the gradual change from the broad amorphous peak to the double crystalline peaks can be quantitatively measured through peak symmetry measurements. Error bars represent standard error of n=3.

2.4.4. Drug Polymer interaction

2.4.4.1. FT-IR intermolecular bonding

FT-IR results show the N-H peak in pure amorphous nifedipine 3342 cm^{-1} (Fig 2.27 A) shifts to 3288 cm^{-1} in freeze-dried formulations of nifedipine in PVP. Indicating a strong intermolecular hydrogen bonding between the N-H group of nifedipine and the carbonyl group in PVP (Rumondor *et al.*, 2009). Equally the shift of the C=O carbonyl group from 1681 cm^{-1} in pure amorphous nifedipine to 1660 cm^{-1} in freeze-dried formulations (Fig 2.27-B) is another strong indication of hydrogen bonding interactions between the carbonyl group of PVP and the N-H group of nifedipine (Rumondor *et al.*, 2009) (Fig 2.28).

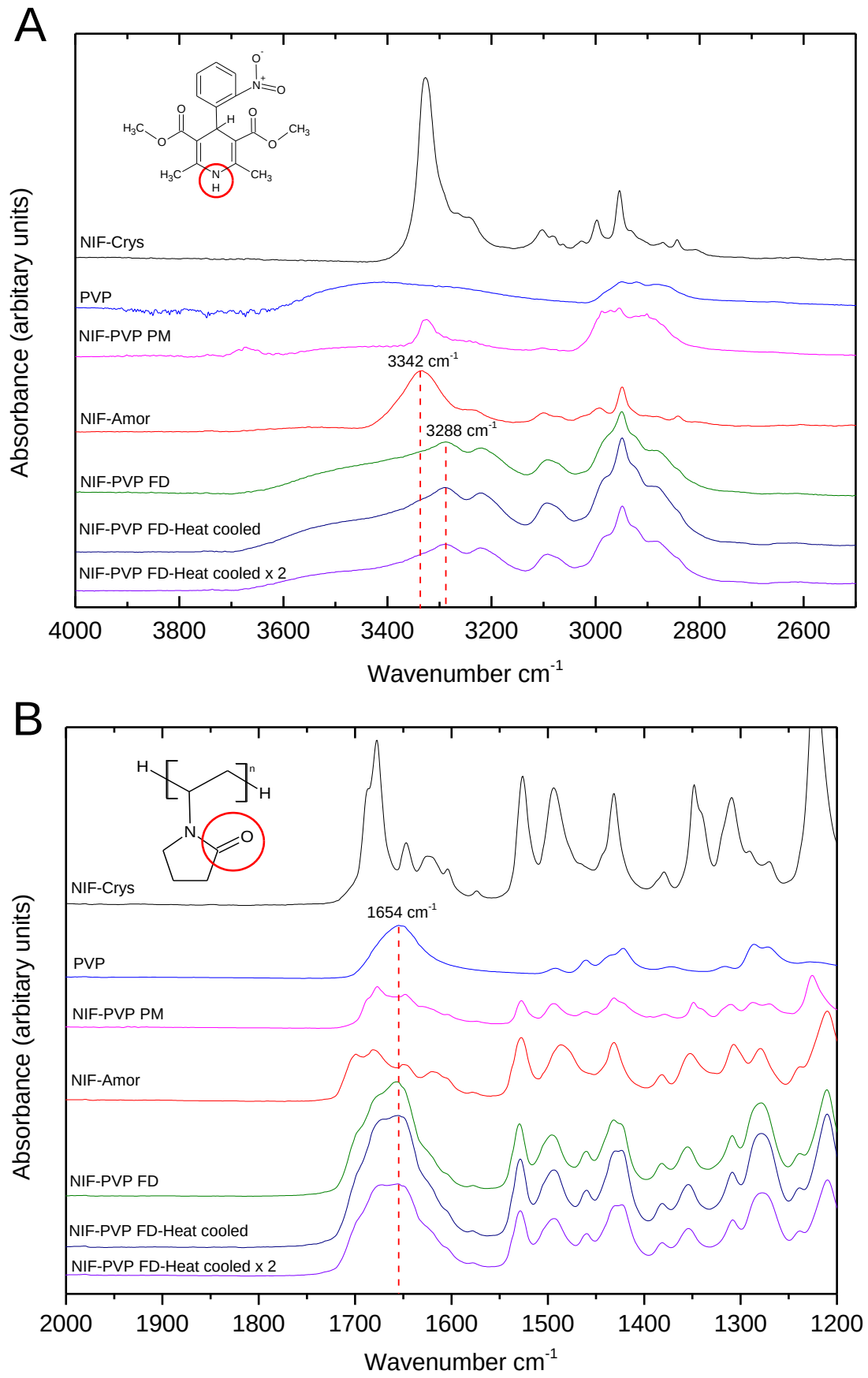

Figure 2.27 **(A)** N-H and **(B)** Carbonyl regions of a range of nifedipine containing samples to demonstrate differences in drug-polymer interactions. Repeats of n=3.

This drug-polymer interaction observed through FT-IR analysis has shown to be present in both freeze-dried formulations as well as heat-cycled formulations resulted by melting freeze-dried samples by DSC. Melting a cooled (heat-melt) sample for the second time has shown not to affect the drug-polymer interactions nor degrade the drug at a detectable level using FT-IR analysis (Fig 2.27). However stability indicating HPLC assay for NIF will be used to further confirm the effect of heating on the chemical stability of NIF in following chapters (Chapter 3).

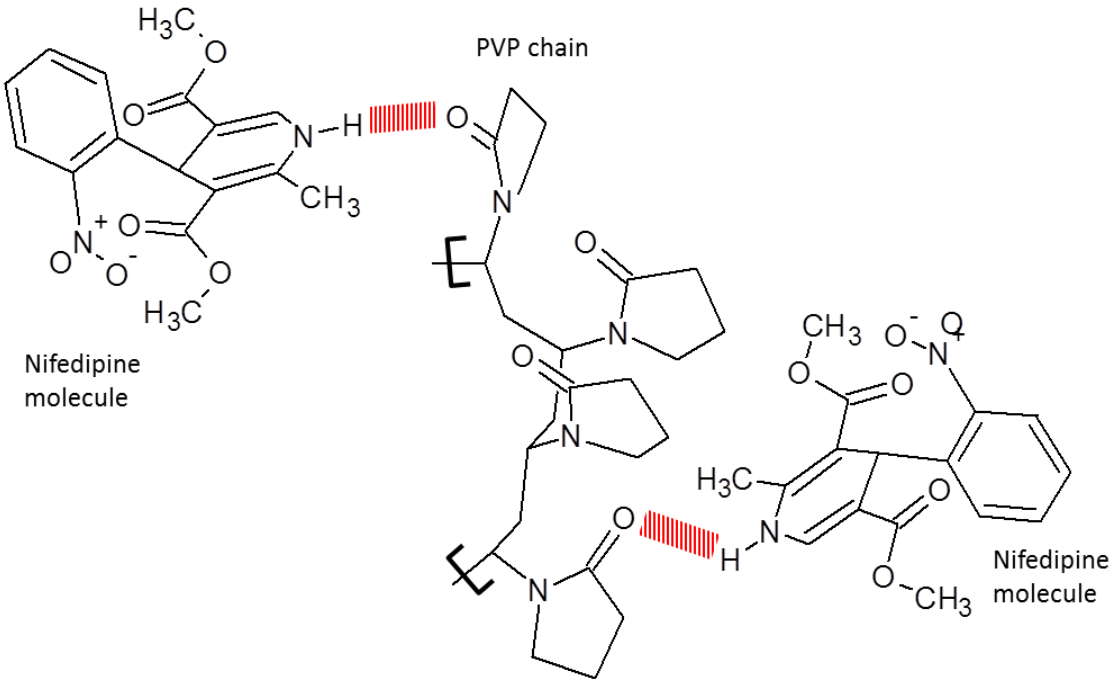

Figure 2.28 A proposed model for the intermolecular hydrogen bonding between nifedipine and PVP based on the IR spectra (Fig 2.27). Hydrogen bonds are presented in red. This figure was constructed using ACD/ChemSketch.

2.4.4.2. Glass Transition

The experimentally determined glass transition temperature (T_g) of pure amorphous nifedipine, created by heat-cooling freeze-dried pure nifedipine in the DSC, was determined to be 46.7 ± 0.8 ^{o}C, which as would be expected, is similar to the determined T_g of amorphous nifedipine prepared by heat-cooling as received nifedipine, in the DSC, (46.7 ± 0.3 ^{o}C). Pure amorphous PVP k10, prepared from freeze-dried pure PVP, showed a reproducible T_g of 151.8 ± 1.5 ^{o}C, slightly higher than the determined T_g of PVP as received 146.1 ±2.8 ^{o}C, both of which determined via second heat DSC. (Literature values listed in section 2.4.2.3.1).

Dispersing the two components into a continuous phase has shown to result in a material with a single compensated T_g value, which as shown by figure 2.29 is dependent on the ratio of both components. One of the most used models to study the dependence of T_g on the composition of binary dispersions is the Gordon-Taylor equation (Brostow *et al.*, 2008):

$$T_g = \frac{x_1 T_{g1} + K_{GT}(1 - x_1)T_{g2}}{x_1 + K_{GT}(1 - x_1)} \qquad \text{Equation 2.1}$$

Where T_{g1} and T_{g2} are the experimentally determined glass transition temperatures of pure component 1 and 2 respectively, x_1 is the mass fraction of component 1, K_{GT} (referred to as Gordon-Taylor's constant) is the constant ratio of thermal expansion coefficient difference between a glassy and a liquid state of the components 1 and 2 (Seo *et al.*, 2006), i.e. the unequal contributions of components 1 and 2 to the T_g of the binary solid dispersion (Brostow *et al.*, 2008, Seo *et al.*, 2006). K_{GT} can sometimes be approximated to the ratio of the density of the 2 components (Royall *et al.*, 1999). Finally T_g is the resulting glass transition temperature of the binary solid dispersion (Brostow *et al.*, 2008). The Gordon-Taylor model assumes perfect volume additivity (Royall *et al.*, 1999), where the size and shape of the 2 components, in the binary mix, is unchanged (Seo *et al.*, 2006); thus the packing fraction of the 2 components in the binary dispersion remains the same with no intermolecular interaction between the 2 components (Royall *et al.*, 1999).

Figure 2.29 below, shows the experimentally determined T_g*'s* for each of the freeze-dried NIF-PVP cakes. Despite the FT-IR based evidence of drug-polymer interactions observed in freeze-dried and hot-melt formulations of NIF in PVP, the observed experimental T_g values were found to fit the Gordon Taylor equation (Fig 2.29) whilst K_{GT} equalled 1.02. The K_{GT} value was correlated to the strength of the interaction between the 2 components (Lu and Weiss, 1992).

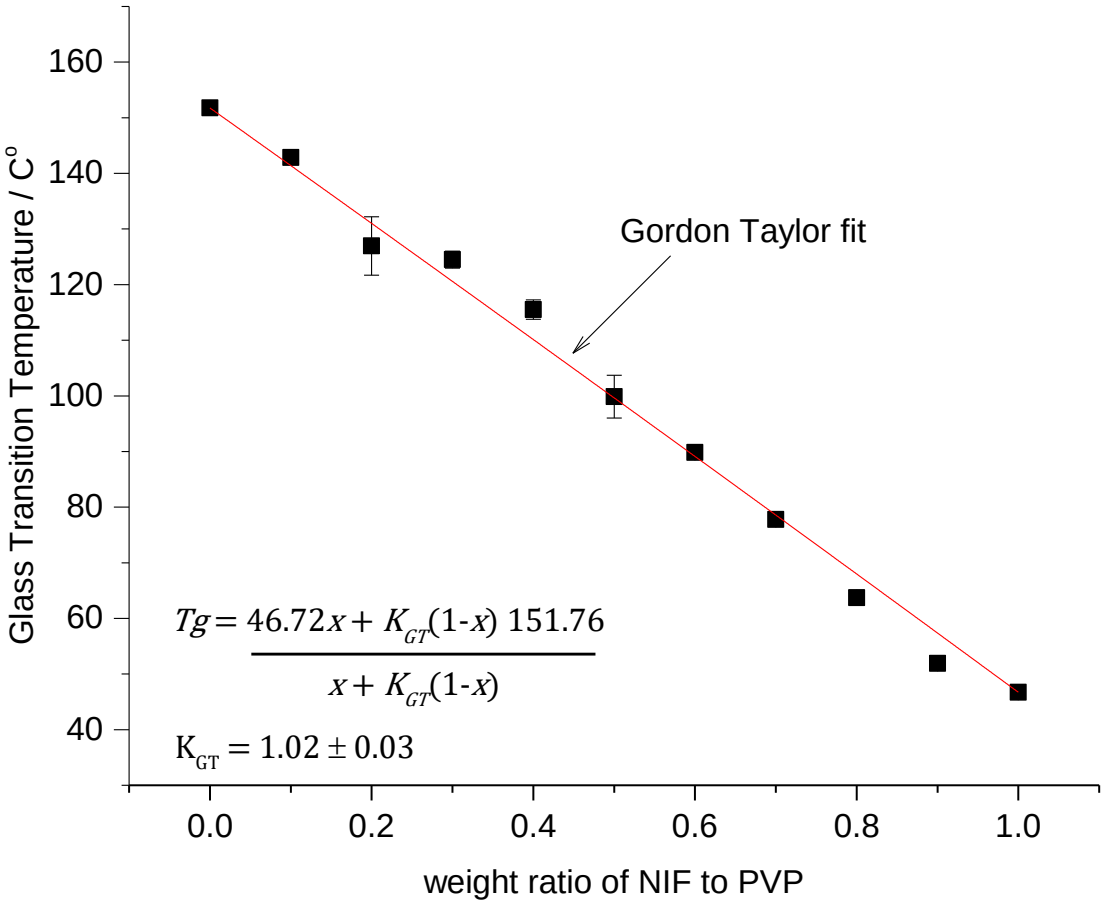

Figure 2.29 Average T_g of heat cycled samples of nifedipine in PVP. The data was fitted with a Gordon Taylor equation using OriginPro. (Error bars represent standard error of n=3).

2.5. Discussion

A freeze-drying method was developed to produce molecularly dispersed amorphous nifedipine in PVP freeze-dried formulations. The freeze-drying cycle was designed to provide the needed conditions to ensure a porous freeze-dried cake is produced with no signs of shrinkage or melting. The freezing stage is one of the critical steps in the process of freeze-drying. Franks and Auffret (2008) have described slow cooling rate as a critical step in the creation of large ice crystals which later have a positive effect on the rate of sublimation. Taking this into account, the TBA based feed solutions in this study were left to crystalize just below room temperature (18-24 ^{o}C) to ensure the formation of large TBA solid crystals. Furthermore, Tang and Pikal (2004) described the disadvantage of using a precooled shelf as a mean to freeze feed solutions, as it was shown to give large heterogeneity in cooling between vials. This therefore supports the initial freezing step performed at stable room temperature. Once feed solutions have crystallized, they were cooled further to -80 ^{o}C to ensure product temperature is below collapse temperature and thus avoid sample melting or collapse during freeze-drying (Tang and Pikal, 2004).

Determining the primary drying end point was directly related to the sublimation process of TBA. Tang and Pikal (2004) described how the end point of primary drying may be determined by chamber pressure. Once all ice crystals have sublimed, or in the case of this study, TBA crystals, the vapour composition in the freeze-drying chamber changes from essentially all TBA vapour during primary drying to mostly air, thus a drop in pressure along with stabilization is a good indication of primary end point. Although product temperature, determined by micro thermocouples, is also used by many to determine the end point of primary drying, it can be very miss leading. Roy and Pikal (1989) have shown that vials containing thermocouples are not representative of the batch as a whole due to the formation of larger ice crystals and thus show a faster sublimation which as a result require shorter primary drying time. Nevertheless the temperature of the drying chamber was monitored throughout the primary drying stage to ensure it is maintained above T'_g.

Secondary drying is a stage at which remaining solvent is removed by desorption to further increase the product stability at room temperature. A critical requirement of

this stage is heating, nevertheless, the laboratory freeze dryer (Lyotrap) used in this study does not provide a heating option, thus secondary drying was performed under room temperature (18-25 ^{o}C) for a period of 24 h. Pikal *et al.* (1990) have shown that short secondary drying stages (3-6 h) at high temperatures are better than a longer secondary drying at a low temperature as water desorption rate decreases dramatically with time at a given temperature. As part of the developed method, quality control tests have been implemented to ensure successful freeze-drying cakes are produced.

Freeze-dried formulations in the range 0-90% w/w NIF in PVP have shown the ability to retain residual solvents significantly greater than FD-100% formulation. This may be used as an indication to the physical state change between the FD-100% and other FD percentages as amorphous material is reported by Tang and Pikal (2004) to have a higher affinity to residual solvents than crystalline materials. Additionally the large jump in % residual solvent (Fig 2.16) may be a direct result of a sharp increase in surface area by developing FD porous structures. Increasing the ratio of PVP to nifedipine in the freeze-dried system has showed to steadily increase the materials ability to retain residual solvent. However a significant drop in w/w % residual solvent was observed in FD 10% w/w NIF in PVP (Fig 2.16). This may indicate that, at this particular ratio of NIF to PVP, some of the PVP hydrogen bonded water molecules were displaced by amorphous nifedipine.

Freeze-drying nifedipine alone has generated poor quality freeze-dried cakes of α crystalline nifedipine. Both DSC thermograms and FT-IR spectra have shown α-NIF characteristics. Addition of low concentrations (≥20% w/w) of PVP to the formulation has shown to improve the quality of the freeze-dried cakes, while crystalline nifedipine remind detectable with DSC analysis. Decreasing the ratio of NIF:PVP in freeze-dried formulations have shown to broaden and decrease the melting peak of nifedipine to a disappear at 50% w/w NIF in PVP. A novel quantitative deferential thermal assay was developed based on the enthalpy of nifedipine endothermic melting peak, determined by differential scanning calorimetry (Fig 2.21). The assay used binary physical mixtures of crystalline nifedipine and amorphous PVP, and was based on the assumption that

the melting enthalpy of crystalline drug is linearly correlated to the content of crystalline drug in the sample (Fig 2.21).

The use of thermal analysis as a quantitative analytical tool has been developed by many studies and used for routine quantitative analysis of polymorphism. A review of studies in this field can be found else were (Giron, 1995). Recent studies in the field of pharmaceutics have developed quantitative deferential thermal analysis for quantifying crystalline drug in formulation. Kushida (2012) developed a DSC based assay for quantifying E1010, a crystalline drug, in binary physical mixtures of amorphous and crystalline drug. The binary mixtures were prepared by mixing different proportions of crystalline and amorphous drug using pestle and mortar. This very action may cause drug recrystallization, thus changing the ratio of amorphous to crystalline nifedipine. Furthermore, heating amorphous drug in the absence of stabilizing polymers can induce recrystallization as part of the thermal test, which as a result would increase the ratio of crystalline to amorphous drug in the sample. The use of an amorphous polymer, in this study, as the diluent for the crystalline drug, prevents the cross contamination between amorphous and crystalline components. However, samples containing high concentrations of PVP seem to give lower melting peaks than expected by the assay in figure 2.21. As the glass transition of PVP is lower than the melting point of nifedipine, it is believed that a small proportion of crystalline nifedipine is dissolving in the viscous PVP liquid above its glass transition, which as a result reduces the size of the melting peak (Fig 2.20). Increasing the PVP concentration in binary physical mixtures has shown to broaden melting peaks and lower onset of melting by as much as 35 ^{o}C (Fig 2.20). PVP is thought to act as an impurity and thus reduce the melting peak onset of nifedipine. The developed DSC assay (Fig 2.21) has a detection limit of about 5%, w/w crystalline nifedipine in formulations, therefore, it may be concluded that ≤50% w/w freeze-dried nifedipine in PVP formulations, are predominantly amorphous.

As demonstrated in this study, DSC limit of detection was previously reported by authors to be in the range of 5-10% w/w (Buckton and Darcy, 1999). As a result, many studies have explored the use of polarized light microscopy (PLM) for the quantitative monitoring of crystalizing formulations and therefore attempting to determine kinetics

of drug crystallization in solution (Xia *et al.*, 2012). As PLM is a visual based technique, it is considered to have a high sensitivity; especially as nucleation, and crystal growth, may be monitored down to the individual crystal. Table 2.6 presents PLM images of different compositions of freeze-dried formulations as well as pure, as received, PVP and crystalline nifedipine. Gunn *et al.* (2012), Raina *et al.* (2014) and others have reported similar PLM based images of crystalline nifedipine. PLM is based on the anisotropic property of crystalline material, and the isotropic property of amorphous material, and therefore observation of birefringence is key in determining the crystallinity of a sample. The results presented in Table 2.6, much like DSC results, show ≤50% w/w freeze-dried nifedipine in PVP to be the cut-off point where crystalline nifedipine is no longer detected. However, visually finding a crystalline particle in formulations with low NIF:PVP ratio is dependent on the amount of sample observed. This is subject to many factors such as the focus of the image, as neighbouring particles may only be visible in different focus settings when particles are of different heights. The spread and thickness of sample is critical as crystalline particles embedded in amorphous material can appear absent. Additionally photo sensitive drugs, such as nifedipine, are more prone to photo degradation when in amorphous state due to their intrinsic instability. Degradation product may show different crystallization behaviour (Miyazaki *et al.*, 2007). Finally, the PLM technique can be dependent on labour intensive consistent counting and measuring of each polarized light micrograph (Wu *et al.*, 2012). Due to the complexity of the different factors influencing the outcome of PLM analysis (Xia *et al.*, 2012), and the lack of a definitive detection limit, many prefer the use of PLM as a qualitative technique (Wu *et al.*, 2012).

ATR FT-IR spectra of amorphous nifedipine in PVP show clear characteristic signs of molecularly dispersed amorphous nifedipine in PVP, these include the single peak located in the carbonyl region (Iqbal and Chan, 2015) and the shift of N-H peak towards lower wavenumbers (Rumondor *et al.*, 2009, Chan *et al.*, 2004). Semi-quantitative analysis of dispersed crystalline nifedipine in PEG was attempted in the past by Iqbal and Chan (2015). The approach was based on the frequently used method of peak response ratio between a crystalline indicative peak (762 cm^{-1}), and a reference peak that is independent of the crystalline state (710 cm^{-1}) in the 800-700

cm^{-1} out of plane δ(C-H) vibration of the ring regions (Shah *et al.*, 2006). Results from this study show the 762 cm^{-1} crystalline indicative peak to be absent in all freeze-dried formulations of nifedipine in PVP, and only present in freeze-dried pure nifedipine and physical mixtures of crystalline nifedipine and PVP (Fig 2.25). Instead a broad peak centred at approximately 754 cm^{-1} was observed in freeze-dried formulations. Careful examination of this peak showed a slight change in peak shape as the ratio of NIF:PVP is increased. Figure 2.25 shows a clear shoulder on the left side of the peak which is thought to be early indications of the crystalline indicative peak 762 cm^{-1}. The peak symmetry was found to be a representative measure of the change in shape observed in the 754 cm^{-1} peak. Figure 2.26 shows the 754 cm^{-1} peak to be asymmetric (0.9-1.1) of freeze-dried 10-60% w/w nifedipine in PVP, with 60% closest to the out of range. The symmetry of the peak further exceeds the 0.8-1 range as the ration of NIF:PVP increases. As the crystalline indicative peak 762 cm^{-1} is not shown in freeze-dried formulations, it is believed that the shape change observed in peak 754 cm^{-1} is indicative of early stages of nifedipine crystal nucleation such as clusters of dimers. This is further supported by PLM images in table 2.6, where smaller crystals of nifedipine are observed in 70% w/w freeze-dried formulations compared to as received nifedipine (Xia *et al.*, 2012).

FT-IR results also show the presence of intermolecular hydrogen bonding between the N-H group of nifedipine and the carbonyl group of PVP (Fig 2.27 & 2.28). The peak shifts observed in N-H region (3342 to 3288 cm^{-1}) between pure amorphous NIF and FD NIF-PVP cakes, is an indication of the presence of hydrogen bonding in FD NIF-PVP cakes compared to amorphous nifedipine. This drug polymer interaction was also observed in het-cycled formulations developed by heat-cycling the freeze-dried formulations via DSC, however, the carbonyl peak of the heat-cycled formulation, at 1660, has, very slightly, changed in size and shape from that in the freeze-dried formulation. This maybe an indication of drug degradation due to thermal stress (Ali, 1989).

Glass transitions of heat-cycled formulations, for all of the ratios of NIF:PVP (Fig 2.29), fitted the Gordon Taylor equation, which is based on volume additivity (Lu and Weiss, 1992, Royall *et al.*, 1999); therefore, the drug-polymer interactions, presented in the

FT-IR work, must not influence the T_g or the mobility of PVP. Furthermore, NIF still acts as a plasticizer to PVP (i.e. lowers the T_g of PVP upon simple mixing), which supports the hypothesis of PVP not to being dramatically affected by being hydrogen bonded to NIF. Knowing that the NIF-PVP system obeys Gordon Taylor is very useful, as it allows the prediction of T_g of un-prepared ratios of NIF:PVP. Figure 2.29 above lists the Gordon Taylor equation and parameters specific for the NIF-PVP system. However, upon further examination the ratios of NIF:PVP, in figure 2.29 did not show to account for the 14.9% w/w residual water carried by PVP and 1.3% w/w by NIF (Fig 2.16). Taking the weight of water away from PVP, figure 2.30 below presents the observed NIF-PVP weight ratios and thus the Gordon Taylor equation and parameters for the binary NIF-PVP systems corrected for the absence of residual solvent. In comparison to authors in the field, where values of K_{GT} above 1 indicates some interaction, the corrected K_{GT} value, supports the IR work, where interactions between PVP and NIF exists, and from IR, this is predicted to be hydrogen bonding.

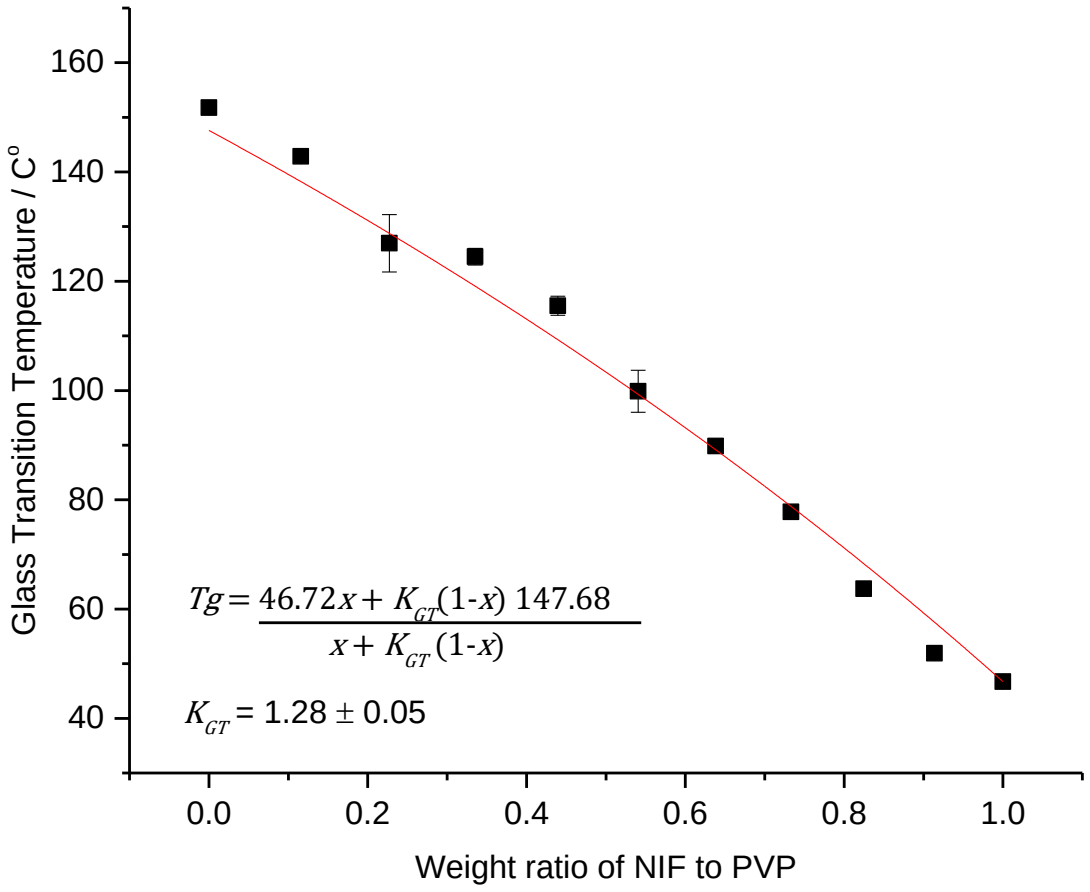

Figure 2.30 Glass transition of NIF-PVP system replotted, from figure 2.29, whilst the ratio of NIF to PVP was corrected for the % w/w of residual water observed in as received PVP (14.9% w/w) and NIF (1.3% w/w).

2.6. Conclusion

A robust and transferable freeze-drying manufacturing method was developed for producing a freeze-dried solid solution of NIF in PVP, using TBA as a common solvent. A 0-100% w/w range of NIF in PVP freeze-dried and physical mix was prepared and characterised using thermal, optical and spectroscopic methods to evaluate phase behaviour of NIF in different NIF:PVP ratios. Differential scanning calorimetry analysis showed freeze-dried ≤50% w/w NIF in PVP formed freely miscible, single T_g, solid solutions that comply to the Gordon Taylor equation with a K_{GT} value of 1.3, indicating intermolecular interactions between NIF and PVP. This was further confirmed by FT-IR analysis, as strong signs of hydrogen bonding were observed in the N-H region for NIF. This therefore provides insights to production, composition and the underpinning mechanism to allow a freeze-dried *in-situ* capsule formulation to be developed; this will be discussed in the following chapter.

Chapter 3. *In-situ* capsule freeze-dried solid solutions of nifedipine

3.1. Introduction

Chapter 3 reports the development of a novel *in-situ* capsule FD formulation of nifedipine and builds on the work reported in the previous sections namely the preparation and characterisation of amorphous nifedipine in PVP. This new knowledge has been used to manufacture an amorphous unit dosage form of nifedipine that enhances both the physical stability of the drug product and the chemical stability of the drug itself. The aim of such work was to overcome the low physical stability of amorphous formulations by avoiding both physical and thermal stress during the manufacturing process (Kaushal *et al.*, 2004, Craig *et al.*, 1999, Vasconcelos *et al.*, 2007). Throughout this research BP regulations were integral, for example the FD capsules were required to consistently deliver a constant mass of the drug, such as conventional tablets and capsules, conforming to regulatory recommendations (MHRA, 2014b).

Aims of the study reported in this chapter were to adapt the freeze-drying method developed in earlier chapters (chapter 2) to manufacture solid oral dosage forms containing 10 $\pm$ 0.5 mg of amorphous nifedipine per unit dosage form. Key indicators of success included developing a predominantly amorphous system, with enhanced dissolution rate and greater apparent solubility, whilst maintaining physical and chemical stability. These indicators will be achieved by developing an *in-situ* freeze-drying method that requires a minimum number of steps to produce the solid dosage form, thus eliminating the risks of crystallisation during the manufacturing process. The effect of varying ratios of NIF:PVP in freeze-dried formulations on dissolution rate and apparent solubility was further investigated. Freeze-dried formulations were compared to physical mixtures to determine the effect of PVP on the dissolution rate and solubility of nifedipine. In addition, the stability of the novel amorphous 10 mg NIF formulation was also investigated.

To achieve the aim of this chapter, the following objectives were set:

1- Adaptation of the method used in chapter 2 for the manufacture of *in-situ* freeze-dried gelatin capsules, containing 10 mg of amorphous nifedipine in PVP.
2- Ensuring the physical and chemical qualities of the *in-situ* capsule freeze-dried formulations are the same as ampoule freeze-dried formulations, taking into account the w/w % of nifedipine in PVP. This will be performed using DSC.
3- Developing and validating a HPLC assay for determining the content and concentration of nifedipine in solution.
4- Determining the effect of the physical state of nifedipine as well as the w/w % of PVP on the rate of dissolution and intrinsic solubility.

3.2. Equipment & materials

3.2.1. Equipment

Basket-rack assembly: ERWEKA GmbH Heusenstamm Germany, Product Type (PT): ZT2, SN: 53462; **Cannula Filters**: SMI-Labhut ltd Gloucestershire UK, Product Number (PN): FIL045-01-100, specification: 45µm UHMW Polyethylene Cannula Dissolution Filters Agilent/VanKel Compatible; **Capsule sinker**: SMI-Labhut ltd Gloucestershire UK, PN: WIRESK-VK, specification: type 316 Stainless Steel Wire 0.6 mm diameter 15 m Roll; **Dissolution instrument**: CALEVA ltd Ascot UK, PT: 6ST, MN: 02042, SN: 3014764; **Falcon tubes**: Fisher scientific Ltd Leicestershire UK, PN: 14-959-49B, BN: E130505S; **High performance liquid chromatography**: Agilent Technologies Co ltd California US, PT: 1100; **Humidity and temperature meter**: Fisher scientific Ltd Leicestershire UK, MN: FB50264, SN: 101822304, specification: Traceable calibration 281-482-1714; **Humidity and temperature meter**: VWR International Ltd Leicestershire UK, PN: I628-0031, SN: 122720346, specification: Traceable calibration 281-482-1714; **Mailbox Box**: Mailbox international ltd city and country, PN: M202A, SN: 0161-330-5577; **pH meter**: InoLab® Werkstätte Germany, PT: inoLab pH Level 2, SN: 02370005; **Sampling Cannual**: SMI-Labhut ltd Gloucestershire UK, PN: CAN575-SH 5.75, specification: 5.75" (120mm) Bent SS Sampling Cannula with Luer Adapter for 900 mL Sampling 0.125" (3.2mm) Diameter VanKel Compatible; **Syringe Filters**: SMI-Labhut ltd Gloucestershire UK, PN: FFPV1345-100, BN: ES129259, specification: Cronus 13 mm PVDF Syringe Filter 0.45µm; **Syringes**: SMI-Labhut ltd Gloucestershire UK, PN: SS20LS-100, specification: 20 mL Luer Slip Polypropylene Syringe, Sterile; **Temperature controlled room air cooler**: GEA Group Düsseldorf Germany, PT: GEA Küba DE professional, MN: A08ID, SN: 6006126, specification: room temperature range from -30 ^{o}C to +30 ^{o}C); **Thermometer**: VWR International Ltd Leicestershire UK, PN: ENICHEM, specification: Spirit thermometer 76 mm immersion 305 mm long -10 to +110 ^{o}C; **Tip holder box**: Starlab Keynes UK, PN: S1126-7810, BN: A108576L specification: TipOne 1000 µL Filter Tip; **Ultraviolet/visible spectroscopy**: PerkinElmer Massachusetts US, PT: Lambda2S, PN: 166351, SN: 6847; **UV/VIS spectroscopy cells**: PerkinElmer Massachusetts US, PN: B0631009; **Verex caps**: Pehnomenex® California US, PN: AR0-8957-13-B; **Verex vial**: Pehnomenex® California US, PN: AR0-3901-13, BN: 004; **Volumetric flask**: Fisher

scientific Ltd Leicestershire UK, PN: 11864020, specification: A100 ±0.8 mL in 20 ^{o}C; **Volumetric flask**: Fisher scientific Ltd Leicestershire UK, PN: 11894020, specification: A25 ±0.04 mL in 20 ^{o}C; **Volumetric flask**: Sigma-Aldrich Company Ltd Dorset UK, PN: Z326437-2EA, specification: ±0.08 mL in 20 ^{o}C; **Volumetric flask**: YORLAB Dunnington UK, PN: 5276453, specification: A1000 ± 0.4 mL in 20 ^{o}C.

Other equipment used in this chapter was listed under equipment section of previous chapters.

All instruments used in this study were calibrated following manufacturer recommendation unless otherwise stated in the method section of this chapter.

3.2.2. Materials

Acetic Acid: Sigma-Aldrich Company Ltd Dorset UK, CAS: 64-19-7, CC: 45740-1L-F; **Ammonium acetate**: VWR International Ltd Leicestershire UK, CAS: 631-61-8, PN: 21198.298, BN: 11K140019; **Bupivacaine hydrochloride**: Santa Cruz Biotechnology Heidelberg, Germany, CAS: 18010-40-7, CC: Sc-252524A, BN: K0410; **Empty capsules**: The-Alchemists Apothecary-amazon.co.uk, PT: Red gelatin capsules size 0, BN: 0299; **Nifedipine 10 mg capsules**: TEVA ltd Castleford UK, BN: 229AG; **Sodium Bromide**: VWR International Ltd Leicestershire UK, CAS: 7647-15-6, CC: 1.06360.1000, BN: K44774260 331; **Sodium Chloride**: VWR International Ltd Leicestershire UK, CAS: 7647-14-5, CC: 567440-1; **Water**: Fisher scientific Ltd Leicestershire UK, CAS: 7732-18-5, PN: W/0106/17, specification: HPLC grade.

3.3. Methods

3.3.1. *In-situ* freeze-drying of nifedipine within capsules

3.3.1.1. Preparation of feed solution

A 2% w/v nifedipine in TBA stock solution was prepared by dissolving pre weighed 200 mg of nifedipine in 20 mL of TBA. Pre weighed PVP K10 (200 mg) was added to the readymade nifedipine solution and dissolved, creating a solution with a 1 to 1 NIF:PVP ratio (equivalent to freeze-dried 50% NIF in PVP). Both nifedipine and PVP were

dissolved in TBA following the method of preparing feeds solutions described in section 2.3.1.1. Feed solutions with varying NIF:PVP ratios were prepared using the same method while maintaining the concentration of nifedipine in all feed solutions constant at 2% w/v.

3.3.1.2. Capsule filling

Up to 30 red opaque gelatin capsules size 0 (distributed by The Alchemists Apothecary) were fitted, facing upwards, into a capsule holder board, designed for this study. Using a positive displacement pipette, a syringe like structured pipette that allows accurate uptake of viscus and volatile samples (Gilson), 0.5 mL of feed solution was transferred into each capsule bottom and allowed to freeze. Capsules containing frozen feed solution, of the same NIF:PVP ratio, were transferred into amber freeze-drying vials as presented in figure 3.2. The vials were then labelled with the corresponding w/w % of NIF in PVP and stored in a -80 ^{o}C freezer (10-14 h).

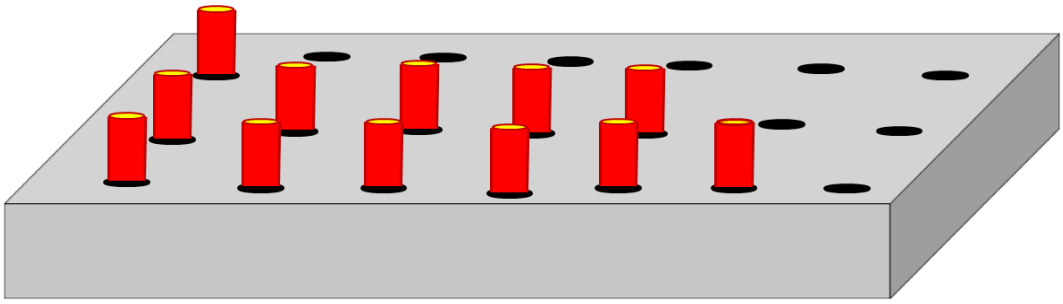

Figure 3.1 Capsule holder used in the process of filling capsule with feed solutions and allowing them to solidify at room temperature (18-25 ^{o}C). This diagram was drawn using Microsoft PowerPoint.

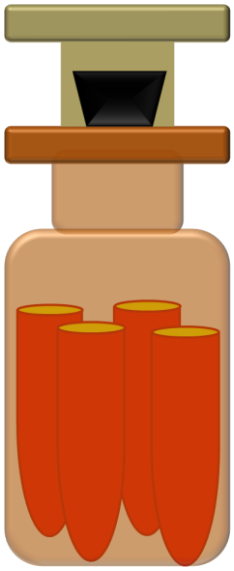

Figure 3.2 Fitting filled capsule bottoms into freeze-drying vials to be freeze-dried. This diagram was drawn using Microsoft PowerPoint.

3.3.1.3. Freeze-drying cycle

In-situ freeze-drying was performed following the same freeze-drying cycle developed in chapter 2, described under section 2.3.1.

3.3.1.4. Recapping capsules

Once secondary drying was completed, vials were re-opened, inside nitrogen bags, for a capsule recapping step. This process was performed inside the previously described nitrogen bags using an adapted version of the method described in section 2.3.1.6. All vials were re-sealed under nitrogen and stored at room temperature (18-25 ^{o}C) over P_2O_5 inside sealed desiccator until tested.

3.3.2. Quality control testing

3.3.2.1. Uniformity of weight and appearance

All capsules were examined for damage or cracks on the outer shell. This was performed as part of the recapping step described above (section 3.3.1.4). Additionally 3 capsules per batch of each of the w/w % formulations were weighed individually.

3.3.2.2. Drug content

The content of nifedipine per capsule was determined for 3 capsules per batch of each of the w/w % formulations. The content of drug was determined using a reproducible and validated stability-indicating HPLC method adapted from a previous study (Helin-Tanninen *et al.*, 2001). The adapted method is described in the below sections (3.4.2.2.1 – 3.4.2.2.7).

3.3.2.2.1 Stability indicating HPLC system

The HPLC system used was the Agilent 1100 HPLC system series. This consisted of an Auto sampler (Agilent ALS – G1313A, SN: DE11115724), a Diode Array detector (Agilent DAD G1315B, SN: DE11112633), a column oven, a binary pump (Agilent 1100 – G1316A, SN: DE11121364) and a degasser unit (Agilent Degasser – G1322A, SN: JPO5027194). For this method a Gemini-NX C18 revers phase column (particle size 5µm, width of 4.60 mm and length of 150mm) was fitted. The mobile phase consisted of 68% (v/v) HPLC grade methanol and 32% (v/v) 0.1M Ammonium acetate (adjusted to pH 5.8 using acetic acid).

3.3.2.2.2 Stability indicating HPLC Method conditions

An isocratic mobile phase was set to a flow of 1.0 mL/min. The flow was not interrupted between samples of a given experiment. The column oven was set to 37 ^{o}C and the DAD unit was set to monitor absorbance at: 238 nm. Injection volume was set to 20 µL and the injection needle was programmed to wash with 100% HPLC grade methanol after each sample.

The system was run with no sample injections for 30 min prior to use for conditioning. The performance of the HPLC instrument was tested on at least 6 repeated injections where flow rate, pressure and measurement response were monitored to ensure system suitability in accordance to ICH guidelines (ICH, 1996).

3.3.2.2.3 Preparation of mobile phase

0.1M Ammonium acetate stock solution was prepared by adding 7.708 g of ammonium acetate to a 1.0 L volumetric flask and diluting to mark using HPLC grade water. The solution was sonicated for 10 min. The pH of the solution was adjusted to 5.8 using acetic acid. HPLC grade methanol was used as received.

3.3.2.2.4 Preparation of internal standard stock solution

Pre-weighed 1.5 g of bupivacaine hydrochloride, as the internal standard, was added into a 1.0 L volumetric flask. 0.1M HCL was added to volumetric flask to make up a solution of 1.0 L. The solution was sonicated until no solid particles are visible. This stock solution was stored at 5 ^{o}C (Helin-Tanninen *et al.*, 2007) for a maximum of 28 days (Karin Janssen, 2009).

3.3.2.2.5 Preparation of nifedipine dilutions for the construction of calibration graph

A calibration curve was constructed by preparing a series of dilutions of nifedipine prepared from stock solution (table 3.1). This was prepared by adding a red gelatin capsule containing pre-weighed 10.0 mg nifedipine to a 50 mL amber volumetric flask. The volumetric flask was then filled up to the mark with 50% v/v HPLC methanol in 0.1M HCL. The solution was then sonicated (using a sonicator water bath) until no solid particles were visible. A range of volumes were pipetted from the nifedipine stock solution into 25 mL volumetric flasks, while a constant 0.83 mL of internal standard stock solution (0.15% w/v bupivacaine hydrochloride) was added to all dilutions (table

3.1) (Helin-Tanninen *et al.*, 2007). 0.1M HCl was used to dilute all solutions to mark. As a result all dilutions contained equal concentrations of internal standard (49.8 µg/mL).

Table 3.1 Pipetted volumes of stock solutions in the preparation of a series of nifedipine dilutions (n=3).

Target concentration of nifedipine. (µg/mL)	Volume of dilution solutions	Pipetted volume of NIF stock solution needed mL	Pipetted volume of internal standard stock solution mL
2	25	0.25	0.83
4	25	0.50	0.83
6	25	0.75	0.83
8	25	1.00	0.83
10	25	1.25	0.83
11	25	1.38	0.83
12	25	1.50	0.83

The series of nifedipine dilutions were prepared in a replicate of 3, each of which was prepared from a different nifedipine stock solution.

3.3.2.2.6 Preparation of finished product HPLC sample

The *In-situ* FD capsule formulation (i.e. the finished product after recapping) was placed inside a 50 mL amber volumetric flask. 25 mL of 50% v/v HPLC grade methanol in 0.1M HCL was added. The resulting solution was sonicated, while limiting temperature of the water bath sonicator to the range 25-37 ^{o}C, to full dissolution. The solution was further diluted, to a total volume of 50 mL, using the same solvent mixture. The resulted solution was mixed by inverting the 50 mL volumetric flask at least 3 times.

A volume of 0.63 mL from the resulting solution was pipetted into an amber 25 mL volumetric flask, to which a standard volume of 0.83 mL of the internal standard stock solution was added. The solution was then diluted to mark using 0.1M HCl. The resulting solution was then analysed using the HPLC stability indicating assay.

3.3.2.2.7 Stability indicating HPLC system validation

A. Specificity

An investigation of specificity was conducted to determine and differentiate response by the drug and impurities as well as the internal standard (ICH, 1996). This was performed by injecting solutions of nifedipine alone, internal standard alone, photo

degraded nifedipine, prepared by exposing NIF solutions to day light for no less than 2h, and finally a solution of all of the analytes to ensure response of impurities and internal standard do not interfere with drug response. Identity of peaks appearing in the presence of impurities were further confirmed using HPLC mass spec, where nifedipine solutions where analysed before and after light degradation (ICH, 1996).

Selectivity was also investigated by ensuring other components of the freeze-dried formulation do not interfere with the response of nifedipine and bupivacaine hydrochloride. This was performed by analysing drug free FD capsule formulation (0% w/w nifedipine in PVP). HPLC samples of drug free formulations were prepared using the same method used for preparing finished product HPLC samples. This experiment was repeated 3 times, using 3 different capsules (ICH, 1996).

B. Linearity & range

To determine the linear working range of the HPLC method, nifedipine standards of known concentration were prepared with concentration range from 2.0 to 12.0 µg/mL. This covers the range of 40% to 240% of the expected sample concentration (5.0 µg/mL) following ICH guidelines (ICH, 1996).

C. Detection and quantification limits

This was performed following the method described in previous chapters (2.4.3.1) following ICH guidelines (ICH, 1996).

D. Accuracy and precision

The HPLC assay was tested for accuracy and precision through the analysis of three standard solutions of nifedipine (5 µg/mL) at three different times of the day following ICH guidelines (ICH, 1996).

E. Robustness

a. Standard solution

The reproducibility of retention time (RT) and PA of nifedipine and bupivacaine hydrochloride was investigated by preparing and testing a standard solution of nifedipine and bupivacaine hydrochloride (5 and 50 µg/mL respectively). The same solution was injected into the column in a replicate of 10 times. The average RT and PA

of nifedipine and bupivacaine hydrochloride was recorded following ICH guidelines (ICH, 1996).

b. Finished product sample

The reproducibility of the RT and PA of nifedipine and bupivacaine hydrochloride was also investigated in finished product HPLC samples. A sample was prepared, using the same method used for preparing finished product HPLC samples, using freeze-dried capsules of 50% w/w nifedipine in PVP. The same sample was injected into the column in a replicates of 10 times. The average RT and PA of nifedipine and bupivacaine hydrochloride was recorded. This experiment was repeated 3 times, using 3 different samples (ICH, 1996).

3.3.2.3. Thermal characterisation

Thermal analysis was performed, following the DSC method described in chapter 2, on freeze-dried material extracted from 3 different capsules per batch of each of the w/w % formulations (ICH, 1996).

3.3.3. Dissolution testing

The optimised dissolution testing method was based on the use of dissolution apparatus 2 (paddle apparatus), of which all parameters were calibrated and adjusted in accordance to Appendix XII B-dissolution of the BP guidelines (MHRA, 2014b).

3.3.3.1. Dissolution medium

The dissolution medium used in this test is 900 mL of 0.1M HCL (MHRA, 2014b), nevertheless a novel method of incorporating the internal standard was implemented, by which a concentration of 50 µg/mL of internal standard was maintained. This was achieved by adding a volume of 33.33 mL of the internal standard stock solution to 100 mL of 1M HCL and making the solution up to 1.0 L using distilled water. Only 900 mL of the resulting solution was poured into the dissolution vessel and the remaining 100 mL was maintained in a separate beaker as a dissolution medium reservoir. This ensures that all samples withdrawn from the dissolution medium contain the same concentration of internal standard.

3.3.3.2. Dissolution assembly and parameters

The dissolution instrument was assembled in accordance to the BP specification of appendix XII B. Dissolution (MHRA, 2014b). In addition to avoid sample contamination or interference from the equipment used, any plasticizers containing tubing was avoided. A special stainless steel cannula was installed to which a 0.45µm non-adsorptive millipore polyvinylidene fluoride syringe membrane filter was fitted. Finally a luer slip polypropylene syringe was fitted to the cannula via the filter to enable sample uptake. The temperature of the dissolution bath was set to 37.0 ^{o}C ± 0.5, paddles were set to rotate at a speed of 50 rotations per minute (MHRA, 2014b). Both the paddle and the sampling cannula were positioned in accordance to the BP guidelines (MHRA, 2014b), this is to ensure samples are withdrawn from a zone midway between the surface of the dissolution medium and the top of the rotating paddle, 1.3 cm away from the vessel wall (MHRA, 2014b). The bottom of the sampling cannula was fitted with a 20 µm Ultra-high-molecular-weight polyethylene cannula dissolution filter, BP compliant (MHRA, 2014b). Figure 3.3 below presents a schematic diagram of the apparatus 2 dissolution setup. To ensure the sampling cannula was securely connected to the various parts and is conditioned to the dissolution medium, a few 5 mL samples were taken up from the dissolution reservoir and then flushed out.

Furthermore to supress light related degradation of nifedipine, the dissolution test was performed in a dark room where only light of long wave lengths is used. Light coming from the dissolution instrument was minimized but not completely eliminated as dissolution parameters were constantly monitored.

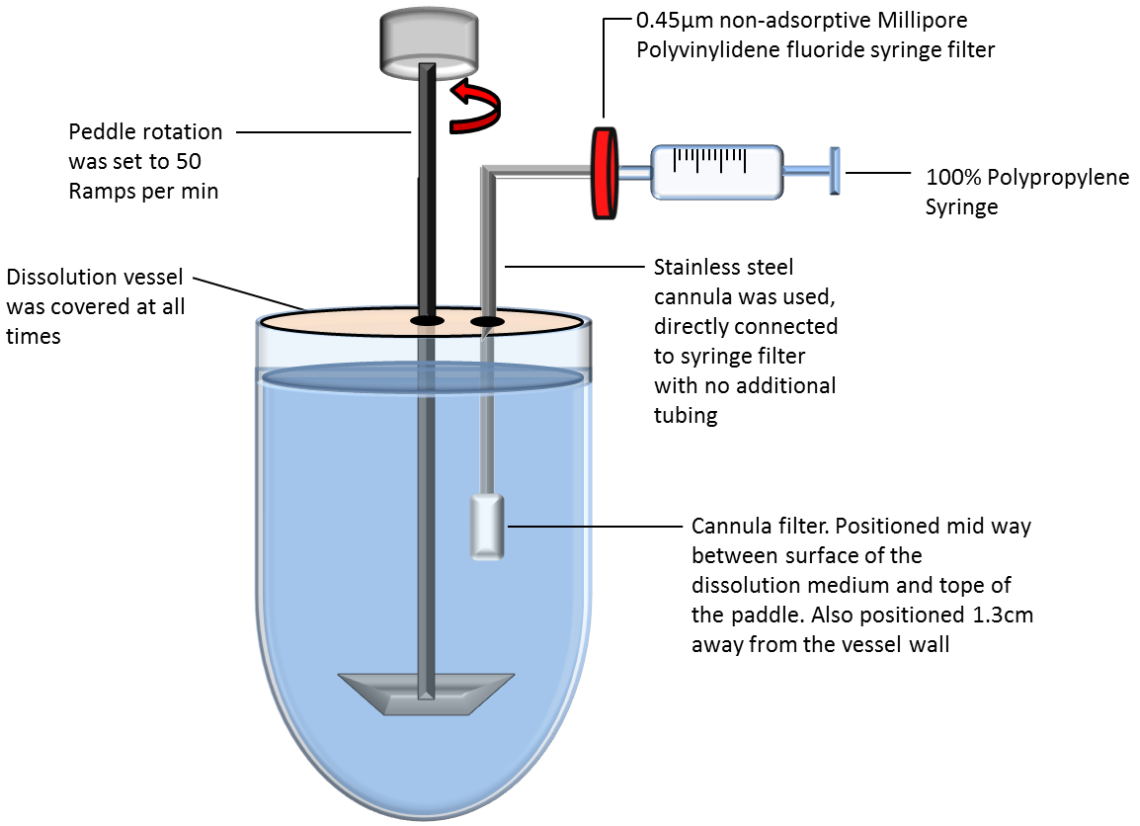

Figure 3.3 USP apparatus 2 dissolution setup following BP guidelines based on (MHRA, 2014b). This diagram was drawn using Microsoft PowerPoint.

3.3.3.3. Method of dissolution testing

The dissolution vessel containing the dissolution medium was allowed to reach the specified temperature and thus equilibrate for 5 min at 37.0 ± 0.5 ^{o}C. Next the capsule to be tested was removed from the amber sealed vial. A small, loose piece of non-reactive stainless steel, wire helix with few turns, was securely attached to the test capsule, to act as a capsule sinker, as recommended by the BP guidelines (MHRA, 2014b). The capsule was then dropped into the dissolution vessel, at which time 0 min was marked. Samples were withdrawn on 1, 2, 3, 4, 5, 6, 10, 20, 45 and 60 minutes. At each time interval a sample of 5 mL was withdrawn into the syringe presented in fig 3.3 above. From the withdrawn sample, 2 mL was injected into 2 mL amber HPLC glass vials, and the remaining 3 mL was injected back to the dissolution medium. Once the dissolution testing was complete, the HPLC vials were analysed immediately using the HPLC assay.

3.3.3.4. Polarized microscopic dissolution

Dissolution testing was mimicked under polarized microscopy. Approximately 1 mg of sample was spread on a clear slide and monitored under polarized microscopy

following method described in previous chapters (2.3.5). 0.5 mL of 0.1M HCl (37.0 ± 0.5 ^{o}C) was pipetted into the formulation and images, through 5X magnification objective, were captured, with 1min interval, for 60 min.

3.3.4. Solubility measurement of nifedipine

The thermodynamic solubility of crystalline nifedipine was measured in 0.1M HCl (37.0 ±0.5 ^{o}C) by adding excess amounts of pure crystalline nifedipine to 25 mL of solvent. Samples were continually shaken by a shaking board and maintained in 37.0 ± 0.5 ^{o}C water bath in a dark room to equilibrate for 5 days. Solutions above excess solid nifedipine were filtered following the same filtering setup used in the dissolution instrument. The concentration of NIF was then determined using the stability indicting HPLC assay described above.

3.3.5. Stability studies

A stability study was performed by storing *in-situ* capsule FD formulations in nitrogen sealed amber vials under two conditions; The first condition 25 ± 2 ^{o}C and 57 ± 0.4% RH, was achieved by storage at a 25 ± 2 ^{o}C controlled room temperature, where by the samples were stored in a sealed box containing saturated solutions of sodium Bromide salt (Greenspan, 1977). The second condition 37 ± 2 ^{o}C and 74 ± 0.13% RH was achieved using the same method while a saturated sodium chloride salt solution was used to maintain the % RH (Greenspan, 1977). Both conditions were monitored periodically to ensure temperature and humidity values are within in specified limits. Samples were withdrawn and tested for physical stability: % w/w of crystalline nifedipine, chemical stability: presence of chemical degradation products, and performance: unit dosage weight uniformity, drug content and dissolution profile.

3.4. Results

3.4.1. HPLC assay method validation

3.4.1.1. Specificity

By separately injecting nifedipine and bupivacaine HCl (internal standard) into the column, it was determined that the RT's of nifedipine and internal standard, under fixed flow rate of 1.0 mL min^{-1}, isocratic mobile phase of 68% v/v methanol in 0.1M ammonium acetate (pH = 5.8-5.5) and a constant column temperature of 37 $^{o}C \pm 1$, are 3.30 $\pm$ 0.005 min and 4.81 $\pm$ 0.007 min respectively (n = 10). A standard solution containing nifedipine and internal standard shows both peaks to appear with a separation factor of 1.94 and a resolution of 2.5 (Figure 3.4-A). Both peaks show ICH acceptable peak symmetry values 0.9-1.4 (Deepti and Pawan, 2013, ICH, 1996, FDA, 2008).

Nifedipine is known to degrade when exposed to light or high temperatures (Ali, 1989), resulting in the production of nitroderivatives of nifedipine: nitrophenylpyridine (NIFII) and nitrosophenylpyridine (NIFIII). These compounds are similar in structure to nifedipine and act as impurities (chapter 2 Fig 2.4). Following ICH guidelines (ICH, 1996) it was important to ensure that the HPLC assay developed allows discrimination and partial identification of impurities that may interfere with measurements of the drug (ICH, 1996). Figures 3.4 B and C, show chromatograms of standard nifedipine solutions after photo and thermal degradations respectively, photo degradation has shown to develop degradation products NIF II and III, which elute at, 2.8 and 3.1 min respectively. The molecular identity of each of the peaks was confirmed using liquid-chromatography-mass-spec (LC/MS), where the same chromatographic conditions were used, while the UV detector was replaced with a mass spec instrument. The mass charge of parent ion molecule was used to confirm the identity of the degradation products and the drug (Deepti and Pawan, 2013). Both HPLC-UV and LC-MS were also performed on placebo samples containing nifedipine, PVP and the internal standard. The average RT of the drug and internal standard in the presence of PVP did not change significantly 3.26 $\pm$ 0.010 min and 4.80 $\pm$ 0.008 min respectively (ICH, 1996).

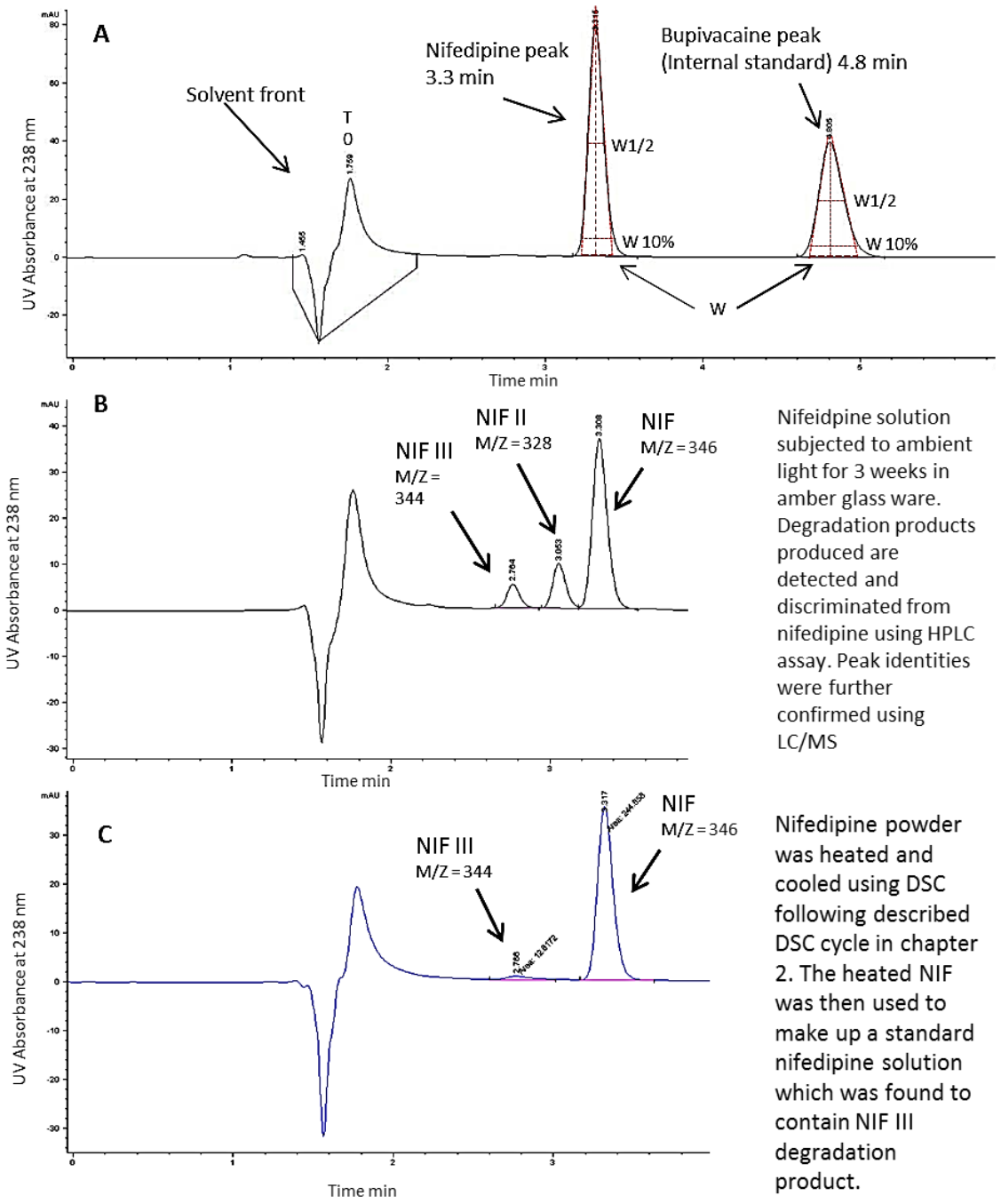

Nifeidpine solution subjected to ambient light for 3 weeks in amber glass ware. Degradation products produced are detected and discriminated from nifedipine using HPLC assay. Peak identities were further confirmed using LC/MS

Nifedipine powder was heated and cooled using DSC following described DSC cycle in chapter 2. The heated NIF was then used to make up a standard nifedipine solution which was found to contain NIF III degradation product.

Figure 3.4 HPLC-UV chromatograms of nifedipine solutions: **A)** Standard NIF solution spiked with internal standard. The solvent front peak indicate T0, otherwise known as the time taken for the sample solvent to reach the detector. Dotted lines show examples of measuring peak width at half height (W1/2), peak width at 10% height (W10%) and peak width (W). **B)** HPLC chromatogram of NIF solution degraded by light while in amber HPLC vial, indicating that amber vials do not fully ensure protection against photo degradation. The identity of NIF-II (RT: 3.1) and NIF-III (RT: 2.8) where further confirmed using LC/MS **C)** HPLC of thermally degraded nifedipine using DSC cycle heating and cooling between 25 and 200 ^{o}C. The observed solvent peak is due to the difference in UV absorbance between the sample solvent and the mobile phase used.

3.4.1.2. Robustness

Following ICH guidelines (ICH, 1996), the HPLC assay was validated for analytical conditions that may influence measurement of nifedipine concentrations. As described above, subjecting nifedipine solutions to either light or high temperatures was shown to induce degradation of NIF (Fig 3.4 and 3.5), and therefore cause a reduction in the content of nifedipine. Repetitive measurements, over the course of 9 hours, were performed on a standard nifedipine solution placed in a clear vial at room temperature (18-25 ^{o}C). The sample was placed in a HPLC sample-stand and was subjected to ambient laboratory light. Figure 3.5 shows the PA (HPLC-UV absorbance) for NIF (RT 3.3 min) to follow zero order kinetics where the PA decreases at a rate constant of 0.042min^{-1}, While peak area of degradation product NIF II (RT 3.1 min) was shown to increase at a rate constant of 0.023 min^{-1} after approximately 2h of subjecting the sample to ambient light. PA values were not converted to concentrations for degradation products, as no calibration graph was constructed for degradation product as part of this study, nevertheless converting the PA values of NIF to concentration values has shown the concentration of NIF to follow the equation (NIF conc. µg/mL = -8.22x10^{-4} x time + 5.439, R^2 = 0.97) when subjected to ambient light, while -8.22x10^{-4} ± 1.5x10^{-5} min^{-1} was the determined rate constant of NIF degradation in clear vials. Performing the same experiment using amber glass vials has shown to decrease the rate of nifedipine degradation by approximately a factor of 5 times as was observed by (Ali, 1989). Fig3.4-B shows the presence of degradation products after 3 weeks of exposure to ambient light at room temperature (18-25 ^{o}C). In the effort to prevent light induced degradation, HPLC vials containing nifedipine solutions were covered with foil where possible, the HPLC sample stand was also covered with foil to further protect vials waiting to be analysed, and were maintained at room temperature (18-25 ^{o}C). Following this method has shown to protect nifedipine solutions from any light degradation for at least 10 hours at the HPLC stand, which is more than the usual needed time for HPLC analysis (3 hours).

The effect of temperature on nifedipine degradation was investigated by heating nifedipine powder to 200 ^{o}C using the heat-cool-heat-cool DSC cycle described in chapter 2. The sample was protected from light at all times to avoid light induced degradation. NIF powder exposed to high temperatures was then used to make

standard solutions with concentrations of 5 µgmL^{-1}, which were then analysed using HPLC assay. Results show a recovery of 79.1 ± 6.4% (n=3) while a peak at 2.8min, corresponding to NIFIII, was detected (Figure 3.4-B). In a separate experiment, the thermal stability of nifedipine solution were tested by storing light protected NIF solutions at moderately high temperatures (40 ± 5 ^{o}C) for >10h. Results show the PA of NIF before and after storage to be < 0.2% RSD (n = 10). Similarly thermal stability at room temperature (18-25 ^{o}C) for > 10h showed < 0.2% RSD between PA of NIF before and after storage.

Fluctuations in RT, flow rate and injection volume have shown to cause irregularity in measurements, especially for low concentrations of nifedipine solutions ≤ 3 µgmL^{-1} (RSD ≥ 20.5% of n=3). As a result the internal standard (bupivacaine HCl) was introduced to the HPLC assay. Using the PA ratio of drug to internal standard has reduced the effect of occasional fluctuations in injection volume on the determined concentration of nifedipine to RSD ≤ 0.5%.

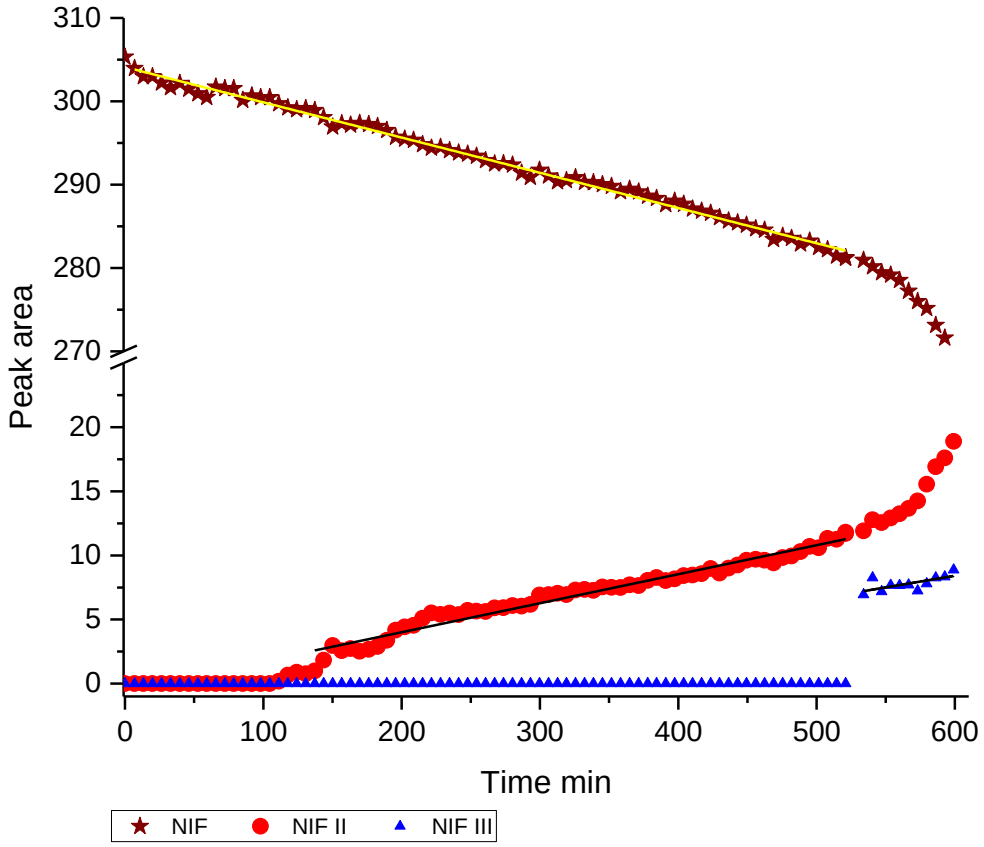

Figure 3.5 PA of NIF, NIF II and NIF III was repeatedly measured from a standard solution held in a clear vial. The vial was subjected to ambient laboratory light and a temperature of 18-25 ^{o}C. Degradation of NIF follows the equation PA=0.042 x time + 301.03. PA of NIF-II = 0.023 x time – 0.517, and finally PA of NIF-III = 0.0183 x time (min) + 2.505.

3.4.1.3. Linearity, range and precision

The linearity of the HPLC assay was validated for drug content uniformity in the developed pharmaceutical product, 10 mg *in-situ* capsule FD NIF in PVP, following the ICH guidelines, with a range that covers at least 70-130% (Fig 3.6) of the test concentration (5 μgmL^{-1}). Furthermore, the assay was also validated for dissolution testing use, where the final expected test concentration is 10 µg ±10%. Following the ICH guidelines, a range of 0-12 μgmL^{-1} was validated for linearity (Fig 3.6). R^2 = 0.9998, slope = 0.138 and the y-intercept = -0.015. The calibration curve presented in figure 3.6 was derived from 3 separate calibration curves, to ensure repeatability (ICH, 1996), performed in 3 different days, from 3 different nifedipine stock solutions, to ensure intermediate precision (ICH, 1996), Error bars represent standard error of n=3. The relationship between PA ratio and concentration of nifedipine was further tested by another analyst, using a different internal standard stock solution, to ensure reproducibility (ICH, 1996). A similar, but different linear equation was determined, where the y-intercept was equal to -0.0077 and a slope of 0.130 (R^2=0.998). The small difference in relationship observed was thought to be due to a small difference in the concentration of internal standard stock solution. To eliminate variance going forward, a new calibration curve was prepared for every new internal standard stock solution prepared, as the concentration of internal standard in the calibration standard and samples must be constant to facilitate quantification of drug following the FDA guidelines (FDA, 2001).

3.4.1.4. Limit of detection and quantification

Using the calibration curve below (Fig 3.6), the limit of detection and quantification were calculated using the standard deviation of intercept. This was calculated using the same method used in section 2.4.3.1.

Table 3.2 Detection and quantification limits of the HPLC assay for NIF.

Equation	**y = 0.13881x - 0.0151**
R^2	0.999
SD of Intercept	0.00465
LOD	0.11 µg/mL
LOQ	0.33 µg/mL

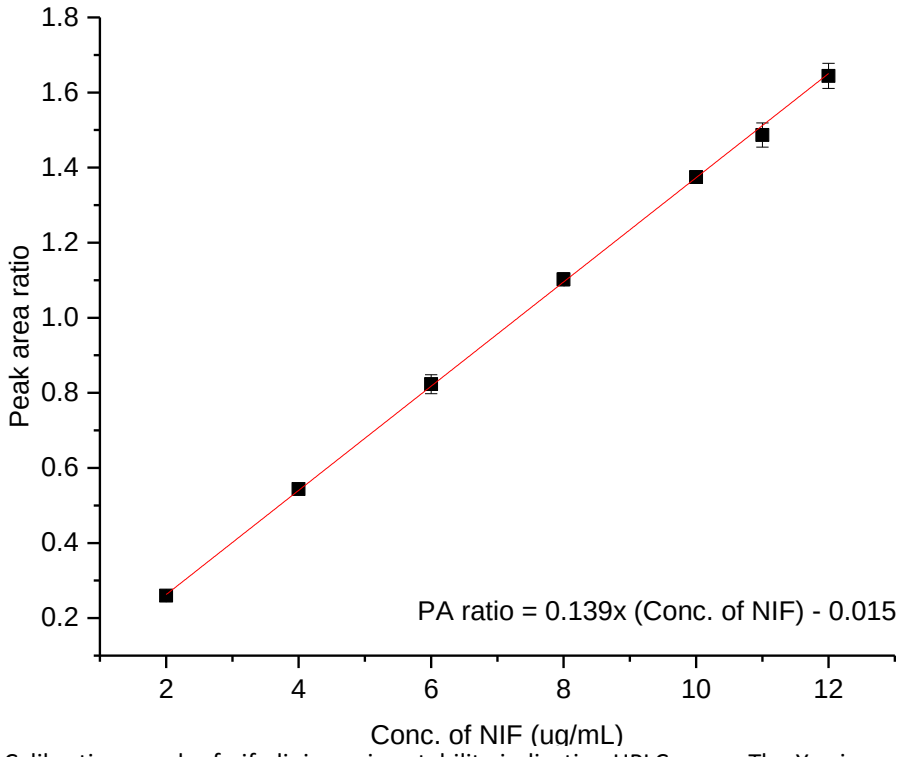

Figure 3.6 Calibration graph of nifedipine using stability indicating HPLC assay. The Y axis represents the PA ratio of nifedipine to bupivacaine HCl. Error bars represent the standard error of three different stock solutions prepared in 3 different days (n=3). R^2 equals 0.9998 indicating that the line of best fit shows a good representation of the data points.

3.4.1.5. System suitability

Prior to starting the analysis of any sample, a standard sample was injected at least 6 times to ensure the system was functioning well. The suitability of the system was assessed by calculating the RSD% of RT for drug and internal standard as well as the PA's. The system was evaluated as suitable to use when RSD values ≤ 2% (Deepti and Pawan, 2013). The low RSD value indicated system suitability following ICH guidelines. In cases where the RSD value was > than 2%, the system was checked and assessed following manufacturer guidelines (Technologies, 1999).

3.4.1.6. Detection of NIF degradation products

As no calibration graph was constructed for the degradation products of NIF (NIFII and NIFIII), percentage PA was used as a method of detection for the presence of these products. Percentage PA is equal to the PA of 1 or both degradation products divided by the total sum PA of NIF, NIF II and NIF III (if present). This method of detection was validated using LC/MS (Figure 3.4).

3.4.2. Dissolution method validation

3.4.2.1. Interference of apparatus

Dissolution test was performed using a placebo capsule, containing only PVP, to ensure no interference was introduced by any of the used parts. All samples showed no peaks at the RT of nifedipine, indicating system suitability for testing the dissolution of nifedipine.

3.4.2.2. Evaluation of filters

Following USP and BP dissolution monographs, samples were filtered in-line while withdrawn from the dissolution bath to ensure removal of any particulates or undissolved drug that may interfere with further analytical procedures. If undissolved drug passes through the filter it may dissolve in collected samples and thus lead to a higher concentrated and more variable results. The method of filtration was developed and validated as described below. USP dissolution paddle apparatus are usually fitted with cannula filters 0.45µm. These filters were tested using marketed nifedipine soft gel formulations (Adalat nifedipine 10 mg). Results showed the percentage dosage released, at ≥ 20 min, to equal 120% ± 5% of the expected drug content (i.e. 12 mg of NIF released), while, in a separate experiment, the drug content of the same formulation and same batch (Adalat nifedipine 10 mg) showed each capsule to contain an average of 10 ± 0.5 mg of NIF. This therefore indicates that the cannula filters are insufficient in filtering undissolved nifedipine particles. To ensure efficient filtration of collected samples, an additional, polyvinylidene fluoride (PVDF) membrane syringe, filter was added between the cannula and sample syringe. This has improved filtration efficiency as the concentrations of collected samples were found to be ± 5% of the expected concentration.

3.4.2.3. Drug degradation

Based on previous findings on the degradation of NIF when NIF solutions are exposed to ambient light, precautions were taken to protect dissolution medium from ambient light. This was achieved by performing all dissolution studies in dark rooms with red light and minimal stray light, coming from instrument's digital screens. This method has not shown to completely prevent light degradation during dissolution studies, but has limited the growth of % accumulative PA of degradation products to a maximum of

12% within the 60 min dissolution test. (% accumulative PA of degradation products is the sum of the PA's for NIF II and NIF III divided by the sum of PA's of NIF, NIFII and NIFIII). It was assumed by the author that the conditions of the dissolution medium; 37 ± 0.5 ^{o}C and continuously stirring by paddle, at 50 rotations min^{-1}, increased the chance of NIF degradation.

3.4.2.4. Calculating dosage percentage dissolved

Using the validated stability indicating HPLC assay, the concentration of NIF in the dissolution medium at each time point was determined. This was then converted into a total amount of NIF released from the formulation, taking into account the small volume of media withdrawn at each time interval. To obtain a percentage value, the amount of drug released was divided by the mean drug content of the specific formulation tested.

3.4.3. Quality control of *in-situ* freeze-dried capsule formulations

3.4.3.1. Successful freeze-drying

The effect of *in-situ* capsule freeze-drying on the structure of freeze-dried cake was investigated. Figure 3.7 below, presents the *in-situ* capsule FD formulations (10-100% w/w NIF in PVP) in clear capsule, allowing visual examination of the FD cakes. FD cakes of formulations containing ≤ 70% w/w NIF in PVP show no shrinkage, indicating successful freeze-drying, while > 70% w/w NIF in PVP FD cakes have shown to loose structural integrity. This is similar to the pattern observed in previous chapters (Chapter 2), where by reducing PVP content was seen to reduce the strength of FD cakes.

10% w/w in red capsules | 10% w/w | 50% w/w | 70% w/w | 100% w/w

Figure 3.7 Images of the *in-situ* capsule freeze-dried formulation. The percentages illustrated are the w/w % of NIF in PVP. *In-situ* clear capsule freeze-drying was performed for the purpose of demonstration. This figure is in agreement with the finding of chapter 1, as low content of PVP (100% NIF) shows fragile FD cakes that loose structural integrity.

3.4.3.2. Quality control of hard gelatin capsule shells

The effect of the freeze-drying process on the quality of gelatin hard capsules was also investigated following the World Health Organization (WHO) general monograph for quality control of capsules.

3.4.3.2.1 Visual inspection

Hard gelatin capsules that have been involved in the *in-situ* capsule freeze-drying process (otherwise refered to here as treated capsules) were visually examined and inspected, results show > 20 treated capsules to be smooth and undamaged. The physical appearance of treated capsules did not suggest a change in the hardness, softness, swelling or mottling of capsule shells. In addition, treated and untreated parts of the capsule were compared using scanning electron microscope (SEM) techniques. Figure 3.8 (B, C & D) below presents a capsule bottom (treated) and top (untreated) under various magnification levels where no significant difference was observed in the treated parts.

3.4.3.2.2 Effect of liquid TBA

The effect of liquid TBA on the physical stability of hard gelatin capsules was further investigated to determine if any colouring additives are released from capsules while adding 0.5 mL of liquid TBA (40 $\pm$ 0.5 ^{o}C) to the inside of a hard red gelatin capsule. Figure 3.8-A present's the corresponding experiment performed using clear gelatin capsules, for presentational purposes. Added TBA was maintained liquid for 60 min by maintaining the temperature of the liquid filling at (40 $\pm$ 0.5 ^{o}C). This was achieved by placing the test capsule in a vial which then was transferred into a (40 $\pm$ 0.5 ^{o}C) water bath. By visual inspection, of which protocol is described above, the capsules remained intact and no leaching of the dye into TBA was observed (n=3). In order to confirm this observation, HPLC method, described below, was run on the TBA contained within the capsule.

In order to validate this approach and check whether the HPLC method, described below, was able to detect the dyes and additive that may leach out from the red capsules, the following control experiment was performed; Red gelatin capsules were filled with 0.5 mL of 0.1M HCl, (n=3), which resulted in the whole capsule dissolving within 60 min, releasing its colouring and food additives (0.19% w/w E123 Amaranth,

0.76% w/w E124 Ponceau-4R and 0.66% w/w E171 Titanium dioxide as described by the manufacturers: The-Alchemists Apothecary).

The generated solutions from the controlled experiment, were examined using UV/Vis instrument, dye absorbance was found to peak at 510nm (Fig 3.9-A); thus using the HPLC method described in section 3.3.2.2.2, with a modified mobile phase (20%v/v methanol, 80%v/v 0.1M ammonium acetate) and monitoring the wavelength 510nm, the generated solutions of both experiments (i.e. liquid TBA from inside the gelatin capsule and the resulted solution from dissolving red capsule in 0.1M HCl) were tested by the modified HPLC method. Results show that the chromatogram of the controlled experiment solutions showed a peak retained at 6.3 $\pm$ 0.01 min with absorbance at 510nm (n=3). The parallel experiment, where by liquid TBA was used, no absorbance at 6.3 min was detected (n=3). Chromatograms of pure TBA was also compared to that withdrawn from inside the red gelatin capsule only to find no differences (n=3). This indicated that using liquid TBA has not resulted in detectable leaching of capsule colure additives.

3.4.3.2.3 Chemical degradation of hard gelatin capsules shell

FT-IR analysis of treated and untreated capsules were compared to determine if the process of freeze-drying has caused chemical changes. Treated capsules in this experiment, are capsule shells used in the manufacture of *in-situ* capsule FD 10% w/w NIF in PVP. Figure 3.9-B below contains an example FT-IR spectrum of both capsules. The correlation between 2 capsules for the range 4000-400 cm^{-1} is > 97%, therefore indicating no chemical changes to the gelatin capsule shell induced by freeze-drying.

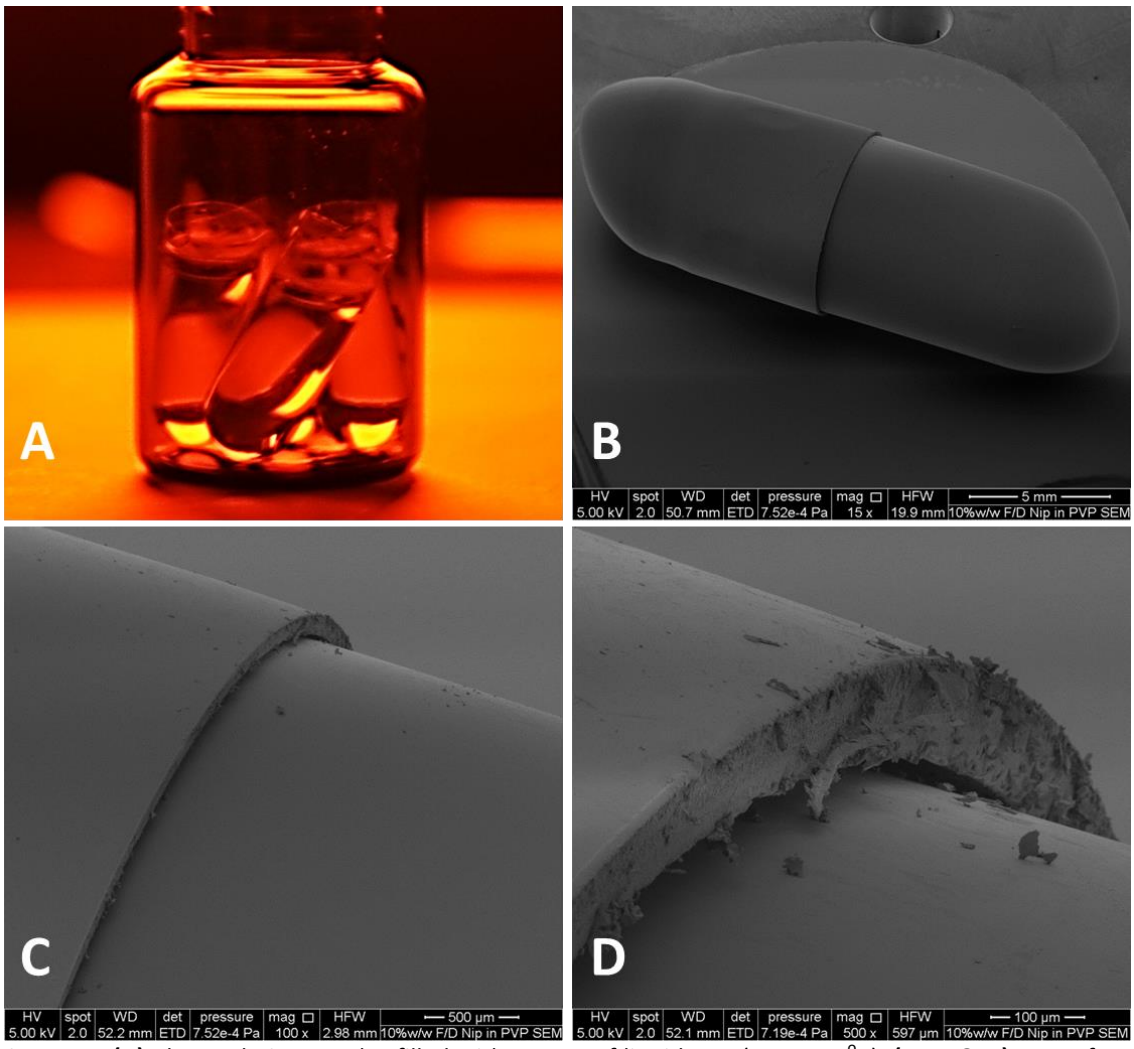

Figure 3.8 **(A)** Clear gelatin capsules filled with 0.5 mL of liquid TBA (40 ± 0.5 ^{o}C). **(B, C, & D)** SEM of *In-situ* red capsule FD formulation. The capsule bottom part was involved in the freeze-drying process, while the top part was not. The structure of both looks identical under SEM.

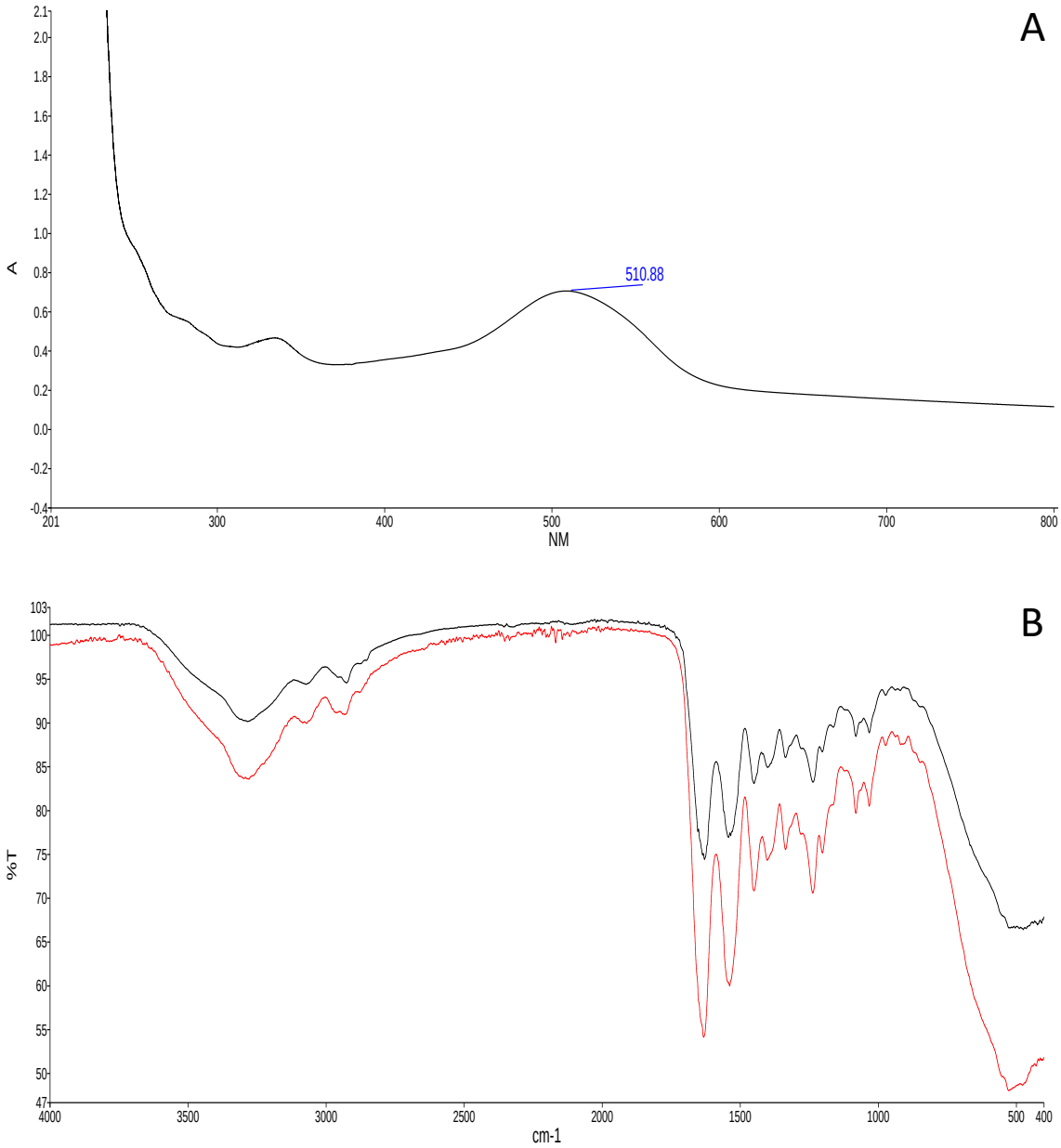

Figure 3.9 **(A)** UV-Vis absrobance spectra of red gelatin capsule disolved in 0.1M HCl. **(B)** FT-IR transmittance spectra of untreated (i.e. not FD) red gelatin capsule (—) and treated (FD) capsule (—), showing > 97% correlation. No chemical differences are observed between the two capsules.

3.4.3.2.4 Uniformity of mass

Following the WHO guidelines, the uniformity of mass of the treated gelatin hard capsules was determined by weighing 20 indicted capsules individually and determining the deviation of each of the treated intact capsules from the average mass. Table 3.3 below presents the weights of 20 intact capsules used in the production of *in-situ* capsule FD 10% w/w NIF in PVP formulation. All capsules show ≤ 2% deviation from the average weight, therefore complying with the WHO limit of 10% deviation from the average weight.

3.4.3.2.5 Disintegration test

Following the international pharmacopeia guidelines (WHO, 2015) on disintegration test of hard capsules, 6 FD capsules were tested using the basket-rack apparatus as described in section 5.3 of the international pharmacopeia (WHO, 2015). The disintegration medium consisted of 1000 mL of water maintained at (35 – 39 ^{o}C). Results show all 6 FD capsules have disintegrated in 5.10 min, while performing the same test on un-FD red hard gelatin capsules showed to disintegrate in 5.5 min. Therefore indicating that the freeze-drying process has not significantly affected the disintegration performance of hard gelatin capsule shells. Both FD and un-FD capsules showed to comply with the international pharmacopeia limits for hard gelatin capsule disintegration time of < 30 min (WHO, 2015).

Table 3.3 Average weight of intact treated capsules. (These capsules were used in the manufacture of *in-situ* capsule FD 10% w/w NIF in PVP formulation) All capsules were within the WHO % deviation limit of 10% from the average weight.

No.	Weight of capsule (mg)	% Deviation from average	Condition	No.	Weight of capsule (mg)	% Deviation from average	Condition
1	195.76	2%	Pass	11	203.34	-2%	Pass
2	197.09	1%	Pass	12	203.53	-2%	Pass
3	197.37	1%	Pass	13	201.14	-1%	Pass
4	197.33	1%	Pass	14	198.65	1%	Pass
5	201.67	-1%	Pass	15	198.59	1%	Pass
6	202.40	-1%	Pass	16	201.36	-1%	Pass
7	201.51	-1%	Pass	17	200.52	0%	Pass
8	200.02	0%	Pass	18	199.29	0%	Pass
9	195.32	2%	Pass	19	202.75	-1%	Pass
10	200.81	0%	Pass	20	201.68	-1%	Pass
Average weight of intact capsule					**200.01 ± 2.34 mg**		

3.4.3.3. Physical state of nifedipine

Thermal analysis output of FD cakes formed by *in-situ* capsule freeze-drying, following the same methods described in previous chapters (Section 2.3.3), was compared to the thermal analysis findings of ampule FD formulations. Table 3.4 below presents a summary output of the average thermal analysis (n=3) for formulations developed by both techniques (*In-situ* capsule and ampule FD). The average % w/w residual solvent in capsule formulations was shown to follow a similar trend to that of the ampule FD formulations. Similarly both techniques have shown to produce predominantly

amorphous formulations in compositions containing <70% w/w NIF in PVP. Nevertheless, a difference of 5% was observed in the % w/w crystalline NIF between the *in-situ* capsule FD and the ampule FD formulation containing 70% w/w NIF in PVP (Table 3.4). With the exception of 30% w/w NIF in PVP, T_g values of *in-situ* capsule FD formulations follow the same trend presented by ampule FD formulations, where by the T_g increases as the content of PVP increases in the formulation (section 2.4.3.1). However, the T_g values of *in-situ* capsule FD formulations were shown to generally be lower than T_g values of ampule FD formulations (with the exception of 70 and 100% w/w NIF in PVP). Figure 3.10 below presents an example second heat thermogram comparing the FD 10% w/w NIF in PVP formulation produced in both techniques. Observed differences in T_g of second heat thermograms may indicate changes in the amount of PVP available in the freeze-dried cake. A hypothesis addressing this difference will be purposed in the discussion, but it is reported in the next section the overall nifedipine content for the formulation that will be taken forward is within BP acceptable limits, so non has been lost form the capsule for this formulation.

Table 3.4 Average thermal analysis of the *in-situ* capsule FD formulations. The percentage of crystalline material is dependent on the average enthalpy value. Crystalline nifedipine was undetected in ≤ 50% w/w NIF in PVP of the *in-situ* capsule FD formulations, which is in agreement with the data generated from ampule FD formulations in chapter 2 (section 2.4.3.).

***In-situ* capsule FD formulations**							
% w/w NIF in PVP	**Average % Weight loss**	**SE**	**Av. Enthalpy***	**SE**	**% w/w crystalline NIF**	**Second heat Av. T_g**	**SE**
100%	3.0%	1.2%	106.93	1.10	-	49.22	0.27
70%	9.0%	0.5%	10.13	2.20	18%	80.12	7.59
50%	10.0%	0.5%	0.00	0.00	0%	96.23	0.25
30%	9.7%	0.3%	0.00	0.00	0%	91.96	0.58
10%	10.8%	0.2%	0.00	0.00	0%	130.26	3.56
Ampule FD formulation							
% w/w NIF in PVP	**Average % Weight loss**	**SE**	**Av. Enthalpy***	**SE**	**% w/w crystalline NIF**	**Second heat Av. T_g**	**SE**
100%	1.8%	0.6%	101.96	3.07	-	46.72	0.44
70%	10.1%	0.9%	4.73	0.58	13%	77.80	0.58
50%	12.6%	1.5%	0.00	0.00	0%	99.87	3.84
30%	13.2%	1.2%	0.00	0.00	0%	124.49	1.52
10%	11.8%	0.2%	0.00	0.00	0%	142.87	0.61

*Measured for melting peaks of first heat in the range (140-180 ^{o}C)

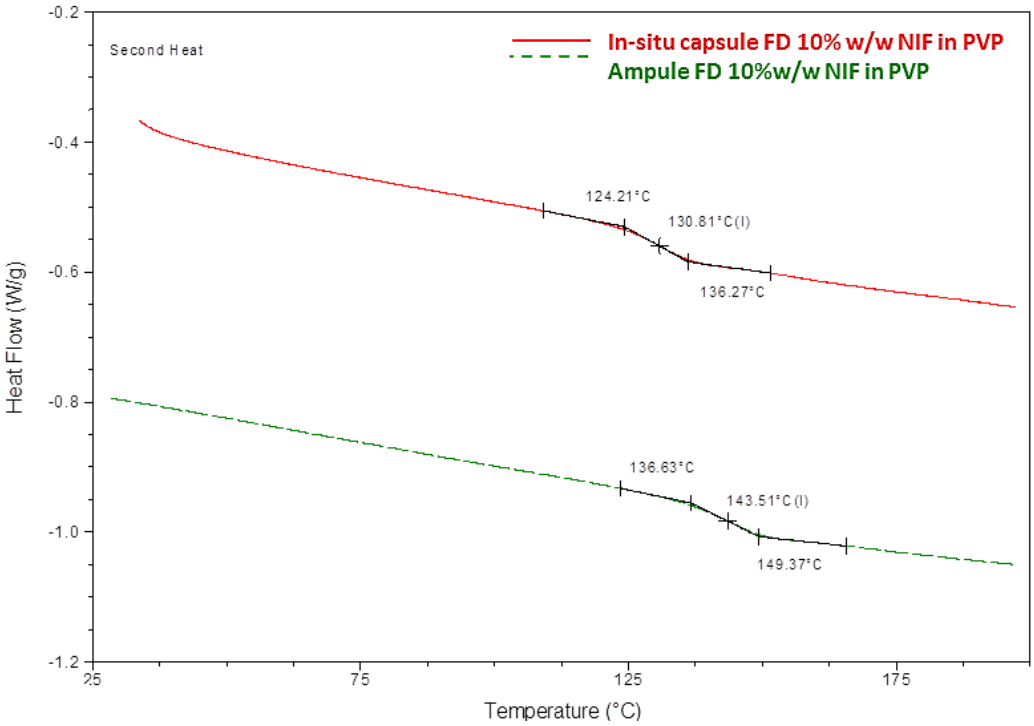

Figure 3.10 Thermogram of the second heat of *in-situ* capsule FD and Ampoule FD 10% w/w NIF in PVP formulation using DSC. (All DSC thermograms in this thesis unless stated will have exothermic transitions upwards).

Despite the absence of a melting peak in DSC thermograms of FD 50% w/w NIF in PVP formulations, scanning electron micrograph (figure 3.11) shows the presence of crystal like structures on top of larger amorphous particles. Such small NIF crystals may be undetected using thermal methods as they may simply dissolve in PVP once heated to temperatures above T_g of the product. Scanning electron micrograph of the FD 10% w/w NIF in PVP shows a much lower number of crystals.

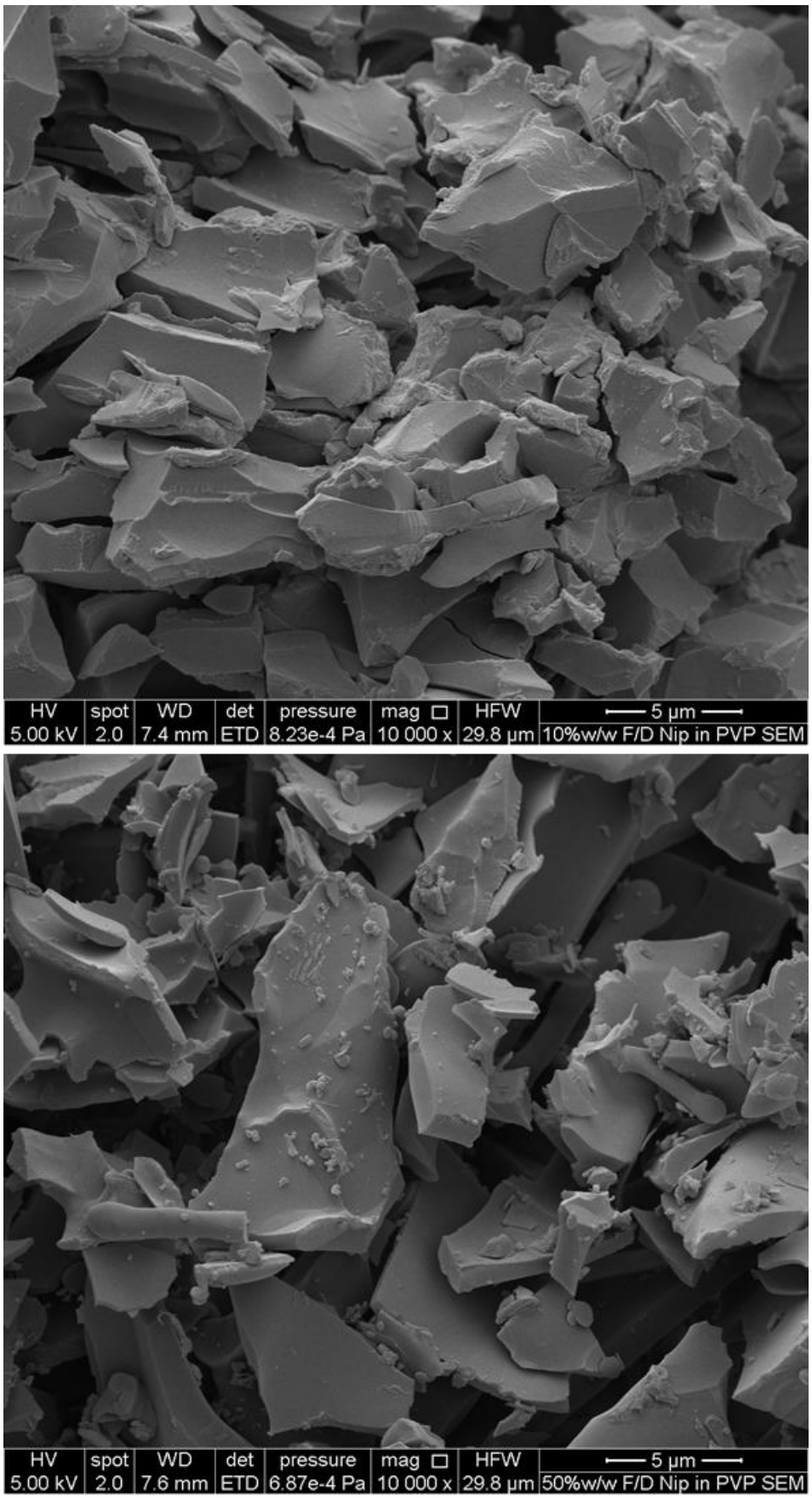

Figure 3.11 Scanning electron micrograph of FD cakes of *in-situ* capsule FD formulations (10 and 50% w/w NIF in PVP). The 50% w/w formulation (lower image) is showing small crystal like particles on top of what appears to be broken amorphous sheets.

3.4.3.4. Uniformity of weight and drug content

The FD capsules of NIF in PVP were tested for uniformity of weight following BP guidelines. As would be expected, the average weight of individual unit dosage form was seen to increase as the content of PVP in the formulation increased, FD 10% w/w (i.e. 10 mg NIF in 90 mg PVP) is approximately 90 mg heavier than the average weight of FD 100% w/w (i.e. 10 mg NIF and 0 mg of PVP). Weight uniformity is presented as relative standard deviation (RSD%). With the exception of 30% w/w NIF in PVP, the weight of formulation was seen to be less uniform as the % w/w of NIF increases (table 3.5). This may be related to the effect of NIF content on the structural strength of FD cakes. Although all formulations have shown variations in unit dosage weight greater than that observed in the marketed (TEVA 10 mg nifedipine fast release soft gel capsule) formulation, the FD 10% w/w NIF in PVP formulation shows a an RSD <2%.

Formulations showing large variations (RSD > 2%) in unit dosage weight (FD 100 - 30% w/w NIF in PVP) have also shown large variations in drug content (≥ 5% RSD). Figure 3.12 presents the average drug content of *in-situ* capsule FD formulations and the marketed TEVA formulation. Both 50 and 70% w/w NIF in PVP formulations show an average drug content below the BP acceptable limit (10 $\pm$ 0.5 mg). This may be due to the weak nature of the produced FD cakes in such formulations. Manual process such as recapping of FD capsules, inside nitrogen bags, have shown the potential to cause loss of capsule content, which may be more effective with weakly held FD cakes. *In-situ* capsule FD 10% w/w NIF in PVP has shown greater potential, in uniformity of weight and drug content, than other *in-situ* FD formulations, in addition it shows BP acceptable drug content (MHRA, 2014b).

Table 3.5 Uniformity of weight for unit dosage (n=3). All formulations are designed to contain 10 mg NIF. The percentage listed under formulation column details the w/w % of NIF in PVP of the *in-situ* capsule FD formulations. Weight of empty capsule = 90 mg.

Formulation and % w/w of NIF in PVP	Expected weight of formulation (mg)	Average observed weight of unit dosage form (mg)	%RSD
Marketed	-	616.39	0.2%
FD 100%	100.00	100.37	4.4%
FD 70%	104.29	103.95	3.0%
FD 50%	110.00	109.72	2.3%
FD 30%	123.30	125.41	3.2%
FD 10%	190.00	200.01	1.2%

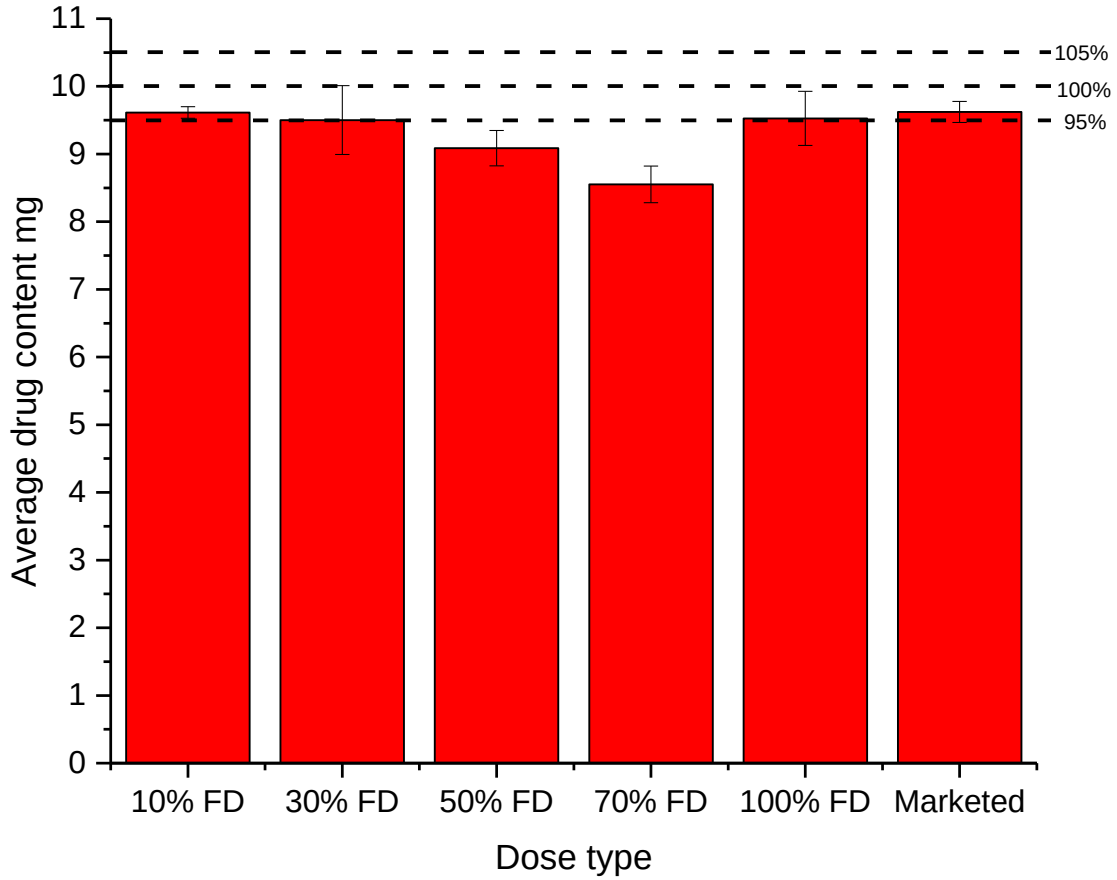

Figure 3.12 Average drug content in each of the tested formulations as well as the marketed formulation. Error bars represent standard error of n=3. The marked dashed lines indicate the BP drug content limits (MHRA, 2014b).

3.4.4. Dissolution studies

3.4.4.1. Comparing dissolution profiles of different formulation types of NIF in PVP

A multivariate approach (MANOVA) test was conducted to clarify differences in dissolution profiles of different formulations of NIF (Yuksel *et al.*, 2000, Costa *et al.*, 2001). Whereby percentage dosage released at individual time intervals are compared for any statistically significant differences. Dissolution rates of different formulations of NIF where further compared using mathematical model dependent methods, whereby dissolution profile curves are fitted to the most representative kinetic model (Costa *et al.*, 2001), allowing a better understanding of the dissolution kinetics and therefore the rate constant of dissolution (Costa *et al.*, 2001). For all dissolution studies in this chapter, a good linear relationship was found when plotting the natural logarithm, ln, of percentage undissolved drug versus time (Figure 3.13-B & Figure 3.14-B), therefore indicating a first-order dissolution process (Chutimaworapan *et al.*, 2000, Costa *et al.*, 2001). The slope of the first order linear relationship is known as the rate constant (k), which may be related to the half-life ($t_{1/2}$) of undissolved drug (i.e. the time taken for the content of undissolved drug to half), using the equation [$t_{1/2}$ = ln2 / k] (Zeuzem *et al.*, 1996).

The average dissolution profile of nifedipine as received (NIF-AR), 10 ± 0.5 mg of drug placed in empty red gelatin capsules, in 0.1M HCL (37.0 ± 0.5 ^{o}C), was found to release approximately 9% of drug content in 60 min of dissolution testing. The addition of PVP to the dissolution medium, in concentrations equivalent to the amount of PVP in 30% w/w NIF in PVP (labelled NIF-AR* in figure 3.13-A), did not show a great effect on the dissolution profile of nifedipine as received (Figure 3.13-A). Applying MANOVA analysis shows to be no significant difference, in the percentage drug released at all time-points, between NIF-AR and NIF-AR*($p > 0.05$). The average dissolution rate constants of NIF-AR and NIF-AR* are 0.00162 ±7.7x10^{-5} min^{-1} and 0.00175 ± 1.0x10^{-4} min^{-1} with no significant difference. Treating NIF-AR as control, a MANOVA analysis was applied to determine if there is a significant difference in dissolution profiles between freeze-dried formulations, physical mix, NIF-AR and NIF-AR*. Using the Wilks' Lambda test of the MANOVA analysis, the 4 dissolution profiles have shown to be significantly

different (P <0.001). Additionally Post hoc analysis was performed using Dunnett (2-sided) test to identify where the significant difference lay between the 4 dissolution profiles (Table 3.13 Appendix 1). Results of the FD formulations show significant difference (P < 0.001) to the control NIF-AR starting from 2 min into the dissolution profile, while the PM formulation starts to show significant difference from 10 min into the dissolution profile (P < 0.05). Repeated measures were applied separately to each drug product to allow comparison of percent dissolved at the sequential times. 30% w/w FD and 30% w/w PM started to show significant differences in the average percentage dissolved at 2 min of the dissolution profile (P < 0.001). Significant differences were observed in all remaining sequential times (P < 0.05).

As MANOVA analysis is based on the assumption that the population of data follows a normal distribution, a Levene's test was applied to compare the variances of percentage dissolved at each time point separately, thus treating each time point as a single population. Results, from the Leven's test, show the variances of percentage dissolved of time points ≤ 10min to be significantly different (i.e. does not follow a normal distribution). Therefore MANOVA results for time points at 10min and below are rendered irrelevant. A data suitable non-parametric test (Kruskal-Wallis test which assumes monotonic relation-ship between the two variables) was applied to determine any significant differences between the percentages dissolved of the different test formulations at each time point 1-10min (Table 3.14 Appendix 1). Results show significant differences in percentage dissolved to arise between the different formulations at ≥6 min table 3.14 (Appendix 1) includes the P values.

A model dependent method was adopted to further study the dissolution kinetics for the fastest segment of each of the dissolution profiles. By plotting the ln of the percentage undissolved drug against time (Figure 3.13-B), a linear relation confirms the reaction follows a first order kinetics (Yuksel *et al.*, 2000, Costa *et al.*, 2001). While dissolution profiles for NIF-AR and NIF-AR* show a lag time, for drug release, of approximately 20 min, drug content below the detection limit are assumed to be released but undetected in this phase. Therefore, no data points were plotted between 0 and 20 min, in figure 3.13-B, for NIF-AR and NIF-AR,* as this may interfere with the slope of the line, which is also defined as the rate constant (k). Figure 3.13-C compares the average k value (n=3) for each of the 4 test formulations. No significant difference was found between the dissolution rate constant of NIF-AR* and NIF-AR

(even at P = 0.1). The k value for the PM formulation shows a significant difference from NIF-AR (P < 0.001 Student's T-test) with approximately 20 times. The FD formulation shows a rate constant, approximately, ten times greater than that of the equivalent PM formulation (P < 0.001 Student's T-test).

The outcome of the above performed statistical compression and analysis on the four test formulations indicates that the dissolution profile of NIF-AR and NIF-AR* show no significant difference in rate or percentage dissolved at individual time points. This concludes that the presence of PVP in dissolution medium, at levels equivalent to 30% w/w NIF in PVP, does not improve the dissolution profile of nifedipine. Nevertheless, grinding PVP with NIF to formulate a physical-mix has shown to improve the percentage dissolved values of nifedipine at ≥ 10 min, and has increased k by approximately 20 times. Presenting NIF in a freeze-dried formulation with an equivalent concentration of PVP has shown to further enhance the dissolution rate constant, from the PM formulations, by approximately 10 times.

For a better grasp on the differences in dissolution rates between the 4 dissolution profiles, $t_{1/2}$ for each of the profiles was determined using the presented average rate constant in figure 3.13-C. Table 3.6 below shows that the $t_{1/2}$ of undissolved NIF in *in-situ* capsule FD formulation of 30% w/w NIF in PVP is shorter than the equivalent physical-mix formulations by approximately 10 time and lower than NIF as received by approximately 100 time.

Table 3.6 A summary of t ½ of undissolved NIF in dissolution profiles of different formulations of NIF

Formulation	**k (min^{-1})**	**$t_{1/2}$ (min)**
Freeze-dried	0.20	3.43
Physical mix	0.02	34.08
NIF AR*	0.18 $x10^{-2}$	396.08
NIF AR	0.16 $x10^{-2}$	435.94

*NIF as received in a PVP containing dissolution medium 2.59$x10^{-3}$% w/v PVP in 0.1M HCl

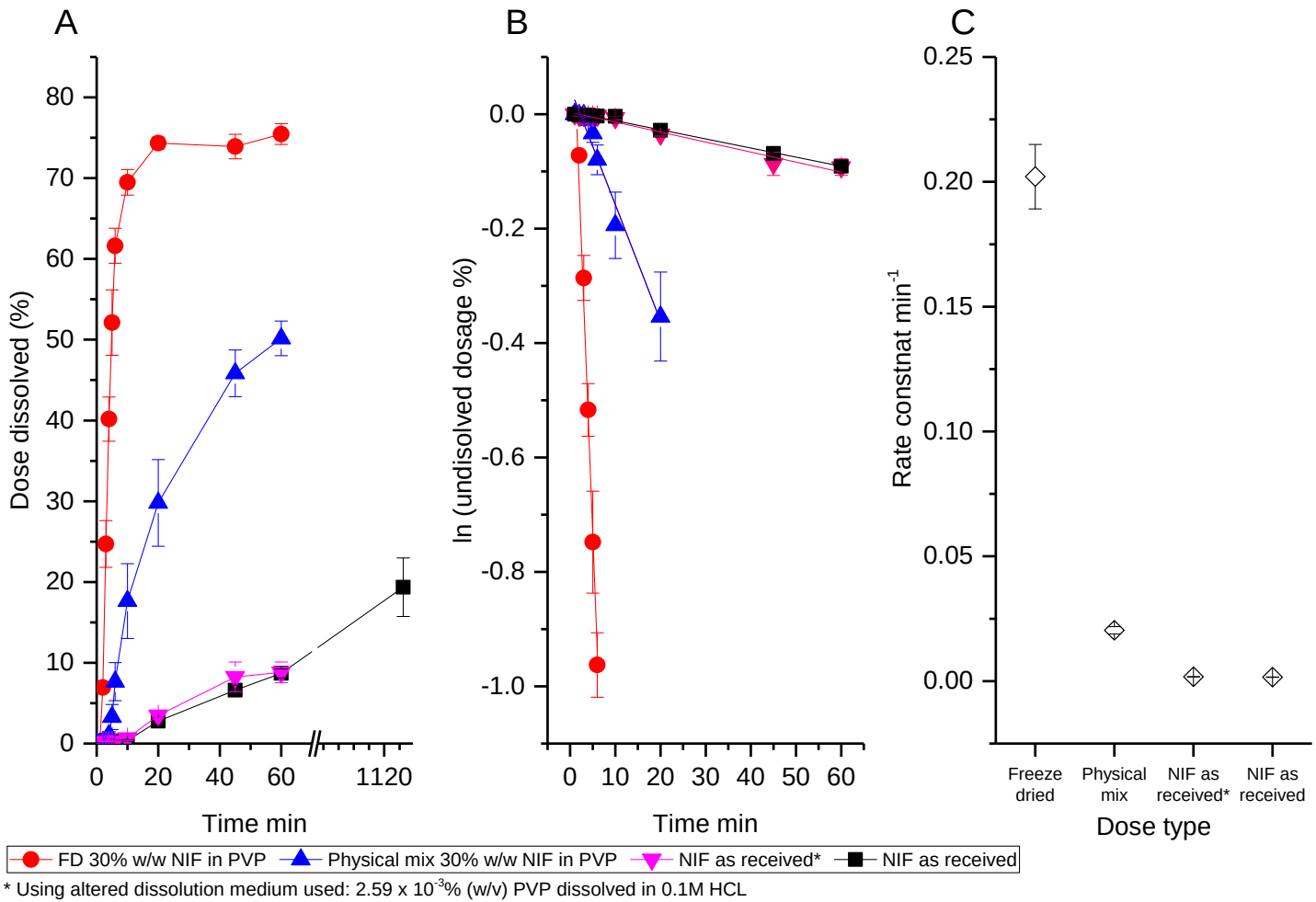

Figure 3.13 Comparing **(A)** dissolution profile, **(B)** dissolution kinetics and **(C)** rate constant of nifedipine in different dosage types. The dissolution medium is 0.1M HCL unless otherwise stated. Temperature of dissolution medium is 37.0 ± 0.5oC and dissolution volume 900mL. Test was performed following USP paddle apparatus 2. Error bars represent standard error of n=3

3.4.4.2. Effect of NIF:PVP ratio on dissolution profile in FD formulations

Dissolution profiles of FD formulations containing different NIF:PVP ratios are presented in figure 3.14-A. Table 3.15 (Appendix 1) presents full descriptive data of percentages dissolved at individual time points. In order to assign the correct statistical test (i.e. parametric or non-parametric), the data was subjected to Levene's test (Table 3.16 Appendix 1). Results show percentages dissolved prior to 5 min of the dissolution profile, for all compared formulations, to have significantly different variances, thus indicating a non-normally distributed data. Therefore, a non-parametric test (Kruskal-Wallis) was used to compare the percentages dissolved for each formulation at time points 1-3 min (Table 3.18 Appendix 1). Results from the Levene's test also show dissolved percentages at 5 and 60 min to follow a normal distribution; therefore a MANOVA analysis was performed following the same method described in the previous sub-section. Results from the Kruskal Wallis test (table 3.18 Appendix 1) indicate that a significant difference was observed between percentages dissolved of different FD formulations and FD-100% at time-points ≥ 2 min ($p < 0.05$). Similarly, MANOVA analysis shows a significant difference at time-points ≥ 45 min ($p < 0.01$). The Dunnett t-test further illustrates these significant differences arise from differences in percentages dissolved between FD-10% and FD-100% at 45 and 60 min (p <0.001), and FD-30% and FD-100% at 45 and 60 min (p <0.001) both with a positive mean difference (table 3.17 Appendix 1). On the other hand a significant difference was observed between FD-70% and FD-100% at 45 and 60 min ($p = 0.001$ and $p < 0.001$ respectively). No significant difference was observed between FD-50% and NIF-AS in percentages dissolved at individual time points.

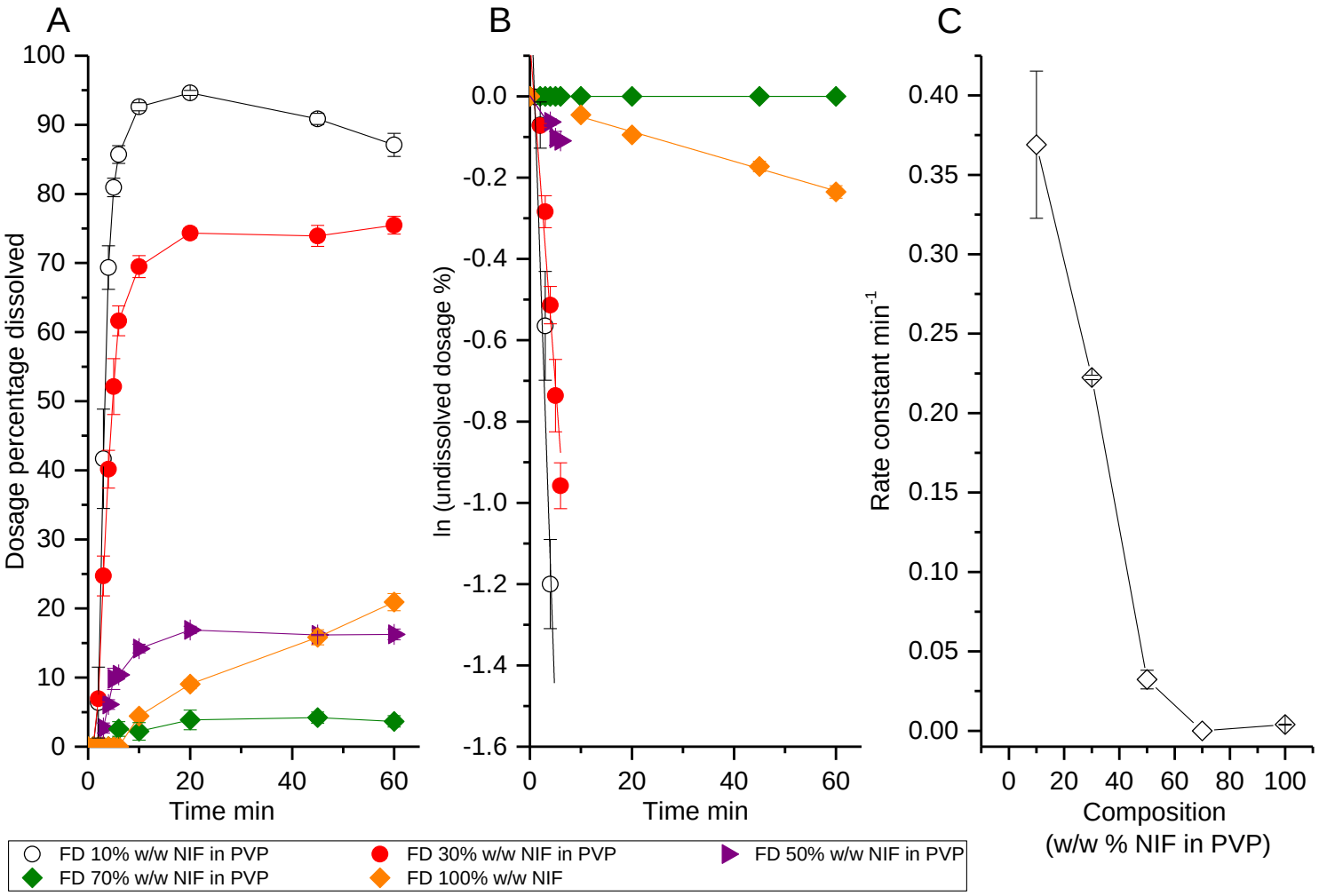

Figure 3.14 Comparing **(A)** dissolution profile, **(B)** dissolution kinetics and **(C)** rate constant of *In situ* FD nifedipine capsules with varying NIF:PVP ratios. The dissolution medium is 0.1M HCL unless otherwise stated. Temperature of dissolution medium is 37.0 ± 0.5°C and dissolution volume 900mL. Test was performed following USP paddle apparatus 2. Error bars represent standard error of n=3

Figure 3.14-B shows all dissolution profiles to follow a first order kinetics. Using student t-test, a significant difference in average k value was observed between FD 10% w/w and FD-100% ($p < 0.001$), with k of FD-10% greater by approximately 86 times. The k value of FD-30% was shown to be approximately 56 times greater than FD-100% with the significant difference observed at ($p < 0.001$). The average k values of FD-50% showed to be approximately 8 times greater than FD-100% with the significant difference observed at ($p < 0.05$). The k value for FD-70% was shown to equal 7.91 x 10^{-4} min^{-1} (table 3.7).

Table 3.7 A Summary of t ½ of undissolved NIF in dissolution profiles of different FD formulations of NIF. Percentages presented in the FD formulations refer to the % w/w NIF in PVP.

FD Formulation	k (min^{-1})	$t_{1/2}$ (min^{-1})
10%	0.37	1.88
30%	0.22	3.12
50%	0.03	21.49
70%	7.91 x10^{-4}	879.00
100%	3.91 x10^{-3}	177.28

3.4.4.3. Effect of PVP and physical state of nifedipine on the kinetic and thermodynamic solubility of nifedipine

Although the presence of PVP in dissolution medium did not show a significant effect on the dissolution profile of nifedipine (Fig 3.14), a further investigation on the effect of PVP on the kinetic or intrinsic solubility of nifedipine is presented in figure 3.15-A and B. The concentration of NIF in dissolution medium at 5 min (Fig 3.16-A) and the maximum concentration of NIF, in dissolution medium, reached within 60min (Fig 3.16-B) are plotted for NIF-AR* against the equivalent % w/w composition. For example, the data mark for NIF-AR* 10% w/w NIF in PVP in figure 3.15-A indicates the concentration of NIF in dissolution medium, at 5 min, whereby the dissolution medium contained a dissolved mass of PVP equivalent to that present in a 10% w/w NIF in PVP. As the content of NIF per unit dosage form, for all formulations, was 10 mg, the equivalent PVP weight was 90 mg in 900 mL, otherwise expressed as 1x10^{-2} w/v%.

Both of figure 3.15-A and B show that the presence of PVP in dissolution medium has no significant effect on the kinetic solubility of as received nifedipine. On the other hand, the content of PVP in FD formulation showed to correlate to an increase in the concentration of NIF in dissolution medium, of 0.1M HCl following [$NIFconc._{5min}$ = 19.3

x C + 11.04] for the concentration of NIF at 5 min of dissolution, and [NIFconc.$_{Max}$ = 19.6 x C + 11.96], where C is the % w/w NIF in PVP composition, for the maximum concentration of NIF reached within the 60 min dissolution test, otherwise defined as the kenitic solubility. Both linear correlations were found significant ($p < 0.05$) when tested with linear regression analysis. Although the content of PVP in FD formulation showed to correlate to the kinetic solubility of NIF, it is important to refer back to the phase diagram described in previous chapters (Chapter 2.4.2.3) where the relation between the content of PVP in FD formulations and the % w/w crystalline NIF showed a linear relationship with a negative slope, therefore suggesting that the enhancement in kinetic solubility is a result of increasing the amorphous NIF content.

Although the presence of PVP in dissolution medium has shown not to affect the kinetic solubility of NIF, results in figure 3.15-C show that the thermodynamic solubility of NIF as received, determined over 5 days of equilibrium at (37.0 $\pm$ 0.5 ^{o}C), to correlate with the concentration of PVP in dissolution medium following the equation [NIF solubility $_{(thermodynamic)}$ = 134.62X + 7.11] where X is the concentration of PVP in dissolution medium in % w/v. An outlier point, thought to be a result of artefact error, presented in figure 3.15-C, was excluded from the regression analysis.

The average kinetic solubility of predominantly amorphous NIF FD-10% (10.16 $\pm$ 0.04 µg/mL) was determined to be 20% greater than the thermodynamic solubility of the equivalent NIF-AR* (8.33 $\pm$ 1.5 µg/mL), therefore presenting evidence of the positive effect on the kinetic solubility of NIF, induced by its amorphous state.

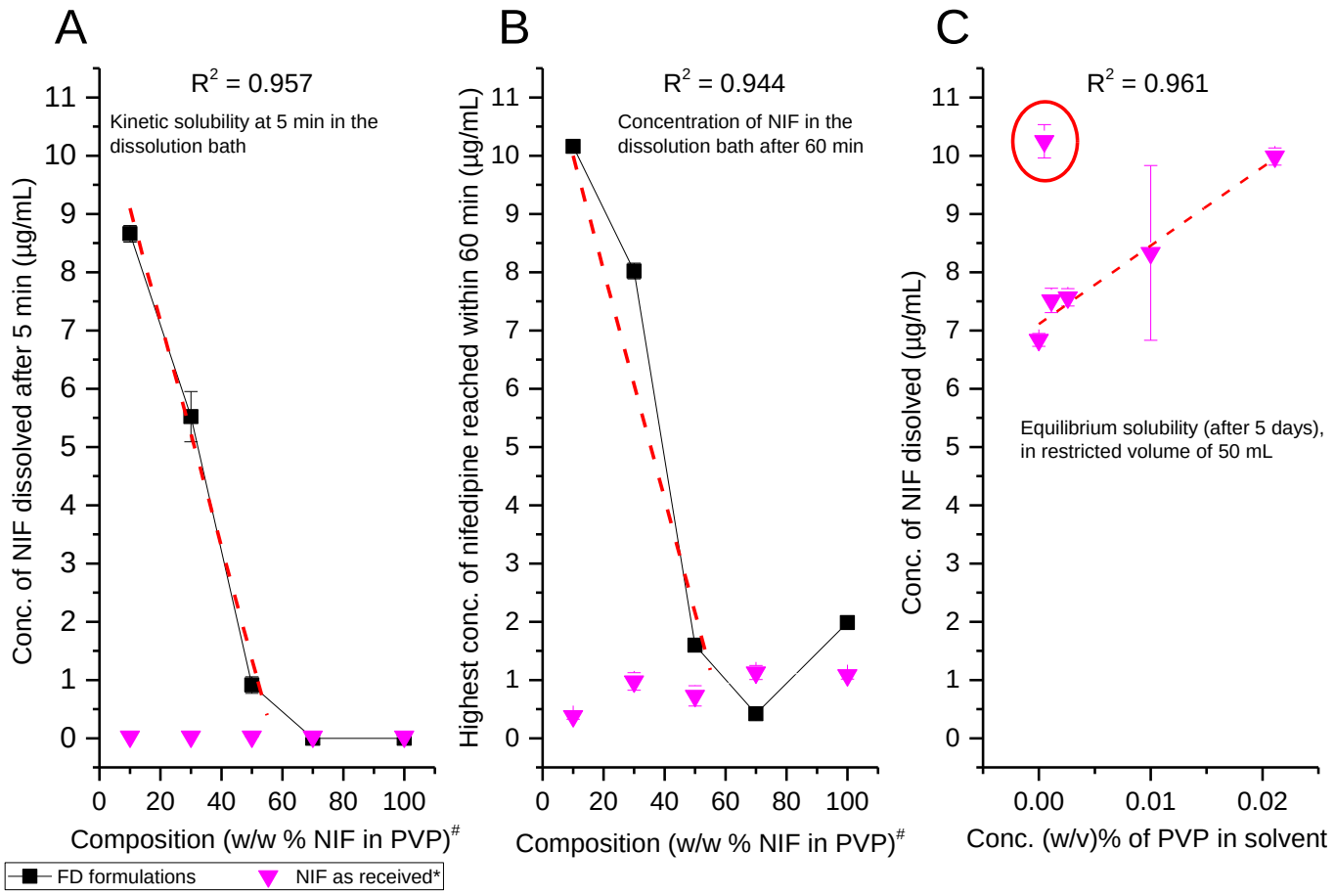

* Dissolution medium contains PVP at concentrations equavelent to the amount of PVP in corresponding FD formulations

Figure 3.15 Comparing the concentration of nifedipine **(A)** after 5 min of dissolution **(B)** after 60 min of dissolution and **(C)** after 5 days of equilibrium (thermodynamic solubility). The dissolution medium is 0.1M HCL, with the exception to NIF as received* in (A) & (B). # Only when testing nifedipine as recived*, the dissolution medium also contained PVP at concnetrations equal to thoes resulted by the full dissolution of PVP from equevelent FD formulations in 900 mL 0.1M HCl (e.g: NIF as received* with an x-axis (composition w/w % NIF in PVP) of 50%, indicates that the dissolution medium for this perticlar test contained a predisolved 10 mg of PVP). Error bars represent standard error (n=3). Circuled data point in (C) was considered an outliyer casued by an artefact, and therfore was not included in linear regression analysis.

3.4.4.4. Comparing FD 10% w/w NIF in PVP to marketed formulation

A currenlty markted fast release formulation of nifedipine has been compared to the performance of the *in-situ* capsule FD formulaiton (10% w/w NIF in PVP). Both formulations contained 10 mg of NIF. The dissolution profile of both formulations is presented in figure 3.16 below. Table 3.8 shows that the predominantly amorphous *in-situ* FD capsule formulation, 10% w/w NIF in PVP, reached a dosage percentage dissolved of 80% in an avage of 4.8 ± 0.2 min (also referd to as T_{80}), thus compatabil with the T_{80} BP guidelines of fast release tablets and capsule (MHRA, 2014b). The marketted formulation on the other hand shows a T_{80} aproximatly 3 times longer than the *in-situ* FD formulation.

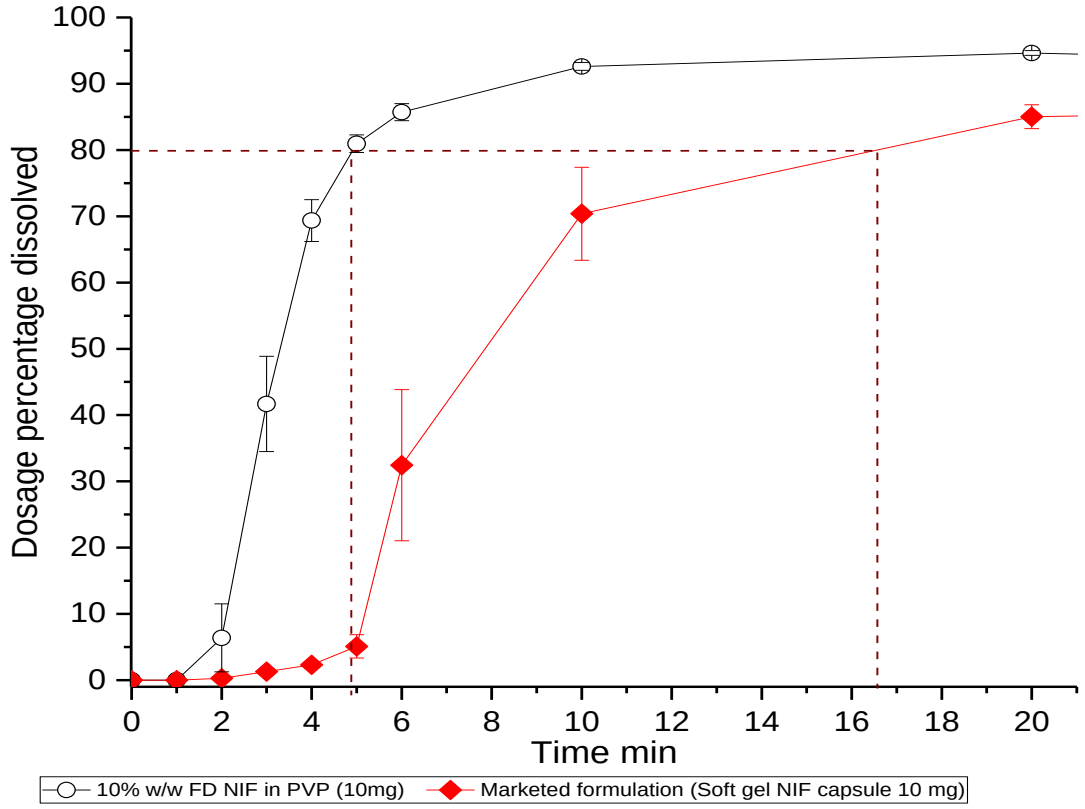

Figure 3.16 Comparing the dissolution profile of the *in-situ* capsule FD formulation 10% w/w NIF in PVP against the TEVA 10 mg NIF marketed formulation consisting of a soft gel capsule. Average T80 for the marketed formulation is approximately 3 times longer than that of the *in-situ* capsule FD formulation (10% w/w NIF in PVP). Error bars represent slandered error of n=3.

Table 3.8 A summary table comparing key parameters of *in-situ* capsule FD 10% w/w NIF in PVP with the marketed formulation soft gel 10 mg NIF TEVA fast release capsule. Variations are shown as SE.

Parameters	*In-situ* capsule FD		Marketed (soft gel)	
Drug content (10 mg)	9.61	± 0.09	9.62	± 0.16
T80 (min)	4.8	± 0.2	13.40	± 2.40
Dissolution rate constant (k)	0.37	± 0.05	0.10	± 0.02
Maximum reached dosage % dissolved	95%	±0.35%	89%	±0.99%

3.4.5. Polarized microscopic dissolution

The observed reduction in the concentration of NIF in dissolution medium after 20 min of the FD-10 dissolution test (Figure 3.14-A), may indicate that recrystallization and precipitation of drug was taking place in dissolution medium. This concept was qualitatively examined as part of this study. The dissolution experiments of FD formulations FD-10% and FD-50% were simulated under a polarized microscopy, whereby a mass of 1 ± 0.2 mg of material was placed on a clear microscopic slide, and a volume of 0.5 mL of 0.1M HCl (37.0 ± 0.5 ^{o}C) dissolution medium was pipetted on top. The dispersion in dissolution media was monitored through polarized light microscopy, where a photo was taken every min over 1 hour. Table 3.9 shows images of polarized microscopy at subsequent time points for both FD formulations and a control PM-50%. As described in previous chapters, crystals are identified by birefringence. Results show that initial recrystallization signs of FD-10% appear at 15 min, where 3 crystals were observed. The number of crystals was shown to stop increasing at 30 min where 6 crystals was the final observed number. FD-50% on the other hand appears to take, approximately 5 min more for recrystallization to initiate. Image at 20 min of the FD-50% dissolution shows weak birefringence of 3 crystals. The number of crystals in FD-50% was shown to sharply increases between 20 and 30 min, reaching approximately 100 crystals, at which point the number of crystals was maintained approximately the same between 40 and 60 min. Figure 3.17-A shows a summary of the number of crystals observed, in FD-10% and FD-50%, over the duration of the experiment. In an attempt to further quantify the outcome of the experiment, individual images were analysed using the software ImageJ, where the mean grey value (MGV) of each image was measured. MGV of polarized images containing no birefringence is equal to 0.00 arbitrary units (AU). The presence of crystals and therefore birefringence causes the measured MGV to increase. The controlled sample, PM-50%, was shown to give a constant MGV of 6.0 ± 0.5 AU (Figure 3.17-B). The MGV of FD-50% showed to continuously increase after a lag time of approximately 25 min and only reaches a plateau at approximately 50 min. Despite the small difference in the number of crystals observed between 40 and 50 min in the dissolution of FD-50%, the MGV was seen to almost double in value between these 2 time points. A closer examination of individual crystals (Fig 3.18) shows individual

crystals to grow in size, therefore increasing the amount of birefringence observed, which was detected through MGV measurements.

Table 3.9 Dissolution of FD-10%, FD-50% and PM50% under polarized light microscopy. Presence of birefringence indicates the presence of crystal materials. This may be due to their presence in a sample prior to dissolution, such as the controlled sample, or due to recrystallization of amorphous materials.

Time min^{-1}	FD-10%	FD-50%	PM-50%
0		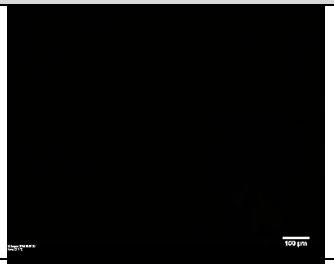	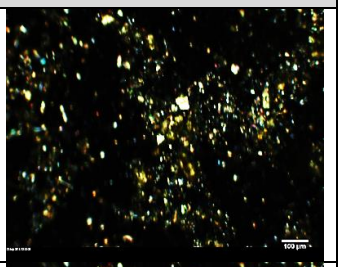
5	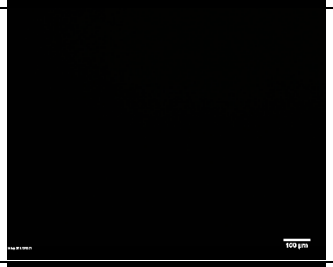	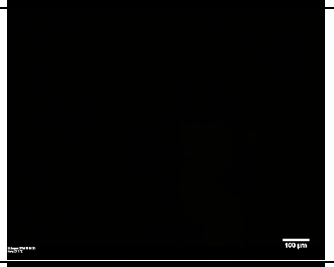	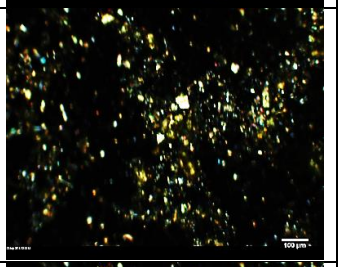
10			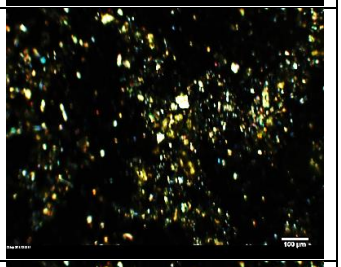
15		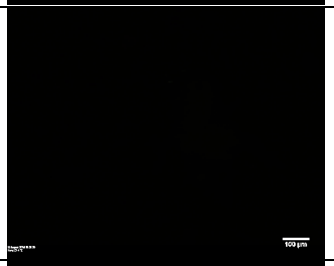	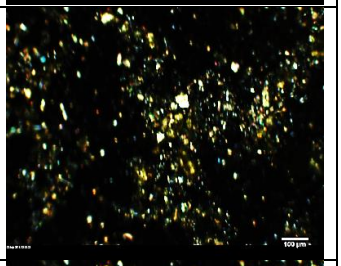
20			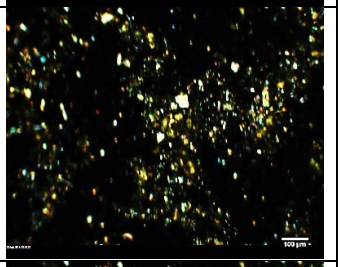
30		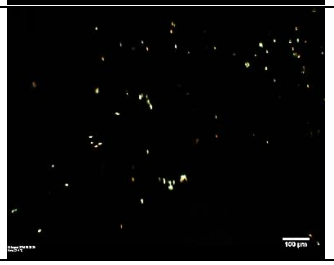	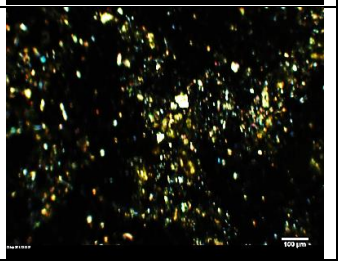

Time min^{-1}	FD-10%	FD-50%	PM-50%
40		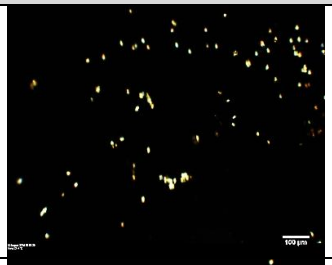	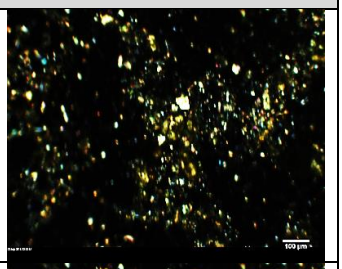
50			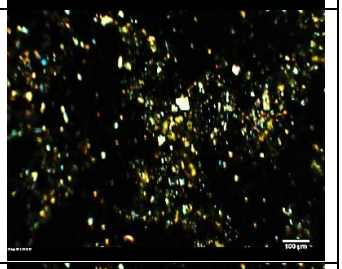
60			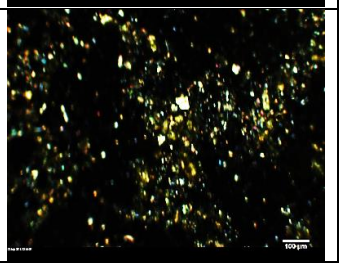

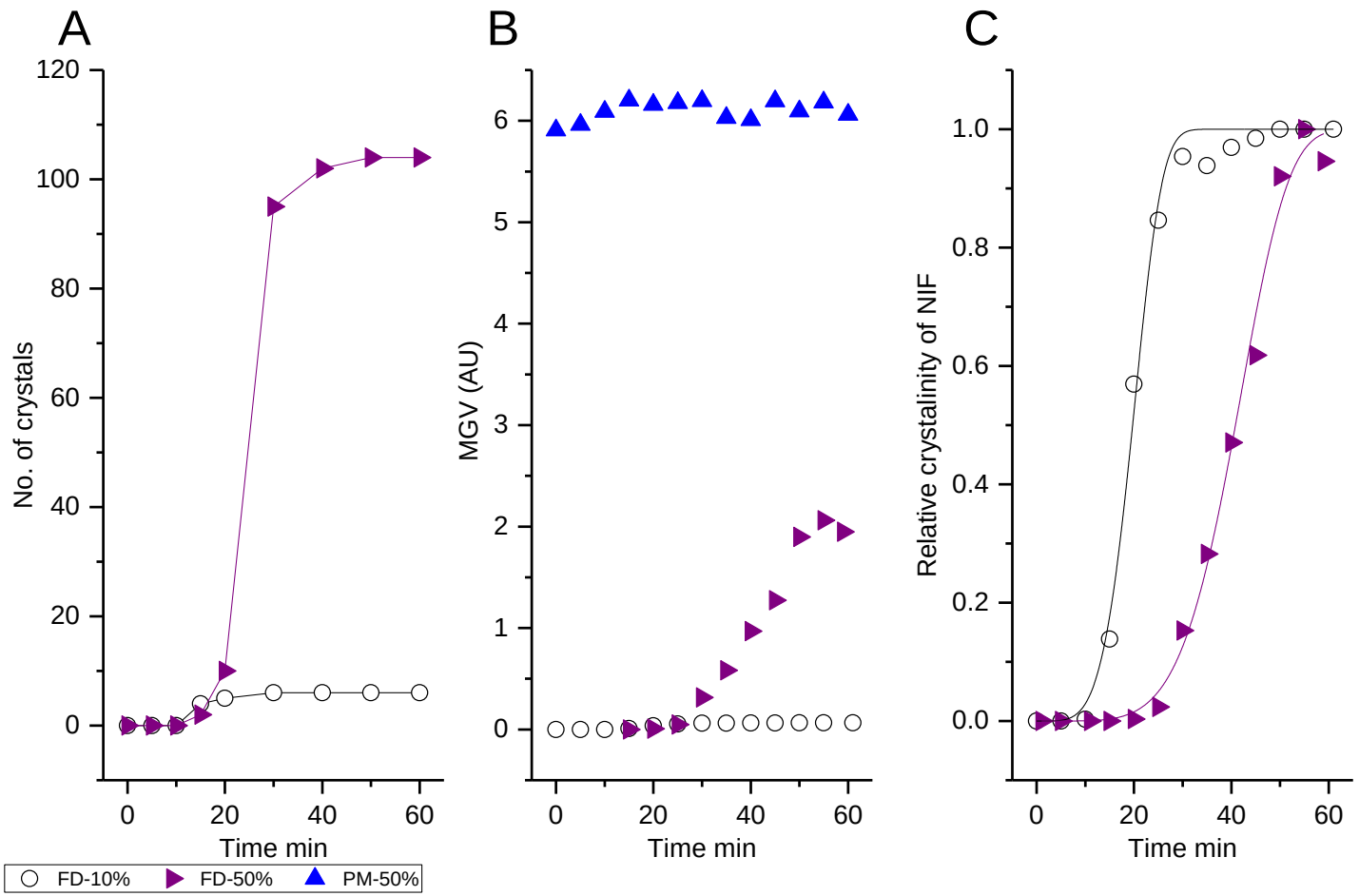

Figure 3.17 Analysis of polarized microscopic dissolution: **(A)** Number of crystals observed under polarized microscopy of FD-10% and FD-50% formulations in a simulated dissolution experiment. **(B)** Mean grey value of polarized microscopy images of simulated dissolution of FD-10% and FD-50% and PM-50%. Although the number of crystals in FD-50% stops increasing at approximately 40 min, the MGV (correlated to birefringence) continues to increase, therefore indicating crystal growth as presented in figure 3.17. **(C)** Relative crystallinity (θ_t) versus time fitted with the Avrami equation to determine the rate constant of NIF crystallisation during microscopic simulated dissolution of FD-10% and FD-50% (table 3.9).

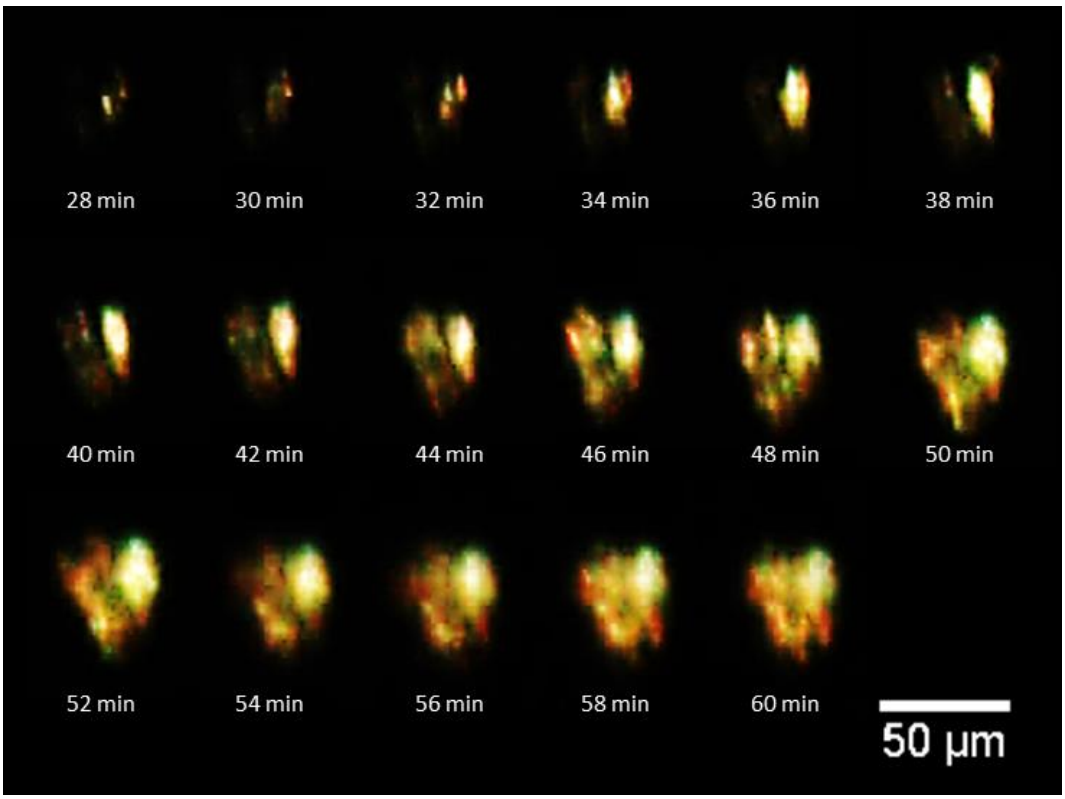

Figure 3.18 Crystal growth observed in the FD 50% NIF in PVP formulation. This image was constructed from individual light polarized microscopic images using ImageJ software.

It is important to note that the FD-50% has the potential of presenting more crystals than the FD-10% in a single image, simply due to the difference in dilution factor of NIF, as NIF in FD-10% is 5 times more diluted than NIF in FD-50%. Therefore, taking the dilution factor into account, the final estimated number of crystals formed by FD-10%, if the same amount of NIF was observed in a single image, is equal to 30 crystals. This was calculated as shown below:

[Observed number of crystals X Dilution factor = Estimated number of crystals]

Taking the dilution factor into account, the number of crystals generated from the dissolution of FD-50% was still greater than that generated by the FD-10% dissolution by approximately 3 times.

To determine the rate of recrystallization, in order to further compare the two FD formulations, the relative crystallinity (θ_t) was plotted as a function of time (Figure 3.17-C). Where θ_t was determined by dividing MGV at interval time points by final MGV determined at the end of the experiment. This gives a relative crystallinity between 0 (no crystallinity) and 1 (maximum crystallinity reached at end point) for both formulations. It is important to note that a relative crystallinity of 1 does not

imply that all nifedipine within a formulation has crystalized, but only nifedipine susceptible to crystallisation with the time frame and the conditions of the experiment. The plots of relative crystallinity (Figure 3.17-C) may subsequently be analysed with a mathematical model, to determine the rate constant (k). One of the commonly used models is the Avrami model (Gaisford *et al.*, 2009):

$$\theta_t = 1 - \exp[-(k_a t)^{na}] \qquad \text{Equation 3.1}$$

(Also presented in section 1.1.3)

Where k_a is the Avrami rate constant and n_a is the Avrami exponent (Gaisford *et al.*, 2009). Figure 3.17-C shows both sets of data points, FD-10% and FD-50%, fitted to the Avrami equation, where the rate constant and Avrami exponential were determined from the equation of the fitted curve (table 3.10). The rate constant of the FD-10% showed to be approximately double that of the rate constant of the FD-50% formulation. With FD-10% showing a half-life of 1.8 min, while FD-50% showing a half-life of 1.9 min.

Table 3.10 Avrami rate constant of crystallization (k_a) and the Avrami exponent (na) determined for both formulations (FD-10% and FD-50%) when in dissolution medium. This was achieved by fitting the Avrami equation to the MGV data points as presented in Figure 3.17-C. The half-life ($t_{1/2}$) was determined from k_a and na using the following equation: $\sqrt[na]{0.693/k}$ (Mazzobre *et al.*, 2003).

Formulation	k_a (min^{-1})	na	$t_{1/2}$
FD-10%	0.04688	4.63767	1.8
FD-50%	0.02285	5.31117	1.9

3.4.6. Stability and shelf life of FD formulation

A stability study was performed on the *in-situ* capsule FD 10% w/w NIF in PVP formulation to allow the estimation of shelf life in storage temperatures ranging from 25-37 ^{o}C and relative humidity ranging from 57-74% RH. The product was packaged in FD amber vials as presented in figure 3.7 and sealed under nitrogen. Quality control tests were performed on the product at time point 0, 1 and 3 months to test for the physical and chemical stability as well as the performance of the product. Table 3.11 below presents a summary output of the stability study showing average measurements before and after storage. The table also includes BP based specifications for nifedipine fast release capsules (MHRA, 2014b).

Table 3.11 Summary of stability study output of the *in-situ* capsule FD formulation (10% w/w NIF in PVP) for 3 months. Values presented as averages ± SE of n=6.

Stability type	Parameters	Spec	Average measurements					
			0 months		3 months 25 °C 57% RH		3 months 37 °C 74% RH	
Physical	Weight of unit dosage form (mg)	201 ± 20	201.57	± 0.30	200.40	± 0.31	201.06	± 0.65
	Tg (°C) 2nd heat	-	130.26	± 3.56	125.04	± 2.19	125.16	± 0.76
	Crystalline NIF % w/w	0%	0.00	± 0.00	0.00	± 0.00	0.00	± 0.00
Chemical	Degradation products (%)*	<5%	0.00	± 0.00	0.00	± 0.00	0.00	± 0.00
Performance	Drug content (mg)	10 ± 0.5	9.61	± 0.12	9.37	± 0.10	9.44	± 0.06
	Rate constant of dissolution (k)	-	0.37	± 0.05	-	-	0.39	± 0.04
	T80 (min)	< 20 min	4.8	± 0.2	-	-	5.27	± 0.1

*based on peak area %

Although the average weight of unit dosage form does not show a great change over the storage period, T_g shows a decrease by approximately 5 °C over the course of 3 months of storage at both temperatures.

Both, chemical stability and performance have shown to be constant throughout the 3 month storage at both temperatures. Figure 3.19 below shows the dissolution profiles of the *in-situ* capsule FD 10% w/w NIF in PVP formulation before and after 3 months storage at 37 °C. No significant difference was observed between the 2 profiles.

To further teste the effect of FD on dissolution performance of red gelatin capsules, empty capsule bottoms were filled with 0.5 mL of pure TBA, which was then FD following the same FD cycle. The empty FD capsules were then loaded with 10 mg of NIF as received and put under a USP apparatus 2 dissolution tests (n=3). Results were compared to the dissolution of 10 mg NIF as received from untreated red gelatin capsules. No difference was observed between the two dissolution profiles ($P > 0.05$).

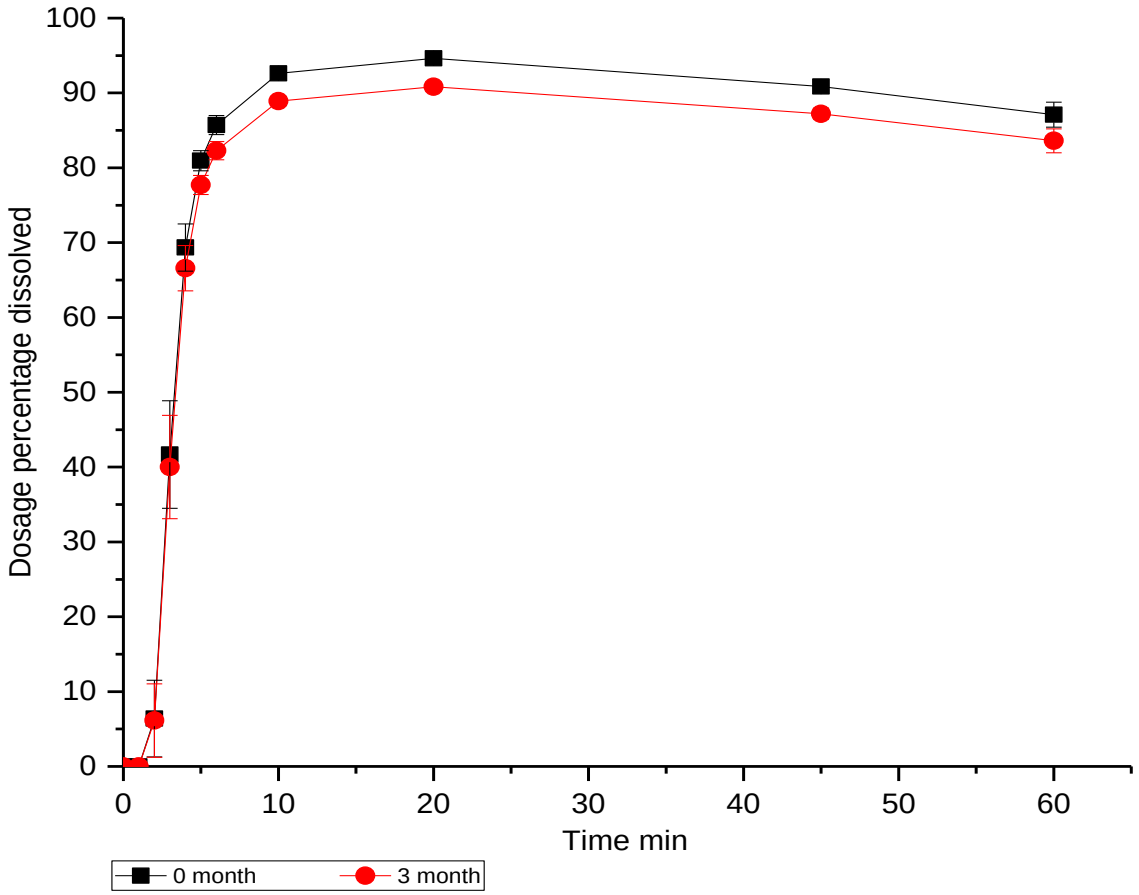

Figure 3.19 Average dissolution profile (n=3) of the FD 10% w/w NIF in PVP at time point 0 months and 3 months of stability storage at 37 ± 2 °C and 75% RH while sealed under nitrogen. No significant difference was found between the two profiles. (*P*>0.05). Error bars represent standard error.

3.5. Discussion

A novel *in-situ* FD capsule platform was successfully developed for the rapid dissolution of PWSD's in their amorphous form. The novel *in-situ* capsule FD formulation containing 10% w/w NIF in PVP met the BP guidelines with regards to drug content and dissolution rate (MHRA, 2014b). Additionally the dissolution rate of the novel formulation was observed to be approximately 3 times faster than that of the marketed, liquid-filled capsule formulation (TEVA). The *in-situ* FD-10% formulation complied with ICH oriented stability testing (ICH, 2006), where the formulation's performance was maintained with in BP specifications after an accelerated stability study.

Nifedipine was chosen as a model drug because of its poor solubility and high permeability (Ali, 1989), thus, this API is an excellent test material as it would greatly benefit from the enhancement of its dissolution rate (Chapter 2.1.4). Red opaque capsules were chosen to protect nifedipine from light degradation, and therefore ensure its chemical stability over storage period.

The platform developed in this study allowed a simple manufacturing process, whereby recrystallization inducing stress was avoided by directly freeze-drying formulations inside capsule shells. The use of TBA was essential for this process, as it was shown not to cause hard gelatin capsules to dissolve (Fig 3.8-A). Residual TBA after the freeze-drying process, for the FD-10%, showed to equal a w/w % of 10.8 $\pm$ 0.2%. This is equivalent to 10.8 $\pm$ 0.2 mg of TBA per capsule. While this value may be reduced through improving the efficiency of the freeze-drying cycle, the content of TBA per capsule a day is still below the limit of human consumption by the NSF, 1.0 mg/kg-day (NSF-Toxicology-Services., 2003), for those above 15 Kg of weight. For example in the case of a 75 Kg patient, currently without extra measures for the removal of TBA, a maximum of 6 capsules per day maybe consumed following NSF guidelines (NSF-Toxicology-Services., 2003). However, employing this platform in the treatment of chronic conditions may raise concerns due to accumulation of TBA in the body (NSF-Toxicology-Services., 2003, McGregor, 2010); therefore, this platform is more suited for the delivery of emergency medicines.

FD capsules were shown to comply with the guidelines for hard gelatin capsule monograph of the international pharmacopeia; where by individual capsules were visually examined, and tested for uniformity of weight (table 3.3) and disintegration performance. FT-IR spectrum of FD capsules were also examined and compared to untreated capsules, where no significant difference was observed, therefore indicating that FD capsules have not chemically degraded. Scanning electron micrograph presented in figure 3.8 showed the physical appearance of FD capsule shells, at various magnifications, to be identical to that of the untreated capsule shells. HPLC results have also confirmed that the red dye, of the red hard gelatin capsule shells, does not leach into liquid TBA (40.0 $\pm$ 0.5 ^{o}C) based solutions. Therefore, confirming the use of hard gelatin capsules fit for the manufacture of *in-situ* capsule FD formulations.

Results from this study, show similar crystalline/amorphous patterns to those observed in chapter 2, where by, using DSC methods, freeze-dried formulations < 60% w/w NIF in PVP showed to be predominantly amorphous. Therefore, indicating that the change from freeze-drying in amber vials to opaque size 0 capsules has not affected the content of amorphous drug in FD formulations. However a significant deviation in the T_g was observed, specifically for FD-10% and FD30%, in the second heat of *in-situ* capsule FD formulation cakes, when compared to the ampule FD cakes (table 3.4). As the deviation, in T_g, is observed in the second heat, this may indicate that it is due to a small change in the amount of PVP available in the freeze-dried cake (as described in section 2.4.2). The overall amount of drug and therefore PVP is as expected, so no loss from the capsule was observed. However it can be hypothesized that due to PVP's adhesive property (Lee, 2005), the polymer may adhere to capsule walls while in solution or during freeze-drying. The loss of small amounts, of PVP from the drug-polymer dispersion can lower the glass transition temperature of the freeze-dried cake by as much as 20 ^{o}C based on the Gordon Taylor theory (Brostow *et al.*, 2008).

Although capsule shells were confirmed not to leach red dye into TBA liquid based solutions, gelatin leaching, from the capsule shells into feed solutions, may still be a possibility. As a result, the diffusion of gelatin to the formulation can affect the T_g of the final product. The glass transition of gelatin can vary from 50-90 ^{o}C (Gugulothu *et al.*, 2015, Sudhakar *et al.*, 2006), therefore if fully dispersed in FD cakes, can contribute

to a minor increase or decrease in the overall T_g following the Gordon-Taylor equation (Lu and Weiss, 1992), assuming no intermolecular interactions are present between gelatin and the other components (Lu and Weiss, 1992).

Using the novel *in-situ capsule* FD platform to manufacture 10 mg NIF fast release capsules, has shown to better comply with BP regulations, when the % w/w of NIF in PVP was maintained at 10%. Higher NIF:PVP ratios (≥ 30% w/w NIF in PVP) were shown to have high variations (RSD% > 2%) in unit dosage weight. While formulations containing ≤ 50% w/w PVP showed to contain drug contents below the BP (MHRA, 2014b) acceptable range of 10 ± 0.5 mg (Table 3.3, Fig 3.12). As discussed in previous chapters (2.4.2.1), low PVP content can reduce the strength of the FD cake, leaving such formulations susceptible to yield loss when handling in processes such as manual recapping under nitrogen, leading to variations in weight and the loss of drug content. This problem may be overcome in larger manufacturing units, where automated recapping processes may be installed in a nitrogen only environment.

Although the recommended BP method of determining the concentration of nifedipine is to use an ultraviolet instrument (MHRA, 2014b), it was found, through preliminary studies of this project, to be unequipped to protect nifedipine from light degradation (Ali, 1989). Repeated readings of the same sample cannot be performed using the UV instrument, as the measurement process leads to the degradation of the sample itself (Ali, 1989). Preliminary experiments using UV showed un-explained fluctuations in absorbance, which later were determined, using ICH validated (ICH, 1996) stability indicating HPLC assay, as absorbance of degradation products (Ali, 1989). In other words, the analytical tool used for assessing stability of NIF, was a factor in accelerating the degradation of NIF. To ensure better photo protection of nifedipine samples, for drug content uniformity and dissolution tests, a stability indicating HPLC-UV assay was tested and validated, according to ICH guidelines (ICH, 1996, Potter and Hulm, 1988, Kuminek *et al.*, 2010), to ensure nifedipine samples are protected from degradation for the duration of analysis. Similar steps were taken towards sample preparation methods and dissolution tests, nevertheless, degradation of nifedipine during dissolution tests proved to be very difficult to eliminate due to its long duration. The maximum accumulative % PA of degradation products observed in the dissolution tests of FD 10% w/w NIF in PVP, an average % PA of 11.3 ± 0.4% (i.e. of the total PA

occupied by nifedipine and degradation products) at 60 min. (concept of percentage PA is explained in section 3.4.1.3). This was clearly observed as a decay in the dosage percentage dissolved, after 20 min, of the FD 10% w/w NIF in PVP dissolution (Fig 3.14-A). Other FD formulations have shown lower accumulative % peak are of degradation products, which may be due to the much lower concentrations of NIF observed in solution. As dissolved NIF degrades at a much faster rate than solid NIF (Ali, 1989).

Method of dissolution testing was further optimised, to specifically account for the extreme hydrophobic properties of nifedipine (Ali, 1989), following previously performed studies (Mehta *et al.*, 1995, Huang *et al.*, 2006, Garbacz *et al.*, 2009, Heller *et al.*, 1999a, Crum *et al.*, 2013). Plasticizer containing tubing and syringes where replaced by polypropylene products, as preliminary results showed variations (RSD > 2%) in nifedipine concentration of repeat sampling (n = 3). In addition, the usually fitted 0.45 µm cannula filters were found inefficient in filtering nifedipine particles as observed in dissolution of soft gel capsules of NIF (described in section 3.4.2.2). Listed information from manufacturer detailed that the pore size value listed was an average value, indicating that particles above 0.45µm may pass through. As a result, a membrane non-adsorptive millipore polyvinylidene fluoride syringe filter was added to further enhance the filtration of nifedipine particles. Non-sink conditions were implemented in dissolution studies, by not adding additional or external surfactant agents such as Sodium dodecyl sulfate (SDS) to enhance the solubility of NIF and therefore create a sink condition in dissolution medium (Schug *et al.*, 2002). Non-sink conditions in dissolution tests have enabled the kinetic solubility of amorphous nifedipine to be determined, a value that may not be obtained if the thermodynamic solubility of NIF was measured. In addition, as the solubility of drug is a factor that influences dissolution rate, as demonstrated by Noyes and Whitney (1897), tests with non-sink conditions, unlike sink conditions, allow better discrimination between dissolution profiles of different formulations where the kinetic solubility of drug is predicted to be different (Liu *et al.*, 2013).

Dissolution studies have shown that the presence of PVP in dissolution medium, with concentrations ≤ 0.024% w/v (equivalent to NIF:PVP ratios of 90-0% w/w PVP in NIF), does not enhance the dissolution rate or the kinetic solubility of pure crystalline nifedipine (Fig 3.13 and 3.15 respectively). Alternatively, using the same amount of

PVP in physical-mix formulations, where the drug and polymer were simply mixed together, has shown to enhance the dissolution rate by a factor of 20 times. This may be due to the dual effect of decreasing the particle size of nifedipine where by increasing the surface are of dissolution, thus enhancing the rate of dissolution (Noyes and Whitney, 1897), and increasing the surface are between the drug and polymer, and therefore allowing more efficient wetting This effect was also observed by (Broman *et al.*, 2001), where enhancing the contact time between polymer and drug was described as key factor in enhancing the wetting of drug, therefore providing access of the dissolution medium to the drug surface and preventing aggregation of particles and subsequent decrease in surface area. In addition Broman *et al.* (2001) suggests that drug-polymer interactions may occur between drug and polymer, when in dissolution medium. Dissolution of NIF as received in PVP containing dissolution medium is thought not to have encouraged drug-polymer interaction in dissolution medium due to the low concentration of PVP, while in dissolution of physical mix formulations, the drug and polymer were mixed prior to dispensing into the dissolution medium. This has increased the concentration of PVP in the vicinity of nifedipine particles and therefore enhanced drug-polymer interactions while in dissolution medium.

Formulating PVP in an amorphous solid dispersion with NIF has shown to further enhance the dissolution rate by a factor of 10 times from the equivalent PM formulation (Fig 3.13). The enhancement in dissolution rate is due to presenting NIF in its amorphous state (in FD formulations) rather than its crystalline state (PM formulations). This was further supported by the pattern observed between the effect of content of crystalline NIF in FD formulation and the rate of dissolution; figure 3.14 shows a sharp increase in the rate constant of FD formulations as the % w/w of NIF in PVP decreases, which, as described as a phase diagram in previous chapters (chapter 2.4.2.3), indicating a decrease in the content of crystalline NIF. Similar patterns were observed by Najib *et al.* (1986) using ibuprofen and PVP solid dispersion and Torrado *et al.* (1996) using albendazole in PVP solid dispersions. Kaushal *et al.* (2004) described high drug content solid solutions to contain small crystals within the dispersion, this was observed in >50% w/w FD NIF in PVP formulations in previous chapters (2.4.2.3.2). The formation of small crystals within solid dispersion showed to limit molecular

dispersion of drug and polymer and as a result has limited the dissolution enhancement usually observed in amorphous materials (Kaushal *et al.*, 2004). A more recent study by Verma and Rudraraju (2015), investigating the wetting kinetics of amorphous solid dispersions of PWSD's, found that the type and content of polymer used in solid dispersion has a great influence over the lowering of the contact angle of drug, a measure of wettability, where the limit of contact angle is 0^o, indicating complete wetting, and 180^o for no wetting (Verma and Rudraraju, 2015). PVP, with a wetting angle of 27 ± 0.5^o (Verma and Rudraraju, 2015) was described to be much more efficient than other polymers (HPMC and Copovidone) in lowering contact angles of PWSD's, such as crystalline cilostazol (68 ± 0.6^o). Higher amounts of PVP were also found to generate higher supersaturated solution from the dissolution of amorphous cilostazol solid dispersion, and were maintained for longer as the recrystallization of super saturated drug was inhibited at higher concentration of PVP (Verma and Rudraraju, 2015). Similar results were observed in this study, where recrystallization of nifedipine supersaturated solution from FD-10% generated less crystals than the FD-50% formulation, taking the dilution factor of NIF in PVP into account as described in section 3.4.5 of this chapter (Table 3.9 and Fig 3.19-A). In addition, the MGV of FD-50% (Fig 3.18-B) showed to continue increasing after 40 min despite reaching a constant number of crystals after 40 min, indicating crystal growth in size (Fig 3.17). FD-10% on the other hand, showed a constant MGV value once the number of crystals reached a plateau, indicating that high content of PVP can also inhibit crystal growth. This may be due to the higher drug-polymer hydrogen bonding interactions, observed at lower % w/w NIF in PVP of the amorphous FD formulations as described in previous chapters (chapter 2.4.3), therefore stabilizing dissolved NIF more efficiently.

To further compare the two formulations in terms of physical stability in dissolution medium, the rate of crystallization was determined using the Avrami model (Gaisford *et al.*, 2009). The Avrami rate constant of crystallization for FD-10% was found higher than that of FD-50% by approximately 2 times. This may be due to the fact that the dissolution rate constant of NIF in FD-10% is approximately 10 times higher than NIF in FD-50%, thus dissolved NIF is more readily available to crystallise in the dissolution of FD-10%.

Verma and Rudraraju (2015) also investigated the effect of polymeric carrier on drug solubility when present in solvent medium. By measuring the thermodynamic solubility of cilostazol in 0, 0.1 and 0.2% w/v PVP solutions, which were allowed to equilibrate over 24h (Verma and Rudraraju, 2015), concluded that the inclusion of PVP in dissolution medium has no significant effect on the solubility of cilostazol. Such polymer concentrations were chosen as they represent concentration of polymer in dissolution medium following the dissolution of formulations. Previous studies of the effect of polymeric carriers (e.g. PVP and polyethylen glycol) in solvent on the solubility of PWSD's (e.g. pofecoxib and ibuproxam) show contradicting results, where the concentration of polymer (0-20% w/v) in solvent, compared to the 0-0.022% w/v polymer in solvent tested in this study, was found to enhance the thermodynamic solubility of PWSD's, which were allowed to equilibrate over 2 days (Cirri *et al.*, 2004). In both studies by Verma and Rudraraju (2015) and Cirri *et al.* (2004), the determined effect of polymeric carrier on solubility was performed in purified water, rather than the dissolution medium used by both studies: 0.1M HCl, pH=1.2 (Hwisa *et al.*, 2013). The difference in pH of solution is known to have an impact on solubility (Ali, 1989), therefore comparing the thermodynamic solubility of crystalline drug in water to the kinetic solubility of amorphous drug in 0.1M HCl may be biased.

Results from this study, investigated the effect of increasing the concentration of PVP in dissolution medium, on the thermodynamic solubility of crystalline nifedipine, which was allowed to equilibrate for 5 days. The concentration range of PVP in dissolution medium 0-0.022% w/v (Fig 3.15-C) was chosen in order to cover the range of PVP concentrations resulted after full dissolution of 10%-100% w/w NIF in PVP in 900 mL of dissolution medium. As presented by figure 3.15-C, a strong correlation between the concentration of PVP in dissolution medium and the thermodynamic solubility of crystalline NIF was observed, where the thermodynamic solubility of NIF in 0% w/v PVP in dissolution medium (0.1M HCl pH = 1.2 and 37.0 $\pm$ 0.5 ^{o}C,) was found to equal 6.8 $\pm$ 0.1 µg/mL. Literature reference for the thermodynamic solubility of nifedipine in 0.1M HCl was not found, however, solubility of NIF in water at pH 4 was published by (Ali, 1989) to equal 5.8 µg/mL. Evidence of the effect of pH (4-9) on the solubility of NIF can be found elsewhere (Ali, 1989, Schug *et al.*, 2002). On the other hand, no correlation was found between the concentration of PVP in dissolution medium and

the kinetic solubility (Kaushal *et al.*, 2004) of NIF in dissolution medium (Fig 3.15). The kinetic solubility of amorphous nifedipine, from FD formulations (≤ 50% w/w NIF in PVP) showed significant enhancement when compared to equivalent NIF-AR*. Results show that at 20 min of dissolution, the FD-10% has reached higher concentrations of NIF than the equivalent NIF-AR*, by approximately 26 times (Fig 3.15-B), which also exceeds the thermodynamic solubility of crystalline NIF in dissolution medium by approximately 1.5 times.

ICH derived stability studies of *in situ* FD-10% w/w NIF in PVP, in nitrogen filled sealed amber glass vials, showed physical and chemical stability of amorphous nifedipine, for at least 3 months, in temperatures ranging between 25-37 ^{o}C and 57-74%RH. Product quality and performance was tested before and after stability study (fig 3.19) in accordance to BP and ICH guidelines and regulations (MHRA, 2014b, ICH, 2006). This platform therefore showed great potential in solving fundamental barriers in formulating amorphous drugs into stable formulations (Kaushal *et al.*, 2004, Trasi *et al.*, 2014, Craig *et al.*, 1999, Vasconcelos *et al.*, 2007, Verma and Rudraraju, 2015). Making it an ideal platform to use for early stages of testing novel water insoluble drugs in animal trials and early stage clinical trials, where amounts of drug manufactured are in short supplies.

A novel polarized light microscopy dissolution method was developed to allow visual qualitative analysis of the recrystallization process during dissolution (Kaushal *et al.*, 2004, Verma and Rudraraju, 2015). The method, very quickly, started showing potential in generating quantitative date to allow accurate comparison between the degree and onset of drug recrystallization during dissolution simulated tests; therefore, this is worth developing in the future. The Avrami model was used to determine the crystallisation rate constant for both FD-10% and FD-50%, as it is based on the assumption that there is no crystal impingement within the system (Gaisford *et al.*, 2009). As the amount of nifedipine in the freeze-dried cakes of both formulations is equal to or less than the amount of PVP, it was assumed that crystals of nifedipine have the potential to grow, during the dissolution simulated test, without being inhibited by their neighbours, thus the Avrami model was found to be fit for use. However, approaching maximum relative crystallinity with the examined freeze-dried systems does not imply that all present nifedipine has crystallised. In fact figure 3.18-B

shows the physical mix (PM-50%) to have an MGV value approximately 3 times greater than the maximum value reached by FD-50%.

In this study, the dissolution profile of FD-10% was compared to that of the marketed soft capsule formulation, TEVA, which consists of a liquid filled soft capsule in which nifedipine was pre-dissolved (Cole *et al.*, 2008). The dissolution profile of the marketed soft gel shows a lag period of approximately 5 min, where by the slow dissolving soft capsule shell (Cole *et al.*, 2008) allowed the release of the liquid formulation at about 6 min. On the other hand, the predominantly amorphous solid FD-10% formulation was dispensed in a conventional fast dissolving, hard gelatin capsule shell (Cole *et al.*, 2008) and thus showed a lag period of only 1 min. Once the FD amorphous formulation was released from the hard gelatin capsule, it only required an additional 4 min for 80% of the drug to dissolve. While the liquid formulation required an additional 11 min (approximately 3 times longer). This clearly shows the dissolution enhancement gained by rendering a drug into its amorphous form (Verma and Rudraraju, 2015).

3.6. Conclusion

A novel platform of *in-situ* capsule FD formulation was successfully developed, and allowed the stable manufacture of solid solution of predominantly amorphous nifedipine formulation. Dissolution studies showed FD-10% to have the highest dissolution rate constant (0.37 min^{-1}) and lowest $t_{1/2}$ (1.88 min) of all FD formulations, reaching T_{80} in less than 5 min, which is more than 3 times faster than the marketed soft gel formulation of NIF (TEVA). *In-situ* capsule FD-10% showed physical and chemical stability over 3 month accelerated stability study at 37 ^{o}C and 75%RH.

Chapter 4. Instant disintegrating buccal tablets for emergency delivery of naloxone

4.1. Introduction

Opioid overdose causes an estimated 69,000 deaths per annum and is a major contributor to the global burden of disease (Degenhardt *et al.*, 2011). Naloxone is a highly effective opioid antagonist but must be delivered rapidly to the systemic circulation of overdose victims, who may be unconscious, so as to prevent fatal outcome from respiratory depression (Strang *et al.*, 2013). Existing published pharmacokinetic–pharmacodynamics studies of naloxone do not enable simple determination of the appropriate dose required to achieve a target concentration or concentration–time profile to maximize its antidote efficacy (Dowling *et al.*, 2008). Speed of onset is critical to reverse the life-threatening respiratory depression which characterizes the opioid overdose (Dowling *et al.*, 2008). Naloxone injection is currently licensed for intravenous (IV) and intramuscular (IM) administration and is available in two concentrations, 0.4 mg/mL and 1 mg/mL injectable solution. Licensing of naloxone has recently changed in the UK to expand access to naloxone as a medicine which is available in emergency situations (MHRA, 2013). Making naloxone available as an emergency medicine is in accordance with the position statements of the American Academy of Clinical Toxicology, the American College of Medical Toxicology, the American Association of Poison Control Centres (Doyon *et al.*, 2014), the American Medical Association (AMA, 2015) and the World Health Organization (WHO, 2014). However, the use of injections in emergency situations is limited by the training required to administer these, ideally using aseptic technique, and syringes are not readily portable (McDermott and Collins, 2012, Weber *et al.*, 2012). Orally ingested dosage forms are unsuitable as they are not easily administered to an unconscious patient and naloxone undergoes extensive first pass metabolism and has low bioavailability (< 1%) after oral administration (Hussain *et al.*, 1987).

Prototype improvised kits for nasal administration have been introduced in ambulance services and clinical trials, but the use of nasal naloxone remains off-licence as

supporting pharmacokinetic data is lacking (Strang *et al.*, submitted). There are reasons for caution about reliance on nasal naloxone, and concerns about the clinical adaptation of untested unlicensed formulations have been expressed (Strang *et al.*, submitted). Other non-injectable options need to be considered.

Buccal delivery provides an attractive alternative route of administration for the emergency delivery of drugs (Sudhakar *et al.*, 2006, Lam *et al.*, 2014, Sankar *et al.*, 2011). The application of a tablet to the inner cheeks of the oral cavity is simple and easily accessible to a non-specialist bystanders or healthcare professionals in emergency situations (Sudhakar *et al.*, 2006). Following naloxone liberation from the dosage form, the buccal mucosa, a 40-50 cell (500-600 μm) thick stratified epithelium, provides the principal absorption barrier (Kulkarni *et al.*, 2009). The vasculature of the buccal mucosa drains into the retromandibular, lingual and facial veins, which in turn drain directly into the internal jugular vein and, via the superior vena cava, into the systemic circulation (Sudhakar *et al.*, 2006, Sattar *et al.*, 2014, Pather *et al.*, 2008). The absorption of naloxone from the human buccal cavity is unknown, but the bioavailability of naloxone from the buccal administration in rats has been reported to be 70%, compared to 0.3% via the oral route due to the extensive first pass metabolism (Hussain *et al.*, 1987), with maximum plasma levels obtained within 15 min (Hussain *et al.*, 1987). Sublingual administration of 2-8 mg of naloxone solution has been reported to precipitate opiate withdrawal in humans within 30 min (Preston *et al.*, 1990).

Dosage forms for buccal delivery include (i) tablets and lozenges, (ii) films, wafers and patches, (iii) liquids, creams, gels, ointments, (iv) sprays, lozenges, chewing gum and mucoadhesive film (Patel *et al.*, 2011). Of these options, tablets provide the simplest, most portable and easily applied formulation as an emergency medicine, but for efficacy will be required to disintegrate immediately on application. Orally disintegrating tablets have recently become widely accepted dosage forms, especially for pediatric and geriatric patients and there are more than 55 products having marketing authorization in the United States, European Union and Japan. However, despite their rapid disintegration, dissolution times for drugs from these formulations is often in minutes rather than seconds (Kraemer *et al.*, 2012). Development of formulations with 'instant' disintegration rates (e.g. ≤ 10 s) is required for emergency

medicines; one strategy to achieve this is to exploit the physicochemical advantages of amorphous materials, which enhance disintegration rate and bioavailability due to their increased molecular mobility compared to corresponding crystalline material (Allesø *et al.*, 2009, Craig *et al.*, 1999). However, a major problem with producing and maintaining amorphous form in a product is physical and chemical instability, i.e. reversion to crystalline structure (Alonzo *et al.*, 2010, Jawad *et al.*, 2012). Production of solid amorphous medicines is typically complex because the quality attributes of the final product are difficult to control, which has proved a limitation for many early phase amorphous formulations entering clinical trials (Kawakami, 2009).

The aim of this study was to develop a safe, easily administered and quick-to-act buccal tablet containing naloxone. A novel instant disintegrating tablet formulation was designed by modifying the ratio of gelatin, sodium bicarbonate and mannitol to produce an amorphous, but stable tablet by freeze-drying. Although freeze-drying is frequently used as a manufacturing technique for pharmaceuticals, its application to instant disintegrating tablets (also referred to as freeze-dried wafer), a technology known as Zydis ®, was commercialized in 1993 (Green and Kearney, 1999). However, as the expiration of Zydis® related patents is near, (Gugulothu *et al.*, 2015 there has been an increase in the research activity associated with this dosage form, therefore creating the need for evaluating the performance of similar freeze-dried systems. Such evaluation should include measurements of solid state behaviour and disintegration times.

The principles of molecular and material science (Sun, 2009) were used to design a formulation and manufacturing process that confers structural and physicochemical properties for optimal stability and performance. Speed of drug liberation is the critical performance or quality attribute for a solid dosage form designed to deliver drug in an emergency. At present there is not a pharmacopoeial method for quantifying disintegration for instant disintegrating tablets (Sattar *et al.*, 2014, Kraemer *et al.*, 2012, Patel *et al.*, 2012). Therefore a buccal disintegration test was developed which proved to be: (i) discriminatory for quality control purposes, and (ii) bio-relevant with potential for future development as an assay to predict *in vivo* performance.

To achieve the aims of this chapter, the following objectives have been set:

1- Utilizing freeze-drying to develop, solid dispersion, instant disintegrating tablet containing 0.8 mg of naloxone HCl with a pharmaceutical manufacture convenient and transferable method.
2- Developing quality control specifications of the novel pharmaceutical formulation for quality assurance and stability measures.
3- Adapting the manufacture and quality control methods to good manufacturing practice to allow for MHRA application for the use of the novel formulation in human clinical trials.
4- Developing novel discriminative disintegration assay with potential for use as a quality control test for the novel instant disintegrating tablet of naloxone.

Table 4.1 Target properties of an ideal fast disintegrating tablet

Property and description	**Target properties**	**Limits**
Solid state	Predominantly amorphous matrix	Absence of peaks associated with crystallinity in both DSC and PXRD
90% Disintegration time	< 10 seconds	Based on BP limits for fast disintegrating tablets < 3min
Drug content	0.8 mg	Based on BP limits for naloxone injections 0.76-0.84 mg
Size; to cover typical fingerprint area.	Lenthg:29 mm Width:16mm	Length: 26-30mm Width: 14-18mm
Physical stability; size, and disintegration time	12 months , not less than a 5% change of the following: Size: Length: 26-30mm Width: 14-18mm 90%Disintegration time < 10 s	6 months , not less than a 5% change of the following: Size: Length: 26-30mm Width: 14-18mm 90%Disintegration time < 10 s
Chemical stability; Drug content	12 months , not less than a 5% change of the following: Based on BP limits for naloxone injection 0.76-0.84 mg	6 months , not less than a 5% change of the following: Based on BP limits for naloxone injection 0.76-0.84 mg

Table 4.2 Details of the physical and chemical characteristics of Naloxone. Naloxone structure was constructed using ACD/ChemSketch.

Molecular Formula	C19H21NO4 (Zhurkovich *et al.*, 2015)
Structure of Naloxone	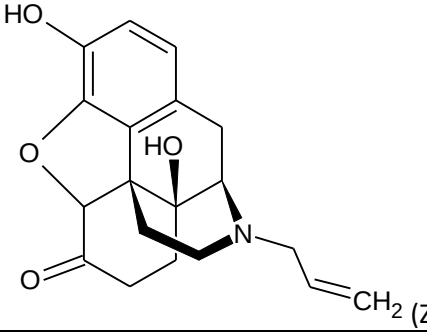 H-Cl (Zhurkovich *et al.*, 2015)
Melting Range	200-205°C (PubChem, 2005)
Solubility	Freely soluble in water, soluble in ethanol 96%, practical insoluble in toluene
Log Partition Coefficient ($C_{octanol}$ / C_{water})	2.09 (Kaliszan *et al.*, 2002)
pKa	7.9 (Kaliszan *et al.*, 2002)
Description	White or almost white, crystalline powder, hygroscopic

4.2. Equipment & Materials

4.2.1. Equipment

Aluminium blister: Zhejang Xinfei Machinery Ltd China, specification: custom made; **Digital Caliper**: DURATOOL distributors- CPC Preston UK, model: DC150, specification: 0-150mm; **Freeze-drying vials**: Packed and provided by Guy's hospital pharmacy manufacturing unit London UK, Catalogue Code (CC): CON/056, specification: 1oz Clear Glass Universal Type 1; **Freezer**: Fisher scientific Ltd Leicestershire UK, Product Number (PN): 1204-8281, specification: -20 ^{o}C laboratory Freezer (Liebherr GGU1500) under bench; **Gel imager box**: Syngene Europe office Cambridge UK, model: G:BOX HR; **Micro thermocouple**: TC Ltd Uxbridge UK, CC: 401-324 specification: Welded Tip PFA with Plug; **Rubber Bung**: Packed and provided by Guy's hospital pharmacy manufacturing unit London UK, CC: CON063/13, specification: Grey 25mm; **Screw cap**: Packed and provided by Guy's hospital pharmacy manufacturing unit London UK, CC: CON/058, specification: 28 mm silver lacquer; **Temperature logger**: TC Ltd Uxbridge UK, CC: 753-671, model: YC-747U, specification: Hand Held Dual Input Multi Thermocouple Type Indicator.

Other equipment used in this chapter, have been listed under the equipment section of previous chapters.

All instruments used in this study were calibrated following manufacturer recommendation unless otherwise stated in the method section of this chapter.

4.2.2. Materials

Gelatin powder: Fagron UK Ltd Newcastle, Chemical Abstracts Service (CAS): 9000-70-8, Product Code (PC): Gelatina pulv, Batch Number (BN): 12E30-B02, specification: Pharma grade 110 g bloom strength; **Mannitol 10% intravenous infusion:** Fresenius Kabi Manor UK, CC: 2275341, specification: BP grade; **Mucin**: Sigma-Aldrich Gillingham UK, CAS: 84082-64-4, CC: M2378-100G, specification: from porcine stomach; **Naloxone HCl dihydrate**: Fagron UK Ltd Newcastle, CAS: 51481-60-8, PN: D603739, BN: 13D22-N07, specification: Pharma grade; **Potassium phosphate monobasic**: Sigma-Aldrich

Gillingham UK, CAS: 7778-77-0, CC: P9791-100G; **Sodium bicarbonate**: Fagron UK Ltd Newcastle, PC: NF100075, specification: Pharma grade; **Sodium phosphate**: Sigma-Aldrich Gillingham UK, CAS: 7558-79-4, CC: S7907-100G; **Water for Injection (WFI)**: Guy's Hospital London UK specification: internally manufactured.

4.2.3. Software

GeneSnap version 6.07.03: Syngene Europe office Cambridge UK; **ImageJ**: Image processing and analysis Java, developed by Wayne Rasband at the national institute of mental health; **Temp monitor_S2**: TC Ltd Uxbridge UK.

4.3. Methods

4.3.1. Manufacture of instant disintegrating tablets of naloxone HCl

Instant disintegrating tablets were produced in the Pharmacy Manufacturing Unit of Guy's Hospital of the Guy's and St Thomas' NHS Foundation Trust, London UK. All equipment and instruments were calibrated, tested and maintained in accordance with ICH guidelines (ICH, 2000). Feed solution for tablet was prepared by dissolving 0.780 g of pre-weighed gelatin powder (Fagron Ltd), 0.132 g of sodium bicarbonate powder (Fagron Ltd) and 2.931 g of mannitol 10% w/v (Fresenius Kabi) in 40 mL of water for injection (WFI) held at 70 ^{o}C. Once all excipients were fully dissolved, a further 40 mL WFI (room temperature) was added and the solution was allowed to cool to room temperature. Naloxone hydrochloride dihydrate (pharm-grade; Fagron Ltd) 0.0586 g was dissolved in the feed solution, which was made up to 100 mL. The same method was used in preparing feed solutions with varying mannitol:gelatin ratios, where the added weights of each of the excipients were adjusted accordingly.

Empty wells of an aluminium blister (Zhejang Xinfei Machinery Ltd), made and designed specifically for this study, were filled with 1.500 g of naloxone HCl feed solution. Filled blister wells were cooled down to -20 ^{o}C to allow feed solutions to freeze, and then were maintained at -20 ^{o}C for 2 h as an annealing step. After annealing, the blisters were cooled down to -80 ^{o}C. Frozen tablets where removed from the wells and placed into pre-cooled freeze-drying vials (1 oz Clear Glass

Universal Type 1) packed inside a temperature controlled freeze-drying chamber, -40 ^{o}C (Lyotrap freeze dryer; LTE Scientific Ltd). The drying chamber was sealed and a 5 day freeze-drying cycle was initiated to ensure all ice within the tablets was sublimed under ≤ 0.1 mbar and ≤ -40 ^{o}C (Tang and Pikal, 2004). At the end of the freeze-drying cycle, the drying chamber was backfilled with nitrogen, allowing it to reach atmospheric pressure with the cooling unit on. The drying chamber was opened and the freeze-drying vials were immediately sealed with rubber stoppers and screw lids while inside the drying chamber. The finished products were removed from inside the drying chamber and inspected for breakage or shrinkage. Detailed methodology of the preparation and usage of the freeze-dryer was described in previous chapters (chapter 2). Following GMP requirements, the manufacturing method was documented following ICH and MHRA guidelines (Appendix 2).

Quality control tests were performed on each of three batches of manufactured tablets to ensure that they matched specifications. Two tablets from each batch were tested for the uniformity of weight and dimensions (using a digital calliper) and disintegration time using an adapted USP method, where by the time taken for 2 tablets to disintegrate in a non-shaking 100 mL beaker containing 25 mL of water, thus making a total of 6 tablets used for each test.

4.3.2. Naloxone HCl HPLC assay

A stability indicating, reverse phase, HPLC assay for naloxone HCl was adapted from a published method (Mostafavi *et al.*, 2009). This assay was based on comparing response, PA, of finished product sample to a standard solution with a known concentration of drug, which is the approach commonly used in the pharmaceutical industry. The concentration of drug in the standard solution is equal to the ideal concentration of finished product sample assuming no drug loss was encountered. Equations used to calculate the concentration of naloxone HCl in finished product samples, and the content of naloxone HCL per instant disintegrating tablet, are described in later sections of this study (Equation 4.1-4.3).

As the drug used in this study was available as naloxone HCl dihydrate, the mass of this sample was used to convert concentrations and amounts from naloxone HCl dihydrate to naloxone HCl.

4.3.2.1. HPLC system and conditions

The method utilizes C-18 Gemini-NX 5 µm reverse phase column, mobile phase of 32% v/v methanol HPLC grade and 68% 0.1 ammonium acetate (pH 5.8), isocratic flow rate of 1 mL/min, column temp of 37 ^{o}C and an injection volume of 20 µL. Absorbance was measured at 229 nm.

4.3.2.2. Preparation of mobile phase

This was performed following the same method described in previous chapters (chapter 3.3.2.2).

4.3.2.3. Preparation of external standard solution

Pre-weighed 88.0 mg of Naloxone HCL dihydrate (the equivalent mass of 80.0 mg of Naloxone HCl) was added into a 100 mL volumetric flask and diluted to the 100 mL mark with distilled water. The developed solution was gently mixed by inverting 3 times. 10 mL of the generated solution was pipetted into a 250 mL volumetric flask and further diluted to the 250 mL mark using distilled water. Therefore, developing a standard naloxone hydrochloride dihydrate solution with the concentration 35.2 µg/mL.

4.3.2.4. Preparation of finished product HPLC sample from a BP adapted disintegration method

Two naloxone instant disintegrating tablets were disintegrated in 25 mL of distilled water as part of a BP adapted disintegration test. This solution was transferred into a 50 mL volumetric flask and diluted to the 50 mL mark using distilled water.

4.3.2.5. HPLC method validation

The HPLC method was validated and tested for specificity, linearity, limits of detection and quantification, accuracy and precision and robustness according to ICH and MHRA guidelines following methods described in previous chapters (chapter 3.3.2.2). As an additional requirement for GMP based analytical assay, the HPLC method was also validated for reproducibility where by the relationship between response and

concentration of naloxone HCl dihydrate determined by two different analysts was compared.

Table 4.3 below presents the dilutions used in validation of linearity in the relationship between PA and concentration of naloxone HCl dihydrate. The tested range covered approximately 50-150% of the target concentration of Naloxone HCl dihydrate in finished product (35.2 µg/mL as described above) as recommended by MHRA guidelines.

Table 4.3 Preparation of naloxone hydrochloride serial dilutions for a HPLC-UV calibration graph, using ultra-purified water as a solvent.

Dilution number	Volume of stock solution pipetted into individual dilutions / mL	Make up to total volume of: / mL	Final conc. µg / mL
1	0.4	25	20
2	0.76	25	38
3	0.8	25	40
4	0.84	25	42
5	1.2	25	60

4.3.3. Differential scanning calorimetry

Differential scanning calorimetry studies were performed over a temperature range of 25–200°C following the same sample preparation methodology described in previous chapters (Chapter 2). Experimental conditions followed an equilibration at 25 ^{o}C for 5 min, ramp to 200 ^{o}C (10 ^{o}C/min), followed by a ramp to 25 ^{o}C (10 ^{o}C/min) and a ramp to 200 ^{o}C (10 ^{o}C/min). All experiments were repeated three times. The sample size used was approximately 5 mg, with the mass for each experiment recorded accurately on a six-figure balance.

4.3.4. Environmental scanning electron microscopy

Samples were adhered to a conventional SEM stub and imaged using a FEI Quanta 200F microscope. The operating conditions were: vacuum pressure 200 Pa, HV 20kV, a gaseous secondary detector and a typical magnification of ×1000.

4.3.5. Powder X-ray diffraction (PXRD)

PXRD analyses were performed on Rigaku MiniFlex 600 diffractometer (Rigaku, Tokyo, Japan). The samples were spread on a zero background holder and placed on a spinner stage. The instrument produces Cu Kα radiation (1.5418 Å) operated at a voltage of 40

kV and a current of 15 mA over a scan range 3-40° 2θ with a step size of 0.01° 2θ at a speed of 5°/min.

4.3.6. Digital image disintegration assay

A digital image or photographic disintegration assay was developed to measure tablet disintegration in small volumes of medium in temperature controlled blisters. Disintegration was quantified using a gel imager to follow tablet disappearance. The disintegration vessel was a thermal-jacketed aluminium blister sheet with black-painted wells of the same dimension as those used for manufacturing the tablets (Fig 4.1). Disintegration medium was phosphate buffered distilled water (pH 7.3 ± 0.2) or a synthetic saliva adapted from the SS5 USP recipe for artificial saliva (Quilaqueo and Aguilera, 2015), which consisted of distilled water, salts (NaCl = 8 g/L, KH_2PO_4 = 0.19 g/L and Na_2HPO_4 = 2.38 g/L) and mucin 2.16 g/L (from porcine stomach).

Assay temperature was adjusted by placing the whole apparatus in a temperature controlled water bath at the target temperature. Disintegration medium, 0.7 mL, was pipetted into the blister wells adjacent to the test well and micro probe thermocouples connected to a data logger thermometer were used to monitor the temperature of the disintegration medium. Once the temperature of the disintegration medium in blister wells reached the target temperature, the apparatus was placed inside a heat-insulting box of polystyrene, and transferred into a closed box gel imager for the disintegration assay. This apparatus allowed accurate temperature logging throughout the disintegration assay to ensure the temperature of the disintegration medium was maintained ± 1 ^{o}C of the target temperature.

Disintegration was measured using a GeneSnap version 6.07.03 gel imager, with the camera located above test blister well. A reference image was then taken of test blister well containing disintegration medium, after which the well was dried and an instant disintegrating tablet was placed in the blister. An image of test well was then taken (t = 0 s) and the assay initiated by adding the required volume of temperature-conditioned disintegration medium onto the tablet, (e.g., 0.7 mL at 35 ^{o}C) after which 100 consecutive images were taken at 0.4 s intervals. Image J analysis software, was used

to analyse the images by determining the mean grey value (MGV), corrected for baseline at each time point and normalized to the assay range.

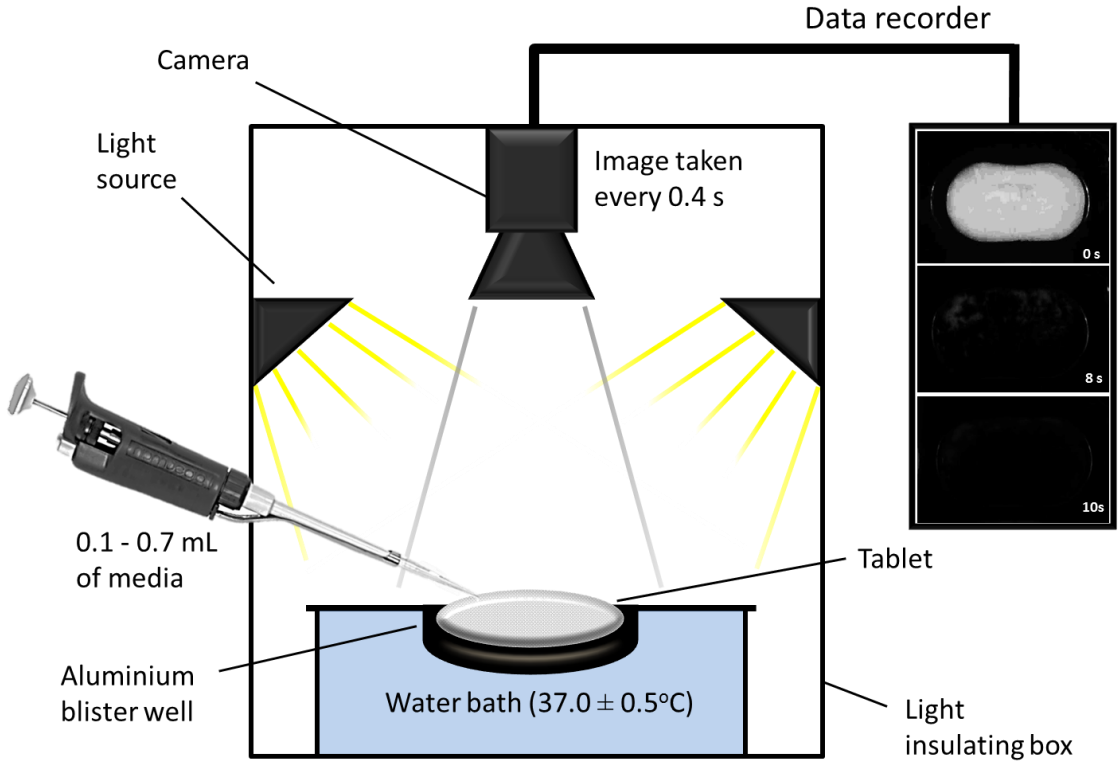

Figure 4.1 Schematic for the digital image disintegration assay, constructed from an aluminium blister sheet with a painted black background to provide contrast for the tablet. Disintegration of the tablet was monitored as the mean grey value using an image analyser.

4.4. Results

4.4.1. HPLC method validation

Following the same steps for, validating analytical methods, described in previous chapters, the stability indicating HPLC assay for naloxone HCl was validated.

4.4.1.1. Naloxone HPLC Assay

The HPLC assay developed in this study was based directly on the relationship between PA ratio of sample to external standard and the concentration of drug in µg/mL. Unlike previous chapters, internal standard was replaced here by using standard solutions of naloxone HCl as an external standard solution. This method was more convenient for GMP dedicated laboratories, where the aim was to avoid introducing foreign compounds to samples of manufactured products and or HPLC instruments which have been dedicated for particular formulations. The concentration of drug in unknown samples was determined by comparing the PA's, at the RT of the drug, of unknown samples to an average PA of standard solution generated by 2 separate HPLC injections before and after the unknown sample, one each, assuming a linear relationship between drug PA and concentration in the range of analysis (this is confirmed in later sections of this study Table 4.5). The following equation was used to convert PA at 2.6 min, for finished product sample, to a concentration of naloxone hydrochloride dihydrate µg/mL:

$$[\text{NLX HCl dihydrate}]\ \mu\text{g/mL} = \frac{\text{PA}_{\text{FPS}} \times \text{Mass of standard (mg)}}{\text{PA}_{\text{STD}} \times 88.0} \times 35.2 \qquad \text{Equation 4.1}$$

To determine the content of naloxone HCl dihydrate per tablet, the following equation is then used:

$$\text{Content of NLX HCl dihydrate (mg)} = \frac{\text{Conc. of naloxone HCl dihydrate (FPS)}}{40} \qquad \text{Equation 4.2}$$

Finally to determine the content of naloxone HCl per tablet the following equation was used:

$$\text{Content of NLX HCl (mg)} = \frac{\text{Content of naloxone HCl dihydrate pert tablet x } 363.83}{399.87} \qquad \text{Equation 4.3}$$

4.4.1.2. Specificity

4.4.1.2.6 Separation adequacy

Table 4.4 HPLC System suitability criteria (FDA, 1994) for the naloxone HPLC assay. Despite not meeting the FDA recommended capacity factor, other aspects of the assay, such as repeatability and reproducibility, were found to meet the required needs. Therefore making the naloxone HPLC assay fit for purpose.

Parameters	Naloxone	FDA recommended criteria
Column efficiency	4020.46	>2000
Capacity factor	0.81	>2
Peak Symmetry	0.88	0.9-1.4
Resolution from noroxymorphone	4.0	>1.5

4.4.1.2.7 Selectivity

Selectivity was investigated through the analysis of 10 different placebo samples. The placebo samples were prepared by disintegrating placebo IDT (Naloxone free IDT) in 100 mL volumetric flask. The resulting solution was tested using the Naloxone stability indicating-HPLC assay.

No interference was detected at the expected RT of Naloxone.

4.4.1.3. Linearity and limitations in quantification and detection

Table 4.5 below shows a summary of the linear relationship between PA of Naloxone HCl dihydrate and the PA response at 2.66 min. the target concentration to be measured is much higher than the limit of detection and quantifications detailed below:

Table 4.5 Calibration curve details for the NLX HPLC assay. LOD and LOQ were calculated following the same steps taken in previous chapters. All values listed below are related to the concentration of naloxone HCl dihydrate.

Linear range	20.0 to 60.0 µg/mL (naloxone HCL dihydrate in distilled water)
HPLC assay	NLX conc. (µg/mL) = (13.5 X PA) – 4.77
R^2	≥ 0.9999
LOD	0.36 µg/mL
LOQ	1.83 µg/mL
Equation to determine content of NLX per tablet	Content of NLX per tablet in mg = [(PA $_{(RT\ 2.6\ min)}$ +4.7696) / 13.505] x 0.025

4.4.1.4. Accuracy and Precision

The calibration graph was tested for accuracy and precision through the analysis of three standard solutions of Naloxone with known concentrations. Results for accuracy are reported as % bias between the estimated and the actual concentration values. All of which are less than 1.5%. Precision of the HPLC assay is described via the inter and intra percentage coefficient variance. All of which is below 0.5%.

Table 4.6 Accuracy of the naloxone HPLC assay; Three standard naloxone solutions were tested on different times of the day. Each sample was injected twice and the average estimated concentration was compared to the actual concentration. Note; the conc. of A, B & C is slightly different (32-33 μg/mL)

Sample analysed	Average*	Accuracy %bias from actual concentration	Inter %CV	Intra %CV
A	32.25	-0.9%	0.1%	
B	32.09	-1.4%	0.1%	0.40%
C	32.40	-0.4%	0.0%	

* Estimated concentration (number of repeat injections = 2)

4.4.1.5. Robustness

4.4.1.5.8 Repeatability of response

The variation in repeatability of RT for 10 different injections of the same standard solution is presented by the percentage coefficient variance (%CV) as 0.0%, while the variation in PA is determined to be 0.1%.

Table 4.7 Summary for repeatability of response, RT and PA, for 10 different HPLC injections of the same standard solution.

Injection number	RT	PA
1	2.66	432.8
2	2.66	432.9
3	2.66	432.4
4	2.66	432.7
5	2.66	432.5
6	2.66	432.4
7	2.66	432.9
8	2.66	432.9
9	2.66	432.7
10	2.66	433.0
Average	2.66	432.7
STD	0.00	0.2
%RSD	0.00%	0.10%

4.4.1.5.9 Stress study

Standard solutions of naloxone were subjected to varies stress factors to determine the ones that can contribute to degradation of naloxone. Degradation of naloxone was detectable using the HPLC assay described above by showing a peak at 2.22 min for Noroxymorphone. It is not necessary to identify or quantify this impurity for demonstration of compliance (BP).

Table 4.8 Summary of stress study: Presenting the different stress tests that were performed on standard solutions of naloxone, to enhance naloxone degradation rate.

Stress condition	RT/ min	Identity	Rs of NLX peak	Average PA	Average determined conc. of NLX µg/mL	% of naloxone hydrochloride concentration*
None	2.6	NLX	-	701.05	31.15	100%
No stress stored for 16 h	2.6	NLX	-	698.55	31.04	100%
Light, solution was subjected to light for 16 h	2.6	NLX	-	698.55	31.04	100%
Heat to 70 ^{o} C for 2.5 hours	2.6 2.2	NLX NOX	3.76	671.90 16.40	29.85	96%
Heat to 70 ^{o} C for 16 hours	2.6 2.2	NLX NOX	4.29	462.95 70.85	20.54	66%

*In relation to solution prior to the stress

4.4.1.6. Reproducibility

4.4.1.6.10 Confirming linearity

A linear relation between the concentration of naloxone (20 – 60 µg/mL) and the PA was confirmed by an additional analyst.

Table 4.9 Validation of linearity by a second analyst

Linear range	20.0 60.0 µg/mL (naloxone I distilled water)
HPLC assay	NLX conc. (µg/mL) = (13.2 X PA) – 11.67
R^2	>0.999

4.4.1.6.11 Variation in drug content analysis by different analysts

Standard sample solution of finished product were analysed by 2 different analysts using the same HPLC method described above. The determined concentrations were compared to one another to show <2% variation from one another.

Table 4.10 Variation in determined drug concentration, between the 2 analysts as a measure of reproducibility.

	PA at 2.6 min	Calculated conc. of NLX using µg/mL	Intra % variation
Analyst 1	302.5	22.75	-0.4%
Analyst 2	301.3	22.66	

4.4.1.7. Summary of HPLC method validation

The method for the assay of naloxone hydrochloride by HPLC has been assessed for specificity, repeatability, linearity, accuracy and precision and was found to be satisfactory. The method is considered fit for purpose and is suitable for use within the 13th Floor Pharmacy QC Lab for routine and stability testing.

Table 4.11 Acceptance criteria (FDA, 1994) and results summary for the validation of HPLC assay for naloxone hydrochloride.

Parameter	Observed values	FDA recommended criteria
Resolution	4.0	>2.0 between additional peaks
Linearity	R2> 0.999	R^2>0.9992
Precision	<0.4%	RSD <2.0%
Precision between analysts	<0.4%	RSD <2.0%
LOD	0.36 µg/mL	Internal acceptance criteria LOQ ≤ 5% of the target concentration. Thus it must not exceed 1.6 µg/mL
LOQ	1.83 µg/mL	Internal acceptance criteria LOQ ≤ 10% of the target concentration. Thus it must not exceed 3.2 µg/mL

4.4.2. Temperature control validation for DIDA

As temperature is believed to be a critical parameter that can influence the rate of table disintegration, it was critical to control the assigned temperature of the 0.1-0.7 mL disintegration medium over the period of the disintegration test. To validate the method used to control the temperature of the disintegration bath, validation experiments were performed, where by the temperature of the disintegration bath was monitored and recorded with an interval of 1 sec at all investigated temperatures (25 ^{o}C, 33 ^{o}C, 35 ^{o}C and 37 ^{o}C-Fig 4.2) for 0.7mL, and all volumes (0.1 mL, 0.2 mL, 0.4 mL -Figure 4.3) for 35 ^{o}C. Each condition was tested 3 times for at least double the duration of the expected disintegration. Results show that temperature, for all conditions, was controlled within a ±1.0 ^{o}C of the target temperature (Fig 4.2 & 4.3).

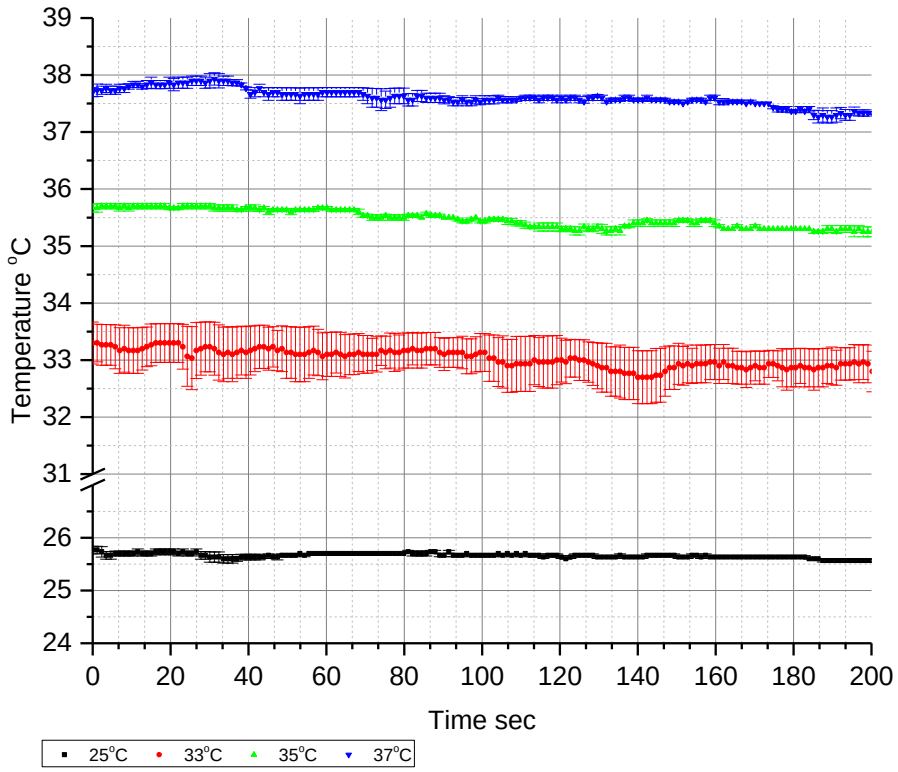

Figure 4.2 Average recorded temperatures for 4 different target temperature conditions of a 0.7 mL DIDA test. (starting from the top, the target temperatures were: 37, 35, 33 and 25 °C). Error bars represent standard error of (n=3).

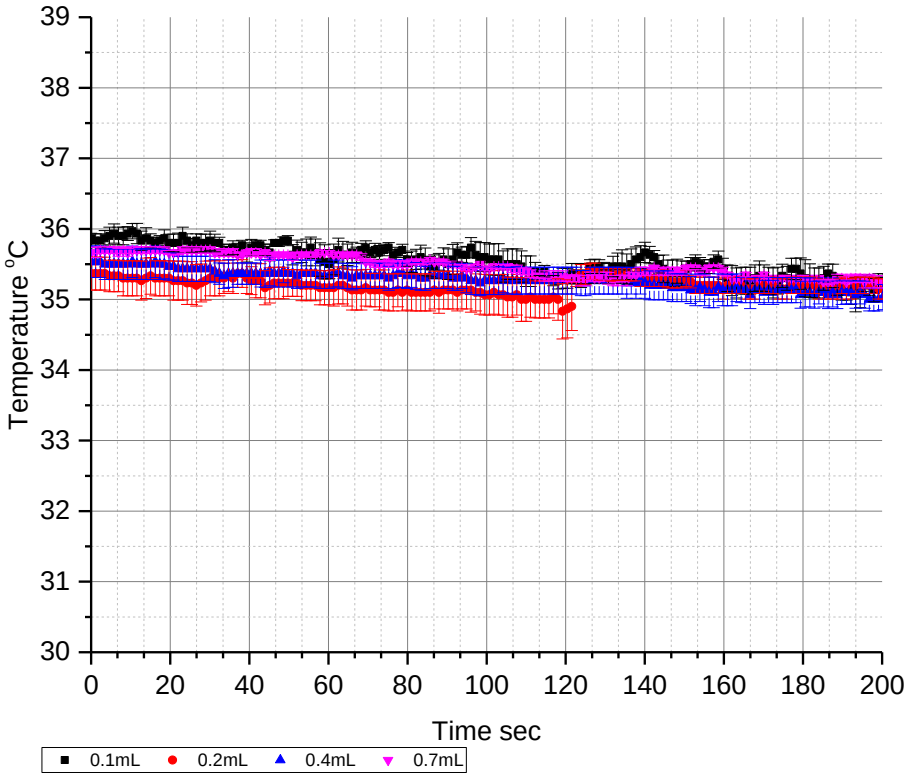

Figure 4.3 Average temperature of disintegration mediums with different volumes for the duration of the experiment. Target temperature is 35 °C Error bars represent standard error of n=3.

4.4.3. Tablet composition

Ratios of mannitol, gelatin and sodium bicarbonate were varied with the aim of identifying a tablet composition that would form an amorphous and porous freeze-dried product. Mannitol was utilized because of its hydrophilic nature, bulking properties and common use as a lyoprotectant (Gugulothu *et al.*, 2015). Gelatin was selected to confer the quality attributes for a successful product; i.e. gelatin typically forms glassy amorphous complexes with relatively high glass transition temperatures, T_g 50-90°C, provides structural strength and has mucoadhesive properties (Sudhakar *et al.*, 2006, Gugulothu *et al.*, 2015).

Preliminary results showed that simply freeze-drying aqueous solutions of pure mannitol and pure gelatin produced tablets of very poor quality. Freeze-dried tablets composed of 100% w/w mannitol possessed a distinct melting peak with an average onset at 163.9 ± 0.5 ^{o}C (n=3), indicative of a crystal melt (Figure 4.4). A small endotherm at approximately 60°C for 100% w/w freeze-dried mannitol was representative of the hemihydrate crystalline form of mannitol (Nunes *et al.*, 2004), indicating that freeze-drying a solution of pure mannitol produced a crystalline product. Comparable studies have demonstrated that freeze-dried mannitol contains a mixture of the hemihydrate together with the anhydrous polymorphs as mannitol hemihydrate is quite unstable (Nunes *et al.*, 2004, Cavatur and Suryanarayanan, 1998). The melting points for the α and β polymorphs are very close together and have been reported to fall between 165 and 166°C (Cornel *et al.*, 2010, Telang *et al.*, 2003). A lower onset for this melting peak of approximately 164°C indicates the presence of an additional phase. Further inspection of the leading edge of the endothermic peak revealed a very small and broad inflexion overlaid on the rapidly falling heat flow curve. Nunes *et al.* have attributed this broadening of the peak onset to conversion of an anhydrous δ polymorph to the β form of mannitol. Dehydration of the hemihydrate form mannitol at 60°C initiates the formation of the δ polymorph (Nunes *et al.*, 2004). The δ polymorph is enantiotropic and thus will undergo transition to the more stable β form over quite a wide temperature range, typically from 140 to 180°C with a relatively small PA when observed by DSC, thus it is often difficult to identify this transition (Telang *et al.*, 2003).

Pure mannitol crystalline tablets were brittle and difficult to remove from their sample vials without collapsing into a powder. In contrast, pure gelatin tablets had a sticky texture and lacked porosity. Formulations containing both mannitol and gelatin proved successful when freeze-dried; addition of gelatin diminished the crystalline melting peak in the freeze-dried product whereas mannitol conferred porosity within the tablets. However, even with high gelatin content, persistent peaks were observed in the amorphous halo of the powder x-ray diffraction results. This indicated a crystalline fraction within the freeze-dried tablet and the unique peak at 9.7° 2θ identified the presence of mannitol hemihydrate (Nunes *et al.*, 2004), an example of this unambiguous peak can be seen in Figure 4.6.

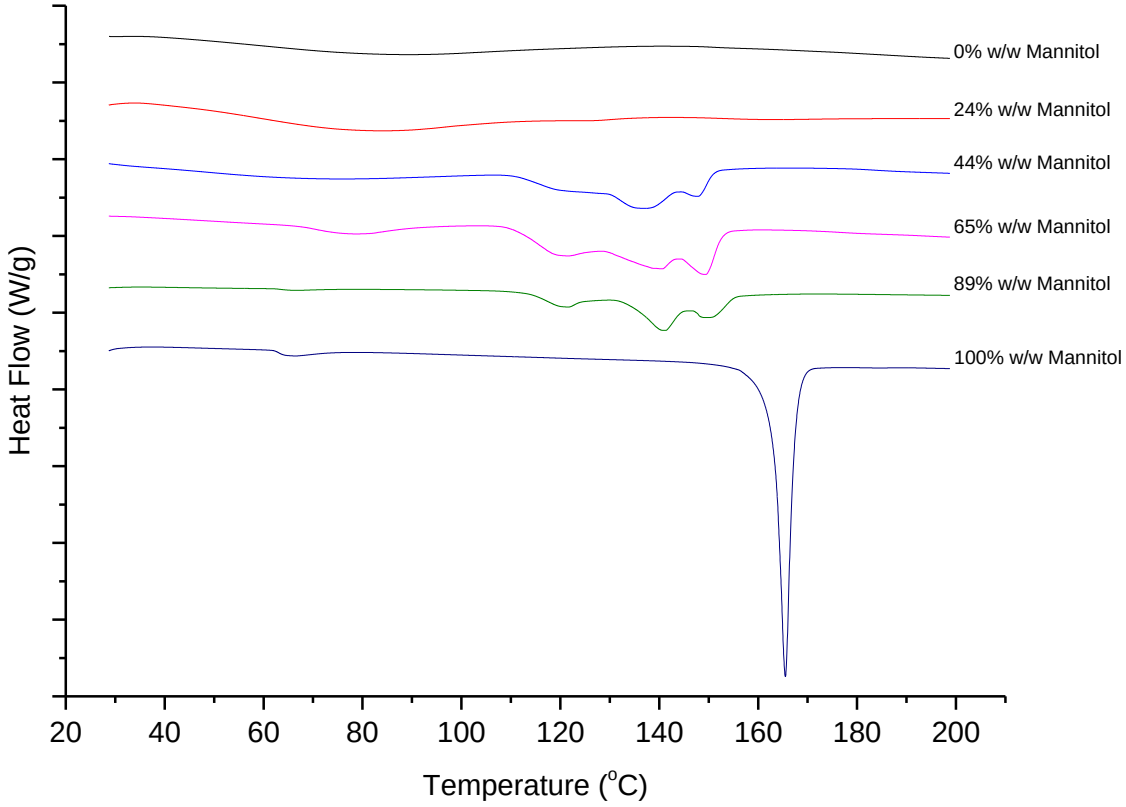

Figure 4.4 Differential scanning calorimetry to show the effect of mannitol:gelatin ratio on the thermal properties of the freeze-dried instant disintegrating tablets.The tablets were composed of mannitol:gelatin in the ratios illustrated, plus sodium bicarbonate 11% w/w, with the exception of the 100% w/w mannitol sample.

Since mannitol has an affinity for inorganic salts and this miscibility often leads to the inhibition of mannitol crystallization when present in freeze-dried solids (Telang *et al.*, 2003), sodium bicarbonate was introduced as a ternary agent. Physical mixtures of mannitol and sodium bicarbonate were investigated by heating to 200°C to melt the mannitol, then analysed by DSC while cooling at 10°C/min back to room temperature.

The addition of sodium bicarbonate reduced the size of the mannitol recrystallization peak in the cooling cycle. At concentrations of sodium bicarbonate above 10% w/w, crystallization of mannitol could no longer be seen. The reduction in the observed mannitol recrystallization enthalpy was linear with increasing sodium bicarbonate concentration ($\Delta_{recry}H$ = -20.3[$NaHCO_3$] + 220.9; r^2 = 0.9, n = 18). The extrapolated line crossed the enthalpy axis at a concentration of sodium bicarbonate at approximately 10.9% w/w (supporting information; Figure 4.5), indicating that this is the concentration of sodium bicarbonate at which crystallization of mannitol is inhibited entirely. Therefore, unless otherwise stated all freeze-dried tablets were formulated to contain 11% w/w sodium bicarbonate. Scanning electron microscopy images revealed that the inclusion of sodium bicarbonate resulted in an increase in pore size but a reduction in the thickness of the pore walls compared to tablets prepared without sodium bicarbonate (data not shown).

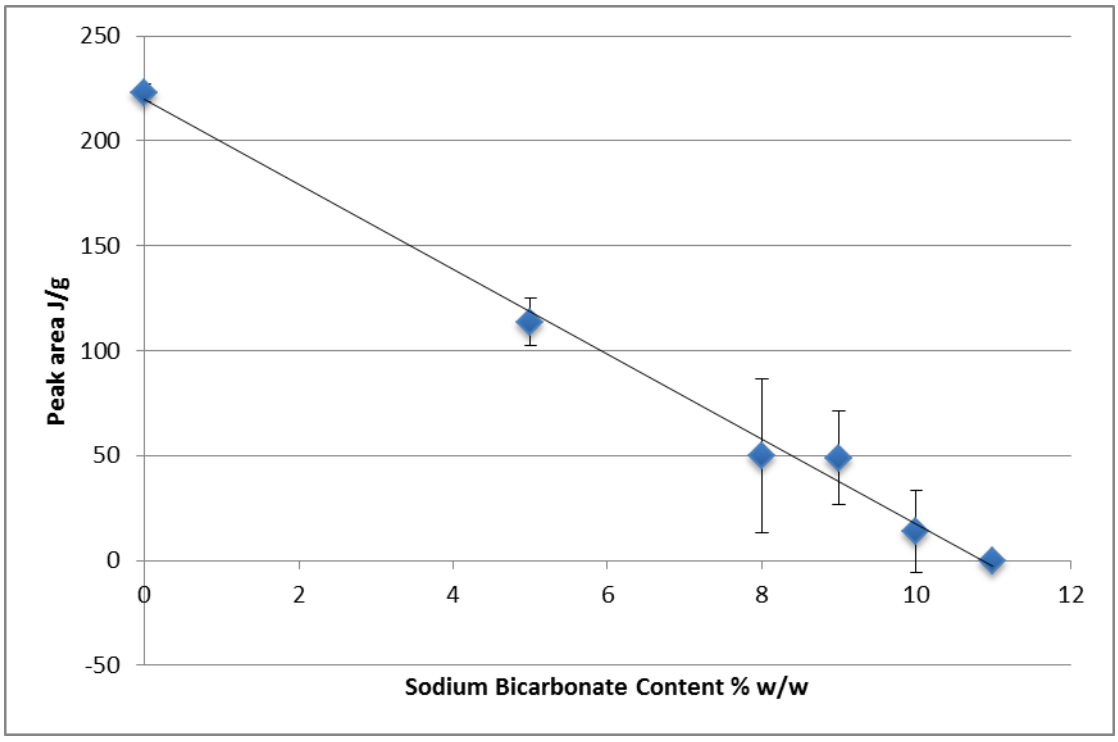

Figure 4.5 Peak area of the mannitol recrystallization peak measured in the cooling cycle by differential scanning calorimetry against the concentration of sodium bicarbonate present in the binary physical mixtures.

The effect of mannitol:gelatin ratio on the crystallinity of the tablet was screened using differential scanning calorimetry. As the proportion of mannitol reduced relative to gelatin, progressively broader peaks with a reduced area appeared at lower temperatures. Peaks were entirely absent from formulations containing < 24% w/w

mannitol (Figure 4.4). These observations were confirmed by X-ray diffraction (Figure 4.6) indicating that the freeze-dried product containing 24% w/w mannitol and 11% w/w sodium bicarbonate was fully amorphous. Characterisation of the tablet excipients by PXRD showed distinct peaks for mannitol, naloxone and sodium bicarbonate, but no peaks for gelatin (Figure 4.7). Thus, an optimised formulation with a composition of 24% w/w mannitol, 65% w/w gelatin and 11% w/w sodium bicarbonate was defined. These tablets were confirmed to be predominately amorphous by PXRD, both with and without the incorporation of naloxone 800 µg (Figure 4.7).

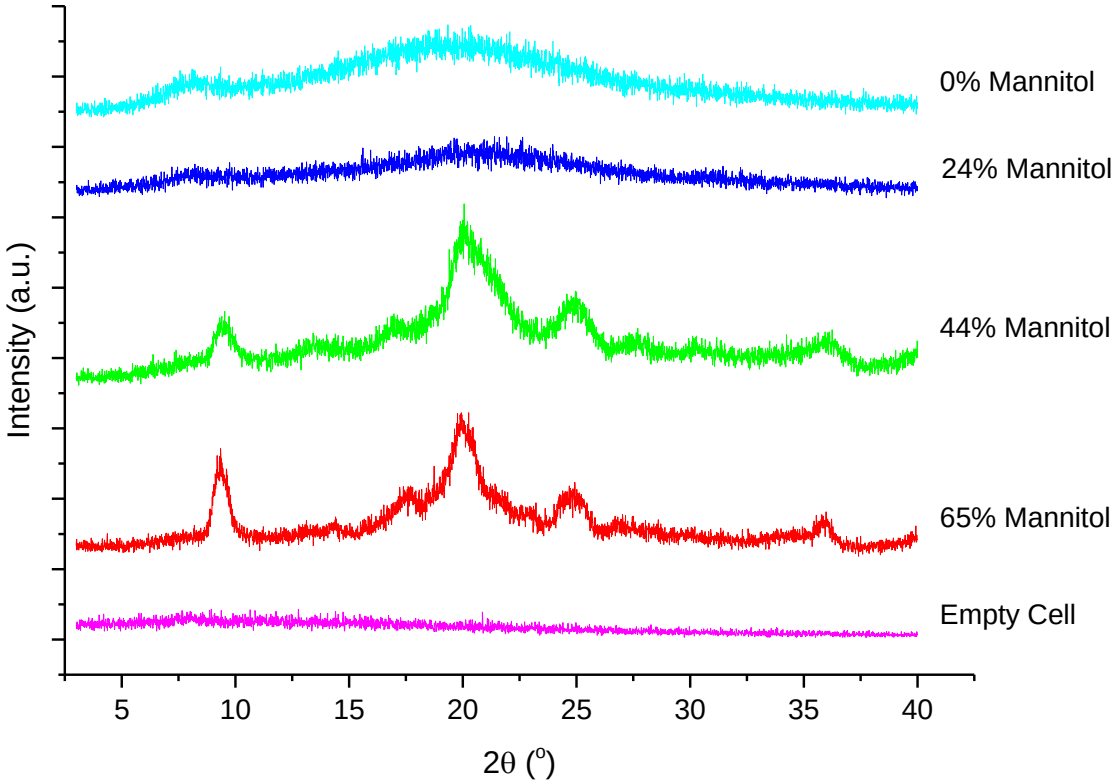

Figure 4.6 Powder X-ray diffraction to show the effect of mannitol:gelatin ratio on the solid state properties of the freeze-dried fast disintegrating tablets. The tablets were composed of mannitol:gelatin in the ratios specified, plus sodium bicarbonate 11% w/w.

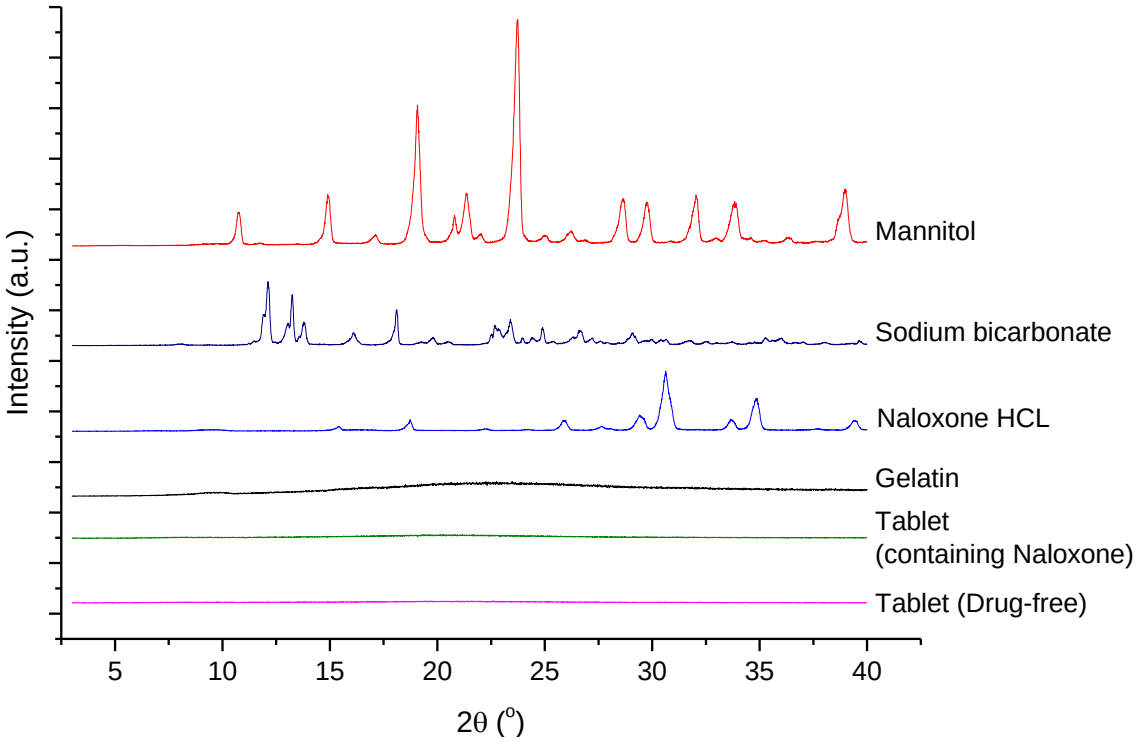

Figure 4.7 Powder X-ray diffraction of individual tablet excipients, plus the formulated product with and without naloxone 800 µg.

4.4.4. Tablet specification and stability

The instant disintegrating buccal tablets conformed reproducibly to quality specifications for weight, size, speed of disintegration and drug content (Table 4.1). The white hemispherical porous tablets were 29.4 ± 0.2 mm in length, 16.1 ± 0.5 mm in width with a depth of 3.0 ± 0.2 mm and weighed 17.7 ± 0.4 mg (Figure 4.8). Scanning electron microscopy revealed the pore size in the tablet to be approximately 100 µm (Figure 4.8). The target drug content, 800 µg of Naloxone HCl/tablet and chemical stability over 9 months when stored under nitrogen at 4 ^{o}C or 25 ^{o}C were confirmed by HPLC assay. The residual moisture content of the tablets was 10.4 ± 3.2% w/w, which is relatively high, but it did not result in chemical degradation of the API or physical instability (Table 4.12).

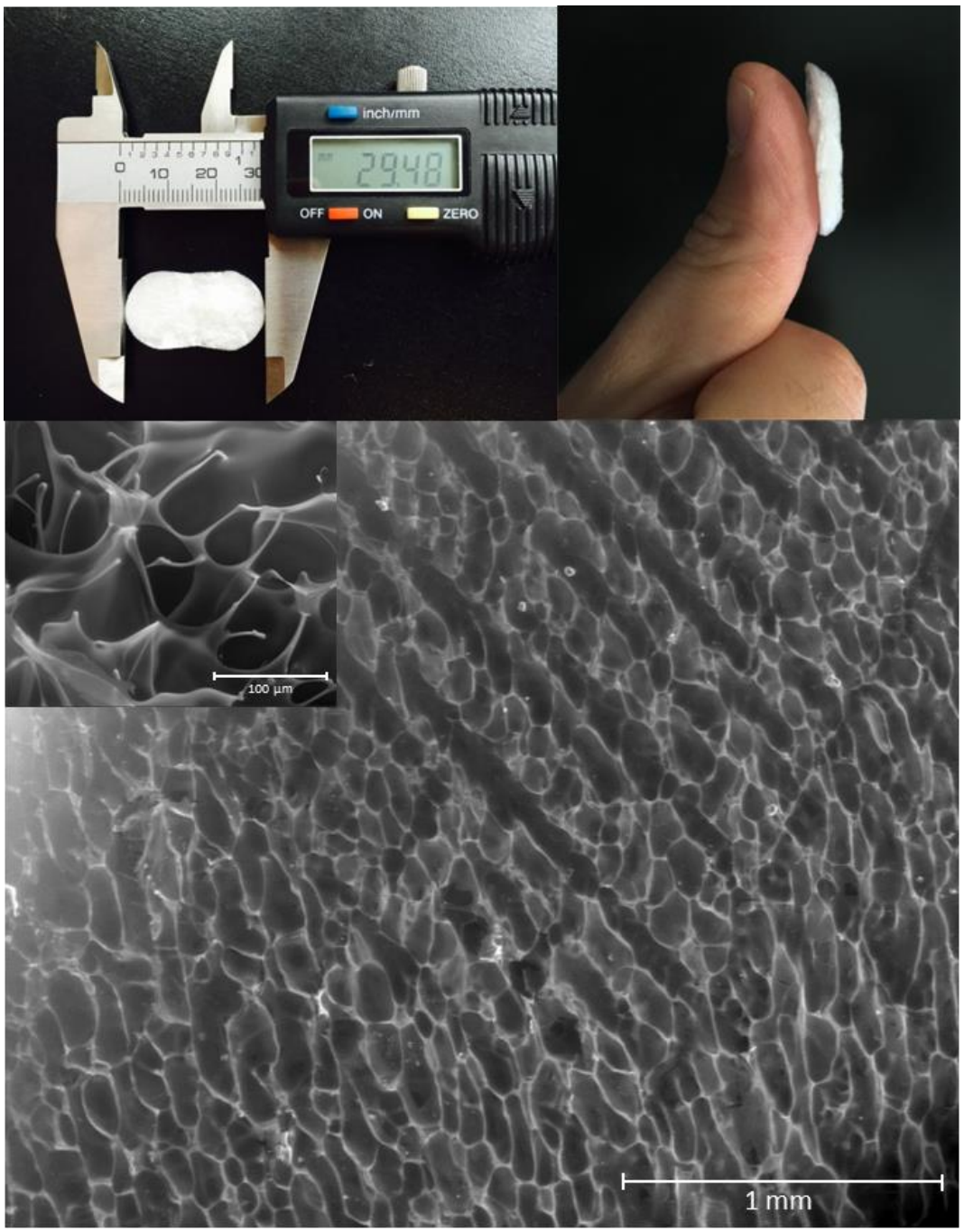

Figure 4.8 FDT's appearance and physical structure; The top left, photograph of the instant disintegrating tablet with the length displayed in mm, top right showing the tablet's intended method of dispensing to an unconscious patent's buccal cavity. Bottom main image; presenting a scanning electron micrograph of the instant disintegrating tablet, with a smaller image to its tope left corner; showing porous structure at higher magnification.

Table 4.12 Summary of naloxone FDT's stability data for 9 months, specifications listed are derived from related BP monographs.

Parameter	Specification	Stability		
		0 months	9 months	
			4 °C	25 °C
Tablet weight (mg)	16.9 - 20.7	17.8 ± 0.5	17.8 ± 0.5	17.6 ± 0.5
Dimension - length (mm)	20.0 - 30.0	29.4 ± 0.2	29.1 ± 0.3	29.1 ± 0.7
Dimension - width (mm)	14.0 - 18.0	16.1 ± 0.5	16.1 ± 0.3	16.0 ± 0.3
Disintegration test* (s)	≤180	14.0 ± 5.9	9.0 ± 5.0	10.0 ± 5.0
Naloxone HCL assay (mg)	0.76 - 0.84	0.80 ± 0.01	0.81 ± 0.02	0.80 ± 0.03

*BP adapted disintegration method.

4.4.5. Good manufacturing practice

For the purpose of meeting GMP requirements, thus to allow application for using naloxone HCl instant disintegrating tablets in clinical trials, the manufacturing method and quality control tests for naloxone HCl IDT were documented following ICH and MHRA guidelines in appendix 2 and 3 respectively. These documents allowed the transfer of laboratory developed methods to be implemented in a control pharmaceutical manufacture environment, and therefore allow for an investigational medicinal product dossier (IMPD) to be submitted to the MHRA for the use of the developed naloxone IDTs to be used in a human clinical trial (Appendix 4).

4.4.6. Rapid Buccal Disintegration

The novel digital imaging disintegration assay (DIDA) was used to explore the effects of temperature, solvent volume and composition on the disintegration of the tablets. Under all conditions the tablets disintegrated fully (>90%) within 30 s. Tablets disintegrated in < 10 s in 0.7 mL of phosphate buffer at 35 °C (Figure 4.9-A). Temperature variation over the range reported to exist in the buccal cavity (Moore *et al.*, 1999), 33-37 °C did not alter the disintegration rate, but the rate was 4-5 times slower at 25 °C. In opiate overdose, the volume of oral fluid available in the buccal cavity may be reduced compared to 0.7 mL in a typical adult human (Patel *et al.*, 2012). Reducing the amount of fluid available to the tablet progressively reduced the rate at which the tablet disintegrated, with disintegration in 0.1 mL being 4.5 times slower than in 0.7 mL (Figure 4.9-B). Interestingly, when phosphate buffer was

replaced with synthetic saliva, a slightly quicker disintegration rate was observed, a result of better spreading and wetting of the tablet caused by the mucin present in the disintegration media (Figure 4.9-C).

Evaluating the discrimination between disintegration profiles in different temperatures and volumes, was performed using the similarity factor (*f2*) test (Shah *et al.*, 1998) rather than MANOVA analysis. This is due to the high number of data points recorded for each disintegration profile, and therefore making the MANOVA analysis impractical. Equation 4.4 below present *f2*:

$$f2 = 50.\log\{[1 + \frac{1}{n}.\sum_{t=1}^{n}(R_t - T_t)^2]^{-0.5}.100\} \quad \text{Equation 4.4}$$

Where n is the number of time points in the disintegration profile, R_t and T_t represent the percentage of matrix reaming in the reference profile and the tested profile respectively. When *f2* is ≥ 50, this indicates a high similarity between the 2 disintegration profiles. Table 4.13 below presents a summary of the *f*2 test output for discrimination against temperature and volume respectively.

Table 4.13 Summary of the *f*2 test for disintegration between profiles with different temperatures and volumes. f2 ≥ 50 shows high similarity between the profiles. Low similarities are only seen between 25 ^{o}C and other temperatures. While discrimination against volume shows low similarities between all volumes with the exception of 0.2 and 0.1 mL

Discrimination against temperature				**Discrimination against volume**			
Reference profile	**Tested profile**	***f*2**	**Similarity**	**Reference profile**	**Tested profile**	***f*2**	**Similarity**
	35 ^{o}C	57.6	High		0.4 mL	28.36	Low
37 ^{o}C	33 ^{o}C	63.32	High	0.7 mL	0.2 mL	19.13	Low
	25 ^{o}C	19.78	Low		0.1 mL	17.09	Low
	37 ^{o}C	57.6	High		0.7 mL	28.36	Low
35 ^{o}C	33 ^{o}C	72.83	High	0.4 mL	0.2 mL	35.26	Low
	25 ^{o}C	22.74	Low		0.1 mL	27.89	Low
	37 ^{o}C	63.32	High		0.7 mL	19.13	Low
33 ^{o}C	35 ^{o}C	72.83	High	0.2 mL	0.4 mL	35.26	Low
	25 ^{o}C	21.75	Low		0.1 mL	48.2	High
	37 ^{o}C	19.78	Low		0.7 mL	17.09	Low
25 ^{o}C	35 ^{o}C	22.74	Low	0.1 mL	0.4 mL	27.89	Low
	33 ^{o}C	21.75	Low		0.2 mL	48.2	High

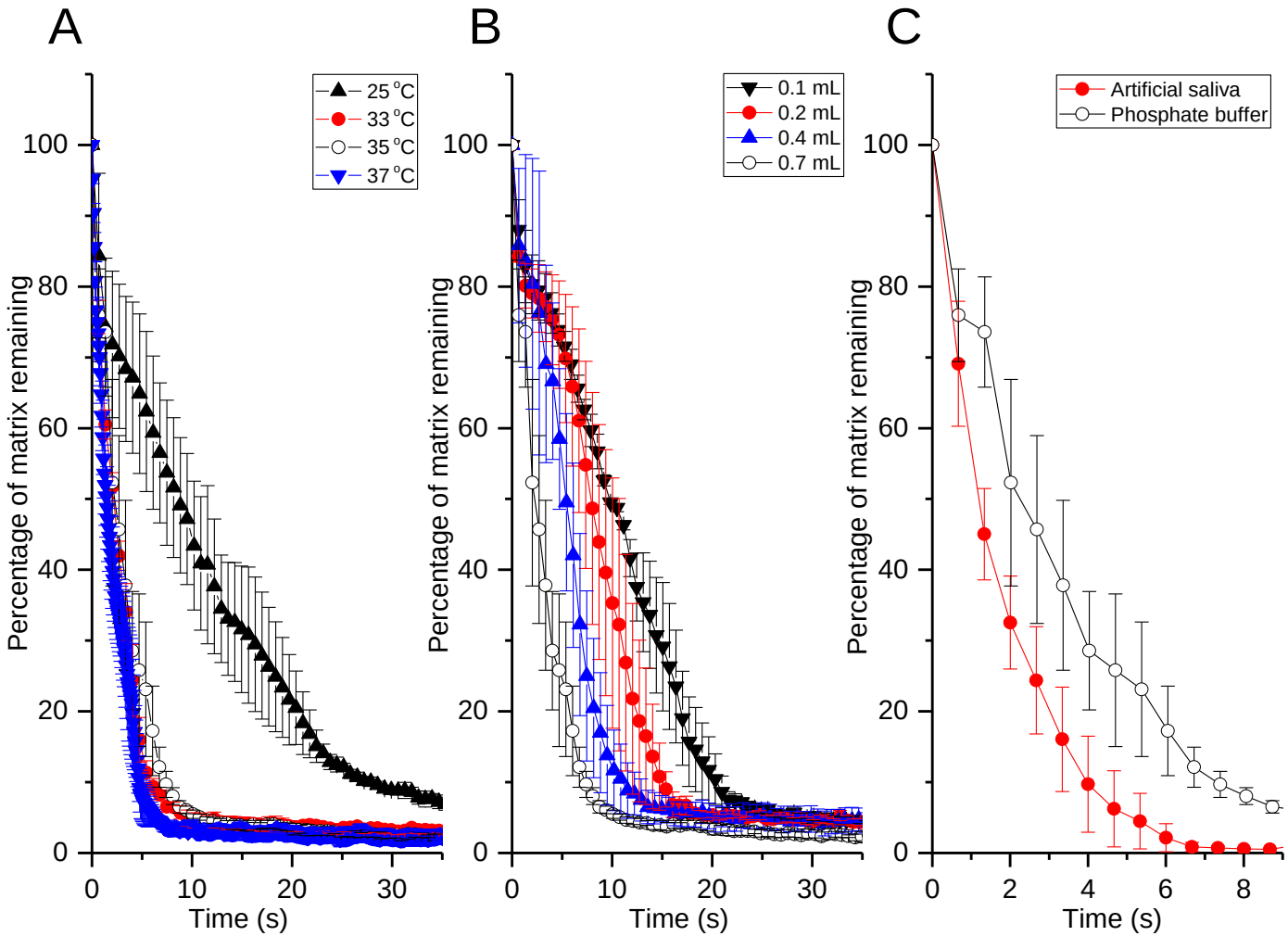

Figure 4.9 Disintegration profiles of naloxone FDT: The effect of (A) temperature [volume 0.7 mL; medium – phosphate buffered saline], (B) volume of disintegration medium [temperature 35 °C; medium – phosphate buffered saline] & (C) disintegration medium [temperature 35 °C; volume 0.7 mL] on the disintegration profile of the FDT; using a digital image disintegration assay. Data represent mean ± standard error, n=3.

4.4.6.1. Comparing naloxone FDT to the Zydis® formulation

The rate of disintegration for naloxone FDT was also compared to the Zydis® formulation, marketed as Imodium® for the release of loperamide HCl. DIDA parameters included 0.7 mL of phosphate buffer and a maintained temperature 37 ^{o}C. As demonstrated by figure 4.10, the disintegration of the Zydis® formulation does not reach a percentage of matrix remaining ≤ 20%. On the other hand, the Zydis® formulation showed to generate a cloudy suspension. While this may not be ideal for a buccal formulation, it is considered fit for purpose as the Zydis® formulation was designed for oral delivery rather than buccal (Green and Kearney, 1999). However the enhancement in matrix disintegration, and disappearance of the naloxone FDT matrix, is clearly emphasised in figure 4.10.

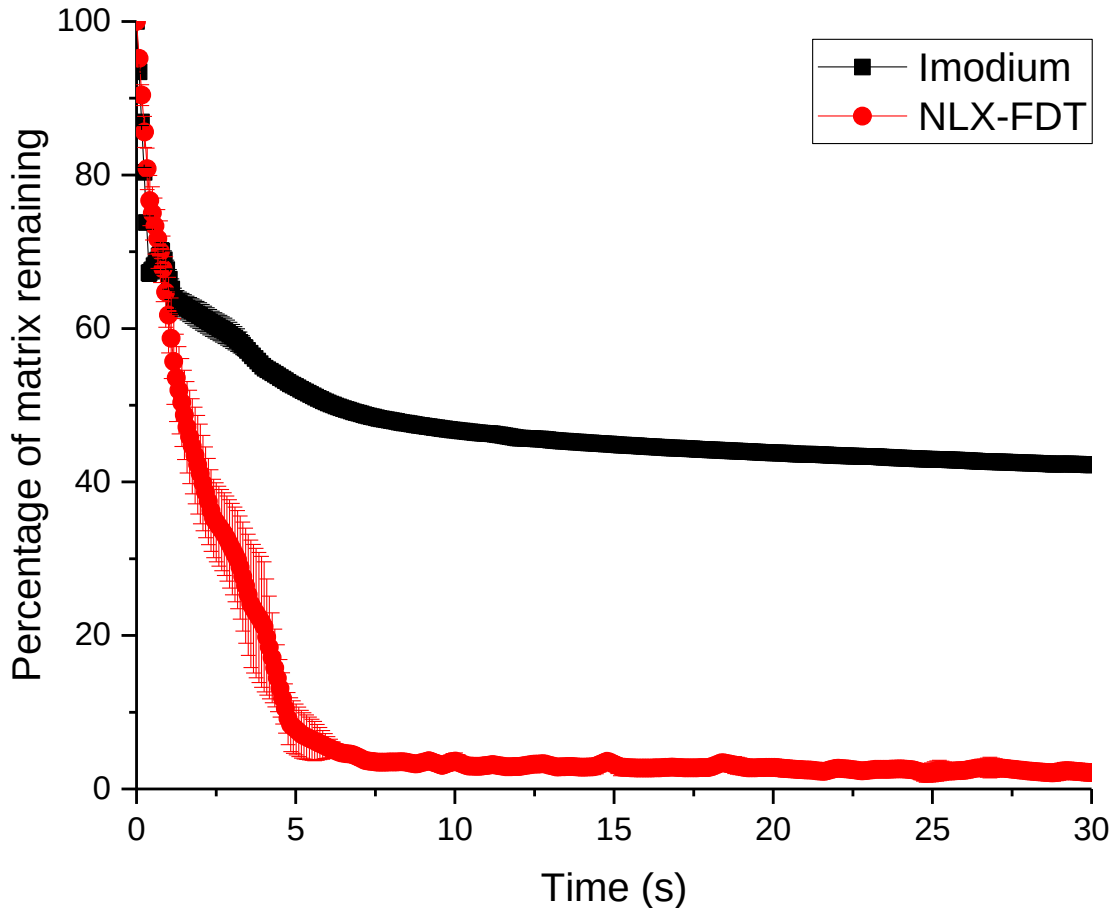

Figure 4.10 Disintegration of the naloxone FDT compared to the Zydis® formulation, marketed as Imodium instants®, at 37 ^{o}C and 0.7 mL of phosphate buffer. The Zydis® produces a cloudy suspension with more than 40% of the matrix remaining, while the novel naloxone FDT generates an almost clear suspension with less than 90% of the matrix remaining.

4.5. Discussion

An instant disintegrating tablet for rapid delivery of naloxone HCl was developed successfully to be tested in a clinical trial for emergency buccal delivery medicine in opioid overdose. The product is suitable for proof of concept clinical trials in humans to determine the pharmacokinetics of naloxone delivered via this route. The size and shape of the developed tablet were designed to ensure a high surface area contact with the buccal epithelium. The open pore structure and amorphous structure of the low density tablet, $11.8 \pm 0.3 \times 10^{-3}$ g/mL, were designed for rapid release of drug in low volumes of fluid. Additionally, the size and shape of the tablet were fashioned based on the recommendations of healthcare professionals experienced in treating overdose patients (Gugulothu *et al.*, 2015). These dimensions contrast with smaller fast disintegrating buccal tablets currently under development (Gugulothu *et al.*, 2015).

A tablet specification was developed for weight, dimensions, rate of disintegration and drug content and used to verify batch-to batch reproducibility and stability (Table 4.12). Tablets containing 24% w/w mannitol showed no shrinkage or collapse from their dimensions after the initial freezing step, confirming that the collapse temperature of the formulation was not exceeded during the drying cycle. If the T_g of mannitol in maximally freeze concentrated aqueous solutions (-27 ^{o}C) is exceeded during drying, collapse and crystallization of the amorphous cake is observed as a dramatic shrinkage of the product (Cavatur and Suryanarayanan, 1998). One of the roles of gelatin in the formulation is to raise the glass transition of both the freeze concentrated solution and the dried amorphous product in which gelatin maintains the amorphous structure. The drying cycle reported within this paper is conservative, incorporating a wide safety margin; when considering scale up and increasing process efficiency, the drying temperature of -40 ^{o}C could be increased.

Gelatin alone was insufficient to prevent crystallization of mannitol within the tablet during freeze-drying. Even at 65% w/w gelatin, sodium bicarbonate was required to eliminate the persistent PXRD peak, indicative of the crystalline hemihydrate form of mannitol. This peak disappeared when 5% sodium bicarbonate was added to the feed solution. However, measurement of recrystallization during the cool cycle using DSC

revealed that concentration of sodium bicarbonate for full suppression of crystallization was 11% w/w. Thermal analysis, especially DSC, is influenced less by particle size and density issues compared to PXRD because the whole of the crystalline fraction present in the sample contributes to the response observed (Kim *et al.*, 1998). Thus DSC was more sensitive for determining the concentration of sodium bicarbonate needed to prevent mannitol crystallization. When salts are present in freeze concentrated solutions of mannitol, the sugar has a greater affinity for ions and water, than with itself and thus the formation of mannitol crystals is inhibited. However water is key to this mechanism; removal of a large proportion of the non-frozen water during secondary drying and this protective effect is lost and mannitol crystals are observed (Telang *et al.*, 2003). Thus secondary drying was negated in the preparation of the tablets reported here and a longer primary drying cycle was applied. This resulted in 10% w/w residual water content for the tablets that maintained their amorphous structure but did not adversely influence the stability of the product.

A wide range of mannitol to gelatin concentration ratios were investigated to allow selection of a predominantly amorphous formulation for further investigation. Gelatin acts as a binder and provides structural strength, resistance to breakage and a highly porous spongy structure (Gugulothu *et al.*, 2015). Too much gelatin can have a negative effect on the rate of disintegration and dissolution as a result of inter-molecular interactions between the polymer chains of gelatin, through both hydrogen bonding and steric hindrance (Sudhakar *et al.*, 2006). Both mannitol and salts are incorporated within freeze-dried materials to bridge and intercalate these tight polymer aggregates and thus expand the porous structure (Jones *et al.*, 2011). Thus, high concentrations of gelatin in the formulation increase the likelihood of strong inter-polymer chain attractions, resulting in water trapping and the subsequent formation of gels (Gugulothu *et al.*, 2015). Unlike in other studies, for example study by Gugulothu *et al.*, where this problem was overcome by lowering the gelatin content and compensating with crystalline mannitol as a supporting agent (Gugulothu *et al.*, 2015), we have shown that it is possible to increase the ratio of gelatin to mannitol and form amorphous tablets (Figures 4.4, 4.6 & 4.7).

To circumvent the issue of strong gelatin intermolecular interaction, small amounts of an ionic salt, i.e. sodium bicarbonate, were used to expand the gelatin network, inhibit

mannitol crystallization and generate an amorphous material (Jones *et al.*, 2011). This resulted in a fast disintegrating, gelatin-mannitol amorphous complex. Gelatin may also play an important role in the long term stability of amorphous mannitol by increasing the glass transition of amorphous mannitol by approximately 13 ^{o}C, as reported by Kim et al. (Kim *et al.*, 1998) Mannitol in turn acts as a lyoprotectant agent for proteins and is thus believed to stabilize the porous structure of gelatin in freeze-dried formulations (Telang *et al.*, 2003). The stabilizing effect of mannitol in freeze-drying decreases with an increase in mannitol crystallinity (Izutsu *et al.*, 1994), which is avoided in the current product. Mannitol in freeze-drying feed solutions is known to crystallize in temperatures close to -26 ^{o}C (Tang and Pikal, 2004). The addition of small amounts of salt stabilizes amorphous mannitol in freeze concentrated solutions (Tang and Pikal, 2004); hence sodium bicarbonate was included in the tablet matrix of this study (Tang and Pikal, 2004). Furthermore, the inclusion of sodium bicarbonate enhanced the porosity of freeze-dried material. To further prevent crystallization of mannitol, the freeze-drying process was performed, at -40 ^{o}C, below the glass transition of amorphous freeze-concentrated mannitol, determined by a previous study to be ~ -27 ^{o}C (Cavatur and Suryanarayanan, 1998).

Mannitol polymorphs were clearly detected in the DSC thermograms for tablets composed of non-optimal ratios of mannitol and gelatin. For the crystalline containing samples, sodium bicarbonate also plays a significant role in the formation and thermal stability of the polymorphs observed. Telang *et al*. have shown that salts will depress the melting points of mannitol polymorphs by up to 15 ^{o}C, with additional broadening of the associated peaks (Telang *et al.*, 2003). The complex thermal and PXRD results show that a mixture of the hemihydrate and β polymorphs are formed during freeze-drying, and when tablets are heated, de-hydration and conversion results in the observation of melting profiles for the δ & α polymorphs as well as the underlying β form. These transitions are broadened and depressed by the presence of sodium bicarbonate.

There is no standard method for *in vitro* disintegration tests for instant disintegrating tablets. Many studies use standard USP apparatus 2 disintegration methods with a disintegration volume of 900 mL, whereas the total volume of saliva in the mouth does not usually exceed 3 mL (Mueller *et al.*, 2010). Other studies have attempted to study

disintegration by applying physical force to the tablet using a texture analyser (Fu *et al.*, 2005), in which case disintegration profiles are therefore dependent on mechanical strength of the tablet rather than its disintegration properties. We report a novel and reproducible digital image disintegration assay to study rapidly disintegrating buccal tablets. The assay allows automated data collection to monitor tablet disintegration in a volume and temperature controlled environment, using conditions relevant to the buccal mucosa. The disintegration of the tablet as a whole is used as a surrogate for drug release, and was rapid, economical, discriminatory and appropriate for the product developed. A factor that may limit the wider application of the assay is its reliance on the disappearance of white colour as a measure of tablet disintegration, which would exclude its use for evaluating the disintegration of tablets with insoluble excipients. Combining image analysis algorithms, common to particle size analysis, with our photographic approach to small volume disintegration is likely to remove this temporary limitation.

The novel disintegration assay was optimized for temperature in the range of 33-37 ^{o}C, corresponding to buccal temperature range (Moore *et al.*, 1999), and for disintegration medium with a volume in the range of 0.1-0.7 mL (Figure 4.9) corresponding to saliva volumes range (DiSabato-Mordarski and Kleinberg, 1996). No significant differences were observed in the disintegration profile over the buccal temperature range, but profiles were significantly different when the test was conducted at 25 ^{o}C (Figure 4.9-A). Directly correlating the disappearance of white colour to the dissolution of the matrix may be partially limited, as several white or off-white polymers form translucent masses of high viscosity within a larger body of water. These gel-like agglomerates cannot be said to be dissolved. However, complementing the novel disintegration assay with a drug quantification method, such as HPLC, performed once full disintegration is achieved, may give assurance of drug dissolution. The assay has the potential for further development as a quality control test for instant disintegrating buccal tablets and, with further exploration of biorelevant test conditions, as an assay that is predictive of *in vivo* performance.

4.6. Conclusion

A novel amorphous instant disintegrating tablet, containing naloxone, was successfully produced to good manufacturing practice standards. The composition, based on three excipients, mannitol, gelatin and sodium bicarbonate, was essential for fulfilling the design aims for a naloxone instant disintegrating buccal tablet. The tablets were both chemically and physically stable for 9 months and may be used as a prototype in clinical trials for the fast buccal delivery of emergency naloxone. A novel disintegration method for the instant disintegrating buccal tablets was developed and used to investigate the disintegration profile of the tablet formulations manufactured in this study. Total disintegration of the developed tablet was achieved in less than 10 s which is critical for their intended application.

Chapter 5. General discussion and future work

Drug solubility and dissolution rate are critical factors for delivering drugs orally, as the drug concentration in the intestinal luminal fluid is one of the main factor that determine the rate and extent of oral absorption (Augustijns *et al.*, 2014) as described by Fick's law (Flynn *et al.*, 1974). Poor water solubility is a central problem for the pharmaceutical industry, as an estimated 40% of new chemical entities are identified as poorly water-soluble (Heimbach *et al.*, 2007, Verma and Rudraraju, 2015). The main parts of this thesis look at utilising freeze-drying as a method of manufacturing solid dosage platforms to enhance the rate of drug release.

Freeze-drying is one of many methods used to make solid dispersions; this is a method of dispersing a drug, often hydrophobic, in a water soluble excipient, most commonly a hydrophilic polymer, to enhance the dissolution rate of the PWSD's (Van den Mooter, 2012, Vasconcelos *et al.*, 2007). Although freeze-drying is categorised as a solvent evaporation method (Vasconcelos *et al.*, 2007), it removes solvent mainly by sublimation (Tang and Pikal, 2004). The use of relatively low temperatures in the process of freeze-drying has made it attractive for the manufacture of solid formulations with an extended shelf-life (Craig *et al.*, 1999). The absence of high temperatures, such as those observed in the HME process (Patil *et al.*, 2015), has also made freeze-drying an ideal method of manufacture for the many thermally sensitive drugs. However, freeze-drying is a time consuming method, and as a result can be very expensive due to its slow production and high demand of power (Fu *et al.*, 2004). Nevertheless, optimizations of freeze-drying cycles and the use of industrial freeze-driers have made it economically efficient for the pharmaceutical industry.

One of the recently overcome limitations of using freeze-drying to formulate PWSD's, is the use of alternative solvents that can allow the drug and polymer to be dissolved while serving to the specific needs of freeze-drying. These include relatively high freezing temperature (≥ -20 ^{o}C) and vapour pressure (≥ 1 mbar); to resemble those of water (Murphy and Koop, 2005). Therefore, allowing a high rate of sublimation to maintain freeze-drying economically efficient (Vessot and Andrieu, 2012). Tert-butanol (TBA), showed to be a successful organic solvent that may be used instead of or in

combination with water as a solvent for freeze-drying feed solutions (Vessot and Andrieu, 2012). In this research TBA was found to be a successful substitute to water in making freeze-drying feed solutions of, the extremely hydrophobic drug, nifedipine, and the water soluble polymer, PVP. Additionally, the relatively high freezing temperature and vapour pressure of TBA (24 ^{o}C and 35.7 mbar at 20 ^{o}C respectively) was vital to its success in substituting water in the freeze-drying process (Teagarden and Baker, 2002a).

Despite recent updates in the utilization of freeze-drying as an industrial method of manufacturing oral solid dosage formulations (Al-Saadi Kumar, 2015), freeze-drying is not fully utilized in manufacturing predominantly amorphous formulations, which is known to enhance dissolution rate of PWSD's (Kaushal *et al.*, 2004). The low physical and chemical stability of amorphous materials (Kaushal *et al.*, 2004, Yu, 2001) makes it difficult to process predominantly amorphous freeze-dried cakes, into conventional solid dosage units such as tablets, without inducing physical or chemical degradation (Yu, 2001, Craig *et al.*, 1999, Vasconcelos *et al.*, 2007, Kaushal *et al.*, 2004). This research investigated the possibility of overcoming this barrier by eliminating intermediate steps, and freeze-drying feed solutions while in a vehicle that would allow the developed, predominantly amorphous freeze-dried cake to be packaged and dispensed with no additional manufactural process. Therefore, adapting the freeze-drying process of TBA based feed solutions, of PWSD's, to manufacture predominantly amorphous solid unit dosage forms. Hard gelatin capsules showed to fulfil this need elegantly, whereby accurately measured feed solutions, containing 10 mg of nifedipine, were added to the inside of capsule bottoms and were *in-situ* freeze-dried. Liquid TBA, and the *in-situ* freeze-drying process, was found to not affect the, international pharmacopeia based, specifications of hard gelatin capsules (WHO, 2015), therefore giving this system great potential to be used in early clinical studies.

Nevertheless, simply freeze-drying TBA based solutions of nifedipine did not produce amorphous nifedipine. While formulating high ratios of PVP:NIF generated freeze-dried solid solutions with enhanced dissolution rate. To understand the mechanism behind the enhancement of dissolution rate, physicochemical properties of freeze-dried formulations, containing a range of NIF:PVP ratios, were examined via thermal analysis, infrared analysis and polarized microscopy. Results indicated that formulating

NIF with PVP (at w/w percentages ≤ 50% NIF in PVP), via freeze-dying, has resulted in a miscible binary molecular dispersion, with a single T_g, where by signs of crystalline nifedipine were undetectable using thermal and microscopic techniques. The miscibility of nifedipine and PVP has also contributed to an increase in the overall T_g, upon the addition of PVP, which is critical for the physical stability of amorphous nifedipine. This has enhanced the stability of amorphous nifedipine during and after manufacture of the solid solution.

When comparing FT-IR analysis of freeze-dried ≥60% w/w NIF in PVP, produced in this study, to equivalent solid dispersions produced by hot-melt extrusion (HME) processes in similar studies, performed by Chan and Iqbal, a clear difference is observed in the IR crystalline NIF characteristics. Where freeze-dried samples do not show the characteristic peaks of crystalline NIF, at 762 cm^{-1} and 793 cm^{-1}, observed in equivalent HME solid dispersions (Iqbal and Chan, 2015, Chan *et al.*, 2004). This may be an indication that crystals detected in freeze-dried formulations may consist only of fragments, such as nifedipine dimers. The mixing of NIF and PVP in feed solutions may have therefore, generated a more dispersed solid solution, leading to a more effective inhibition of NIF crystal growth. However, another reported factor that may affect the tendency of amorphous materials to crystalize is the thermal history (Bhugra and Pikal, 2008). Tsukushi *et al.* (1994) found that amorphous tri-omethyl-b-cyclodextrin generated by melt quenching, has much lower enthalpy relaxation than that generated by milling, and therefore a lower tendency to crystalize. Although the temperature range used in the freeze-drying methods of this project are relatively low, the normal temperature range used in secondary drying can vary from 40 ^{o}C to 50 ^{o}C, therefore creating a thermal history that would lead to higher recrystallization tendency (Bhugra and Pikal, 2008). Surana *et al.* (2004) compared the physical stability of amorphous trehalose manufactured by freeze-drying, melt quenching, spray drying and dehydration. The authors concluded, from crystallisation studies during water sorption, that amorphous trehalose prepared by quench melting has the least tendency to crystallise, followed by freeze-drying and spray drying, showing equal tendencies, and finally amorphous trehalose prepared by dehydration, showing the highest tendency to crystallise.

In this project, the *in-situ* capsule formulation of NIF in PVP was only subjected to a secondary drying temperature range of (18-25 ^{o}C), and was sealed and stored under nitrogen gas. Therefore, it is concluded by the author, in light of the above described FT-IR analysis, that the developed *in-situ* freeze-dried formulation shows potential for higher physical stability than that produced by HME. Further FT-IR analysis has shown strong indications of hydrogen bonding between the nifedipine and PVP (NH and carbonyl group respectively). Such drug-polymer interactions are believed to further discourage molecular mobility of amorphous nifedipine, and therefore enhance its physical stability. Similar observations were published by Aso and Yoshioka (2006) using ^{13}C- NMR analysis. The enhancement of physical stability of amorphous nifedipine in the novel *in-situ* freeze-dried platform has led to a significant increase in the dissolution rate of nifedipine. However, although no signs of nifedipine crystals were detected in the 30% w/w NIF in PVP, a reduction in the % w/w NIF in PVP, showed to further enhance the dissolution rate by approximately 1.7 times and the kinetic solubility by approximately 1.3 times. This enhancement was observed despite that both formulations did not show any detectable nifedipine crystals using thermal, spectral and microscopic methods.

A closer look at the dissolution of freeze-dried formulations, using a novel polarized microscopic dissolution test, showed crystallization and precipitation of drug after dissolution to be a possibility. Based on the assumption, that observed birefringence is directly proportional to the amount of recrystallized and precipitated nifedipine, FD-10% generated less birefringence, measured in MGV, than FD-50% by almost 20 times (taking a dilution factor of 5 times into account). This may indicate that the role of PVP to stabilize amorphous nifedipine is not limited to the physical stability of amorphous nifedipine during manufacture and shelf life, but also in solution. This may be achieved via drug-polymer interactions while in dissolution medium (Broman *et al.*, 2001), thus an increase in concentration of PVP in the vicinity of nifedipine in dissolution medium, may result in the formation of a highly viscous boundary layer (Kaushal *et al.*, 2004) around nifedipine molecules. This can inhibit the recrystallisation and precipitation of nifedipine, which as a result increases the kinetic solubility of nifedipine in dissolution medium. Additionally, as presented by the Noyes and Whitney equation, enhancement in solubility results in dissolution rate enhancement (Noyes and Whitney, 1897).

The novel *in-situ* capsule freeze-dried platform developed as part of this project was recently proposed by Crum *et al.* (2013) before there was an opportunity to publish the work presented in this thesis. However, Crum *et al.* (2013) failed to meet the dissolution rate requirements of the BP (MHRA, 2014b), as all formulations described by the authors only showed ≤ 50% dosage released at 20 min, while the minimum BP acceptance criteria is ≥ 80% dosage released at 20 min. The FD-10% formulation developed in this thesis has shown to supersede the dissolution rate of the 10 mg nifedipine marketed fast release soft gel formulations TEVA® by more than 3 times. The developed FD-10% formulation has also showed to conform to fast release nifedipine capsule specification of the BP (MHRA, 2014b), making it fit for use, as a formulation platform, in early stages of a clinical trial.

The *in-situ* FD platform described in this project has shown great potential for a much needed enhancement in the dissolution and kinetic solubility of PWSD's (Verma and Rudraraju, 2015, Heimbach *et al.*, 2007). This as a result, is expected to improve the oral bioavailability of class II drugs of the BCS (Vasconcelos *et al.*, 2007, Leuner and Dressman, 2000). However, drug potency may act as a limiting factor, as the amount of drug needed must be molecularly dispersed in a high w/w % of polymer. This puts the estimated maximum amount of drug to be approximately 15 mg per capsule. Therefore drugs with low potency, such as Ibuprofen, my not be suitable candidates for this platform. However, relatively higher dose size, such as 30 mg, may still be achieved by administering multiple dose units at each time point. The miscibility of drug in polymer as well as the solubility of drug and polymer in TBA, or TBA and water co-solvent (Vessot and Andrieu, 2012), is another crucial factor for the success of the platform design. Table 5.1 below presents a number of drugs which may potentially be delivered using the *in-situ* FD platform for dissolution rate enhancement.

Freeze-drying was also utilized to develop a predominantly amorphous buccal tablet with enhanced release of the antagonist naloxone. This was performed as part of a project, aiming to support wider availability of non-injectable emergency naloxone in community settings, to overcome fatal outcomes from opioid overdose in the absence of medically trained personal (Alqurshi *et al.*, submitted, Strang *et al.*, submitted, Degenhardt *et al.*, 2011). The designed buccal platform was optimised to contain a predominantly amorphous matrix, for enhanced dissolution rate. This was confirmed

by the absence of peaks, indicative of crystalline structure, in powder X-ray diffraction and differential scanning calorimetry analysis. The tablet was also made to have an oval shape and a large size to allow ease of applying in emergency situations (Gugulothu *et al.*, 2015).

Using principles of molecular and material science (Sun, 2009), the porous freeze-dried instant disintegrating tablet was designed by modifying the ratios of mannitol, gelatin and sodium bicarbonate to develop a stable predominantly amorphous freeze-dried solid dispersion. Varying the ratios of individual excipients relied on understanding the role of each excipient and its effect on the physical stability of the amorphous matrix. While mannitol was used as a fast disintegrating agent, gelatin, acting as a high T_g polymer, was critical to stabilise its amorphous form during and after freeze-drying. Nevertheless, gelatin was not sufficient to stabilise amorphous mannitol even at high ratios, and therefore the addition of sodium bicarbonate determined to be essential for the physical stability of predominantly amorphous matrix. In addition to the analytical methods used in development of the NIF-PVP *in-situ* FD capsule formulations, PXRD analysis was also used in the development of the predominantly amorphous instant disintegrating tablet. This allowed comparison of analysis between DSC and PXRD.

The rate of disintegration for the instant dissolving tablet is the most critical quality to control for the success of fast dissolving buccal tablets. Nevertheless, to the best of my knowledge, there was no discriminative disintegration method found in regulatory recourses or in the literature. The use of conventional USP apparatus I, with high disintegration volumes, such as 900 mL, is a common approach in current published studies, investigating fast release buccal formulations (Hirani *et al.*, 2009, Ray *et al.*, 2011, Malik *et al.*, 2012a, Kraemer *et al.*, 2012). In this thesis, a novel digital image disintegration assay was developed, where biologically relevant volumes and temperatures are implemented. The novel assay showed great potential of being used as a quality control assay for fast disintegrating tablets. In general, the use of sequence imaging as a monitoring technique, in this thesis, has shown to be quite useful in both monitoring the stability of amorphous nifedipine, in dissolution medium, and the rate of disintegration by the naloxone amorphous matrix. Such technique may also be

extended to monitor accelerated stability studies of amorphous formulations, where samples are stored under high temperatures and humidity levels.

The buccal platform design developed in this project was intended for a clinical trial in humans to determine the pharmacokinetics of naloxone delivered via the buccal route, and therefore evaluate the potential of emergency buccal naloxone through rapid releasing tablets (See appendix 2-4 for the manufacturing and quality control of naloxone buccal IDT, and a copy of the investigational medicinal product dossier respectively). Table 5.1 below lists a number of potential candidates for emergency rapid delivery, via the fast disintegrating buccal tablets.

Conclusion

The aims of the research reported in this thesis were successfully fulfilled, where two novel freeze-dried platform designs, for formulations with enhanced drug release, were developed. The first platform design, the *in-situ* freeze-dried capsule formulation, showed to significantly enhance the release of, the poorly water-soluble drug, nifedipine. The second platform design: instant disintegrating tablet, showed rapid matrix disintegration in biorelevant conditions to the buccal cavity, including limited disintegration volumes of 0.1mL. Both novel formulations were compared to equivalent marketed formulations, and showed a superior enhancement in the rate of drug release, for the *in-situ* freeze-dried platform, and a superior matrix disintegration for the IDT platform. The underpinning science behind the success of both formulations was investigated using various analytical tools and techniques, including characterisation of physical state and intermolecular forces. Additionally, the development of novel techniques, described in this thesis, such as polarized microscopy dissolution and the digital image disintegration assay (DIDA), allowed better understanding of the mechanism behind the enhancement in formulation performance. Additionally, the novel DIDA test successfully demonstrated great potential in the quality control of rapid disintegration by FDT's.

Table 5.1 A list of potential drugs for both or either of the developed platforms designed in this thesis.

Drug	Indication	Molecular weight	BCS class	Solubility	Permeability	Recommended dosage / mg	Type of formulation	Ref.
Ketoprofen	Analgesic/anti-inflammatory	254.3	II	Low	High	12.5	*In-situ* freeze-dried capsules	(Reddy and Karunakar, 2011, Tixier *et al.*, 2003)
Glibenclamide	Antidiabetic, Sulfonylureas	494	II	Low	High	1.25, 2.5 & 5.0	FDT and *In-situ* freeze-dried capsules	(Reddy and Karunakar, 2011, Massi-Benedetti, 2003)
Phenytoin	Antiepileptic	252.3	II	Low	High	25.0	*In-situ* freeze-dried capsules	(Lindenberg *et al.*, 2004)
Amlodipine	Antihypertensive	408.9	I	High	High	5.0	FDT	(WHO, 2005)
Diazepam	Psychotherapeutic medicine	284.7	I	High	High	5.0	FDT	
Amiloride hydrochloride	Diuretic	229.6	I	High	High	5.0	FDT	(Lindenberg *et al.*, 2004, WHO, 2005)
Biperiden hydrochloride	Antimuscarinic agent	347.92	III	High	Low	2.0	FDT	
Chlorpheniramine hydrogen maleate	Antiallergic	274.8	I/III	High	insufficient literature	4.0	FDT	

References

Agarwal, V. & Bajpai, M. 2013. "Stability issues related to nanosuspensions: a review". *Pharm. Nanotechnol.,* 1**,** 85-92.

Aguiar, A. J., Krc, J., Kinkel, A. W. & Samyn, J. C. 1967. "Effect of Polymorphism on Absorption of Chloramphenicol from Chloramphenicol Palmitate". *Journal of Pharmaceutical Sciences,* 56**,** 847-&.

Ahmed, H., Buckton, G. & Rawlins, D. A. 1996. "The use of isothermal microcalorimetry in the study of small degrees of amorphous content of a hydrophobic powder". *International Journal of Pharmaceutics,* 130**,** 195-201.

Al-Saadi Kumar, Z. 2015. *Evaluating excipients commonly used in freeze-drying to develop a novel buccal formulation.* MPharm, King's College London.

Ali, S. L. 1989. "Nifedipine". *Anal. Profiles Drug Subst.,* 18**,** 221-88.

Allen, P. V., Rahn, P. D., Sarapu, A. C. & Vanderwielen, A. J. 1978. "Physical Characterization of Erythromycin - Anhydrate, Monohydrate, and Dihydrate Crystalline Solids". *Journal of Pharmaceutical Sciences,* 67**,** 1087-1093.

Allesø, M., Chieng, N., Rehder, S., Rantanen, J., Rades, T. & Aaltonen, J. 2009. "Enhanced dissolution rate and synchronized release of drugs in binary systems through formulation: Amorphous naproxen–cimetidine mixtures prepared by mechanical activation". *Journal of Controlled Release,* 136**,** 45-53.

Alonzo, D. E., Zhang, G. G., Zhou, D., Gao, Y. & Taylor, L. S. 2010. "Understanding the behavior of amorphous pharmaceutical systems during dissolution". *Pharmaceutical research,* 27**,** 608-618.

Alqurshi, A., Kumar, Z., McDonald, R., Strang, J., Buanz, A., Ahmed, S., Allen, E., Cameron, P., Rickard, J., Sandhu, V., C., H., Stansfield, R., Taylor, D., Forbes, B. & Royall, P. G. submitted. "Instant disintegrating buccal tablets for the emergency delivery of naloxone". *Molecular pharmaceutics*.

AMA. 2015. *AMA Adopts New Policies to Improve Health of Nation on First Day of Voting at Annual Meeting* [Online]. Available: http://www.ama-assn.org/ama/pub/news/news/2015/2015-06-08-new-policies-annual-meeting.page [Accessed Jun 26 2015].

Andrews, G. P. 2007. "Advances in solid dosage form manufacturing technology". *Philosophical Transactions of the Royal Society a-Mathematical Physical and Engineering Sciences,* 365**,** 2935-2949.

Arakawa, T., Prestrelski, S. J., Kenney, W. C. & Carpenter, J. F. 2001. "Factors affecting short-term and long-term stabilities of proteins". *Advanced drug delivery reviews,* 46**,** 307-326.

Aso, Y. & Yoshioka, S. 2006. "Molecular mobility of nifedipine-PVP and phenobarbital-PVP solid dispersions as measured by C-13-NMR spin-lattice relaxation time". *Journal of Pharmaceutical Sciences,* 95**,** 318-325.

Aso, Y., Yoshioka, S. & Kojima, S. 2004. "Molecular mobility-based estimation of the crystallization rates of amorphous nifedipine and phenobarbital in poly(vinylpyrrolidone) solid dispersions". *Journal of Pharmaceutical Sciences,* 93**,** 384-391.

Augustijns, P., Wuyts, B., Hens, B., Annaert, P., Butler, J. & Brouwers, J. 2014. "A review of drug solubility in human intestinal fluids: Implications for the prediction of oral absorption". *European Journal of Pharmaceutical Sciences,* 57**,** 322-332.

Aulton, M. E. 2007. *Pharmaceutics : the design and manufacture of medicines,* Edinburgh ; New York, Churchill Livingstone.

Badgujar, B. P. & Mundada, A. S. 2011. "The technologies used for developing orally disintegrating tablets: A review". *Acta Pharmaceutica,* 61**,** 117-139.

Baird, J. A., Van Eerdenbrugh, B. & Taylor, L. S. 2010. "A classification system to assess the crystallization tendency of organic molecules from undercooled melts". *J. Pharm. Sci.,* 99**,** 3787-3806.

Barbaree, J. M., Sanchez, A. & Sanden, G. N. 1985. "Problems in freeze-drying 1. Stability in glass-sealed and rubber-stoppered vials". *Developments in Industrial Microbiology***,** 397-406.

Bates, T. R. 1969. "Dissolution characteristics of reserpine-polyvinylpyrrolidone co-precipitates". *Journal of Pharmacy and Pharmacology,* 21**,** 710-2.

Bhugra, C. & Pikal, M. J. 2008. "Role of thermodynamic, molecular, and kinetic factors in crystallization from the amorphous state". *Journal of pharmaceutical sciences,* 97**,** 1329-1349.

Briggner, L. E., Buckton, G., Bystrom, K. & Darcy, P. 1994. "The Use of Isothermal Microcalorimetry in the Study of Changes in Crystallinity Induced during the Processing of Powders". *International Journal of Pharmaceutics,* 105**,** 125-135.

Brittain, H. G., Grant, D. J. R. & Myrdal, P. B. 2009. Effects of Polymorphism and Solid-State Solvation on Solubility and Dissolution Rate. *Polymorphism in Pharmaceutical Solids.*

Brodin, B., Steffansen, B. & Nielsen, C. U. 2010. "Passive diffusion of drug substances: the concepts of flux and permeability". *Chapter,* 3**,** 135-151.

Broman, E., Khoo, C. & Taylor, L. S. 2001. "A comparison of alternative polymer excipients and processing methods for making solid dispersions of a poorly water soluble drug". *International Journal of Pharmaceutics,* 222**,** 139-151.

Brostow, W., Chiu, R., Kalogeras, I. M. & Vassilikou-Dova, A. 2008. "Prediction of glass transition temperatures: Binary blends and copolymers". *Materials Letters,* 62**,** 3152-3155.

Brouwers, J., Brewster, M. E. & Augustijns, P. 2009. "Supersaturating Drug Delivery Systems: The Answer to Solubility-Limited Oral Bioavailability?". *Journal of Pharmaceutical Sciences,* 98**,** 2549-2572.

Buckton, G. & Darcy, P. 1999. "Assessment of disorder in crystalline powders - a review of analytical techniques and their application". *International Journal of Pharmaceutics,* 179**,** 141-158.

Buera, M. D., Levi, G. & Karel, M. 1992. "Glass-transition in poly(vinylpyrrolidone) - effect of molecular-weight and diluents". *Biotechnology Progress,* 8**,** 144-148.

Carlton, R. A. 2011. *Pharmaceutical Microscopy*, Springer.

Cavatur, R. K. & Suryanarayanan, R. 1998. "Characterization of phase transitions during freeze-drying by in situ X-ray powder diffractometry". *Pharmaceutical development and technology,* 3**,** 579-86.

Chahiyan, H., Gharib, F. & Farajtabar, A. 2014. "Thermodynamic studies on solubility and protonation constant of acetaminophen at different ionic strengths and various temperatures". *Journal of Molecular Liquids,* 199**,** 137-142.

Chan, K. L. A., Fleming, O. S., Kazarian, S. G., Vassou, D., Chryssikos, G. D. & Gionis, V. 2004. "Polymorphism and devitrification of nifedipine under controlled humidity: a combined FT-Raman, IR and Raman microscopic investigation". *Journal of Raman Spectroscopy,* 35**,** 353-359.

Chaumeil, J. C. 1998. "Micronization: A method of improving the bioavailability of poorly soluble drugs". *Methods and Findings in Experimental and Clinical Pharmacology,* 20**,** 211-215.

Chiou, W. L. & Riegelma.S 1969. "Preparation and Dissolution Characteristics of Several Fast-Release Solid Dispersions of Griseofulvin". *Journal of Pharmaceutical Sciences,* 58**,** 1505-&.

Chiou, W. L. & Riegelman, S. 1971. "Pharmaceutical applications of solid dispersion systems". *J Pharm Sci,* 60**,** 1281-302.

Chowdary, K. P. R. & Pavan Kumar, A. 2013. "Recent research on formulation development of BCS class II drugs - a review". *Int. Res. J. Pharm. Appl. Sci.,* 3**,** 173-181, 9 pp.

Chutimaworapan, S., Ritthidej, G. C., Yonemochi, E., Oguchi, T. & Yamamoto, K. 2000. "Effect of water-soluble carriers on dissolution characteristics of nifedipine solid dispersions". *Drug Development and Industrial Pharmacy,* 26**,** 1141-1150.

Cilurzo, F., Minghetti, P., Casiraghi, A. & Montanari, L. 2002. "Characterization of nifedipine solid dispersions". *International Journal of Pharmaceutics,* 242**,** 313-317.

Cirri, M., Mura, P., Rabasco, A. M., Gines, J. M., Moyano, J. R. & Gonzalez-Rodriguez, M. L. 2004. "Characterization of ibuproxam binary and ternary dispersions with hydrophilic carriers". *Drug Development and Industrial Pharmacy,* 30**,** 65-74.

Cole, E. T., Cadé, D. & Benameur, H. 2008. "Challenges and opportunities in the encapsulation of liquid and semi-solid formulations into capsules for oral administration". *Advanced Drug Delivery Reviews,* 60**,** 747-756.

Cornel, J., Kidambi, P. & Mazzotti, M. 2010. "Precipitation and Transformation of the Three Polymorphs of D-Mannitol". *Industrial & Engineering Chemistry Research,* 49**,** 5854-5862.

Corveleyn, S. & Remon, J. P. 1997. "Formulation and production of rapidly disintegrating tablets by lyophilisation using hydrochlorothiazide as a model drug". *International Journal of Pharmaceutics,* 152**,** 215-225.

Costa, P., Manuel, J. & Lobo, S. 2001. "Modeling and comparison of dissolution profiles". *European Journal of Pharmaceutical Sciences,* 13**,** 123-133.

Costantino, H. R. & Pikal, M. J. 2004. *Lyophilization of biopharmaceuticals*, Springer.

Craig, D. Q. M., Royall, P. G., Kett, V. L. & Hopton, M. L. 1999. "The relevance of the amorphous state to pharmaceutical dosage forms: glassy drugs and freeze dried systems". *International Journal of Pharmaceutics,* 179**,** 179-207.

Crowley, K. J. & Zografi, G. 2003. "The Effect of Low Concentrations of Molecularly Dispersed Poly(Vinylpyrrolidone) on Indomethacin Crystallization from the Amorphous State". *Pharm. Res.,* 20**,** 1417-1422.

Crum, M., Elkordy, A. A., Zarara, M. & Elkordy, E. A. 2013. "In situ lyophilisation of nifedipine directly in hard gelatine capsules". *Pharmaceutical Development and Technology,* 18**,** 1379-1390.

Cui, J., Li, C., Deng, Y., Wang, Y. & Wang, W. 2006. "Freeze-drying of liposomes using tertiary butyl alcohol/water cosolvent systems". *International journal of pharmaceutics,* 312**,** 131-136.

de Waard, H., Hinrichs, W. L. J. & Frijlink, H. W. 2008. "A novel bottom-up process to produce drug nanocrystals: Controlled crystallization during freeze-drying". *Journal of Controlled Release,* 128**,** 179-183.

Deepti, J. & Pawan, K. B. 2013. "ICH guideline practice: application of validated RP-HPLC DAD method for determination of tapentadol hydrochloride in dosage form". *journal of analytical science and technology,* 4.

Degenhardt, L., Bucello, C., Mathers, B., Briegleb, C., Ali, H., Hickman, M. & McLaren, J. 2011. "Mortality among regular or dependent users of heroin and other opioids: a systematic review and meta-analysis of cohort studies". *Addiction,* 106**,** 32-51.

Dehring, K. A., Workman, H. L., Miller, K. D., Mandagere, A. & Poole, S. K. 2004. "Automated robotic liquid handling/laser-based nephelometry system for high throughput measurement of kinetic aqueous solubility". *J. Pharm. Biomed. Anal.,* 36**,** 447-456.

Desai, J., Alexander, K. & Riga, A. 2006. "Characterization of polymeric dispersions of dimenhydrinate in ethyl cellulose for controlled release". *International Journal of Pharmaceutics,* 308**,** 115-23.

Devinder Gupta, L. W., Leonard M, Hanseen, Jack J, Hsia, Raju U, Dalta 1995. Polystyrene Films for Calibration the Wavelength Scale of Infrared Spectrometers. *In:* COMMERCE, U. S. D. O. (ed.). NIST special publication.

DiSabato-Mordarski, T. & Kleinberg, I. 1996. "Measurement and comparison of the residual saliva on various oral mucosal and dentition surfaces in humans". *Archives of Oral Biology,* 41**,** 655-665.

Dobetti, L. 2001. "Fast-melting tablets: Developments and technologies". *Pharm. Technol. North Am.*, 44-46,48-50.

Dowling, J., Isbister, G. K., Kirkpatrick, C. M. J., Naidoo, D. & Graudins, A. 2008. "Population pharmacokinetics of intravenous, intramuscular, and intranasal naloxone in human volunteers". *Therapeutic Drug Monitoring,* 30**,** 490-496.

Doyon, S., Aks, S. E. & Schaeffer, S. 2014. "Expanding access to naloxone in the United States". *Clinical Toxicology,* 52**,** 989-992.

Edwards, B. 2010. *Instruction Manual RV3, RV5, RV8 and RV12 Rotary Vane Pumps* [Online]. http://www.ultimatevacuum.dk/A652_01_880%20RV%20instr%20manual.pdf: BOC Edwards. [Accessed 23rd Sep 2014].

FDA. 1994. *Reviewer Guidance: Validation of Chromatographic methods* [Online]. http://www.fda.gov/downloads/Drugs/.../Guidances/UCM134409.pdf: CDER-FDA. Available: http://www.fda.gov/downloads/Drugs/.../Guidances/UCM134409.pdf.

FDA. 2001. *Guidance for Industry Bioanalytical Method Validation* [Online]. http://www.fda.gov/downloads/Drugs/.../Guidances/ucm070107.pdf: U.S. Department of Health and Human Services, Food and Drug Administration. Available: http://www.fda.gov/downloads/Drugs/.../Guidances/ucm070107.pdf.

FDA. 2004. *Guidance for Industry Q1E Evaluation of Stability Data* [Online]. http://www.fda.gov/downloads/drugs/guidancecomplianceregulatoryinformation/guidances/ucm073380.pdf: U.S. Department of Health and Human Services. Available: http://www.fda.gov/downloads/drugs/guidancecomplianceregulatoryinformation/guidances/ucm073380.pdf [Accessed 24/08/2015 2015].

FDA. 2007. *Guidance for Industry ANDAs: Pharmaceutical Solid Polymorphism* [Online]. Center for Drug Evaluation and Research (CDER). Available: http://www.fda.gov/downloads/Drugs/Guidances/UCM072866.pdf [Accessed 24/08/2015 2015].

FDA. 2008. *Guidance for Industry Drug Stability Guidelines* [Online]. http://www.fda.gov/downloads/AnimalVeterinary/GuidanceComplianceEnforcement/GuidanceforIndustry/ucm051556.pdf: U.S. Department of Health and Human Services. Available: http://www.fda.gov/downloads/AnimalVeterinary/GuidanceComplianceEnforcement/GuidanceforIndustry/ucm051556.pdf.

Fix, I. & Steffens, K. J. 2004. "Quantifying low amorphous or crystalline amounts of alpha-lactose-monohydrate using X-ray powder diffraction, near-infrared spectroscopy, and differential scanning calorimetry". *Drug Development and Industrial Pharmacy,* 30**,** 513-523.

Florence, A. T. & Attwood, D. 1988. *Physicochemical principles of pharmacy,* N ew Y ork , NY, Chapman and Hall.

Flory, P. J. 1942. "Thermodynamics of high-polymer solutions". *J. Chem. Phys.,* 10**,** 51-61.

Flynn, G. L., Yalkowsk.Sh & Roseman, T. J. 1974. "Mass-Transport Phenomena and Models - Theoretical Concepts". *Journal of Pharmaceutical Sciences,* 63**,** 479-510.

Franks, F. & Auffret, T. 2008. *Freeze-drying of pharmaceuticals and biopharmaceuticals : [principles and practice],* Cambridge, RSC Pub.

Fu, Y., Yang, S., Jeong, S. H., Kimura, S. & Park, K. 2004. "Orally fast disintegrating tablets: developments, technologies, taste-masking and clinical studies". *Crit Rev Ther Drug Carrier Syst,* 21**,** 433-76.

Fu, Y. R., Jeong, S. H. & Park, K. 2005. "Fast-melting tablets based on highly plastic granules". *Journal of Controlled Release,* 109**,** 203-210.

Fujii, S., Ishizawa, K., Sakurada, T., Yamano, N., Izawa-Ishizawa, Y., Imanishi, M., Nuno, A., Suzuki, Y., Kihira, Y., Ikeda, Y., Tomita, S., Tsuchiya, K. & Tamaki, T. *Nitrosonifedipine, a photodegradation product of nifedipine, prevents the progression of diabetic nephropathy in type ii diabetic mice*, Hypertension. Conference: High Blood Pressure Research 2012 Scientific Sessions, HBPR 2012 Washington, DC United States.

Conference Start: 20120919 Conference End: 20120922. Conference Publication: (var.pagings). 60 (3 Meeting Abstracts) , 2012. Date of Publication: September 2012.

Gaisford, S., Verma, A., Saunders, M. & Royall, P. G. 2009. "Monitoring crystallisation of drugs from fast-dissolving oral films with isothermal calorimetry". *International Journal of Pharmaceutics,* 380**,** 105-111.

Garbacz, G., Blume, H. & Weitschies, W. 2009. "Investigation of the Dissolution Characteristics of Nifedipine Extended-Release Formulations Using USP Apparatus 2 and a Novel Dissolution Apparatus". *Dissolution Technologies,* 16**,** 7-13.

Gardner, D., Casper, R., Leith, F. & Wilding, I. 1997. "Noninvasive methodology for assessing regional drug absorption from the gastrointestinal tract". *Pharmaceutical Technology International,* 9**,** 46, 48, 50, 52-53.

George Burton, J. H., John Lazonby, Gwen Pilling, David Waddington 2000. *Salters Advanced Chemistry: Chemical Ideas*, Heinemann.

Gerber, A., Kohaupt, I., Lauterbach, K. W., Buescher, G., Stock, S. & Lungen, M. 2008. "Quantification and classification of errors associated with hand-repackaging of medications in long-term care facilities in Germany". *The American Journal of Geriatric Pharmacotherapy,* 6**,** 212-219.

Ghayas, S., Sheraz, M., Anjum, F. & Baig, M. T. 2013. "Factors influencing the dissolution testing of drugs". *Pakistan Journal of Health Research,* 1**,** 1-11.

Gibaldi, M. & Weintrau.H 1968. "Dissolution of salicylic acid and polyvinylpyrrolidone from compressed mixtures". *Journal of Pharmaceutical Sciences,* 57**,** 832-&.

Gilmartin, J. F.-M., Hussainy, S. Y. & Marriott, J. L. 2013. "Medicines in Australian nursing homes: A cross-sectional observational study of the accuracy and suitability of re-packing medicines into pharmacy-supplied dose administration aids". *Research in Social and Administrative Pharmacy,* 9**,** 876-883.

Gilson. *The working principle of positivedisplacement pipettes* [Online]. http://www.gilson.com/Resources/PDTechniques.pdf: Gilson. Available: http://www.gilson.com/Resources/PDTechniques.pdf [Accessed 31/08 2015].

Gilson.S.A.S 2006. Microman. *In:* GILSON (ed.). http://www.gilson.com/: Gilson.

Giron, D. 1995. "Thermal-analysis and calorimetric methods in the characterization of polymorphs and solvates". *Thermochimica Acta,* 248**,** 1-59.

Goldberg, A. H., Gibaldi, M., Kanig, J. L. & Mayersohn, M. 1966. "Increasing dissolution rates and gastrointestinal absorption of drugs via solid solutions and eutectic mixtures. IV. Chloramphenicol-urea system". *J. Pharm. Sci.,* 55**,** 581-3.

Green, R. & Kearney, P. 1999. Process for preparing fast dispersing solid oral dosage form. Google Patents.

Greenspan, L. 1977. "Humidity fixed-points of binary saturated aqueous-solutions". *Journal of Research of the National Bureau of Standards Section a-Physics and Chemistry,* 81**,** 89-96.

Grisedale, L. C., Moffat, J. G., Jamieson, M. J., Belton, P. S., Barker, S. A. & Craig, D. Q. M. "Development of Photothermal FTIR Microspectroscopy as a Novel Means of Spatially Identifying Amorphous and Crystalline Salbutamol Sulfate on Composite Surfaces". *Mol. Pharmaceutics***,** Ahead of Print.

Grodowska, K. & Parczewski, A. 2010. "Analytical methods for residual solvents determination in pharmaceutical products". *Acta Poloniae Pharmaceutica,* 67**,** 13-26.

Gugulothu, D., Desai, P., Pandharipande, P. & Patravale, V. 2015. "Freeze drying: exploring potential in development of orodispersible tablets of sumatriptan succinate". *Drug Development and Industrial Pharmacy,* 41**,** 398-405.

Gunn, E., Guzei, I. A., Cai, T. & Yu, L. 2012. "Polymorphism of Nifedipine: Crystal Structure and Reversible Transition of the Metastable beta Polymorph". *Crystal Growth & Design,* 12**,** 2037-2043.

Guo, J. H. 1994. "A theoretical and experimental study of additive effects of physical aging and antiplasticization on the water permeability of polymer film coatings". *Journal of pharmaceutical sciences,* 83**,** 447-449.

Habib, W., Khankari, R. & Hontz, J. 2000. "Fast-dissolve drug delivery systems". *Crit Rev Ther Drug Carrier Syst,* 17**,** 61-72.

Haines, P. J. 2002. *Principles of thermal analysis and calorimetry,* Cambridge, Royal Society of Chemistry.

Hancock, B. C., Shamblin, S. L. & Zografi, G. 1995. "Molecular mobility of amorphous pharmaceutical solids below their glass-transition temperatures". *Pharmaceutical Research,* 12**,** 799-806.

Hancock, B. C. & Zografi, G. 1997. "Characteristics and significance of the amorphous state in pharmaceutical systems". *Journal of Pharmaceutical Sciences,* 86**,** 1-12.

Hasegawa, S., Hamaura, T., Furuyama, N., Kusai, A., Yonemochi, E. & Terada, K. 2005. "Effects of water content in physical mixture and heating temperature on crystallinity of troglitazone-PVP K30 solid dispersions prepared by closed melting method". *Int. J. Pharm.,* 302**,** 103-112.

Heimbach, T., Fleisher, D. & Kaddoumi, A. 2007. *Overcoming Poor Aqueous Solubility of Drugs for Oral Delivery*.

Helin-Tanninen, M., Naaranlahti, T., Kontra, K. & Savolainen, K. 2007. "Nifedipine capsules may provide a viable alternative to oral powders for paediatric patients". *Journal of Clinical Pharmacy and Therapeutics,* 32**,** 49-55.

Helin-Tanninen, M., Naaranlahti, T., Kontra, K. & Wallenius, K. 2001. "Enteral suspension of nifedipine for neonates. Part 1. Formulation of nifedipine suspension for hospital use". *Journal of Clinical Pharmacy and Therapeutics,* 26**,** 49-57.

Heller, M. C., Carpenter, J. F. & Randolph, T. W. 1999a. "Application of a thermodynamic model to the prediction of phase separations in freeze-concentrated formulations for protein lyophilization". *Archives of Biochemistry and Biophysics,* 363**,** 191-201.

Heller, M. C., Carpenter, J. F. & Randolph, T. W. 1999b. "Protein formulation and lyophilization cycle design: Prevention of damage due to freeze-concentration induced phase separation". *Biotechnology and Bioengineering,* 63**,** 166-174.

Hibler, S., Wagner, C. & Gieseler, H. 2012. "Vial freeze-drying, part 1: New insights into heat transfer characteristics of tubing and molded vials". *Journal of Pharmaceutical Sciences,* 101**,** 1189-1201.

Hirani, J. J., Rathod, D. A. & Vadalia, K. R. 2009. "Orally Disintegrating Tablets: A Review". *Tropical Journal of Pharmaceutical Research,* 8**,** 161-172.

Hishikawa, Y., Togawa, E., Kataoka, Y. & Kondo, T. 1999. "Characterization of amorphous domains in cellulosic materials using a FTIR deuteration monitoring analysis". *Polymer,* 40**,** 7117-7124.

Horter, D. & Dressman, J. B. 1997. "Influence of physicochemical properties on dissolution of drugs in the gastrointestinal tract". *Advanced Drug Delivery Reviews,* 25**,** 3-14.

Hosono, T., Tsuchiya, S. & Matsumaru, H. 1980. "Model of interaction of ajmaline with poly(vinylpyrrolidone)". *J. Pharm. Sci.,* 69**,** 824-6.

Huang, J. J., Wigent, R. J., Bentzley, C. M. & Schwartz, J. B. 2006. "Nifedipine solid dispersion in microparticles of ammonio methacrylate copolymer and ethylcellulose binary blend for controlled drug delivery - Effect of drug loading on release kinetics". *International Journal of Pharmaceutics,* 319**,** 44-54.

Hussain, M. A., Aungst, B. J., Kearney, A. & Shefter, E. 1987. "Buccal and oral bioavailability of naloxone and naltrexone in rats". *International Journal of Pharmaceutics,* 36**,** 127-130.

Hwisa, N. T., Adiki, S. K., Katakam, P. & Chandu, B. R. 2013. "Design of dissolution media for in-vitro bioequivalence testing of Lamivudine".

ICH. 1996. *Validation of analytical procedures: Text and methodology q2(r1)* [Online]. http://www.ich.org/home.html: International conference on harmonisation of

technical requirements for registration of pharmaceuticals for human use. [Accessed 02/07/2015 2015].

ICH. 2000. *Good manufacturing practice guide for active pharmaceutical ingredients q7* [Online]. http://www.ich.org/fileadmin/Public_Web_Site/ICH_Products/Guidelines/Quality/Q7/Step4/Q7_Guideline.pdf: International conference on harmonisation of technical requirements for registration of pharmaceuticals for human use. Available: http://www.ich.org/fileadmin/Public_Web_Site/ICH_Products/Guidelines/Quality/Q7/Step4/Q7_Guideline.pdf [Accessed 13/07/2015 2015].

ICH. 2006. *Stability testing of new drug substances and products q1a(r2)* [Online]. http://www.ich.org/: International conference on harmonisation of technical requirements for registration of pharmaceuticals for human use Available: http://www.ich.org/fileadmin/Public_Web_Site/ICH_Products/Guidelines/Quality/Q1A_R2/Step4/Q1A_R2__Guideline.pdf [Accessed 13/07/2015 2015].

ICH. 2009. *Pharmaceutical development q8(r2)* [Online]. http://www.ich.org/fileadmin/Public_Web_Site/ICH_Products/Guidelines/Quality/Q8_R1/Step4/Q8_R2_Guideline.pdf: International conference on harmonisation of technical requirements for registration of pharmaceuticals for human use Available: http://www.ich.org/fileadmin/Public_Web_Site/ICH_Products/Guidelines/Quality/Q8_R1/Step4/Q8_R2_Guideline.pdf [Accessed 24/08/2015 2015].

Ikegami, K., Tagawa, K. & Osawa, T. 2006. "Bioavailability and in vivo release behavior of controlled-release multiple-unit theophylline dosage forms in beagle dogs, cynomolgus monkeys, and Gottingen minipigs". *Journal of Pharmaceutical Sciences,* 95**,** 1888-1895.

Iqbal, W. S. & Chan, K. L. A. 2015. "FTIR Spectroscopic Study of Poly(Ethylene Glycol)-Nifedipine Dispersion Stability in Different Relative Humidities". *Journal of Pharmaceutical Sciences,* 104**,** 280-284.

Izutsu, K., Yoshioka, S. & Kojima, S. 1997. "Phase separation and crystallization of components in frozen solutions: Effect of molecular compatibility between solutes". *Therapeutic Protein and Peptide Formulation and Delivery,* 675**,** 109-118.

Izutsu, K., Yoshioka, S. & Terao, T. 1994. "Effect of mannitol crystallinity on the stabilization of enzymes during freeze-drying". *Chemical & Pharmaceutical Bulletin,* 42**,** 5-8.

Jachowicz, R. & Nürnberg, E. 1997. "Enhanced release of oxazepam from tablets containing solid dispersions". *International Journal of Pharmaceutics,* 159**,** 149-158.

Jawad, R., Elleman, C., Vermeer, L., Drake, A. F., Woodhead, B., Martin, G. P. & Royall, P. G. 2012. "The Measurement of the beta/alpha Anomer Composition Within Amorphous Lactose Prepared by Spray and Freeze Drying Using a Simple H-1-NMR Method". *Pharmaceutical Research,* 29**,** 511-524.

Jiang, S. & Nail, S. L. 1998. "Effect of process conditions on recovery of protein activity after freezing and freeze-drying". *European Journal of Pharmaceutics and Biopharmaceutics,* 45**,** 249-257.

Jin, J., Sklar, G. E., Min Sen Oh, V. & Chuen Li, S. 2008. "Factors affecting therapeutic compliance: A review from the patient's perspective". *Ther Clin Risk Manag,* 4**,** 269-86.

Johnson, S. R. & Zheng, W. F. 2006. "Recent progress in the computational prediction of aqueous solubility and absorption". *Aaps Journal,* 8**,** E27-E40.

Jones, R. J., Rajabi-Siahboomi, A., Levina, M., Perrie, Y. & Mohammed, A. R. 2011. "The influence of formulation and manufacturing process parameters on the characteristics of lyophilized orally disintegrating tablets". *Pharmaceutics,* 3**,** 440-57.

Kaliszan, R., Haber, P., Bczek, T., Siluk, D. & Valko, K. 2002. "Lipophilicity and pKa estimates from gradient high-performance liquid chromatography". *Journal of Chromatography A,* 965**,** 117-127.

Kanig, J. L. 1964. "Properties of Fused Mannitol in Compressed Tablets". *J Pharm Sci,* 53**,** 188-92.

Karavas, E., Georgarakis, E. & Bikiaris, D. 2006a. "Application of PVP/HPMC miscible blends with enhanced mucoadhesive properties for adjusting drug release in predictable pulsatile chronotherapeutics". *European Journal of Pharmaceutics and Biopharmaceutics,* 64**,** 115-126.

Karavas, E., Ktistis, G., Xenakis, A. & Georgarakis, E. 2006b. "Effect of hydrogen bonding interactions on the release mechanism of felodipine from nanodispersions with polyvinylpyrrolidone". *European Journal of Pharmaceutics and Biopharmaceutics,* 63**,** 103-114.

Karin Janssen, P. R. W., B App Sci; Charles Geerlings, PharmD; Jan Pieter Schouten, PharmD, MBM 2009. "Chemical stability of a solution of bupivacaine hydrochloride 0.125% and sufentanil citrate 0.5 µg/mL for filling syringes using a repeater pump". *EJHP Science* 15 11-14.

Kassem, M. A. A., ElMeshad, A. N. & Fares, A. R. 2014. "Enhanced bioavailability of buspirone hydrochloride via cup and core buccal tablets: Formulation and in vitro/in vivo evaluation". *International Journal of Pharmaceutics,* 463**,** 68-80.

Kaur, J., Aggarwal, G., Singh, G. & Rana, A. C. 2012. *Improvement of drug solubility using solid dispersion*, International Journal of Pharmacy and Pharmaceutical Sciences. 4 (2) (pp 47-53), 2012. Date of Publication: 2012.

Kaushal, A. M., Gupta, P. & Bansal, A. K. 2004. "Amorphous drug delivery systems: molecular aspects, design, and performance". *Crit Rev Ther Drug Carrier Syst,* 21**,** 133-93.

Kawakami, K. 2009. "Current Status of Amorphous Formulation and Other Special Dosage Forms as Formulations for Early Clinical Phases". *Journal of Pharmaceutical Sciences,* 98**,** 2875-2885.

Kawase, Y., Uehara, S. & Nasu, S. 1990. "Dynamical observation of the structure change at the melting point of indium metal by a time-differential perturbed angular correlation method". *J. Non-Cryst. Solids,* 117-118**,** 76-9.

Kazarian, S. G. & Chan, K. L. A. 2013. "ATR-FTIR spectroscopic imaging: recent advances and applications to biological systems". *Analyst,* 138**,** 1940-1951.

Kerc, J. & Srcic, S. 1995. "Thermal-analysis of glassy pharmaceuticals". *Thermochimica Acta,* 248**,** 81-95.

Khougaz, K. & Clas, S.-D. 2000. "Crystallization inhibition in solid dispersions of MK-0591 and poly(vinylpyrrolidone) polymers". *Journal of Pharmaceutical Sciences,* 89**,** 1325-1334.

Kim, A. I., Akers, M. J. & Nail, S. L. 1998. "The physical state of mannitol after freeze-drying: Effects of mannitol concentration, freezing rate, and a noncrystallizing cosolute". *Journal of Pharmaceutical Sciences,* 87**,** 931-935.

Kraemer, J., Gajendran, J., Guillot, A., Schichtel, J. & Tuereli, A. 2012. "Dissolution testing of orally disintegrating tablets". *Journal of Pharmacy and Pharmacology,* 64**,** 911-918.

Kulkarni, U., Mahalingam, R., Pather, S. I., Li, X. & Jasti, B. 2009. "Pharmaceutics, preformulation and drug delivery porcine buccal mucosa as an in vitro model: Relative contribution of epithelium and connective tissue as permeability barriers". *Journal of Pharmaceutical Sciences,* 98**,** 471-483.

Kumar, A., Sahoo, S. K., Padhee, K., Kochar, P. P. S., Satapathy, A. & Pathak, N. 2011. "Review on solubility enhancement techniques for hydrophobic drugs". *Pharm. Globale,* 2**,** No pp. given.

Kuminek, G., Tagliari, M. P., Granada, A., Bertol, C. D., Langassner, S. Z., Segatto Silva, M. A. & Stulzer, H. K. 2010. "Development and validation of a rapid and simple stability-indicating lc method for nifedipine". *Journal of Liquid Chromatography & Related Technologies,* 33**,** 1601-1611.

Kushida, I. 2012. "Quantitative crystallinity determination for E1010, a novel carbapenem antibiotic, using differential scanning calorimetry". *Journal of Pharmacy and Pharmacology,* 64**,** 366-371.

Kuu, W. Y., Hardwick, L. A. & Akers, M. J. 2005. "Correlation of laboratory and production freeze drying cycles". *International Journal of Pharmaceutics,* 302**,** 56-67.

Laidler, K. J. 1987. *Chemical kinetics,* New York, Harper & Row.

Lam, J. K. W., Xu, Y., Worsley, A. & Wong, I. C. K. 2014. "Oral transmucosal drug delivery for pediatric use". *Advanced Drug Delivery Reviews,* 73**,** 50-62.

Lee, J. 2005. "Intrinsic adhesion properties of poly (vinyl pyrrolidone) to pharmaceutical materials: humidity effect". *Macromolecular bioscience,* 5**,** 1085-1093.

Legendre, B. & Sghaier, M. 2011. "Curie temperature of nickel". *Journal of Thermal Analysis and Calorimetry,* 105**,** 141-143.

Leucuta, S. E. 2014. "Selecting oral bioavailability enhancing formulations during drug discovery and development". *Expert Opin Drug Discov,* 9**,** 139-50.

Leuner, C. & Dressman, J. 2000. "Improving drug solubility for oral delivery using solid dispersions". *Eur J Pharm Biopharm,* 50**,** 47-60.

Levy, G. 1963. "Effect of particle size on dissolution and gastrointestinal absorption rates of pharmaceuticals". *Am J Pharm Sci Support Public Health,* 135**,** 78-92.

Li, C. & Deng, Y. 2004. "A novel method for the preparation of liposomes: freeze drying of monophase solutions". *Journal of pharmaceutical sciences,* 93**,** 1403-1414.

Lindenberg, M., Kopp, S. & Dressman, J. B. 2004. "Classification of orally administered drugs on the World Health Organization Model list of Essential Medicines according to the biopharmaceutics classification system". *European Journal of Pharmaceutics and Biopharmaceutics,* 58**,** 265-278.

Liu, P., De Wulf, O., Laru, J., Heikkila, T., van Veen, B., Kiesvaara, J., Hirvonen, J., Peltonen, L. & Laaksonen, T. 2013. "Dissolution Studies of Poorly Soluble Drug Nanosuspensions in Non-sink Conditions". *Aaps Pharmscitech,* 14**,** 748-756.

Liu, R. 2008. *Water-insoluble drug formulation,* Boca Raton, FL, CRC Press.

Lloyd, G. R., Craig, D. Q. M. & Smith, A. 1999. "A calorimetric investigation into the interaction between paracetamol and polyethlene glycol 4000 in physical mixes and solid dispersions". *European Journal of Pharmaceutics and Biopharmaceutics,* 48**,** 59-65.

Loftsson, T. 1998. "Increasing the cyclodextrin complexation of drugs and drug biovailability through addition of water-soluble polymers". *Pharmazie,* 53**,** 733-40.

Loftsson, T. & Brewster, M. E. 1996. "Pharmaceutical applications of cyclodextrins .1. Drug solubilization and stabilization". *Journal of Pharmaceutical Sciences,* 85**,** 1017-1025.

Ltd, L. S. 2014. OPERATING INSTRUCTIONS LTE Product: LYOTRAP FREEZE DRYING MACHINE Cat No: LF/LYO/01/1. 6 ed.

Lu, X. & Weiss, R. A. 1992. "Relationship between the glass-transition temperature and the interaction parameter of miscible binary polymer blends". *Macromolecules,* 25**,** 3242-3246.

Mackenzie, A. P. 1966. "Basic principles of freeze-drying for pharmaceuticals". *Bull Parenter Drug Assoc,* 20**,** 101-30.

Majerik, V., Charbit, G., Badens, E., Horvath, G., Szokonya, L., Bosc, N. & Teillaud, E. 2007. "Bioavailability enhancement of an active substance by supercritical antisolvent precipitation". *Journal of Supercritical Fluids,* 40**,** 101-110.

Malik, K., Arora, G. & Singh, I. 2012a. "Ocimum sanctum seeds, a natural superdisintegrant: Formulation and evaluation of fast melt tablets of nimesulide". *Polim Med,* 42**,** 49-59.

Malik, K., Arora, G. & Singh, I. 2012b. "Ocimum Sanctum seeds, a natural superdisintegrant: formulation and evaluation of fast melt tablets of nimesulide". *Polimery w medycynie,* 42**,** 49-59.

Marsac, P. J., Li, T. & Taylor, L. S. 2009. "Estimation of Drug-Polymer Miscibility and Solubility in Amorphous Solid Dispersions Using Experimentally Determined Interaction Parameters". *Pharm. Res.,* 26**,** 139-151.

Marsac, P. J., Shamblin, S. L. & Taylor, L. S. 2006. "Theoretical and Practical Approaches for Prediction of Drug-Polymer Miscibility and Solubility". *Pharm. Res.,* 23**,** 2417-2426.

Marwaha, M., Sandhu, D. & Marwaha, R. K. 2010. "Coprocessing of excipients: a review on excipient development for improved tabletting performance". *Int. J. Appl. Pharm.,* 2**,** 41-47.

Massi-Benedetti, M. 2003. "Glimerpiride in type 2 diabetes mellitus: A review of the worldwide therapeutic experience". *Clinical therapeutics,* 25**,** 799-816.

Matsumoto, T. & Zografi, G. 1999a. "Physical properties of solid molecular dispersions of indomethacin with poly(vinylpyrrolidone) and poly(vinylpyrrolidone-co-vinyl-acetate) in relation to indomethacin crystallization". *Pharm. Res.,* 16**,** 1722-1728.

Matsumoto, T. & Zografi, G. 1999b. "Physical properties of solid molecular dispersions of indomethacin with poly(vinylpyrrolidone) and poly(vinylpyrrolidone-co-vinylacetate) in relation to indomethacin crystallization". *Pharmaceutical Research,* 16**,** 1722-1728.

Mayersoh.M & Gibaldi, M. 1966. "New Method of Solid-State Dispersion for Increasing Dissolution Rates". *Journal of Pharmaceutical Sciences,* 55**,** 1323-&.

Maynard, R. L. 1997. "The Merck Index: 12th edition 1996". *Occupational and Environmental Medicine,* 54**,** 288-288.

Mazzobre, M. F., Aguilera, J. M. & Buera, M. P. 2003. "Microscopy and calorimetry as complementary techniques to analyze sugar crystallization from amorphous systems". *Carbohydrate Research,* 338**,** 541-548.

McDermott, C. & Collins, N. C. 2012. "Prehospital medication administration: a randomised study comparing intranasal and intravenous routes". *Emergency medicine international,* 2012**,** 476161-476161.

McGregor, D. 2010. "Tertiary-Butanol: A toxicological review". *Critical Reviews in Toxicology,* 40**,** 697-727.

McPhillips, H., Craig, D. Q. M., Royall, P. G. & Hill, V. L. 1999. "Characterisation of the glass transition of HPMC using modulated temperature differential scanning calorimetry". *International Journal of Pharmaceutics,* 180**,** 83-90.

Mehta, A. C., Hartdavies, S. & Kay, E. A. 1995. "In-Vitro Dissolution Studies on Nifedipine Capsules". *Journal of Clinical Pharmacy and Therapeutics,* 20**,** 243-245.

Mehta, K. A., Kislalioglu, M. S., Phuapradit, W., Malick, A. W. & Shah, N. H. 2002. "Multi-unit controlled release systems of nifedipine and nifedipine : Pluronic (R) f-68 solid dispersions: Characterization of release mechanisms". *Drug Development and Industrial Pharmacy,* 28**,** 275-285.

Meng, F., Dave, V. & Chauhan, H. 2015. "Qualitative and quantitative methods to determine miscibility in amorphous drug-polymer systems". *European journal of pharmaceutical sciences : official journal of the European Federation for Pharmaceutical Sciences,* 77**,** 106-11.

Meryman, H. T. 1976. "Historical recollections of freeze-drying". *Developments in biological standardization,* 36**,** 29-32.

MHRA. 2013. *Proposal to Allow Wider Access to Naloxone for Use in Emergencies* [Online]. www.gov.uk. Available: https://www.gov.uk/government/consultations/proposal-to-allow-wider-access-to-naloxone-for-use-in-emergencies 2015].

MHRA. 2014a. *Medicines and Healthcare Products Regulatory Agency* [Online]. Available: http://www.mhra.gov.uk/#page=DynamicListMedicines [Accessed 01/10/2014 2014].

MHRA, T. B. P. C. S. o. t. 2014b. *The British Pharmacopoeia, 2014*, The Stationery Office.

Milanovic, L., Bosch, H. A. & Hoover, W. G. 1998. ""What is liquid'? Understanding the states of matter". *Molecular Physics,* 95**,** 281-287.

Miyazaki, T., Yoshioka, S., Aso, Y. & Kawanishi, T. 2007. "Crystallization rate of amorphous nifedipine analogues unrelated to the glass transition temperature". *International Journal of Pharmaceutics,* 336**,** 191-195.

Miyazaki, T., Yoshioka, S., Aso, Y. & Kojima, S. 2004. "Ability of polyvinylpyrrolidone and polyacrylic acid to inhibit the crystallization of amorphous acetaminophen". *J. Pharm. Sci.,* 93**,** 2710-2717.

Moore, R. J., Watts, J. T. F., Hood, J. A. A. & Burritt, D. J. 1999. "Intra-oral temperature variation over 24 hours". *European Journal of Orthodontics,* 21**,** 249-261.

Mostafavi, A., Abedi, G., Jamshidi, A., Afzali, D. & Talebi, M. 2009. "Development and validation of a HPLC method for the determination of buprenorphine hydrochloride,

naloxone hydrochloride and noroxymorphone in a tablet formulation". *Talanta,* 77**,** 1415-1419.

Mueller, K., Figueroa, C., Martinez, C., Medel, M., Obreque, E., Pena-Neira, A., Morales-Bozo, I., Toledo, H. & Lopez-Solis, R. O. 2010. "Measurement of saliva volume in the mouth of members of a trained sensory panel using a beetroot (Beta vulgaris) extract". *Food Quality and Preference,* 21**,** 569-574.

Muller, R. H., Jacobs, C. & Kayser, O. 2000. "Nanosuspensions for the formulation of poorly soluble drugs". *Drugs Pharm. Sci.,* 105**,** 383-407.

Mullin, J. W. 2001. *Crystallization*, Butterworth-Heinemann.

Murphy, D. M. & Koop, T. 2005. "Review of the vapour pressures of ice and supercooled water for atmospheric applications". *Quarterly Journal of the Royal Meteorological Society,* 131**,** 1539-1565.

Nainar, S., Rajiah, K., Angamuthu, S., Prabakaran, D. & Kasibhatta, R. 2012. "Biopharmaceutical Classification System in Invitro/In-vivo Correlation: Concept and Development Strategies in Drug Delivery". *Tropical Journal of Pharmaceutical Research,* 11**,** 319-329.

Najib, N. M., Suleiman, M. & Malakh, A. 1986. "Characteristics of the invitro release of ibuprofen from polyvinylpyrrolidone solid dispersions". *International Journal of Pharmaceutics,* 32**,** 229-236.

Ni, N., Tesconi, M., Tabibi, E. S., Gupta, S. & Yalkowsky, S. H. 2001. "Use of pure t-butanol as a solvent for freeze-drying: a case study". *International Journal of Pharmaceutics,* 226**,** 39-46.

Noyes, A. A. & Whitney, W. R. 1897. "The rate of solution of solid substances in their own solutions". *J. Am. Chem. Soc.,* 19**,** 930-4.

NSF-Toxicology-Services. 2003. *t-BUTANOL oral risk assesment document* [Online]. NSF International. Available: http://www.documents.dgs.ca.gov/bsc/pex/exibit_nsf_t_butanol.pdf [Accessed 01-05-2014 2014].

Nunes, C., Suryanarayanan, R., Botez, C. E. & Stephens, P. W. 2004. "Characterization and crystal structure of D-mannitol hemihydrate". *Journal of Pharmaceutical Sciences,* 93**,** 2800-2809.

Oesterle, J., Franks, F. & Auffret, T. 1998. "The influence of tertiary butyl alcohol and volatile salts on the sublimation of ice from frozen sucrose solutions: implications for freeze-drying". *Pharmaceutical development and technology,* 3**,** 175-83.

Ohara, T., Kitamura, S., Kitagawa, T. & Terada, K. 2005. "Dissolution mechanism of poorly water-soluble drug from extended release solid dispersion system with ethylcellulose and hydroxypropylmethylcellulose". *International Journal of Pharmaceutics,* 302**,** 95-102.

Opie, L. H. 1987. "Calcium channel antagonists, part I: fundamental properties: mechanisms, classification, sites of action". *Cardiovasc. Drugs Ther.,* 1**,** 411-30.

Ozaki, S., Kushida, I., Yamashita, T., Hasebe, T., Shirai, O. & Kano, K. 2012. "Evaluation of drug supersaturation by thermodynamic and kinetic approaches for the prediction of oral absorbability in amorphous pharmaceuticals". *Journal of Pharmaceutical Sciences,* 101**,** 4220-4230.

Papadimitriou, S. A., Barmpalexis, P., Karavas, E. & Bikiaris, D. N. 2012. "Optimizing the ability of PVP/PEG mixtures to be used as appropriate carriers for the preparation of drug solid dispersions by melt mixing technique using artificial neural networks: I". *European Journal of Pharmaceutics and Biopharmaceutics,* 82**,** 175-186.

Patel, V. F., Liu, F. & Brown, M. B. 2011. "Advances in oral transmucosal drug delivery". *Journal of Controlled Release,* 153**,** 106-116.

Patel, V. F., Liu, F. & Brown, M. B. 2012. "Modeling the oral cavity: in vitro and in vivo evaluations of buccal drug delivery systems". *J Control Release,* 161**,** 746-56.

Paterson, A. H. J., Ripberger, G. D. & Bridges, R. P. 2015. "Measurement of the viscosity of freeze dried amorphous lactose near the glass transition temperature". *International Dairy Journal,* 43**,** 27-32.

Pather, S. I., Rathbone, M. J. & Senel, S. 2008. "Current status and the future of buccal drug delivery systems". *Expert Opinion on Drug Delivery,* 5**,** 531-542.

Patil, H., Tiwari, R. V. & Repka, M. A. 2015. "Hot-melt extrusion: from theory to application in pharmaceutical formulation". *AAPS PharmSciTech***,** 1-23.

Patravale, V. B., Date, A. A. & Kulkarni, R. M. 2004. "Nanosuspensions: a promising drug delivery strategy". *J Pharm Pharmacol,* 56**,** 827-40.

Pikal, M. J. 1993. "Freeze-Drying of Proteins - Process, Formulation and Stability". *Abstracts of Papers of the American Chemical Society,* 205**,** 144-BIOT.

Pikal, M. J. 1994. "Freeze-Drying of Proteins - Process, Formulation, and Stability". *Formulation and Delivery of Proteins and Peptides,* 567**,** 120-133.

Pikal, M. J., Roy, M. L. & Shah, S. 1984. "Mass and heat transfer in vial freeze-drying of pharmaceuticals: role of the vial". *J Pharm Sci,* 73**,** 1224-37.

Pikal, M. J. & Shah, S. 1990. "The Collapse Temperature in Freeze-Drying - Dependence on Measurement Methodology and Rate of Water Removal from the Glassy Phase". *International Journal of Pharmaceutics,* 62**,** 165-186.

Pikal, M. J. & Shah, S. 1997. "Intravial distribution of moisture during the secondary drying stage of freeze drying". *PDA J Pharm Sci Technol,* 51**,** 17-24.

Pikal, M. J., Shah, S., Roy, M. L. & Putman, R. 1990. "THE SECONDARY DRYING STAGE OF FREEZE-DRYING - DRYING KINETICS AS A FUNCTION OF TEMPERATURE AND CHAMBER PRESSURE". *International Journal of Pharmaceutics,* 60**,** 203-217.

Pikal, M. J., Shah, S., Senior, D. & Lang, J. E. 1983. "Physical-Chemistry of Freeze-Drying - Measurement of Sublimation Rates for Frozen Aqueous-Solutions by a Microbalance Technique". *Journal of Pharmaceutical Sciences,* 72**,** 635-650.

Popović, G., Čakar, M. & Agbaba, D. 2009. "Acid–base equilibria and solubility of loratadine and desloratadine in water and micellar media". *Journal of Pharmaceutical and Biomedical Analysis,* 49**,** 42-47.

Potter, H. & Hulm, M. 1988. "Assay of nifedipine and its by-product and degradation product in the drug substance and dragees by liquid-chromatography on formamide-saturated silica-gel columns". *Journal of Pharmaceutical and Biomedical Analysis,* 6**,** 115-119.

Pouton, C. W. 2006. "Formulation of poorly water-soluble drugs for oral administration: physicochemical and physiological issues and the lipid formulation classification system". *Eur J Pharm Sci,* 29**,** 278-87.

Prabhu, S., Ortega, M. & Ma, C. 2005. "Novel lipid-based formulations enhancing the in vitro dissolution and permeability characteristics of a poorly water-soluble model drug, piroxicam". *International Journal of Pharmaceutics,* 301**,** 209-216.

Preston, K. L., Bigelow, G. E. & Liebson, I. A. 1990. "Effects of sublingually given naloxone in opioid-dependent human volunteers". *Drug and Alcohol Dependence,* 25**,** 27-34.

PubChem. 2005. *Naloxone HCl CID=5464092* [Online]. PubChem Compound Database: National Center for Biotechnology Information. Available: https://pubchem.ncbi.nlm.nih.gov/compound/Naloxone_hydrochloride#section=Top [Accessed 12-12-2015 2015].

Quilaqueo, M. & Aguilera, J. M. 2015. "Dissolution of NaCl crystals in artificial saliva and water by video-microscopy". *Food Research International,* 69**,** 373-380.

Raina, S. A., Alonzo, D. E., Zhang, G. G. Z., Gao, Y. & Taylor, L. S. 2014. "Impact of Polymers on the Crystallization and Phase Transition Kinetics of Amorphous Nifedipine during Dissolution in Aqueous Media". *Molecular Pharmaceutics,* 11**,** 3565-3576.

Rasenack, N. & Muller, B. W. 2002. "Crystal habit and tableting behavior". *International Journal of Pharmaceutics,* 244**,** 45-57.

Raudonus, J., Bernard, J., Janssen, H., Kowalczyk, J. & Carle, R. 2000. "Effect of oligomeric or polymeric additives on glass transition, viscosity and crystallization of amorphous isomalt". *Food Res. Int.,* 33**,** 41-51.

Ray, C., Arora, V. & Sharma, V. 2011. "Fast Dissolving Tablets-A Novel Drug Delivery System for Pediatric & Geriatric Patient". *International Bulletin of Drug Research,* 1**,** 55-70.

Reddy, B. B. K. & Karunakar, A. 2011. "Biopharmaceutics classification system: a regulatory approach". *Dissolution Technologies,* 18**,** 31-37.

Roudaut, G., Simatos, D., Champion, D., Contreras-Lopez, E. & Le Meste, M. 2004. "Molecular mobility around the glass transition temperature: a mini review". *Innovative Food Science & Emerging Technologies,* 5**,** 127-134.

Roy, I. & Gupta, M. N. 2004. "Freeze-drying of proteins: some emerging concerns". *Biotechnology and applied biochemistry,* 39**,** 165-177.

Roy, M. L. & Pikal, M. J. 1989. "Process-control in freeze-drying - determination of the end-point of sublimation drying by an electronic moisture sensor". *Journal of Parenteral Science and Technology,* 43**,** 60-66.

Royall, P. G., Craig, D. Q. M. & Doherty, C. 1998. "Characterisation of the glass transition of an amorphous drug using modulated DSC". *Pharmaceutical Research,* 15**,** 1117-1121.

Royall, P. G., Craig, D. Q. M. & Doherty, C. 1999. "Characterisation of moisture uptake effects on the glass transitional behaviour of an amorphous drug using modulated temperature DSC". *International Journal of Pharmaceutics,* 192**,** 39-46.

Royall, P. G., Kett, V. L., Andrews, C. S. & Craig, D. Q. M. 2001. "Identification of crystalline and amorphous regions in low molecular weight materials using microthermal analysis". *Journal of Physical Chemistry B,* 105**,** 7021-7026.

Rumondor, A. C. F., Marsac, P. J., Stanford, L. A. & Taylor, L. S. 2009. "Phase Behavior of Poly(vinylpyrrolidone) Containing Amorphous Solid Dispersions in the Presence of Moisture". *Molecular Pharmaceutics,* 6**,** 1492-1505.

Sankar, V., Hearnden, V., Hull, K., Juras, D. V., Greenberg, M. S., Kerr, A. R., Lockhart, P. B., Patton, L. L., Porter, S. & Thornhill, M. 2011. "Local drug delivery for oral mucosal diseases: challenges and opportunities". *Oral Diseases,* 17**,** 73-84.

Santivarangkna, C., Aschenbrenner, M., Kulozik, U. & Foerst, P. 2011. "Role of Glassy State on Stabilities of Freeze-Dried Probiotics". *Journal of Food Science,* 76**,** R152-R156.

Sastry, S. V., Nyshadham, J. R. & Fix, J. A. 2000. "Recent technological advances in oral drug delivery - a review". *Pharm Sci Technolo Today,* 3**,** 138-145.

Sattar, M., Sayed, O. M. & Lane, M. E. 2014. "Oral transmucosal drug delivery - Current status and future prospects". *International Journal of Pharmaceutics,* 471**,** 498-506.

Savjani, K. T., Gajjar, A. K. & Savjani, J. K. 2012. "Drug solubility: importance and enhancement techniques". *ISRN pharmaceutics,* 2012.

Schug, B. S., Brendel, E., Wolf, D., Wonnemann, M., Wargenau, M. & Blume, H. H. 2002. "Formulation-dependent food effects demonstrated for nifedipine modified-release preparations marketed in the European Union". *European Journal of Pharmaceutical Sciences,* 15**,** 279-285.

Seager, H. 1998. "Drug-delivery products and the Zydis fast-dissolving dosage form". *J Pharm Pharmacol,* 50**,** 375-82.

Sekiguchi, K. & Obi, N. 1961. "Studies on Absorption of Eutectic Mixture .1. Comparison of Behavior of Eutectic Mixture of Sulfathiazole and That of Ordinary Sulfathiazole in Man". *Chemical & Pharmaceutical Bulletin,* 9**,** 866-+.

Sekiguchi, K., Ueda, Y. & Obi, N. 1964. "Studies on Absorption of Eutectic Mixture .2. Absorption of Fused Conglomerates of Chloramphenicol + Urea in Rabbits". *Chemical & Pharmaceutical Bulletin,* 12**,** 134-+.

Seo, J.-A., Kim, S., Kwon, H.-J., Yang, Y., Kim, H. K. & Hwang, Y.-H. 2006. "The glass transition temperatures of sugar mixtures". *Carbohydrate research,* 341**,** 2516-2520.

Shah, B., Kakumanu, V. K. & Bansal, A. K. 2006. "Analytical techniques for quantification of amorphous/crystalline phases in pharmaceutical solids". *Journal of Pharmaceutical Sciences,* 95**,** 1641-1665.

Shah, V. P., Tsong, Y., Sathe, P. & Liu, J.-P. 1998. "In vitro dissolution profile comparison—statistics and analysis of the similarity factor, f2". *Pharmaceutical research,* 15**,** 889-896.

Shalaeva, M., Kenseth, J., Lombardo, F. & Bastin, A. 2008. "Measurement of dissociation constants (pKa values) of organic compounds by multiplexed capillary electrophoresis using aqueous and cosolvent buffers". *J. Pharm. Sci.,* 97**,** 2581-2606.

Shamblin, S. L., Huang, E. Y. & Zografi, G. 1996. "The effects of co-lyophilized polymeric additives on the glass transition temperature and crystallization of amorphous sucrose". *J. Therm. Anal.,* 47**,** 1567-1579.

Shamblin, S. L. & Zografi, G. 1999. "The effects of absorbed water on the properties of amorphous mixtures containing sucrose". *Pharm. Res.,* 16**,** 1119-1124.

Shang, C., Sinka, I. C., Jayaraman, B. & Pan, J. 2013. "Break force and tensile strength relationships for curved faced tablets subject to diametrical compression". *International Journal of Pharmaceutics,* 442**,** 57-64.

Simmons, C. T. 2008. "Henry Darcy (1803-1858): Immortalised by his scientific legacy". *Hydrogeology Journal,* 16**,** 1023-1038.

Simonelli, A. P., Mehta, S. C. & Higuchi, W. I. 1969. "Dissolution rates of high energy polyvinylpyrrolidone (PVP)-sulfathiazole coprecipitates". *J Pharm Sci,* 58**,** 538-49.

Singh, P., Guillory, J. K., Sokolosk.Td, Benet, L. Z. & Bhatia, V. N. 1966. "Effect of inert tablet ingredients on drug absorption .1. Effect of polyethylene glycol 4000 on interestinal absorption of 4 barbiturates". *Journal of Pharmaceutical Sciences,* 55**,** 63-&.

Smith, E. B. 1982. *Basic chemical thermodynamics,* Oxford, Clarendon Press.

Snider, M. E., Nuzum, D. S. & Veverka, A. 2008. "Long-acting nifedipine in the management of the hypertensive patient". *Vasc. Health Risk Manage.,* 4**,** 1249-1257.

Soltanpour, S., Zohrabi, F. & Bastami, Z. 2014. "Thermodynamic solubility of pioglitazone HCl in polyethylene glycols 200, 400 or 600 + water mixtures at 303.2 and 308.2 K—Data report and modeling". *Fluid Phase Equilibria,* 379**,** 180-184.

Srinarong, P., Kouwen, S., Visser, M. R., Hinrichs, W. L. J. & Frijlink, H. W. 2010. "Effect of drug-carrier interaction on the dissolution behavior of solid dispersion tablets". *Pharmaceutical Development and Technology,* 15**,** 460-468.

Stone, A. J. & Editor 1996. *The Theory of Intermolecular Forces*, Oxford Univ Press.

Strang, J., Bird, S. M. & Parmar, M. K. B. 2013. "Take-Home Emergency Naloxone to Prevent Heroin Overdose Deaths after Prison Release: Rationale and Practicalities for the N-ALIVE Randomized Trial". *Journal of Urban Health-Bulletin of the New York Academy of Medicine,* 90**,** 983-996.

Strang, J., McDonald, R., Alqurshi, A., Royall, P. G., Taylor, D. & Forbes, B. submitted. "Naloxone without the needle – structured review of potential non-injectable routes, the consequent rationale for, and next steps in development of new nasal and buccal naloxone formulations". *Drug and alcohol dependence*.

Streubel, A., Siepmann, J. & Bodmeier, R. 2006. "Drug delivery to the upper small intestine window using gastroretentive technologies". *Curr Opin Pharmacol,* 6**,** 501-8.

Strickley, R. G., Iwata, Q., Wu, S. & Dahl, T. C. 2008. "Pediatric drugs—a review of commercially available oral formulations". *Journal of pharmaceutical sciences,* 97**,** 1731-1774.

Struik, L. C. E. 1977. *Physical aging in amorphous polymers and other materials.* TU Delft, Delft University of Technology.

Sudhakar, Y., Kuotsu, K. & Bandyopadhyay, A. K. 2006. "Buccal bioadhesive drug delivery - A promising option for orally less efficient drugs". *Journal of Controlled Release,* 114**,** 15-40.

Sugawara, M., Kadomura, S., He, X., Takekuma, Y., Kohri, N. & Miyazaki, K. 2005. "The use of an in vitro dissolution and absorption system to evaluate oral absorption of two weak

bases in pH-independent controlled-release formulations". *European Journal of Pharmaceutical Sciences,* 26**,** 1-8.

Sun, C. C. 2009. "Materials Science Tetrahedron-A Useful Tool for Pharmaceutical Research and Development". *Journal of Pharmaceutical Sciences,* 98**,** 1671-1687.

Surana, R., Pyne, A. & Suryanarayanan, R. 2004. "Effect of preparation method on physical properties of amorphous trehalose". *Pharmaceutical research,* 21**,** 1167-1176.

Tachibana, T. & Nakamura, A. 1965. "A method of preparing an aqueous colloidal dispersion of organic materials by using water-soluble polymers: dispersion of β-carotene by poly(vinylpyrrolidinone)". *Kolloid-Z.,* 203**,** 130-3.

Tan, J. Z. Y. & Kwan, Y. H. 2014. "Stability of chronic medicines in dosage administration aids. How much have been done?". *Saudi Pharmaceutical Journal*.

Tanaka, N., Imai, K., Okimoto, K., Ueda, S., Tokunaga, Y., Ibuki, R., Higaki, K. & Kimura, T. 2006. "Development of novel sustained-release system, disintegration-controlled matrix tablet (DCMT) with solid dispersion granules of nilvadipine (II): in vivo evaluation". *Journal of Controlled Release,* 112**,** 51-6.

Tang, X. & Pikal, M. J. 2004. "Design of freeze-drying processes for pharmaceuticals: practical advice". *Pharm Res,* 21**,** 191-200.

Teagarden, D. L. & Baker, D. 2004. "Practical aspects of freeze-drying of pharmaceutical and biological products using non-aqueous co-solvent systems". *Drugs and the pharmaceutical sciences,* 137**,** 239-276.

Teagarden, D. L. & Baker, D. S. 2002a. "Practical aspects of lyophilization using non-aqueous co-solvent systems". *Eur. J. Pharm. Sci.,* 15**,** 115-133.

Teagarden, D. L. & Baker, D. S. 2002b. "Practical aspects of lyophilization using non-aqueous co-solvent systems". *European Journal of Pharmaceutical Sciences,* 15**,** 115-133.

Technologies, A. 1999. *Agilent 1100 Series HPLC Value System User's Guide* [Online]. https://www.agilent.com/cs/library/usermanuals/Public/G1380-90000.pdf: Agilent Technologies Available: https://www.agilent.com/cs/library/usermanuals/Public/G1380-90000.pdf.

Telang, C., Suryanarayanan, R. & Yu, L. 2003. "Crystallization of D-mannitol in binary mixtures with NaCl: Phase diagram and polymorphism". *Pharmaceutical Research,* 20**,** 1939-1945.

Tenjarla, S., Puranajoti, P., Kasina, R. & Mandal, T. 1998. "Preparation, Characterization, and Evaluation of Miconazole-Cyclodextrin Complexes for Improved Oral and Topical Delivery". *J. Pharm. Sci.,* 87**,** 425-429.

Thakkar, A. L., Hirsch, C. A. & Page, J. G. 1977. "Solid dispersion approach for overcoming bioavailability problems due to polymorphism of nabilone, a cannabinoid derivative". *J. Pharm. Pharmacol.,* 29**,** 783-4.

Thomas, V. H., Bhattachar, S., Hitchingham, L., Zocharski, P., Naath, M., Surendran, N., Stoner, C. L. & El-Kattan, A. 2006. "The road map to oral bioavailability: an industrial perspective". *Expert Opinion on Drug Metabolism & Toxicology,* 2**,** 591-608.

Tixier, C., Singer, H. P., Oellers, S. & Müller, S. R. 2003. "Occurrence and fate of carbamazepine, clofibric acid, diclofenac, ibuprofen, ketoprofen, and naproxen in surface waters". *Environmental science & technology,* 37**,** 1061-1068.

Torrado, S., Torrado, S., Torrado, J. J. & Cadorniga, R. 1996. "Preparation, dissolution and characterization of albendazole solid dispersions". *International Journal of Pharmaceutics,* 140**,** 247-250.

Trasi, N. S., Baird, J. A., Kestur, U. S. & Taylor, L. S. 2014. "Factors Influencing Crystal Growth Rates from Undercooled Liquids of Pharmaceutical Compounds". *J. Phys. Chem. B,* 118**,** 9974-9982.

Tropin, T. V., Schmelzer, J. W. P. & Schick, C. 2011. "On the dependence of the properties of glasses on cooling and heating rates I. Entropy, entropy production, and glass transition temperature". *Journal of Non-Crystalline Solids,* 357**,** 1291-1302.

Tsinontides, S. C., Rajniak, P., Pham, D., Hunke, W. A., Placek, J. & Reynolds, S. D. 2004. "Freeze drying - principles and practice for successful scale-up to manufacturing". *International Journal of Pharmaceutics,* 280**,** 1-16.

Tsukushi, I., Yamamuro, O. & Suga, H. 1994. "Heat capacities and glass transitions of ground amorphous solid and liquid-quenched glass of tri-O-methyl-ß-cyclodextrin". *Journal of Non-Crystalline Solids,* 175**,** 187-194.

Urbanetz, N. A. 2006. "Stabilization of solid dispersions of nimodipine and polyethylene glycol 2000". *Eur J Pharm Sci,* 28**,** 67-76.

Van den Mooter, G. 2012. "The use of amorphous solid dispersions: A formulation strategy to overcome poor solubility and dissolution rate". *Drug Discovery Today: Technologies,* 9**,** e79-e85.

van den Mooter, G., Weuts, I., De Ridder, T. & Blaton, N. 2006. "Evaluation of Inutec SP1 as a new carrier in the formulation of solid dispersions for poorly soluble drugs". *International Journal of Pharmaceutics,* 316**,** 1-6.

van Dooren, A. A. & Müller, B. W. 1984. "Purity determinations of drugs with differential scanning calorimetry (DSC)—a critical review". *International Journal of Pharmaceutics,* 20**,** 217-233.

van Drooge, D. J., Hinrichs, W. L. J., Visser, M. R. & Frijlink, H. W. 2006. "Characterization of the molecular distribution of drugs in glassy solid dispersions at the nano-meter scale, using differential scanning calorimetry and gravimetric water vapour sorption techniques". *International Journal of Pharmaceutics,* 310**,** 220-229.

Varma, M. V. S., Kaushal, A. M., Garg, A. & Garg, S. 2004. "Factors Affecting Mechanism and Kinetics of Drug Release from Matrix-Based Oral Controlled Drug Delivery Systems". *American Journal of Drug Delivery,* 2**,** 43-57.

Vasconcelos, T., Sarmento, B. & Costa, P. 2007. "Solid dispersions as strategy to improve oral bioavailability of poor water soluble drugs". *Drug Discovery Today,* 12**,** 1068-1075.

Venables, R., Batchelor, H., Hodson, J., Stirling, H. & Marriott, J. 2015. "Determination of formulation factors that affect oral medicines acceptability in a domiciliary paediatric population". *International journal of pharmaceutics,* 480**,** 55-62.

Verma, S. & Rudraraju, V. 2015. "Wetting Kinetics: an Alternative Approach Towards Understanding the Enhanced Dissolution Rate for Amorphous Solid Dispersion of a Poorly Soluble Drug". *AAPS PharmSciTech***,** 1-12.

Vessot, S. & Andrieu, J. 2012. "A Review on Freeze Drying of Drugs with tert-Butanol (TBA) + Water Systems: Characteristics, Advantages, Drawbacks". *Drying Technol.,* 30**,** 377-385.

Vippagunta, S. R., Brittain, H. G. & Grant, D. J. W. 2001. "Crystalline solids". *Advanced Drug Delivery Reviews,* 48**,** 3-26.

Vippagunta, S. R., Maul, K. A., Tallavajhala, S. & Grant, D. J. W. 2002. "Solid-state characterization of nifedipine solid dispersions". *International Journal of Pharmaceutics,* 236**,** 111-123.

Vippagunta, S. R., Wang, Z. R., Hornung, S. & Krill, S. L. 2007. "Factors affecting the formation of eutectic solid dispersions and their dissolution behavior". *Journal of Pharmaceutical Sciences,* 96**,** 294-304.

Vogt, M., Kunath, K. & Dressman, J. B. 2008. "Dissolution enhancement of fenofibrate by micronization, cogrinding and spray-drying: Comparison with commercial preparations". *European Journal of Pharmaceutics and Biopharmaceutics,* 68**,** 283-288.

Wang, X., Michoel, A. & Van den Mooter, G. 2005. "Solid state characteristics of ternary solid dispersions composed of PVPVA64, Myrj 52 and itraconazole". *International Journal of Pharmaceutics,* 303**,** 54-61.

Weber, J. M., Tataris, K. L., Hoffman, J. D., Aks, S. E. & Mycyk, M. B. 2012. "Can nebulized naloxone be used safely and effectively by emergency medical services for suspected opioid overdose?". *Prehospital Emergency Care,* 16**,** 289-292.

White, G. W. & Cakebread, S. H. 1966. "The glassy state in certain sugar-containing food products *". *International Journal of Food Science & Technology,* 1**,** 73-82.

WHO. 2002. *Guidelines on packaging for pharmaceutical products* [Online]. http://www.who.int/medicines/areas/quality_safety/quality_assurance/GuidelinesPackagingPharmaceuticalProductsTRS902Annex9.pdf: WHO Technical Report Series. Available: http://www.who.int/medicines/areas/quality_safety/quality_assurance/GuidelinesPackagingPharmaceuticalProductsTRS902Annex9.pdf.

WHO. 2005. *Proposal to waive in vivo bioequivalence requirements for the who model list of essential medicines immediate release, solid oral dosage forms* [Online]. World Health Organization. Available: http://www.who.int/medicines/services/expertcommittees/pharmprep/QAS04_109Rev1_Waive_invivo_bioequiv.pdf [Accessed 04-12-2015 2015].

WHO. 2009. *Stability testing of active pharmaceutical ingredients and finished pharmaceutical products* [Online]. Available: http://apps.who.int/medicinedocs/en/d/Js19133en/953].

WHO. 2014. *Community management of opioid overdose* [Online]. Available: http://www.who.int/substance_abuse/publications/management_opioid_overdose/en/ [Accessed June 26 2015].

WHO. 2015. *The International Pharmacopoeia Fifth Edition* [Online]. WHO. Available: http://apps.who.int/phint/en/p/docf/ [Accessed 10-09-2015 2015].

Wittaya-Areekul, S., Needham, G. F., Milton, N., Roy, M. L. & Nail, S. L. 2002. "Freeze-drying of tert-butanol/water cosolvent systems: A case report on formation of a friable freeze-dried powder of tobramycin sulfate". *Journal of Pharmaceutical Sciences,* 91**,** 1147-1155.

Wu, J. X., Xia, D., van den Berg, F., Amigo, J. M., Rades, T., Yang, M. & Rantanen, J. 2012. "A novel image analysis methodology for online monitoring of nucleation and crystal growth during solid state phase transformations". *International Journal of Pharmaceutics,* 433**,** 60-70.

Wu, Y., Kildsig, D. O. & Ghaly, E. S. 2004. "Effect of hydrodynamic environment on tablets dissolution rate". *Pharmaceutical Development and Technology,* 9**,** 25-37.

Xia, D., Wu, J. X., Cui, F., Qu, H., Rades, T., Rantanen, J. & Yang, M. 2012. "Solvent-mediated amorphous-to-crystalline transformation of nitrendipine in amorphous particle suspensions containing polymers". *European Journal of Pharmaceutical Sciences,* 46**,** 446-454.

Xiao, H., Chi, Y. & Buekens, A. 2014. "Combustion Characteristics of Waste Printed Circuit Boards in Thermogravimetric Analyzers". *Environmental Progress & Sustainable Energy,* 33**,** 1105-1110.

Yalkowsky, S. H. & Dannenfelser, R. M. 1992. "Aquasol database of aqueous solubility". *College of Pharmacy, University of Arizona, Tucson, AZ*.

Yoshihashi, Y., Iijima, H., Yonemochi, E. & Terada, K. 2006. "Estimation of physical stability of amorphous solid dispersion using differential scanning calorimetry". *Journal of Thermal Analysis and Calorimetry,* 85**,** 689-692.

Yoshioka, M., Hancock, B. C. & Zografi, G. 1995. "Inhibition of Indomethacin Crystallization in Poly(vinylpyrrolidone) Coprecipitates". *J. Pharm. Sci.,* 84**,** 983-6.

Youn, Y. S., Jung, J. Y., Oh, S. H., Yoo, S. D. & Lee, K. C. 2006. "Improved intestinal delivery of salmon calcitonin by Lys(18)-amine specific PEGylation: Stability, permeability, pharmacokinetic behavior and in vivo hypocalcemic efficacy". *Journal of Controlled Release,* 114**,** 334-342.

Yu, L. 2001. "Amorphous pharmaceutical solids: preparation, characterization and stabilization". *Advanced drug delivery reviews,* 48**,** 27-42.

Yuan, X. D., Sperger, D. & Munson, E. J. 2014. "Investigating Miscibility and Molecular Mobility of Nifedipine-PVP Amorphous Solid Dispersions Using Solid-State NMR Spectroscopy". *Molecular Pharmaceutics,* 11**,** 329-337.

Yuksel, N., Kanik, A. E. & Baykara, T. 2000. "Comparison of in vitro dissolution profiles by ANOVA-based, model-dependent and -independent methods". *International Journal of Pharmaceutics,* 209**,** 57-67.

Zeng, X. M., Martin, G. P. & Marriott, C. 2001. "Effects of molecular weight of polyvinylpyrrolidone on the glass transition and crystallization of co-lyophilized sucrose". *Int. J. Pharm.,* 218**,** 63-73.

Zeuzem, S., Schmidt, J. M., Lee, J., Ruster, B. & Roth, W. K. 1996. "Effect of interferon alfa on the dynamics of hepatitis C virus turnover in vivo". *Hepatology,* 23**,** 366-371.

Zhang, G. G. Z., Law, D., Schmitt, E. A. & Qiu, Y. 2004. "Phase transformation considerations during process development and manufacture of solid oral dosage forms". *Advanced Drug Delivery Reviews,* 56**,** 371-390.

Zhurkovich, I., Rudenko, A., Chelovechkova, V., Merkusheva, I., Lugovkina, N., Kovrov, N., Pchelintsev, M., Verbitskaya, E. & Zvartau, É. 2015. "Determination of Buprenorphine and Naloxone in Patient Blood Plasma Using HPLC-MS". *Pharmaceutical Chemistry Journal,* 48**,** 690-695.

Zijlstra, G. S., Rijkeboer, M., van Drooge, D. J., Sutter, M., Jiskoot, W., van de Weert, M., Hinrichs, W. L. J. & Frijlink, H. W. 2007. "Characterization of a cyclosporine solid dispersion for inhalation". *Aaps Journal,* 9**,** E190-E199.

Appendix 1. Statistical analysis of *in-vitro* dissolution of nifedipine

Table **Error! No text of specified style in document.**.1 Dissolution data and descriptive analysis of the 4 dissolution profiles in figure 3.13-A.

Time	Dosage type	n	Mean	Std. Deviation	Std. Error	95% Confidence Interval for Mean		Minimum	Maximum
						Lower Bound	Upper Bound		
1 min	30% FD	3	0.000	0.000	0.000	0.000	0.000	0.000	0.000
	30% PM	3	0.000	0.000	0.000	0.000	0.000	0.000	0.000
	100% AR*	3	0.000	0.000	0.000	0.000	0.000	0.000	0.000
	100% AR	3	0.000	0.000	0.000	0.000	0.000	0.000	0.000
	Total	12	0.000	0.000	0.000	0.000	0.000	0.000	0.000
2 min	30% FD	3	6.933	1.002	0.578	4.445	9.422	5.800	7.700
	30% PM	3	0.170	0.147	0.085	-0.196	0.536	0.000	0.260
	100% AR*	3	0.180	0.128	0.074	-0.137	0.497	0.040	0.290
	100% AR	3	0.267	0.045	0.026	0.155	0.379	0.220	0.310
	Total	12	1.888	3.074	0.887	-0.066	3.841	0.000	7.700
3 min	30% FD	3	24.713	6.138	3.544	9.465	39.962	20.020	31.660
	30% PM	3	0.170	0.147	0.085	-0.196	0.536	0.000	0.260
	100% AR*	3	0.180	0.128	0.074	-0.137	0.497	0.040	0.290
	100% AR	3	0.267	0.045	0.026	0.155	0.379	0.220	0.310
	Total	12	6.333	11.389	3.288	-0.904	13.569	0.000	31.660
4 min	30% FD	3	40.170	5.788	3.342	25.791	54.549	34.620	46.170
	30% PM	3	1.047	0.906	0.523	-1.205	3.299	0.000	1.580
	100% AR*	3	0.180	0.128	0.074	-0.137	0.497	0.040	0.290
	100% AR	3	0.267	0.045	0.026	0.155	0.379	0.220	0.310
	Total	12	10.416	18.119	5.231	-1.096	21.928	0.000	46.170
5 min	30% FD	3	52.117	8.591	4.960	30.776	73.458	45.410	61.800
	30% PM	3	3.283	3.270	1.888	-4.840	11.407	0.000	6.540
	100% AR*	3	0.253	0.040	0.023	0.153	0.354	0.210	0.290
	100% AR	3	0.267	0.045	0.026	0.155	0.379	0.220	0.310
	Total	12	13.980	23.365	6.745	-0.865	28.825	0.000	61.800
6 min	30% FD	3	61.630	4.582	2.645	50.247	73.013	56.970	66.130
	30% PM	3	7.660	5.010	2.893	-4.786	20.106	4.050	13.380
	100% AR*	3	0.333	0.150	0.086	-0.039	0.705	0.210	0.500
	100% AR	3	0.267	0.045	0.026	0.155	0.379	0.220	0.310
	Total	12	17.473	26.968	7.785	0.338	34.607	0.210	66.130
10 min	30% FD	3	69.483	3.366	1.943	61.122	77.845	66.770	73.250
	30% PM	3	17.647	9.829	5.675	-6.771	42.064	9.920	28.710

Time	Dosage type	n	Mean	Std. Deviation	Std. Error	95% Confidence Interval for Mean		Minimum	Maximum
						Lower Bound	Upper Bound		
	100% AR*	3	0.373	0.217	0.125	-0.167	0.913	0.210	0.620
	100% AR	3	0.667	0.653	0.377	-0.955	2.288	0.270	1.420
	Total	12	22.043	29.857	8.619	3.072	41.013	0.210	73.250
20 min	30% FD	3	74.343	1.540	0.889	70.519	78.168	72.670	75.700
	30% PM	3	29.790	11.382	6.571	1.516	58.064	18.780	41.510
	100% AR*	3	2.763	1.002	0.578	0.275	5.252	1.730	3.730
	100% AR	3	3.480	0.567	0.327	2.071	4.889	2.850	3.950
	Total	12	27.594	30.795	8.890	8.028	47.160	1.730	75.700
45 min	30% FD	3	73.920	3.217	1.857	65.929	81.911	70.280	76.380
	30% PM	3	45.840	6.144	3.547	30.577	61.103	40.430	52.520
	100% AR*	3	6.607	1.255	0.725	3.489	9.724	5.270	7.760
	100% AR	3	8.250	3.889	2.245	-1.411	17.911	4.810	12.470
	Total	12	33.654	29.496	8.515	14.914	52.395	4.810	76.380
60 min	30% FD	3	75.463	2.721	1.571	68.703	82.224	72.510	77.870
	30% PM	3	50.163	4.561	2.633	38.834	61.493	45.650	54.770
	100% AR*	3	8.683	1.185	0.684	5.739	11.627	7.440	9.800
	100% AR	3	8.813	2.739	1.582	2.008	15.618	6.250	11.700
	Total	12	35.781	29.853	8.618	16.813	54.749	6.250	77.870

Table **Error! No text of specified style in document.**.2 Post Hoc Analysis of the 4 dissolution profiles in figure 3.13-A. Dunnett t-tests treat one group as a control, and compare all other groups against it.

Time	(I)	(J)	Mean[a] Difference (I-J)	Std. Error	Sig.(*P*)	95% Confidence Interval	
						Lower Bound	Upper Bound
20 min	30% FD	100% AR	70.8633****	4.712	0.000	57.293	84.433
	30% PM	100% AR	26.3100****	4.712	0.001	12.740	39.880
	100% AR*	100% AR	-0.717	4.712	0.997	-14.287	12.853
45 min	30% FD	100% AR	65.6700****	3.286	0.000	56.207	75.133
	30% PM	100% AR	37.5900****	3.286	0.000	28.127	47.053
	100% AR*	100% AR	-1.643	3.286	0.923	-11.107	7.820
60 min	30% FD	100% AR	66.6500****	2.487	0.000	59.488	73.812
	30% PM	100% AR	41.3500****	2.487	0.000	34.188	48.512
	100% AR*	100% AR	-0.130	2.487	1.000	-7.292	7.032

(I) Dose type. (J) Control sample

[a] difference between average percentage dissolved of test formulations and controlled NIF-AR*

*As received nifedipine dissolved in 2.59×10^{-3} (w/v) PVP in 0.1M HCl.

**The mean difference is significant at P< 0.05 level

***The mean difference is significant at P< 0.01 level.

****The mean difference is significant at P< 0.001 level.

Table **Error! No text of specified style in document.**.3 Non parametric analysis (α =0.05) of percentage dissolved at time points 1-10 min for the dissolution of FD and PM 30% w/w NIF in PVP, as received nifedipine in PVP containing dissolution medium (equivalent to 30% w/w NIF in PVP) and NIF as received.

	Null Hypothesis	Test	Sig.	Decision
1	The distribution of 1 min is the same across categories of Dosage type.	Independent-Samples Kruskal-Wallis Test	1.000	Retain the null hypothesis.
2	The distribution of 2 min is the same across categories of Dosage type.	Independent-Samples Kruskal-Wallis Test	.066	Retain the null hypothesis.
3	The distribution of 3 min is the same across categories of Dosage type.	Independent-Samples Kruskal-Wallis Test	.066	Retain the null hypothesis.
4	The distribution of 4 min is the same across categories of Dosage type.	Independent-Samples Kruskal-Wallis Test	.075	Retain the null hypothesis.
5	The distribution of 5 min is the same across categories of Dosage type.	Independent-Samples Kruskal-Wallis Test	.082	Retain the null hypothesis.
6	The distribution of 6 min is the same across categories of Dosage type.	Independent-Samples Kruskal-Wallis Test	.025	Reject the null hypothesis.
7	The distribution of 10 min is the same across categories of Dosage type.	Independent-Samples Kruskal-Wallis Test	.024	Reject the null hypothesis.

Table **Error! No text of specified style in document.**.4 Descriptive analysis of the 5 dissolution profiles in figure 3.14-A.

Time	Dosage type	n	Mean	Std. Deviation	Std. Error	95% Confidence Interval for Mean		Minimum	Maximum
						Lower Bound	Upper Bound		
1 min	10% FD	3	0.000	0.000	0.000	0.000	0.000	0.000	0.000
	30% FD	3	0.000	0.000	0.000	0.000	0.000	0.000	0.000
	50% FD	3	0.000	0.000	0.000	0.000	0.000	0.000	0.000
	70% FD	3	0.000	0.000	0.000	0.000	0.000	0.000	0.000
	100% FD	3	0.000	0.000	0.000	0.000	0.000	0.000	0.000
	Total	15	0.000	0.000	0.000	0.000	0.000	0.000	0.000
2 min	10% FD	3	6.390	10.860	6.270	-20.588	33.368	0.120	18.930
	30% FD	3	6.933	1.002	0.578	4.445	9.422	5.800	7.700
	50% FD	3	0.000	0.000	0.000	0.000	0.000	0.000	0.000
	70% FD	3	0.000	0.000	0.000	0.000	0.000	0.000	0.000
	100% FD	3	0.000	0.000	0.000	0.000	0.000	0.000	0.000
	Total	15	2.665	5.332	1.377	-0.288	5.618	0.000	18.930
3 min	10% FD	3	41.677	15.249	8.804	3.796	79.557	29.500	58.780
	30% FD	3	24.713	6.138	3.544	9.465	39.962	20.020	31.660
	50% FD	3	2.707	1.538	0.888	-1.115	6.528	1.640	4.470
	70% FD	3	0.000	0.000	0.000	0.000	0.000	0.000	0.000

Time	Dosage type	n	Mean	Std. Deviation	Std. Error	95% Confidence Interval for Mean		Minimum	Maximum
						Lower Bound	Upper Bound		
	100% FD	3	0.000	0.000	0.000	0.000	0.000	0.000	0.000
	Total	15	13.819	18.411	4.754	3.624	24.015	0.000	58.780
4 min	10% FD	3	69.353	6.690	3.863	52.734	85.973	63.960	76.840
	30% FD	3	40.170	5.788	3.342	25.791	54.549	34.620	46.170
	50% FD	3	6.103	1.500	0.866	2.376	9.830	4.460	7.400
	70% FD	3	0.000	0.000	0.000	0.000	0.000	0.000	0.000
	100% FD	3	0.000	0.000	0.000	0.000	0.000	0.000	0.000
	Total	15	23.125	28.687	7.407	7.239	39.012	0.000	76.840
5 min	10% FD	3	80.947	2.826	1.632	73.926	87.968	78.700	84.120
	30% FD	3	52.117	8.591	4.960	30.776	73.458	45.410	61.800
	50% FD	3	9.817	3.269	1.887	1.697	17.937	6.180	12.510
	70% FD	3	0.000	0.000	0.000	0.000	0.000	0.000	0.000
	100% FD	3	0.000	0.000	0.000	0.000	0.000	0.000	0.000
	Total	15	28.576	33.839	8.737	9.837	47.315	0.000	84.120
6 min	10% FD	3	85.717	2.715	1.567	78.973	92.461	82.800	88.170
	30% FD	3	61.630	4.582	2.645	50.247	73.013	56.970	66.130
	50% FD	3	10.383	1.111	0.642	7.623	13.144	9.120	11.210
	70% FD	3	2.563	2.224	1.284	-2.961	8.088	0.000	3.980
	100% FD	3	0.000	0.000	0.000	0.000	0.000	0.000	0.000
	Total	15	32.059	36.285	9.369	11.965	52.153	0.000	88.170
10 min	10% FD	3	92.607	1.247	0.720	89.509	95.705	91.320	93.810
	30% FD	3	69.483	3.366	1.943	61.122	77.845	66.770	73.250
	50% FD	3	14.200	1.333	0.770	10.889	17.511	13.290	15.730
	70% FD	3	1.477	2.558	1.477	-4.877	7.830	0.000	4.430
	100% FD	3	4.437	0.964	0.556	2.042	6.831	3.710	5.530
	Total	15	36.441	38.737	10.002	14.989	57.892	0.000	93.810
20 min	10% FD	3	94.633	0.760	0.439	92.745	96.521	94.080	95.500
	30% FD	3	74.343	1.540	0.889	70.519	78.168	72.670	75.700
	50% FD	3	16.887	1.106	0.638	14.140	19.633	15.610	17.540
	70% FD	3	3.873	3.020	1.744	-3.629	11.375	1.600	7.300
	100% FD	3	9.047	1.409	0.813	5.547	12.546	8.060	10.660
	Total	15	39.757	38.651	9.980	18.352	61.161	1.600	95.500
45 min	10% FD	3	90.850	1.724	0.995	86.568	95.132	88.890	92.130
	30% FD	3	73.920	3.217	1.857	65.929	81.911	70.280	76.380
	50% FD	3	16.167	0.182	0.105	15.714	16.620	15.970	16.330
	70% FD	3	4.213	1.716	0.991	-0.050	8.476	2.420	5.840
	100% FD	3	15.823	2.316	1.337	10.070	21.576	13.150	17.220
	Total	15	40.195	36.402	9.399	20.036	60.353	2.420	92.130
60 min	10% FD	3	87.093	3.527	2.036	78.333	95.854	83.190	90.050
	30% FD	3	75.463	2.721	1.571	68.703	82.224	72.510	77.870
	50% FD	3	16.253	1.657	0.957	12.137	20.370	14.340	17.220
	70% FD	3	3.663	1.758	1.015	-0.703	8.029	1.700	5.090
	100% FD	3	20.920	2.616	1.511	14.421	27.419	17.900	22.500

Time	Dosage type	n	Mean	Std. Deviation	Std. Error	95% Confidence Interval for Mean		Minimum	Maximum
						Lower Bound	Upper Bound		
	Total	15	40.679	35.081	9.058	21.252	60.106	1.700	90.050

Table **Error! No text of specified style in document.**.5 Levene's Test of Equality of Error Variancesa (α =0.05)

Time	F	df1	df2	Sig.
1 min		4	10	
2 min	15.237	4	10	.000
3 min	8.103	4	10	.004
4 min	4.705	4	10	.021
5 min	7.234	4	10	.005
6 min	2.305	4	10	.130
10 min	2.699	4	10	.092
20 min	2.833	4	10	.083
45 min	3.215	4	10	.061
60 min	.843	4	10	.529

Table **Error! No text of specified style in document.**.6 Post Hoc Analysis (α =0.05) of the 5 dissolution profiles in figure 3.14-A. Dunnett t-tests treat one group as a control, and compare all other groups against it.

Time	(I)	(J)	Mean Difference (I-J)	Std. Error	Sig.	95% Confidence Interval	
						Lower Bound	Upper Bound
5 min	10% FD	100% FD	80.9467***	3.51143	.000	70.7969	91.0964
	30% FD	100% FD	52.1167***	3.51143	.000	41.9669	62.2664
	50% FD	100% FD	9.8167	3.51143	.058	-.3331	19.9664
	70% FD	100% FD	0.0000	3.51143	1.000	-10.1497	10.1497
6 min	10% FD	100% FD	85.7167***	2.14622	.000	79.5130	91.9203
	30% FD	100% FD	61.6300***	2.14622	.000	55.4264	67.8336
	50% FD	100% FD	10.3833**	2.14622	.002	4.1797	16.5870
	70% FD	100% FD	2.5633	2.14622	.595	-3.6403	8.7670
10 min	10% FD	100% FD	88.1700***	1.71784	.000	83.2046	93.1354
	30% FD	100% FD	65.0467***	1.71784	.000	60.0813	70.0120
	50% FD	100% FD	9.7633**	1.71784	.001	4.7980	14.7287
	70% FD	100% FD	-2.9600	1.71784	.307	-7.9254	2.0054
20 min	10% FD	100% FD	85.5867***	1.42714	.000	81.4615	89.7118
	30% FD	100% FD	65.2967***	1.42714	.000	61.1715	69.4218
	50% FD	100% FD	7.8400**	1.42714	.001	3.7149	11.9651
	70% FD	100% FD	-5.1733*	1.42714	.015	-9.2985	-1.0482
45 min	10% FD	100% FD	75.0267***	1.69940	.000	70.1146	79.9388
	30% FD	100% FD	58.0967***	1.69940	.000	53.1846	63.0088
	50% FD	100% FD	.3433	1.69940	.999	-4.5688	5.2554
	70% FD	100% FD	-11.6100***	1.69940	.000	-16.5221	-6.6979
60 min	10% FD	100% FD	66.1733***	2.08242	.000	60.1541	72.1925

30% FD	100% FD	54.5433***	2.08242	.000	48.5241	60.5625
50% FD	100% FD	-4.6667	2.08242	.142	-10.6859	1.3525
70% FD	100% FD	-17.2567***	2.08242	.000	-23.2759	-11.2375

*The mean difference is significant at P< 0.05 level
**The mean difference is significant at P< 0.01 level.
*** The mean difference is significant at P< 0.001 level.

Table **Error! No text of specified style in document.**.7 Non parametric analysis (α =0.05) of percentage dissolved at time points 1-4 min for the dissolution of FD formulations containing 10, 30, 50, 70 and 100% w/w NIF in PVP.

	Null Hypothesis	Test	Sig.	Decision
1	The distribution of 1 min is the same across categories of Dose type.	Independent-Samples Kruskal-Wallis Test	1.000	Retain the null hypothesis.
2	The distribution of 2 min is the same across categories of Dose type.	Independent-Samples Kruskal-Wallis Test	.011	Reject the null hypothesis.
3	The distribution of 3 min is the same across categories of Dose type.	Independent-Samples Kruskal-Wallis Test	.009	Reject the null hypothesis.
4	The distribution of 4 min is the same across categories of Dose type.	Independent-Samples Kruskal-Wallis Test	.008	Reject the null hypothesis.

Appendix 2. Batch work sheet for the manufacture of naloxone buccal FDT

Please refer to the CD attached for a complete copy

Guy's and St Thomas' NHS
NHS Foundation Trust

NON-STERILE BATCH WORKSHEET

-PRODUCT TITLE: **Naloxone HCL Instant Melt Tablet 0.8 mg Stability Batch**		
FORM: **Buccal Tablet**	PRODUCT CODE: **PHD001**	BATCH NO: **PHD001 / _____**
WORK AREA: **Extemp Prep Room 1.12** **Fire Rated Room 1.7**	PACK SIZE: **1 Tablet**	QC SPEC NO: **NS462**
EXPECTED FINAL YIELD: **18 TABLETS**	DATE MANUFACTURING COMMENCED:	
EXPIRY DATE: **To be determined**	STORAGE CONDITIONS: **STORE AT ROOM TEMPERATURE**	

SPECIAL PRECAUTIONS:
1. **Wear gloves throughout the manufacturing and tablet handling.**
2. **Always ensure the dust control cabinet is switched on when weighing powders.**
3. **Do not touch dry ice without gloves.**
4. **Avoid inhaling sublimed CO_2 from Dry Ice.**
5. **Keep Dry Ice in closed container.**

Version A: New product, PhD project.
Version B:
Producing 30 frozen tablets rather than 20, however only 20 complete tablets are to be freeze dried.
Space is allocated in the work sheet to record the number of tablets that are included in the freeze dried batch and frozen tablets that are disposed of
Using 10% w/v Mannitol IV solution BP instead of Mannitol powder BP
Using large weighing boats in the process of weighing and filling blister wells
Using large weighing boats filled with dry ice in the process of easing tablets out of blister wells
Increased volume of Hot water to 40 mL to ensure gelatine fully dissolved.
Excluding the usage of Ci-DMS(not necessary for stability batches).
Version C:
Changed the quantity of raw material Naloxone Hydrochloride Dihydrate powder BP to give an equivalent dose of 0.8 mg of Naloxone Hydrochloride per tablet.
Changed Quantity of Naloxone Hydrochloride dehydrate added to stock solution accordingly
Changed the ±% range allowed for the weighed raw materials when preparing the stock solution from ±5% to ±1%

Formula:	**Quantity**
Naloxone Hydrochloride Dihydrate Powder BP	0.88 mg
Gelatine Powder BP	11.70 mg
10% w/v Mannitol IV solution BP (quantity refers to equivalent quantity of mannitol powder)	4.26 mg
Sodium Bicarbonate Powder BP	1.98 mg
Water for Injection WFI (Cold/Hot) (-removed on drying) BP	To 1.5 g

ORDER GENERATION and DISPENSING OF RAW MATERIALS (RM)

1. Following procedure MA-GE-001 using the Episys Ultimate system, print labels for the batch, complete label reconciliation table.
2. Only the containers are dispensed in the Basement Raw Material Dispensary following SOP MA-GE-036. The low weight of all the API's means the active Raw Materials are all dispensed in Extemp Prep Room 1.12.
3. Raw Materials for the batch are dispensed in the Extemp-prep room 1.12 and the containers disposed in RMD.

RAW MATERIAL AND CONTAINERS ARE TRANSFERRED FROM RAW MATERIAL DISPENSARY TO 13th FLOOR FOLLOWING MA-GE-040.

Written by Abdulmalik Alqurshi_____PhD student

Checked by Rebecca Stansfield _____ Title Production Pharmacist Version C

Checked by Verity Sandhu _____ Title Senior Production Pharmacist

Authorised by _____ Title Pharmacy QA _____ Review Date 30 Dec 2014

Appendix 3. Finished product quality control for naloxone buccal FDT

Please refer to the CD attached for a complete copy

QC Spec No: QC-NS-462-03 Page 1 of 13

Guy's and St Thomas' NHS
NHS Foundation Trust
FINISHED PRODUCT ANALYTICAL PROCEDURE

TITLE:	Naloxone Hydrochloride Instant Melt Tablets (0.8mg)	Product Spec: PHD001	
Written By:	Abdulmalik Alqurshi	Signed	
Checked By:	James Rickard	Signed	
Approved by Quality Assurance:	Signed:	Approval Date:	Review Date:

FORMULA		AMOUNT	
Raw Material	Grade	Per Batch	Per Tablet
Naloxone Hydrochloride Dihydrate Powder	BP	0.0586g	0.88mg
Gelatine Powder	BP	0.780g	11.70mg
10% w/w Mannitol solution EP (equivalent quantity of mannitol)	BP	2.931g	4.26mg
Sodium hydrogen carbonate Powder	BP	0.132g	1.98mg

CONTAINER & CLOSURE	DESCRIPTION
Container	Universal glass vials
Closure	Rubber stopper and an aluminium cap

SHELF-LIFE & STABILITY DATA	
Shelf-life	To be determined
Stability data	To be determined

Appendix 4. Investigational medicinal product dossier for naloxone buccal FDT

Please refer to the CD attached for a complete copy

Investigational Medicinal Product Dossier

For Naloxone Hydrochloride Instant melt buccal tablet

Name	:	Naloxone buccal immediate melt tablets
Research Number	:	IPS-NALOX-2014-01
Version No. Date	: :	2 15th Jul 2015

MAIN AUTHOR: Mr Abdulmalik Alqurshi

Signatures: _____

AUTHOR: Mr James A Rickard

Signatures: _____

AUTHOR: Miss Mary Nguyen

Signatures: _____

AUTHOR: Mr Timothy White

Signatures: _____

AUTHOR: Dr. Ben Forbes

Signatures: _____

AUTHOR: Dr. Paul Royall

Signatures: _____

Sponsor: Institute of Pharmaceutical Science, King's College London
Tel: 020 7848 4823
Fax: n/a
E-mail: Ben.forbes@kcl.ac.uk

Appendix 5. Digital Image Disintegration Assay (DIDA) for the Quality Control (QC) of fast disintegrating tablets

Digital Image Disintegration Assay (DIDA) for the Quality Control (QC) of fast disintegrating tablets

A. Alqurshi[1], B. Forbes[1], P.G. Royall[1]
[1] King's College London, Institute of Pharmaceutical Science, Franklin-Wilkins Building, 150 Stamford Street, London, UK, SE1 9NH.

Objectives
Despite the growing popularity of fast disintegrating buccal tablets [1], there is no *in-vitro* disintegration test currently available. The objective of this work was to develop and validate a novel, quality control disintegration assay for fast disintegrating buccal tablets (FDT).

Methods
A digital image or photographic disintegration assay was developed to measure tablet disintegration in temperature controlled (25-37°C) small volumes of medium (0.7-0.1 mL). The test tablets used were novel naloxone FDT prepared for a clinical trial associated with an ongoing project by the authors. The disintegration vessel was a thermal-jacketed aluminum blister sheet with black-painted wells of the same dimension and complementary shape to the naloxone tablets. Disintegration medium was phosphate buffered distilled water (pH 7.3 ± 0.2) or a synthetic saliva adapted from the SS5 USP recipe for artificial saliva. Disintegration was quantified using a camera fitted gel imager box to follow tablet disappearance by analyzing sequence images for the remaining percentage of test FDT using the software imagJ.

Results
Validation tests showed that the temperature of the disintegration medium, within in the disintegration vessel, was maintained at ±1.0°C of the target temperature for all disintegration volumes used. Whilst keeping the volume constant the DIDA test discriminated the dissolution profiles, in terms of temperature, for the naloxone FDT, e.g. time to reach T_{80} (time point at which 80% of the tablet has disappeared) at 25°C was equal to 28 sec, whereas for 37°C it was 6 sec. On the other hand, maintaining a constant temperature at 35°C and varying the disintegration volume, showed to significantly affect the rate of disintegration, where T_{80} showed to decrees as the disintegration volume increases, following the exponential equation [$T80 = 18.617e^{-1.672\,(volume\,mL)}$], e.g. disintegration in 0.1 mL showed to reach T_{80} at 17 sec, almost 3 times slower than disintegration in 0.7 mL. The DIDA test also demonstrated potential for use in *in-vivo* prediction, as it discriminated between the use of buffered water and artificial saliva, reaching T80 at 3 sec and 6 sec respectively.

Conclusions
A novel disintegration method for fast disintegrating buccal tablets was developed and partially validated for potential use as a quality control assay. The test has also shown to be useful in investigating disintegration profile and may have potential in future development as an assay to predict *in-vivo* performance.

References

1. Jeong, S.H., Y. Fu, and K. Park, *Frosta: a new technology for making fast-melting tablets.* Expert Opin Drug Deliv, 2005. **2**(6): p. 1107-16.

Acknowledgment: **This study was very generously funded by the Saudi Arabian ministry of education**

Appendix 5. Digital Image Disintegration Assay (DIDA) for the Quality Control (QC) of fast disintegrating tablets

Digital Imaging Disintegration Assay (DIDA) for the quality control of fast disintegrating tablets.

Abdul Alqurshi, Ben Forbes, Paul G. Royall
Institute of Pharmaceutical Science, King's college of London.
150 Stamford Street London SE1 9NH

KING'S College LONDON

1- Naloxone FDT composition

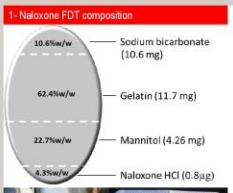

2- Dissolution vessel setup

Image of the DIDA disintegration vessel

3- Developing *In-vitro* QC testing for the rapid disintegration of FDT's

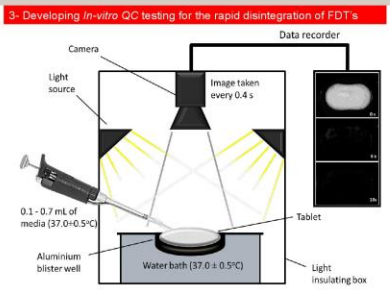

Schematic for the digital image disintegration assay

6- Effect of Temp, volume and media on disintegration rate

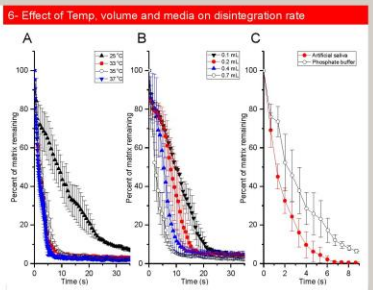

Disintegration of naloxone FDT (A) 0.7 mL*, (B) 35 °C * & (C) 0.7 mL, 35°C

4- Monitoring disintegration volume Temperature

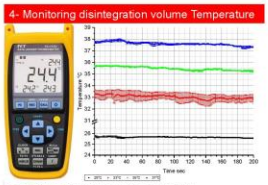

Monitoring disintegration medium temperature.

5- ImageJ software

MGV measurement of FDT. Image was taken at time point 4s of 0.1mL/35 °C

7- T_{80} against disintegration volume

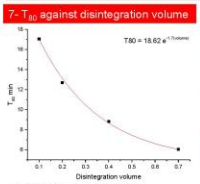

Effect of disintegration volume on T_{80}.

8- Fast disintegrating tablet**

Introduction

Fast disintegrating tablets (FDT), also referred to as mouth-dissolving and fast-melts, have become very common in the past decade[1]. With more formulations predicted as the Zydis® patent has expired[1]. These have been developed for various indications, including delivery of emergency medicines[1].

Slow disintegration of conventional tablets may be tested using BP methods, where sink conditions are applied. However, due to the limited amount of saliva in the mouth, a non-sink quality control (QC) test is more applicable for the disintegration of FDT's.[1]

Why is a specific QC test for fast disintegration needed?

1) Speed of disintegration is a key property of FDT's, which may vary widely (10s-3min).
2) Classify various FDT formulations under different speed of onsets, thus different indications.
3) Evaluate the disintegration of FDT's under different conditions (e.g. different disintegration volumes) in biorelevant volumes and temperatures.

Goal

To develop an *in-vitro* QC disintegration test, that can allow accurate monitoring of FDT's disintegration in biorelevant conditions.

Method

i. Test tablets used, were novel naloxone FDT prepared for a clinical trial associated with an ongoing project by the authors.[1]
ii. The disintegration vessel was a thermal-jacketed aluminum blister sheet, with black-painted wells, of the same dimension and complementary shape to the naloxone tablets (Fig 2 and 3).
iii. Disintegration medium was phosphate buffered distilled water (pH 7.3 ± 0.2) or a synthetic saliva adapted from the SS5 USP recipe for artificial saliva.
iv. Disintegration volumes used, varied from 0.7-0.1 mL, to represent the volume range of saliva in the mouth,[1] while the controlled temperatures varied from 37 to 25 ± 1.0 °C, to cover the temperature range of the oral cavity,[1] monitored and recorded using a micro-thermocouple data logger (Fig 4).
v. Disintegration was quantified using a camera fitted gel imager box (Fig 3) to follow tablet disappearance by analyzing sequence images for the remaining percentage of test FDT using the software imagJ.

Results

- DIDA setup allowed accurate temperature control (±1.0 °C) of disintegration medium for all volumes (Fig 3).
- Monitoring disappearance of tablet showed to be reproducible if all conditions are maintained constant (Fig 6).
- Discrimination against temperature change, while maintaining a constant disintegration volume, was only observed between 25 °C and all other tested temperatures (Fig 6-A).
- Maintaining a constant temperature, at 35 °C and varying the disintegration volume, showed to significantly affect the rate of disintegration (Fig 6-B). Where T_{80} (time point at which 80% of the tablet has disappeared) showed to decrees as the disintegration volume increases, following the equation [$T_{80} = 18.617e^{-1.672\,(\text{volume mL})}$] as presented in figure 7.
- DIDA also demonstrated potential for *in-vivo* prediction, as it discriminated between the use of buffered water and artificial saliva, reaching T_{80} at 3 sec and 6 sec respectively (Fig 6-C).

Discussion

- DIDA setup allowed high resolution monitoring of FDT disintegration using biorelevant volumes and temperatures.[1]
- Reducing disintegration volume, has decreased the rate of disintegration, and therefore T_{80}. This had complex kinetics of a non-integral order between the different volumes, nevertheless, figure 6 showed T_{80} of different volumes to fit an exponential decay model.
- DIDA has potential to be used as a QC test to discriminate between FDT's of different batches and possibly different formulations.

Conclusion

A novel disintegration method for fast disintegrating tablets was successfully developed and partially validated for potential use as a quality control assay. The test has also shown to be useful in investigating disintegration profile and may have potential in future development as an assay to predict *in-vivo* performance.

References

1) Alqurshi, A., Kumar, Z., McDonald, R., Strang, J., Buanz, A., Ahmed, S., Allen, E., Cameron, P., Rickard, J.A., Sandhu, V., Stansfield, R., Taylor, D., Forbes, B., & Royall, P.G. (submitted). Instant dissolving buccal tablets for the emergency delivery of naloxone. *Molecular Pharmaceutics*.

Next steps:

(1) Utilising DIDA to compare marketed FDT's (example Imodium ** Nurofen), · (2) Utilizing DIDA to study the effect of solid state on disintegration rate.

Acknowledgment: I would like to thank Somaiah Alqurashi, Barry Panaretou, Farzana Chowdhury & Thomas Littlewood, for their efforts and support.

SAUDI ARABIAN MINISTRY OF EDUCATION
وزارة التعليم بالمملكة العربية السعودية

Appendix 6. Design of a novel *in-situ* freeze-dried capsule for dissolution rate enhancement

Design of a novel *in-situ* freeze-dried capsule for dissolution rate enhancement

Abdulmalik Al Qurshi, Peter C. Riggs, Paul G. Royall
Institute of Pharmaceutical Science, Faculty of Life Sciences & Medicine, King's College London.

A commonly used approach for the potential improvement of dissolution is to render a poorly soluble drug into its amorphous or disordered form. However, such amorphous materials are physically unstable and are difficult to formulate due to their sensitivity to physical and thermal processing. The aim of the study was to design a manufacture-convenient novel platform to enhance the dissolution of poorly soluble drugs, utilising freeze-drying as a method for the production of amorphous solids *in-situ* within a capsule.

Nifedipine and polyvinylpyrrolidone K10 (PVP) were dissolved in tert-butanol at 37 °C to provide a range of drug to polymer ratios. These solutions were then dispensed into gelatine capsules, freeze-dried, sealed and packaged in amber vials under nitrogen. The nifedipine content was maintained at 10 mg per capsule, the PVP concentration within the freeze-dried formulations was increased from 0 to 90% w/w with respect to the polymer. The resulting product was analysed by differential scanning calorimetry to assess the percentage of amorphous drug present. *In-vitro* dissolution profiles of freeze-dried formulations with different drug to polymer ratios were determined, as well as physical mixes of the drug and polymer. Dissolution profiles of nifedipine as received in a PVP containing dissolution medium and the dissolution of marketed TEVA nifedipine soft capsule formulation were recorded. The physical and chemical stability of the in-situ freeze-dried capsules was investigated by running a 3 month stability study at 25^{o}C, 57%RH and 37^{o}C, 74%RH.

Nifedipine 10-70% w/w in PVP was successfully freeze dried in capsules to produce a dispersed, purely amorphous, porous solid (n=3) with a DSC measured glass transition ranging from 142.9 ± 1.1 ^{o}C to 77.8 ±1.3 ^{o}C, respectively. The absence of crystalline nifedipine was further confirmed by polarized light microscopy images and infrared spectroscopy. A 22 fold increase in the amount of drug released from the dissolution of a 10%w/w nifedipine in PVP capsule when compared to a 70% w/w formulation. The time taken for 80% of the loaded drug to be released from the freeze-dried 10% w/w nifedipine in PVP was equal to 8.7 ± 5.1 min approximately half of the time required by the marketed liquid filled capsule formulation. Stability data showed no crystallised nifedipine in all conditions examined, the amber vial packed formulation however showed 16% ±13% loss in drug content due to photo-degradation.

Tert-butanol has been shown to facilitate the production of stable, *in-situ* freeze-dried, capsule formulations containing the poorly soluble drug nifedipine. The novel but simple formulation design led to enhanced dissolution times, indicating the potential for *in-situ* freeze-dried capsules to provide an elegant approach for the improvement in dissolution rates of aqueous insoluble drugs. *Acknowledgement: This study was funded by the Saudi Arabian ministry of education.*

Design of novel formulations for dissolution rate enhancement.

Abdulmalik AlQurshi, Peter C. Riggs and Paul G. Royall

Institute of pharmaceutical sciences, school of Biomedical Sciences, King's college
The Franklin-Wilkins Building 150 Stamford Street, London SE1 9NH

Nifedipine PVP

Introduction

- A common problem encountered with oral solid dosage forms is low dissolution rate of poorly water soluble drugs. As a direct result low bioavailability and mucosal toxicity are observed[1-4]
- Dispensing the drug as an amorphous material has shown to be a very effective approach for enhancing the dissolution rate of oral solid dosage forms and increasing the apparent solubility of poorly water soluble drugs[2, 5-8]

Aim

- To design a manufacture-convenient novel platform to enhance the dissolution of poorly water soluble drugs, utilising freeze-drying as a method for the production of amorphous solid in-situ within a capsule.

Methods

1. Polyvinylpyrrolidone K10 (PVP) and nifedipine (NIF) were dissolved in tert-butanol at 37°C in concentrations ranging from 0 to 100% w/w (NIF in PVP).
2. Solutions were dispensed into freeze drying vials.
3. A rapid freezing stage was performed at -50°C for 2h.
4. Using a basic freeze dryer, the samples were subjected to a primary drying stage at -40°C and 0.076mbar for a period of 144h.
5. A secondary drying stage was performed at room temperature over P_2O_5.
6. The physicochemical properties of the freeze dried material and related controlled physical mixtures were analysed using differential scanning calorimetry (DSC), FT-IR and polarized microscopy.
7. Control samples were prepared by grinding physical mixtures of NIF and PVP using pestle and mortar.
8. Method was adapted to freeze drying optimal ratios of NIF to PVP in capsules while maintaining a constant mass of 10mg of NIF per capsule. Stock solutions of NIF in PVP (37°C) were dispensed into capsules bottoms which were arranged inside a freeze drying vial. The freeze drying followed the same method stated above.
9. *In-situ* freeze dried capsule formulations were analysed for drug content and *in-vitro* dissolution rate using a stability indicating HPLC assay.
10. Physical and chemical stability of the optimised formulation was investigated between room temperature 25°C, 60%RH and 35°C, 75% RH. Samples were tested for drug content, dissolution rate, content of crystallinity, solvent content and presence of chemical degradation product.

Results

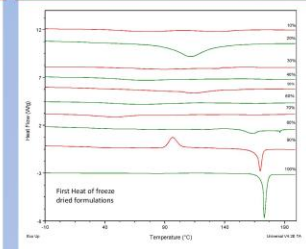

Figure 1: DSC thermograms for each of the freeze dried formulations. Negative heat flow indicates an endothermic process, hence peaks at 170-180°C indicate melting of nifedipine. Area of peak is equal to enthalpy J/g. Note formulations 10-70 w/w% of nifedipine in PVP k10 show no sign of nifedipine melting, and therefore supporting that nifedipine is dispersed as an amorphous material.

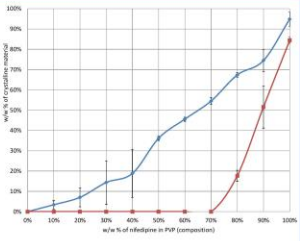

Figure 2: Presents an amorphous/crystalline phase diagram of 0-100% w/w nifedipine in PVP K10 for freeze dried (■) and physical mix formulations (◆). Error bars represent standard deviation (n=3). Note crystalline nifedipine is only present in freeze dried formulations above 70% w/w nifedipine in PVP. Whereas crystalline nifedipine is present in all nifedipine containing physical mix samples (thus controlled samples).

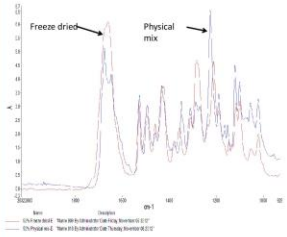

Figure 3: FT-IR normalized spectra of freeze dried 50% w/w NIF in PVP and the corresponding control sample. Note the sharpness in the blue trace (spectrum representing crystalline containing controlled sample). On the other hand the orange trace (spectrum representing freeze dried amorphous sample) shows a less defined trace indicating a difference in the intermolecular forces between the freeze dried and the controlled sample. The disordered nature of an amorphous material reduces the frequency of intermolecular bonds possible.

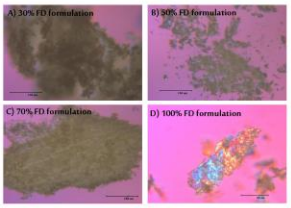

Figure 4: A)FD 30% w/w NIF in PVP, B)FD 50% w/w NIF in PVP, C)FD 70% w/w NIF in PVP and D)FD 100% w/w NIF. Note the absence of birefringence in figures A, B and C, thus indicating the presence of amorphous material in figures A to C. Figure D on the other hand shows birefringence and thus that nifedipine is present as a crystalline material.

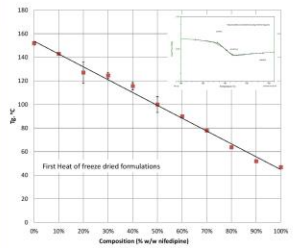

Figure 5: Presenting the glass transition temperature (T_g) of freeze dried material for the second-heat of the sample (first-heat traces were distorted by the removal of residual solvent). Error bars represent standard deviation (n=3). Note that increasing the w/w% of PVP increases the T_g value and therefore shows a strong indication of stability increase in the formulation.

Figure 6: Novel freeze dried capsule formulation of nifedipine. Freeze drying in situ was successfully performed, thus a one step elegant method of producing an amorphous product was developed. Note formulations with higher PVP content show better structural support and therefore occupy a higher volume of the capsule.

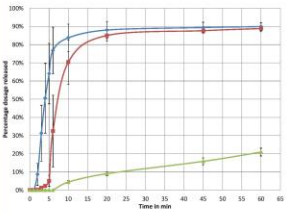

Figure 7: In-vitro dissolution profile of the In-situ freeze dried 10% w/w nifedipine in PVP formulation compared with the marketed liquid capsule formulation. The figure illustrates that although the novel formulation is of a solid dosage form, it is showing a higher rate of dissolution to the liquid capsule formulation. Error bars represent standard deviation (n=3)

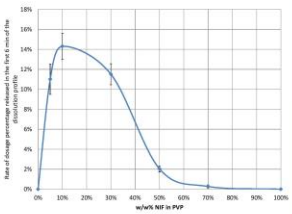

Figure 8: Rate of dissolution was determined as the as the rate of percentage dosage released in the first 6 minutes of *in-vitro* dissolution of varies ratios of NIF to PVP of the *in-situ* freeze dried formulation. Error bars represent standard deviation (n=3).

Discussion

DSC thermograms of NIF as received was used to determine the melting peak area of a 100% crystalline NIF. This data was used to calculate the content of crystalline NIF in freeze dried material.
The absence of crystalline material was further confirmed by comparing FTIR spectrum and polarized microscopy images.
A linear relation ship between glass transition and content of PVP was observed using the DSC, this is an indication of drug-polymer interaction as it deviates from the assumptions of the Gordon-Taylor equation.
Preliminary results of stability study show that content of crystalline NIF is maintained undetected when storing formulation in a sealed vial under nitrogen at either conditions (25°C, 60%RH and 35°C, 75% RH). Chemical stability determined through drug content before and after was shown to be maintained at 10mg $_{(\pm 5\%)}$ when maintaining formulations in red opaque capsules.

Conclusions

- Nifedipine was successfully dispersed in PVP K10 as an amorphous material.
- A novel freeze dried capsule formulation was successfully developed by a simple one step elegant method.
- FD formulation was shown to deliver 80% of the dose in half the time required by a liquid marketed formulation.

Acknowledgments

I Would like to thank God for giving me the strength to carry this research. I would also like to specially thank my supervisor Dr. Paul Royall who has been ever so supportive. Without his guidance and wisdom this research would have not been possible. I would also like to thank Dr. Jawad, Steve Inghamn Dan Asker and David Stanton for their help and support. Last but not least I would like to thank the Saudi Arabian Ministry of higher education for sponsoring my research.

References

1. Streubel, A., J. Siepmann, and R. Bodmeier, *Drug delivery to the upper small intestine window using gastroretentive technologies*. Curr Opin Pharmacol, 2006. **6**(5): p. 501-8.
2. Kaur, J., et al., *Improvement of drug solubility using solid dispersion* 2012: International Journal of Pharmacy and Pharmaceutical Sciences. 4 (2) (pp 47-53), 2012. Date of Publication: 2012.
3. Gardner, D., et al., *Noninvasive methodology for assessing regional drug absorption from the gastrointestinal tract*. Pharmaceutical Technology International, 1997. **9**(Jun): p. 46, 48, 50, 52-53.
4. Vasconcelos, T., B. Sarmento, and P. Costa, *Solid dispersions as strategy to improve oral bioavailability of poor water soluble drugs*. Drug Discovery Today, 2007. **12**(23-24): p. 1068-1075.
5. Ozaki, S., et al., *Evaluation of drug supersaturation by thermodynamic and kinetic approaches for the prediction of oral absorbability in amorphous pharmaceuticals*. Journal of Pharmaceutical Sciences, 2012. **101**(11): p. 4220-4230.
6. Brouwers, J., M.E. Brewster, and P. Augustijns, *Supersaturating Drug Delivery Systems: The Answer to Solubility-Limited Oral Bioavailability?*Journal of Pharmaceutical Sciences, 2009. **98**(8): p. 2549-2572.

Appendix 7. Buccal naloxone for opioid overdose reversal: rationale for and development of a novel instant-dissolving tablet

Abstract

Authors: Rebecca McDonald[1], Abdul Alqurshi[2], Ben Forbes[2], Paul Royall[2], David Taylor[2, 3], & John Strang[1]

Authors' affiliation: (1) Addictions Department, IoPPN, (2) Institute of Pharmaceutical Science, (3) Pharmacy Department, South London and Maudsley NHS Foundation Trust (SLaM)

Primary author email: rebecca.s.mcdonald@kcl.ac.uk

TITLE:

Buccal naloxone for opioid overdose reversal: rationale for and development of a novel instant-dissolving tablet formulation

Background: Opioid overdose annually accounts for ~69,000 preventable deaths worldwide. Opioid overdose is easily reversed with the antidote naloxone. However, naloxone is only licensed as injection.

Aim: To develop an injection-free naloxone formulation for the community-based prevention of opioid overdose.

Methods: All potential routes of drug delivery were reviewed for suitability of layperson administration during overdose. A buccal instant-dissolving tablet was developed using freeze-drying technology and evaluated.

Results: The tablets showed chemical and physical stability over 9-months' storage (25°C) and dissolved fully in vitro within 30 seconds.

Conclusion: Instant-dissolving buccal naloxone tablets are suitable for first-in-human study to determine pharmacokinetics.

100 words (excluding section headers)

References:

Alqurshi, A., Kumar, Z., McDonald, R., Strang, J., Buanz, A., Ahmed, S., Allen, E., Cameron, P., Rickard, J.A., Sandhu, V., Stansfield, R., Taylor, D., Forbes, B., & Royall, P.G. (submitted). Instant dissolving buccal tablets for the emergency delivery of naloxone. *Molecular Pharmaceutics*.

Strang, J., McDonald, R.*, Alqurshi, A., Royall, P., Taylor, D., & Forbes, B. (submitted). Naloxone without the needle - structured review of routes of administration, the rationale for non-injectable naloxone, and next steps in development of nasal and buccal naloxone formulations. *Drug and Alcohol Dependence*.

Strang, J., McDonald, R.*, Tas, B., Day, E. (in press). Clinical provision of nasal naloxone without prior experimental testing and without regulatory approval – imaginative shortcut or dangerous bypass of essential safety procedures? *Addiction*.

Buccal naloxone for opioid overdose reversal: rationale for and development of a novel instant-dissolving tablet formulation

Rebecca McDonald [1], Abdul Alqurshi [2], Ben Forbes [2], Paul Royall [2], David Taylor [2,3], & John Strang [1]

(1) Addictions Department, Institute of Psychiatry, Psychology and Neuroscience (IoPPN)
(2) Institute of Pharmaceutical Science · (3) Pharmacy Department, SLaM NHS Foundation Trust

KING'S College LONDON

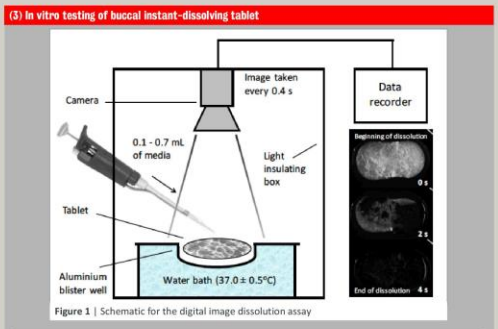

Figure 1 | Schematic for the digital image dissolution assay

Table 1 | Instant-dissolving tablet specification and stability (n=6; 2 tablets per 3 batches)

		Stability		
		0 months	9 months	9 months
Parameter	Specification		4°C	25°C
Tablet weight (mg)	16.9 - 20.7	17.8 ± 0.5	17.8 ± 0.5	17.6 ± 0.5
Dimension - length (mm)	20.0 - 30.0	29.4 ± 0.2	29.1 ± 0.3	29.1 ± 0.7
Dimension - width (mm)	14.0 - 18.0	16.1 ± 0.5	16.1 ± 0.3	16.0 ± 0.3
Disintegration test (s)	≤180	14.0 ± 5.9	9.0 ± 5.0	10.0 ± 5.0
Naloxone HCL assay (mg)	0.76 - 0.84	0.80 ± 0.01	0.81 ± 0.02	0.80 ± 0.03

Introduction

Opioid overdose annually accounts for ~69,000 preventable deaths worldwide.
In England and Wales alone, there were 952 deaths from heroin and morphine in 2014.

Opioid overdose is easily reversed with the antidote naloxone. However, naloxone is only licensed as injection.*

Why is injection-free naloxone needed?

1) Administering injections can be intimidating, requires training
2) Injections bear the risk of needle-stick-injury and blood-borne virus transmission (HIV, HBV, HCV)
3) Injections have prescription-only (POM) status**

Goal

To develop an injection-free naloxone formulation for the community-based prevention of opioid overdose.

* Exception: U.S. (as of Nov 18 2015)
**Exception: Italy

Method

(1) All potential 112 FDA-recognized routes of administration were reviewed for suitability of layperson administration during overdose.

Inclusion criteria

i. Injection or invasive procedure
ii. Medical procedure / medical training
iii. Not publicly acceptable (e.g. rectal)
iv. Inadequate bioavailability
v. Not sufficiently rapid drug absorption

Exclusion criteria

i. Suitable for OD emergency situation
ii. No major risk of compromise from OD complication

The buccal, nasal, and sublingual routes met the above criteria. The latter routes were not pursued due to existing industry investment.

(2) A buccal instant-dissolving tablet was developed using freeze-drying technology from naloxone-HCl solution.

(3) The buccal instant-dissolving tablet was evaluated in vitro.

Results

- Optimised composition defined as: 24% mannitol + 65% gelatine + 11% sodium bicarbonate (w/w)
- The tablets conformed reproducibly to quality specifications (see Table 1).
- The tablets showed chemical and physical stability over 9-months' storage (25° C), with target drug content of 0.8 mg of naloxone HCl/tablet (HPLC assay).
- Digital imaging dissolution assay (see Fig 1): under all conditions, tablets dissolved fully (>90%) within 30 seconds (variation of: temperature, volume of fluid, dissolution medium).

Discussion

- Advantage over solution: tablets typically have greater stability and ease of unit dose application – awaiting 12+ mo. stability data.
- Effect of excipients/formulation on absorption unknown: human PK data needed.
- Addition of absorption enhancers possible.
- Buccal instant-dissolving tablet technology may be adapted for other active ingredients, e.g. naltrexone.

Conclusion

Instant-dissolving buccal naloxone tablets are suitable for first-in-human study to determine pharmacokinetics.

References

Alqurshi, A., Kumar, Z., McDonald, R., Strang, J., Buanz, A., Ahmed, S., Allen, E., Cameron, P., Rickard, J.A., Sandhu, V., Stansfield, R., Taylor, D., Forbes, B., & Royall, P.G. (submitted). Instant dissolving buccal tablets for the emergency delivery of naloxone.

Strang, J., McDonald, R.*, Alqurshi, A., Royall, P., Taylor, D., & Forbes, B. (submitted). Naloxone without the needle - structured review of routes of administration, the rationale for non-injectable naloxone, and next steps in development of nasal and buccal naloxone formulations.

Strang, J., McDonald, R.*, Tas, B., Day, E. (in press). Clinical provision of nasal naloxone without prior experimental testing and without regulatory approval – imaginative shortcut or dangerous bypass of essential safety procedures? *Addiction*.

Patent

King's College London has registered intellectual property on the novel buccal naloxone tablet formulation with which all authors are involved (GB 1504482.9).

Next steps:

First-in-human clinical trials | (1) PK study: buccal naloxone HCl vs IM, IV (EudraCT 2014-001-80216) · (2) PK study: buccal naloxone tablet vs IM, IV

KING'S HEALTH PARTNERS

Pioneering better health for all

Appendix 8. Instant disintegrating buccal tablets for the emergency delivery of naloxone

Please refer to the CD attached for the complete paper

Instant disintegrating buccal tablets for the emergency delivery of naloxone.

Abdulmalik Alqurshi [a], Zahrae Kumar [a], Rebecca McDonald [b], John Strang [b], Asma Buanz [c], Shagufta Ahmed [d], Elizabeth Allen [d], Peter Cameron [e], James A. Rickard [e], Verity Sandhu [e], Chris Holt [e], Rebecca Stansfield [e], David Taylor [a], Ben Forbes [a], Paul G. Royall [a,]*

[a] King's College London, Institute of Pharmaceutical Science, Franklin-Wilkins Building, 150 Stamford Street, London, UK, SE1 9NH. [b] Institute of Psychiatry, Psychology & Neuroscience (IoPPN), King's College London Addictions Sciences Building, 4 Windsor Walk, Denmark Hill, London, UK SE5 8BB. [c] UCL School of Pharmacy, University College London, 29-39 Brunswick Square, London, WC1N 1AX. [d] Quintiles Ltd Quintiles Drug Research Unit at Guy's Hospital, 6 Newcomen Street London SE1 1YR. [e] Guy's and St Thomas' NHS Foundation Trust Pharmacy Manufacturing Unit, Guy's Hospital Great Maze Pond, London, UK, SE1 9RT

[*]Corresponding author & corresponding author contact details: e-mail: paul.royall@kcl.ac.uk; Telephone number: 020 7848 4369; Fax number: 020 7848 4500

KEYWORDS amorphous, instant disintegrating tablets, naloxone, inhibition of crystallization, opioid overdose, buccal delivery, buccal disintegration assay

ABSTRACT The aim of this study was to develop a freeze-dried buccal tablet for the rapid delivery of naloxone in opioid overdose. Tablet composition was optimized to maintain an amorphous matrix confirmed by the absence of peaks associated with crystallinity observed by differential scanning calorimetry and powder X-ray diffraction. Tablets with high gelatin content lacked adequate porosity. Mannitol was added to the formulation to bridge and intercalate gelatin's tight polymer aggregates, however sodium bicarbonate was also required to reduce crystallization within the tablets. A linear reduction in mannitol's re-crystallization enthalpy was observed with increasing sodium bicarbonate concentration ($\Delta_{re\text{-}cry}H$ = -20.3[$NaHCO_3$] + 220.9; r^2 = 0.9, n = 18). The minimum sodium bicarbonate concentration for the inhibition of mannitol crystallization was 10.9% w/w. Freeze dried tablets with lower amounts of sodium bicarbonate included a crystalline fraction that PXRD identified as mannitol hemihydrate from the unique peak at 9.7° 2θ. Mannitol's greater affinity for both ions and residual water rather than its affinity for self-association was the mechanism for the inhibition of crystallization observed here. The optimized tablet (composition mannitol 24% w/w (4.26 mg), gelatin 65% w/w (11.7 mg), sodium bicarbonate 11% w/w (1.98 mg) and naloxone 800 μg) formed predominantly amorphous tablets that disintegrated in less than 10 s. Optimized tablets were both chemically and physically stable over 9 months storage at 25°C. As speed of drug liberation is the critical performance attribute for a solid dosage form designed to deliver drug in an emergency, a novel photographic and imaging based disintegration assay was developed to represent conditions in the buccal cavity: i.e. temperature 33-37°C, disintegration volumes (0.1-0.7 mL), mucin containing disintegration medium. The disintegration assay was discriminatory for quality control purposes In conclusion, rapidly disintegrating tablets have been developed which are suitable for proof-of-concept clinical trial in humans to determine the pharmacokinetics of naloxone delivered via the buccal route.

Appendix 9. Naloxone without the needle – structured review of potential non-injectable routes, the consequent rationale for, and next steps in development of new nasal and buccal naloxone formulations

Please refer to the CD attached for the complete paper

Naloxone without the needle – structured review of routes of administration, the rationale for non-injectable naloxone, and next steps in development of nasal and buccal naloxone formulations

Authors: John Strang [a +], Rebecca McDonald [a *], Abdulmalik Alqurshi [b], Paul Royall [b], David Taylor [b, c] and Ben Forbes [b]

Affiliations:
[a] Addictions Department, Institute of Psychiatry, Psychology and Neuroscience (IoPPN), King's College London, 4 Windsor Walk, Denmark Hill, London SE5 8BB (UK)
[b] Institute of Pharmaceutical Science, King's College London, 150 Stamford Street, London SE1 9NH (UK)
[c] Pharmacy Department, South London and Maudsley NHS Foundation Trust (SLaM), Pharmacy Department, Maudsley Hospital, Denmark Hill, London SE5 8AZ (UK)

[+] **Corresponding author:** john.strang@kcl.ac.uk

Email addresses other authors:
Rebecca McDonald: rebecca.s.mcdonald@kcl.ac.uk
Abdulmalik Alqurshi: abdul.al_qurshi@kcl.ac.uk
Paul Royall: paul.royall@kcl.ac.uk
David Taylor: David.Taylor@slam.nhs.uk
Ben Forbes: ben.forbes@kcl.ac.uk

Words: 4,319 words excluding Title, Abstract, Declarations, Headings.

Running head: Development of novel injection-free naloxone formulations

Abstract: (words 250, excluding section headers)

Introduction: Fatal outcome from opioid overdose can be prevented through administration of the antagonist naloxone, which has been licensed for injection since the 1970s. To support wider availability of naloxone in community settings, novel non-injectable naloxone formulations are required, suitable for emergency use by non-medical personnel.

Objectives: This review 1) identifies candidate routes of injection-free administration potentially suitable for naloxone delivery in the overdose emergency situation; and 2) describes pathways for developing and evaluating novel naloxone formulations.

Methods: A three-stage analysis of candidate routes of administration was conducted: 1) All 112 routes of administration identified by FDA were assessed against exclusion criteria. 2) Empirical data were gathered for all remaining routes by searching PubMed and the WHO International Clinical Trials Registry Platform using the search query "naloxone AND [route of administration]". 3) Non-excluded routes were examined for feasibility and against the inclusion criteria.

Results: Only two routes of administration met inclusion criteria: nasal and buccal. Products specific to both routes are currently in development and being studied in clinical trials. Pharmacokinetic data only exists for nasal naloxone, and product development is more advanced. Buccal dosage forms have the advantage of greater portability, and the buccal mucosa has lesser risk of blockage by opioid-induced vomiting.

Conclusion: After 40 years of injection-based naloxone treatment, non-injectable delivery routes are being investigated. Both nasal and buccal naloxone products appear feasible. The development and approval of reliable non-jectable formulations will facilitate wider naloxone provision across the community, but their ongoing exploration must not be mistaken as evidence of effectiveness.

Key words: naloxone, drug development, opioid, overdose, nasal, buccal